Post-Transcriptional Regulation of ALAS1 Expression by Haem

By

Sadie Jane Redding

A thesis submitted in candidature for the degree of Philosophiae Doctor

Department of Medical Biochemistry and Immunology
Wales College of Medicine
Cardiff University

September 2007

ProQuest LLC
789 East Eisenhower Parkway
P.O. Box 1346
Ann Arbor, MI 48106-1346

Declaration and Statements

DECLARATION

This work has not previously been accepted in substance for any degree and is not concurrently submitted in candidature for any degree.

Signed ..... (candidate) Date 07/12/07

STATEMENT 1

This thesis is being submitted in partial fulfillment of the requirements for the degree of PhD.

Signed ..... (candidate) Date 07/12/07

STATEMENT 2

This thesis is the result of my own independent work/investigation, except where otherwise stated.
Other sources are acknowledged by explicit references.

Signed ..... (candidate) Date 07/12/07

STATEMENT 3

I hereby give consent for my thesis, if accepted, to be available for photocopying and for inter-library loan, and for the title and summary to be made available to outside organisations.

Signed ..... (candidate) Date 07/12/07

STATEMENT 4 - BAR ON ACCESS APPROVED

I hereby give consent for my thesis, if accepted, to be available for photocopying and for inter-library loans **after expiry of a bar on access** approved by the Graduate Development Committee.

Signed ..... (candidate) Date 07/12/07

Acknowledgements

Firstly I would like to thank my supervisors Dr. Andrew Roberts and Dr. David Llewellyn for their help and guidance throughout my PhD. Many thanks to Professor G.H Elder and Professor M Badminton for guidance on the direction of my studies. Thank you also to Professor B.P Morgan and the Department of Medical Biochemistry for supporting and funding my project.

I am most grateful for the technical advice on RNA-binding assays, given by those in Dr. Nancy Standart's laboratory in the University of Cambridge, especially Dr. Lucy Colgrave. Also, thank you to Barrie Francis for help with DNA sequencing, and to Dr Sharon Whatley and Nicola Mason for general advice and making the conferences we attended most enjoyable.

Thank you to all the members of the Department of Medical Biochemistry and fellow UWCM PhD students. In particular, thank you to Tarnjit, Jon, Tom, Ben and Karolina for making my time there enjoyable and being readily available for coffee breaks.

I would like to thank my family: mum, dad and Paul, for all their encouragement and motivation to work hard and achieve my goal. Finally, thank you to Alistair for his constant support and for keeping me happy throughout the writing-up stage.

Publications Relevant to this Thesis

Roberts AG, Redding SJ, Llewellyn DH. An alternatively-spliced exon in the 5'-UTR of human ALAS1 mRNA inhibits translation and renders it resistant to haem-mediated decay. FEBS Letters (2005) 579: 1061-1066.

Unrefereed Abstracts

Redding SJ. Haem-mediated destabilisation of ALAS1 mRNA. The Tetrapyrrole Discussion group, University of Cambridge, 16th-17th September 2004.

Redding SJ. Haem-mediated destabilisation of human ALAS1 mRNA. Proceedings of the 19th Annual Postgraduate Research Day, Cardiff University, 19th November 2004.

Redding SJ, Roberts AG, Llewellyn DH. Haem-mediated destabilisation of human ALAS1 mRNA. Porphyrins and Porphyrias International Conference, South Africa Congress, Cape Town, 26th February – 3rd March 2005.

Redding SJ, Roberts AG, Llewellyn DH. Haem-mediated destabilisation of human ALAS1 mRNA. Proceedings of the 20th Annual Postgraduate Research Day, Cardiff University, 25th November 2005.

Summary

Haem is the prosthetic moiety of numerous haemoproteins critical for the function of all aerobic cells. Its biosynthesis is a tightly controlled process since high intracellular haem concentrations are cytotoxic, whilst haem deficiency impedes the activity of essential haemoproteins. In the liver and probably all other non-erythroid cells, haem supply is regulated primarily through feedback regulation of the stability of the mRNA encoding aminolaevulinic acid synthase 1 (ALAS1), the first and rate-limiting enzyme in the haem biosynthetic pathway. However, the underlying mechanism of this destabilisation is unknown. Consequently, the primary aim of this thesis was to determine how haem regulates ALAS1 mRNA stability to control its own synthesis in non-erythroid cells, using the human hepatoma cell line, HepG2.

In humans, the ALAS1 exon 1b in the 5'-untranslated region (UTR) is alternatively spliced to produce a minor and major form of the enzyme. This thesis has demonstrated that unlike the major ALAS1 5'-UTR, the minor 5'-UTR causes a downstream heterologous RNA to be poorly translated. In addition, the minor ALAS1 isoform is relatively resistant to haem-mediated decay. Using reporter assays and RT-PCR, we have shown that the human ALAS1 mRNA contains a coding region determinant (CRD) that mediates its haem-sensitivity in HepG2 cells. This CRD can function independently of the ALAS1 5'- and 3'-UTR. Furthermore, this haem-mediated CRD has to be translated to function. RNA-electromobility shift assays (EMSAs) have defined two fragments of the ALAS1 coding region that can bind to HepG2 cytosolic protein. However, this binding does not seem to be affected by the addition or depletion of haem. From the data presented in this thesis, a mechanism into how haem destabilises the ALAS1 mRNA in humans has been proposed.

Contents

Abbreviations and Symbols

α	Alpha
β	Beta
γ	Gamma
Δ	Delta
κ	Kappa
µg	Microgram(s)
µM	Micromolar
aa	Amino acid
ADH5/FDH	Human x-alcohol dehydrogenase/formaldehyde dehydrogenase
Ado-CBL	Adenosylcobalamin
ADRES	ALAS drug-responsive enhancer sequence
ALA	5'-aminolaevulinic acid
ALAD	ALA dehydratase
ALAS	ALA synthase
AONS	8-amino-7-oxononanoate synthase
APP	Amyloid precursor protein
ARE	AU rich element
ATP	5'-adenosine triphosphate
AU	Adenylate and uridylate
AUBP	AU-binding protein
bp	Base pair(s)
BCA	Bicinchoninic acid
BSA	Bovine serum albumin
cAMP	Cyclic AMP
CAR	Constitutive androstane receptor
CAT	Chloramphenicol acetyltransferase
CBL	Cobalamin
cDNA	Complementary DNA
CEB	Cytoplasmic extraction buffer
CMV	Cytomegalovirus
CNS	Central nervous system
CO	Carbon monoxide
CO_2	Carbon dioxide
CoA	Coenzyme A
cpm	Counts per minute
CPOX	Coproporphyrinogen oxidase

CRD	Coding region determinant
CREB	cAMP element binding protein
Da	Dalton
dATP	2'-deoxyadenosine 5'-triphosphate
dCTP	2'-deoxycytosine 5'-triphosphate
dGTP	2'-deoxyguanosine 5'-triphosphate
DLRA	Dual luciferase reporter assay
DMEM	Dulbecco's modified Eagle medium
DMSO	Dimethylsulphoxide
DNA	Deoxyribonucleic acid
dNTPs	Equimolar mix of dATP, dCTP, dGTP, dTTP
dsDNA	Double stranded DNA
DTT	Dithiothreitol
dTTP	2'-deoxythymidine 5'-triphosphate
E. coli	Escherichia coli
EDTA	Ethylenediaminetetra acetic acid
eIF	Eukaryotic initiation factor
EMSA	Electromobility shift assay
ER	Endoplasmic reticulum
FCS	Foetal calf serum
FECH	Ferrochelatase
g	Gravity
GAPDH	Glyceraldehyde phosphate dehydrogenase
Glc6P	Glucose-6-phosphatase
h	Hour(s)
HBS	HIF-1 DNA binding site
HCP1	Haem carrier protein 1
HIF-1	Hypoxia-inducible factor–1
HMB	Hydroxymethylbilane
HN3Fβ	Hepatocyte nuclear factor
HO-1	Haem oxygenase 1
IF	Initiation factor
IL	Interleukin
Ins RE	Insulin responsive element
I.p.	Intraperitoneally
IRE	Iron response element
IRP	Iron response protein
kb	Kilobase(s)

KCl	Potassium Chloride
K_d	Equilibrium dissociation constant
kDa	Kilodalton
KOH	Potassium Hydroxide
LB	Luria-Bertani
LDL	Low-density lipoprotein
LMH	Leghorn male hepatoma cells
m^7G	7-methyl-guanylate
M	Molar
MAPK	Mitogen-activated protein kinase
MCS	Multiple cloning site
MEL	Murine erythroleukaemia
Mg	Milligram(s)
$MgCl_2$	Magnesium Chloride
MIP-1β	Macrophage inflammatory protein-1β
MKK	MAP kinase kinase
ml	Millilitre(s)
mM	Millimolar
mRNA	Messenger RNA
mt-acon	Mitochondrial aconitase
MW	Molecular weight
NaCl	Sodium chloride
NEB	New England Biolabs
NF-L	Neurofilament light peptide
ng	Nanogram
NGF	Nerve Growth Factor
nM	Nanomolar
NMD	Nonsense-mediated mRNA decay
NMDA	n-methyl-D-aspartate
NO	Nitric oxide
NR	Nuclear receptor
NRF-1	Nuclear respiratory factor-1
NSAP1	NS1-associated protein
nt	Nucleotide
OD	Optical Density
ORF	Open reading frame
OTC	Ornithine transcarbamoylase precursor
PABP	Poly(A)-binding protein

PAGE	Polyacrylamide gel electrophoresis
PAI-2	Plasminogen activator inhibitor type 2
PAIP	PABP-interacting protein
PB	Phenobarbital
PBG	Porphobilinogen
PBGD	PBG deaminase
PBS	Phosphate-buffered saline
PC	Pyruvate carboxylase
PCR	Polymerase Chain Reaction
PEPCK	Phosphoenolpyruvate carboxykinase
PGC-1α	Proliferator-activated receptor γ co-activator 1α
PKC	Protein kinase C
PLB	Passive lysis Buffer
PLP	Pyridoxal 5-phosphate
pmol	Picomole
PPOX	Protoporphyrinogen oxidase
PXR	Pregnane X receptor
RBB	RNA binding buffer
RES	Reticuloendothelial system
RNA	Ribonucleic Acid
RNA-BP	RNA binding protein
RNase	Ribonuclease
RNP	Ribonucleoprotein
RPA	RNase protection assay
rpm	Revolutions per minute
RPMI	Roswell park memorial institute
rRNA	Ribosomal RNA
RT-PCR	Reverse transcription polymerase chain reaction
SA	Succinyl acetone
SCN	Suprachiasmatic nuclei
SCSβA	Succinyl CoA synthase beta A subunit
S.D.	Standard deviation
SDS	Sodium dodecyl sulphate
ssDNA	Single stranded DNA
Strep-AP	Streptavidin-alkaline phosphatase
TE	Tris-EDTA buffer
TfR	Transferrin receptor
TGF-β	Transforming growth factor-β

TNF	Tumour necrosis factor
tRNA	Transfer RNA
TX	Triton X-100
U	Unit
uAUG	Upstream AUG
UHW	University Hospital of Wales
Unr	Upstream of N-ras
uORF	Upstream open reading frame
UROD	Uroporphyrinogen III decarboxylase
UROS	Uroporphyrinogen III (co-) synthase
UTR	Untranslated Region
UV	Ultraviolet
UWCM	University of Wales College of Medicine
VEGF	Vascular endothelial growth factor
v/v	Volume/volume
w/v	Weight/volume
XLSA	X-linked sideroblastic anaemia

CHAPTER 1

General introduction

1.1 Structure and Chemistry of Haem

Haem (ferroprotoporphyrin IX) is essential for life, playing a vital role in many ubiquitous and tissue-specific cellular processes. It serves as the prosthetic moiety of numerous haemoproteins, essential for the function of all aerobic cells (Ponka, 1999). The unique property of haem, in having an iron molecule coordinated within a tetrapyrrole, allows it to function both as an electron carrier and a catalyst for redox reactions, as well as an oxygen carrier (figure 1-1). The haem molecule plays specific roles in oxygen binding, electron transport, reduction of oxygen and transfer of oxygen for hydroxylation reactions. These roles are in turn determined by the structure of the protein moiety of each specific haemoproteins, their substrates and the intracellular environment where it functions (Bottomley & Muller-Eberhard, 1988).

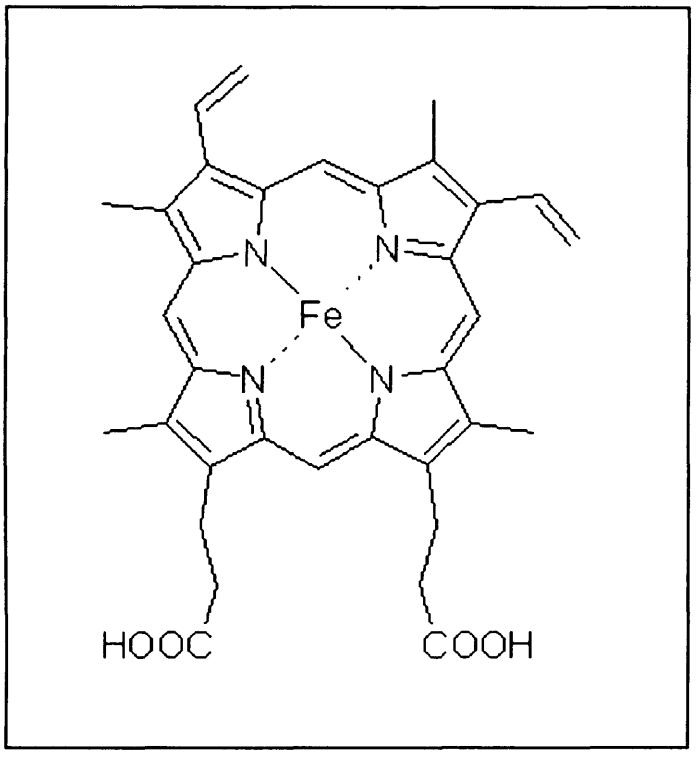

Figure 1-1 Structure of haem.

Structurally, haem is a metallo-compound composed of an iron atom coordinated to the tetrapyrrole (4 pyrroles) ring system known as the protoporphyrin moiety through its 4 nitrogen atoms (Kaplan, 1977). Haem bears 4 methyl, 2 propionate, and 2 vinyl groups attached as substituents to the pyrrole rings. The 4 pyrrole rings are joined to one another via methene bridges. Iron in haem is bound to a histidine residue of the globin chain and to oxygen that binds at other coordinated position of iron (Tsiftsoglou *et al.*, 2006).

Haem is an iron-protoporphyrin complex consisting of four substituted pyrrole rings linked by via methene bridges. When the iron is in the ferrous state, the complex is called ferroprotoporphyrin or haem, and the molecule is electrically neutral (figure 1-1). When the iron atom is in the ferric state, the complex is called ferriprotoporphyrin or haemin, and the molecule carries a unit positive charge (and is consequently associated with an anion). Haem is hydrophobic in nature and contains methyl groups in positions 1, 3, 5 and 8; vinyl groups in positions 2 and 4; and propionic acid groups in positions 6 and 7 (Kumar & Bandyopadhyay, 2005).

Four types of haem are known in eukaryotes, which differ in the composition of the side chains of the pyrrole rings: protohaem, haem *a*, *b*, and *c*. Protohaem is a pool of "free haem" that is not associated, or only loosely associated, with proteins, e.g. tryptophan pyrrolase and is the precursor for the other types of haem (reviewed in Atamna *et al.,* 2002). The most ubiquitous type of haem is haem *b*, and constitutes the prosthetic group of all haemoproteins, except cytochromes types *c* and *a*. In these cytochromes, haem *c* and *a*, respectively, form their prosthetic moiety (Moraes *et al.,* 2004; Kumar & Bandyopadhyay, 2005). Haem *b* and *c* are similar to protohaem, with minor modifications that take place as it is incorporated into each specific protein. The synthesis of haem *a* from protohaem requires two minor modifications: the farnesylation and addition of a formyl group to position 8 of the protohaem (Atamna *et al.,* 2002).

1.2 Function of Haem

Haemoproteins are involved in a remarkable array of crucial biological functions including oxygen binding (haemoglobin, myoglobin), oxygen metabolism (oxidases, peroxidases, and catalases), oxidative phosphorylation (cytochrome c) and electron transfer (cytochrome P450's) (reviewed in Ponka, 1999) (see table 1-1 for examples of haemoproteins).

Cytochrome P450 is the collective term for a large superfamily of haem-containing proteins that play an important role in the oxidative metabolism of numerous endogenous and foreign compounds (Nelson *et al.,* 1996). Four of the P450-families, families 1 to 4, are involved in drug metabolism and are preferentially expressed in the liver. Drug-metabolizing P450 isoforms also occur in extra-hepatic tissue (Strobel *et al.,* 1997), and several of the P450s expressed

in the brain are inducible by alcohol, neuroleptics, anticonvulsants, and endocrine factors (Volk *et al.*, 1995; Hedlund *et al.*, 1996).

Haemoproteins (proteins containing haem as prosthetic group) and haem-based sensors
Respiratory cytochromes – cytochrome c, cytochrome c oxidase, cytochrome reductase
Cytochromes P450
Catalases
Peroxidases
Globin-like coupled sensors
Histidine kinases
eIF2α-kinase (translational initiation factor)
Nitric oxide synthases (NOS): haem-based sensors
Soluble guanylate cyclases (SGC): haem-based sensors
Cyclic nucleotides phosphodiesterases
Haemoglobins (haem-based sensors)
Myoglobins (haem-based sensors)
Hydroxylamine oxidoreductase

Table 1-1 Examples of haemoproteins and haem-based sensors in humans.

Table adapted from Tsiftsoglou *et al.*, 2006.

Haem is also the prosthetic group of numerous haemoproteins that synthesise important regulatory or signalling molecules including cyclic GMP (guanylate cyclase), steroid hormones (hydroxylases) and nitric oxide (nitric oxide synthase). The haem molecule also plays an important role in controlling the expression of numerous proteins (globin, haem biosynthetic enzymes, cytochromes, myeloperoxidase, haem oxygenase-1 (HO-1), transferrin receptor (TfR)) and by providing carbon monoxide (CO), which may have a regulatory role akin to that of nitric oxide (NO) (Ponka, 1999).

CO is a biologically active product of the degradation of haem by the haem oxygenases 1, 2 and 3. Furthermore, this reaction produces the anti-oxidant biliverdin, Fe^{2+} and H_2O_2, which also have biological effects. CO is a signalling molecule with significant vasoactive and anti-inflammatory characteristics (Otterbein *et al.*, 2000). CO selectively inhibits the expression of pro-inflammatory cytokines tumour necrosis factor-α (TNFα), interleukin 1β (IL-1β) and macrophage inflammatory protein-1β (MIP-1β), and the anti-inflammatory cytokine IL-10 (Otterbein *et al.*, 2000). These effects are mediated independently of nitric oxide (NO) or cGMP which has been hypothesised to mediate the effects

of CO in cell culture systems (Morita *et al.,* 1995). CO has been shown *in vivo* to exert its anti-inflammatory effects specifically through the MAP kinase kinase (MKK) 3/p38 pathway (Otterbein *et al.,* 2000).

The requirements for haem vary significantly among various cells and tissues, with the highest amounts made in erythroid cells and hepatocytes (Ponka, 1999). Approximately 85% of haem in the body is synthesised by erythroid cells and utilised for haemoglobin formation (Harigae *et al.,* 2003), whereas about 15% of the daily production takes place in the liver for the formation of haem-containing enzymes. Between 20 and 35% of newly formed haem is directly converted to bile pigments, suggesting a continuous demand for haem biosynthesis (Atamna, 2004). In senescing erythrocytes, haemoglobin undergoes degradation in the reticuloendothelial system of the liver, kidney, and especially the spleen (Ryter & Tyrrell, 2000). Haem biosynthesis in the brain varies according to the type of brain cell, and appears to be higher in non-neuronal cells and lower in neuronal cells (Atamna, 2004; Atamna *et al.*, 2002).

Free haemoglobin and haem released from methemoglobin may also enter the bloodstream during haemolysis. Such extracellular haem circulates in the serum as complexes with the serum proteins, haemopexin, and albumin. Free vascular haemoglobin is often captured by its scavenger haptoglobin and transported to the reticuloendothelial system (RES) (Muller-Eberhard & Fraig, 1993). Haem and haemoglobin are then imported into the liver parenchyma by receptor-mediated endocytosis, and the haem subsequently degraded by HO activity in the liver microsomes. However, any intracellular "free" haem undergoes degradation *in situ*, rather than exportation to serum and subsequent hepatic degradation (Ryter & Tyrrell, 2000).

1.3 Haem Biosynthesis

The synthesis of haem involves eight enzymes, four of which are cytoplasmic and four are mitochondrial (reviewed in Ponka, 1999) (figure 1-2). The intermediate products formed in the haem biosynthetic pathway are the reduced forms of porphyrins – porphyrinogens. These undergo rapid oxidation in air to become porphyrins, which are the usual forms of the cyclic tetrapyrroles found in biological specimens. There are four basic processes of the haem biosynthetic pathway (Ajioka *et al.,* 2006): (1) Formation of the pyrrole; (2) Assembly of the

tetrapyrrole; (3) Modification of the tetrapyrrole side chains; (4) Oxidation of protoporphyrinogen IX to protoporphyrin IX and insertion of iron.

All mammalian haem pathway enzymes have been cloned and the genes encoding these enzymes reside on different chromosomes (table 1-2).

Haem Biosynthetic Enzyme		Chromosome	Reference
Aminolaevulinic acid synthase	ALAS1	3p21.1	Bishop, 1990; Cotter *et al.*, 1995
	ALAS2	Xp11.21	Cotter *et al.*, 1992
Aminolaevulinic acid dehydratase		9q34	Potluri *et al.*, 1987
Porphobilinogen deaminase		11q24	Namba *et al.*, 1991
Uroporphyrinogen III synthase		10q25.2 - q26.3	Astrin *et al.*, 1991
Uroporphyrinogen III decarboxylase		1p34	Dubart *et al.*, 1986
Coproporphyrinogen III oxidase		3q12	Cacheux *et al.*, 1994
Protoporphyrinogen III oxidase		1q22	Taketani *et al.*, 1995
Ferrochelatase		18q21.3	Taketani *et al.*, 1992

Table 1-2 Chromosomes on which the human haem biosynthetic enzymes reside.

In animal cells, anabolic and catabolic pathways are frequently confined to a single cellular compartment unless the process involves import or export of products or substrates. In contrast, the tetrapyrrole biosynthetic pathway in animal cells has its first and its last three steps catalysed by mitochondrial enzymes, whereas the intermediate four steps are catalysed by cytosolic enzymes (Ponka, 1999). All pathway enzymes are nuclear-encoded and are synthesized in the cytosol with the mitochondrially located proteins being post-translationally translocated to their appropriate mitochondrial space (Dailey *et al.*, 2005). To facilitate their high-level erythroid expression, the first four enzymes in the pathway are encoded by erythroid-specific transcripts generated by separate genes (ALAS; Bishop, 1990) or by genes with alternative housekeeping and erythroid promoters (ALA-dehydratase; Kaya *et al.*, 1994; porphobilinogen deaminase; Grandchamp *et al.*, 1987; and uroporphyrinogen III synthase; Aizencang *et al.*, 2000). In contrast, each of the last four genes in the pathway has a single promoter that contains both erythroid-specific and housekeeping binding elements for housekeeping and enhanced erythroid expression (Delfau-Larue *et al.*, 1994; Romana *et al.*, 1987; Taketani *et al.*, 1995; Tugores *et al.*, 1994).

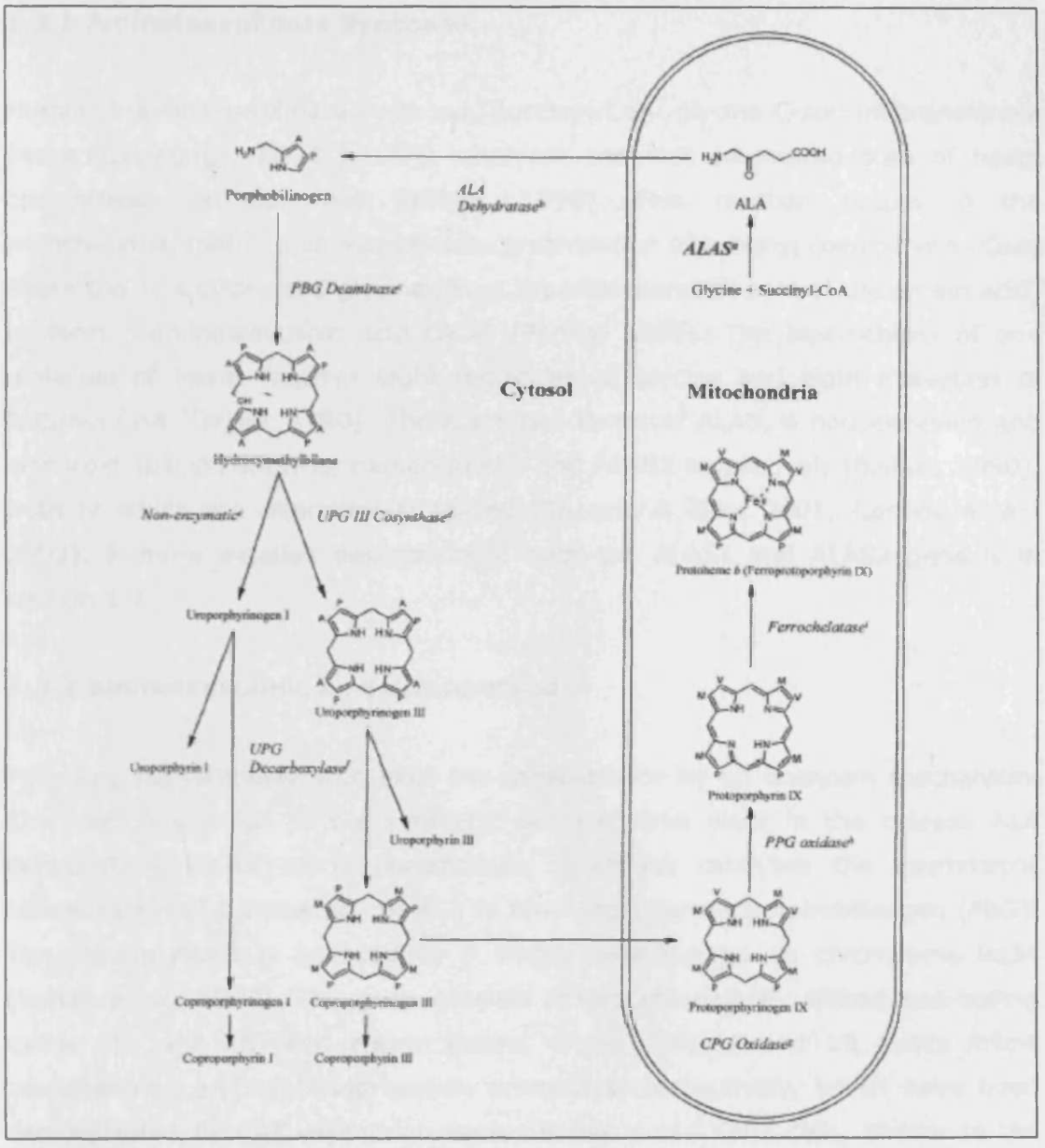

Figure 1-2 The haem biosynthetic pathway, from Ryter & Tyrrell, 2000.

Tetrapyrrole side chains: A=acetyl, M=methyl, P=propionyl, V=vinyl. ALAS[a]=ALAS condenses glycine with succinyl-Co-A to form ALA and CO_2. ALA dehydratase[b]=ALAD condenses 2 molecules of ALA to PBG, eliminating 2 molecules of H_2O. PBG deaminase[c]=PBGD polymerizes PBG (4 molecules) to HMB, eliminating ammonia. UPG III cosynthase[d]=UROS cyclizes HMB to uroporphyrinogen III. e=Non-enzymatic cyclization of HMB produces the useless uroporphyrinogen I. Further metabolism yields copropophyrinogen I. Porphyrinogens undergo non-enzymatic oxidation to corresponding porphyrins, (uroporphyrin I, III; coproporphyrin I, III) which accumulate in porphyrias. UPG decarboxylase[f]=UROD converts uroporphyrinogen III to coproporphyrinogen III by serial decarboxylation. CPG oxidase[g]=CPOX converts coproporphyrinogen III to protoporphyrinogen IX (PPGIX) by decarboxylation and oxidation of 2 propionyl residues to vinyl groups. PPG oxidase[h]=PPOX dehydrogenates protoporphyrinogen to protoporphyrin IX (PPIX). Ferrochelatase[i] incorporates ferrous iron, Fe (II), into PPIX, generating protohaem.

1.3.1 Aminolaevulinate Synthase

Human 5-aminolaevulinate synthase [Succinyl-CoA: glycine C-succinyltransferase (decarboxylating); EC 2.3.1.37]) catalyses the first committed step of haem biosynthesis in mammals (Bishop, 1990). This reaction occurs in the mitochondrial matrix and involves the condensation of succinyl coenzyme A (CoA) (from the TCA cycle) and glycine (from the mitochondrial pool of the amino acid) to form 5-aminolaevulinic acid (ALA) (Ponka, 1999). The biosynthesis of one molecule of haem requires eight molecules of glycine and eight molecules of succinyl CoA (Dailey, 1990). There are two forms of ALAS, a housekeeping and erythroid-specific enzyme, named ALAS1 and ALAS2 respectively (Bishop, 1990). Both of which are alternatively spliced (Roberts & Elder 2001; Conboy *et al.,* 1992). A more detailed description of both the ALAS1 and ALAS2 gene is in section 1.7.

1.3.2 Aminolaevulinic acid dehydratase

Following its synthesis, ALA exits the mitochondria by an unknown mechanism. The next four steps of the synthetic pathway take place in the cytosol. ALA dehydratase (ALAD or porphobilinogen synthase) catalyses the asymmetric condensation of 2 molecules of ALA to form monopyrrole porphobilinogen (PBG). The human ALAD is encoded by a single gene located on chromsome 9q34 (Potluri *et al.,* 1987). This gene consists of two alternatively spliced non-coding exons (1A and 1B) and eleven coding exons. The 1A and 1B genes follow housekeeping and erythroid-specific promoters, respectively, which have been demonstrated by CAT expression assays in HeLa and K562 cells. Similar to the ALAS1 gene, the housekeeping promoter of ALAD is active in both erythroid and non-erythroid cells, whereas the erythroid-specific promoter is active only in erythroid cells. As these alternatively spliced exons are present in the 5'-UTR, both transcripts encode identical 36kDa ALAS polypeptides in all cell types (Kaya *et al.,* 1994). The human ALAD gene is similar to that of the mouse (Bishop *et al.,* 1989). This suggests that an early mammalian evolutionary event of the separation of the housekeeping and erythroid-specific upstream exonic promoter sequences occurred to enable sufficient haem production for erythropoiesis (Kaya *et al.,* 1994).

1.3.3 Porphobilinogen deaminase

The next two enzymatic steps convert four molecules of PBG into the cyclic tetrapyrrole uroporphobilinogen III, which is then decarboxylated to form coproporphyrinogen III. Porphobilinogen deaminase (PBGD; hydroxymethylbilane synthase) is located in the cytosol and is the third enzyme of the haem biosynthetic pathway, which catalyses the stepwise condensation of four PBG units to form the linear tetrapyrrole hydroxymethylbilane (HMB) (Battersby *et al.,* 1980). Similar to ALAS and ALAD, two isoforms of PBGD exist which differ by approximately 2kDa, one present in all cells and the other erythroid-specific (Grandchamp *et al.,* 1987). The PBGD gene is 10kb long, located at chromosome 11q24, and split into 15 exons (Namba *et al.,* 1991; Yoo *et al.,* 1993). Alternative splicing in the 5'-UTR results in two different primary transcripts, where the human PBGD gene is expressed in all tissues due to a housekeeping promoter, whereas the erythroid-specific promoter located 3kb downstream, is switched on during erythroid differentiation (Chretien *et al.,* 1988). The isoforms differ only at their NH_2 ends, where the ubiquitous isoforms extend for an additional 17 residues, making a polypeptide of 361 amino acids (Grandchamp *et al.,* 1987).

1.3.4 Uroporphyrinogen III synthase

Uroporphyrinogen III synthase (URO-synthase, UROS) then rapidly converts HMB to uroporphyrinogen III, the first cyclic tetrapyrrole of the haem biosynthetic pathway, by an intramolecular rearrangement of the D-pyrrole group and ring closure. The UROS human gene is ~34kb and consists of 10 exons. Its expression is controlled by having two distinct erythroid and housekeeping promoters in its 5'-UTR, rather than the use of alternative splicing (Aizencang *et al.,* 2000).

1.3.5 Uroporphyrinogen III decarboxylase

Human uroporphyrinogen III decarboxylase (UROD) catalyses the fifth step of the haem biosynthetic pathway. This is the sequential elimination of the carboxyl groups from each of the four acetate side chains of the uroporphyrinogen III substrate, yielding coproporphyrinogen III. The UROD gene has been assigned to the p34 band of chromosome 1 (Dubart *et al.,* 1986), consisting of 10 exons, and is over 3kb long (Romana *et al.,* 1987). RNase mapping and primer extension analysis has shown that transcription is initiated at two start sites, only 6 bases

apart. These initiation sites are used in all tissue types, with no specific promoter used for erythroid cells (Romana *et al.,* 1987).

1.3.6 Coproporphyrinogen oxidase

The last three steps of the biosynthetic pathway take place in the mitochondria (Ponka *et al.,* 1973). These are the oxidative decarboxylation of coproporphyrinigen III to protoporphyrinogen IX, followed by the six-electron oxidation of protoporphyrinogen to protoporphyrin IX, and finally the insertion of ferrous iron to form haem, catalysed by the enzymes coproporphyrinogen oxidase (CPOX), protoporphyrinogen oxidase (PPOX) and ferrochelatase respectively (reviewed in Dailey, 2002).

CPOX is a soluble mitochondrial protein that is localised in the intermembrane space within mammalian cells, and catalyses the sixth step in haem biosynthesis, the conversion of the two propionate groups at positions 2 and 4 of coproporphyrinogen III to two vinyl groups, thus producing protoporphyrinogen IX (Elder & Evans, 1978; Martasek *et al.,* 1994). The CPOX gene has been mapped to chromosome band 3q12 (Cacheux *et al.,* 1994), spanning 14kb and consisting of seven exons and six introns (Delfau-Larue *et al.,* 1994). This protein possesses an unusually long N-terminal leader sequence of more than 120 amino acids, which is proteolytically removed (Delfau-Larue *et al.,* 1994). The mature protein is a homodimer and possesses no known cofactor (Medlock & Dailey, 1996).

1.3.7 Protoporphyrinogen oxidase

PPOX is the penultimate enzyme of the pathway, and catalyses the six electron oxidation of protoporphyrinogen IX to form protoporphyrin IX. The enzyme is located in the inner mitochondrial membrane of various tissues including liver, lymphocytes and cultured fibroblasts. Its gene is mapped to chromosome 1q22, which spans approximately 8kb and consists of 13 exons and 12 introns (Taketani *et al.,* 1995). Human PPOX contains 477 amino acids and has a molecular mass of 50.8 kDa (Nishimura *et al.,* 1995). Eukaryotic mitochondrial PPOXs are strongly associated with the mitochondrial inner membrane, and the active site has been suggested to be on the cytosolic surface of the membrane (Deybach *et al.,* 1985; Ferreira *et al.,* 1988). The information required for efficient import of human PPOX into the mitochondria is contained within the first 250 amino acid

residues. Fully efficient targeting requires both a major targeting signal, which may be contained between residues 151 and 175, and involved in anchoring to the inner mitochondrial membrane, together with sequences within the first 150 residues (Morgan *et al.,* 2004). Primer extension analysis has shown that PPOX mRNA synthesis is initiated at two major sites, used similarly by both erythroid and non-erythroid cells (Taketani *et al.,* 1995).

1.3.8 Ferrochelatase

The terminal enzyme of the haem biosynthetic pathway is ferrochelatase (FECH), catalysing the insertion of ferrous iron into protoporphyrin IX, and yielding haem. In eukaryotic cells this enzyme is a mitochondrial inner-membrane associated protein, with the active site facing the matrix (Ferreira *et al.,* 1995). The ferrochelatase gene is located on chromosome 18, at region q21.3. It contains a total of 11 exons with a minimum size of approximately 45kb. Primer extension analysis shows that transcription of ferrochelatase initiates at the same site in both hepatoma HepG2 and erythroleukemia K562 cell mRNA, suggesting that there is a single transcript which functions in both erythroid and non-erythroid cells (Taketani *et al.,* 1992).

1.4 Mammalian Haem Transport

Protohaem made by ALAS1 is released into the mitochondrial matrix, where part of it is utilised for assembly of mitochondrial proteins, and an appreciable fraction is exported to the cytosol to be assembled into different cytosolic proteins (Ponka *et al.,* 1973).

Newly formed haem is rapidly incorporated into cellular haem proteins, among which the microsomal cytochromes P-450 are quantitatively the most important in non-erythroid cells. In rats, turnover of these cytochromes appears to consume at least 50% of the haem produced in the liver (Grandchamp *et al.,* 1981). After the translocation of haem across the mitochondrial membranes to varying locations, a proportion is then recruited to the endoplasmic reticulum to be degraded by haem oxygenase (HO) (Atamna *et al.,* 2002).

Transmembrane transport of haem is essential both for the absorption in the gastrointestinal tract to maintain body iron homeostasis and for intracellular trafficking in other cells and tissues. Due to its lipophillic nature, haem can diffuse

into cell membranes; however in several cases transmembrane transport of haem is an energy-dependent process, requiring haem transport proteins (Latunde-Dada *et al.*, 2006).

The carrier proteins and general mechanism that mediate this shuttling of haem between the different compartments of the cell have not been well understood. There have been a number of different putative haem-transport-associated proteins, of which their function and tissue localisation is listed in table 1-3.

Protein	Localization	Function	References
HCP1	Duodenum, liver, kidney	Duodenal apical haem transporter, possible haem scavenging or recovery	Shayeghi *et al.*, 2005
FLVCR	Haematopoietic cells, liver, kidney, pancreas	Haem efflux in erythroid progenitor cells	Quigley *et al.*, 2004
ABCG2	Haematopoietic cells, fetal liver, pancreas, kidney, intestine	Haem porphyrin efflux	Krishnamuphy *et al.*, 2004
SOUL	Eye	Putative haem-binding protein	Sato *et al.*, 2004
ABCme	Erythroid cells, inner mitochondrial membrane	Possible transport of haem from mitochondria to cytosol	Lill & Kispal, 2001
ABC3, ABC7, ABCme	Mitochondria	Transport of haem derivatives	Lill & Kispal, 2001
Haemopexin receptor LRP or CD91	Hepatocyte	Haem endocytosis from citculation	Hvidberg *et al.*, 2005
Haptoglobulin receptor. CD163	Macrophages	Haemoglobin clearance from circulation	Kristiansen *et al.*, 2001
Megalin and cubilin receptors	Kidney	Renal haemoglobin reabsorption	Gburek *et al.*, 2002 & 2003

Table 1-3 Function and tissue localisation of putative haem-transport-associated proteins; table adapted from Latunde-Dada *et al.*, 2006.

HCP1 = haem carrier protein 1; FLVCR = Feline leukaemic virus receptor; ABC = ATP binding cassette transporter; LRP/CD91 = low-density lipoprotein receptor-related protein CD91.

Recently, Krishnamurthy *et al* (2006) identified the ATP-binding cassette transporter, ABCB6, as a mammalian mitochondrial porphyrin transporter. Their experiments showed that the *Acbc6* mRNA and ABCB6 protein are strongly elevated by exogenously added haemin, in murine erythroleukaemia (MEL) cells. Treatment of MEL cells with ALA to endogenously induce haem biosynthesis caused a dose and time-dependent increase in ABCB6 protein and mRNA and intracellular protoporphyrin IX (PPIX) and ABCBC6 concentrations were correlated. Conversely, the inhibition of haem biosynthesis by the addition of succinyl acetone (SA) to MEL cells prevented an increase in intracellular PPIX and blocked upregulation of ABCB6 synthesis by ALA. Thus ABCB6 expression levels respond directly to the intracellular PPIX concentration. This has also been confirmed *in vivo*, using two mouse models. Moreover, not only does ABCB6 protein increase during erythroid differentiation and haem biosynthesis and is directly upregulated by increased intracellular porphyrin, ABCB6 overexpression also enhances porphyrin biosynthesis by upregulating the key genes for transferrin receptor, ALAD, ALAS and coporphyrinogen oxidase (Krishnamurthy *et al.,* 2006).

Work published by Smith & Morgan (1984) and Morgan (1976) indicated that haem released from haemoglobin in plasma, following red blood cell degradation in spleen, is transported into liver cells via haemopexin, a carrier plasma protein. Haemopexin forms stable complexes with haem that are internalized inside the cells. Haemopexin returns intact to the extracellular space just after releasing exogenous haem into intracellular cytosolic compartment for reutilization. This carrier-mediated import of haem via haemopexin is a saturation-, time-, and energy-dependent as well as tissue-specific process. Iron released from haem by microsomal haem oxygenase is then stored into ferritin. This haemopexin-mediated import of haem does not account for all, but only a portion of transported haem (reviewed in Baker *et al.,* 2003; Hvidberg *et al.,* 2005).

The intestinal haem transporter HCP1 was identified by Shayeghi *et al* (2005), which is capable of mediating energy-dependent transmembrane uptake of the intact metal-porphyrin ring, and is used to absorb haem from the diet into the gut (Latunde-Dada *et al.,* 2006). The identification of this transporter revealed the mechanism by which haem is absorbed from the diet by the gut, as an important source of dietary iron.

1.5 Role of Haem Biosynthesis in Disease

Both inherited mutations and environmental factors may affect the haem biosynthetic pathway and lead to diseases including X-linked sideroblastic anaemia (XLSA), lead poisoning and the porphyrias (table 1-4) (Anderson *et al.*, 2000; Sassa, 2000; Jordan & Dailey, 1990). Porphyrias are mainly inherited in an autosomal dominant manner with incomplete penetrance, but autosomal recessive and more complex patterns of inheritance are also possible (reviewed in Kauppinen, 2005).

Porphyrias represent overproduction syndromes with the formation of toxic haem precursors, which are overproduced under particular circumstances, with acute porphyrias resulting in neurovisceral manifestations. Overproduction of porphyrins causes photosensitivity in cutaneous porphyrias (Kauppinen, 2005). Compelling evidence has been generated indicating that neurovisceral symptoms are due to neurotoxic affects of the pre-porphyrin precursors, which is primarily ALA. The photosensitivity is due to the fluorescent properties of the porphyrins (Sassa, 2006).

A convenient way to classify the porphyrias is to divide them according to the dominant clinical feature, although some authors prefer to divide the porphyrias based on whether excess substrate is generated in the liver (hepatic porphyrias) or the erythrocyte (erythropoietic porphyrias) (Sassa, 2006).

During an acute attack, ALAS1, the hepatic isoform of the first enzyme in the haem biosynthetic pathway is induced. The acute hepatic porphyrias are ALA dehydratase porphyria (ADP), acute intermittent porphyria (AIP), variegate porphyria (VP) and hereditary coproporphyria (HCP). ALAS1 formation in normal hepatocytes is repressed by feedback inhibition by the final product, haem. Metabolic inhibition along the pathway in the liver leads to reduced production of haem, resulting in de-repression of ALAS1. This leads to increased production of haem precursors in an effort to overcome the metabolic block, and contributes to the accumulation of intermediates prior to the deficient enzymatic step. This abnormality continues until sufficient haem synthesis is restored (Sassa, 2006).

Enzyme in Haem Biosynthesis	Disease	Type	Symptoms	Products
ALAS2	X-linked sideroblastic anaemia (XLSA)	Erythroid	Microcytic anaemia	Sideroblasts
ALAD	ALA dehydratase porphyria (ADP)	Hepatic	Neurovisceral	Urinary ALA
PBGD	Acute intermittent porphyriea (AIP)	Hepatic	Neurovisceral	Urinary ALA, PBG
UROS	Congenital erythropoietic porphyria (CEP)	Erythropoietic	Photosensitivity Haemolytic anaemia	Urinary & RBC Uroporphyrinogen I, Coproporphyrinogen I
UROD	Porphyria cutanea tarda (PCT)	Hepatic	Photosensitivity	7-C porphyrin; faecal isocoproporphyrin
	Hepatoerythropoietic porphyria (HEP)	Erythropoietic	Haemolytic anaemia	
CPOX	Hereditary coproporphyria (HCP)	Hepatic	Neurovisceral Photosensitivity	Urinary ALA, PBG, coproporphyrin
PPOX	Variegate porphyria (VP)	Hepatic	Neurovisceral Photosensitivity	Urinary ALA, PBG; faecal protoporphyrin
FECH	Erythropoietic protoporphyria (EPP)	Erythropoietic	Photosensitivity	RBC protoporphyrin Faecal protoporphyrin

Table 1-4 Classification of the porphyrias; adapted from Sassa, 2006.

Enzymatic defects, associated diseases, major symptoms and principal accumulation products are shown. ALAS2 defect is responsible for XLSA but is not associated with any porphyria, since the enzymatic defect blocks production of ALA, the precursor for porphyrin formation. ADP and AIP are accompanied by acute hepatic porphyria but not by photocutaneous porphyria, because their enzymatic defects do not result in an increase in porphyrin synthesis. Enzymatic defects beyond UROS are all associated with photocutaneous porphyrias, because they produce excessive amounts of various porphyrins. HCP and VP are additionally associated with acute hepatic porphyria.

Transcription of ALAS1 can also be upregulated by the peroxisome proliferators-activated receptor γ-coactivator 1α (PGC-1α) (described in more detail in section 1.8.2.2). Under conditions of low glucose, PGC-1α production increases, leading to increased levels of ALAS1 and creating conditions for attacks of acute porphyrias (Handschin *et al.*, 2005).

1.5.1 Haem Excess

Haem is absolutely required for aerobic life. However, haem has to be tightly regulated by cells as a deficiency or excess can have cytotoxic effects (figure 1-3), particularly in the presence of oxidants or activated phagocytes (Yoo *et al.,* 1999; Kumar & Bandyopadhyay, 2005). Of all the sites of the body, the vasculature, and in particular the endothelial lining, may be at greatest risk of exposure to free haem. This is because erythrocytes contain haem in a concentration of 20mmol/L and are vulnerable to unexpected lysis. The extramolecular haemoglobin is easily oxidised to ferrihaemoglobin, which, in turn, will readily release haem. Given the hydrophobic nature of haem, it easily crosses cell membranes, then concentrates within the hydrophobic milieu of intact cells, and can synergistically enhance oxidant damage. Both *in vitro* and *in vivo*, cells will accumulate exogenous haem and synergistically amplify the cytotoxic effects of oxidants of reagent, enzymatic, or cellular origin (Balla *et al.,* 1991).

Haem also acts as a catalyst for the oxidation of low-density lipoprotein (LDL), generating products toxic to endothelium (Camejo *et al.,* 1998). These toxic effects may be important in a number of pathologies such as the acute conditions intravascular haemolysis as well as insidious processes such as atherogenesis. As a defence against such toxicity, normal cells upregulate HO-1 and ferritin (Jeney *et al.,* 2002). High levels of free haem are found in pathological states of increased haemolysis, such as sickle cell disease, malaria and ischemia reperfusion. Under these conditions, the physiological mechanisms of removing free haem from the circulation, especially its binding to haemopexin, collapse, allowing non-specific haem uptake and haem-catalysed oxidation reactions (Arruda *et al.,* 2004).

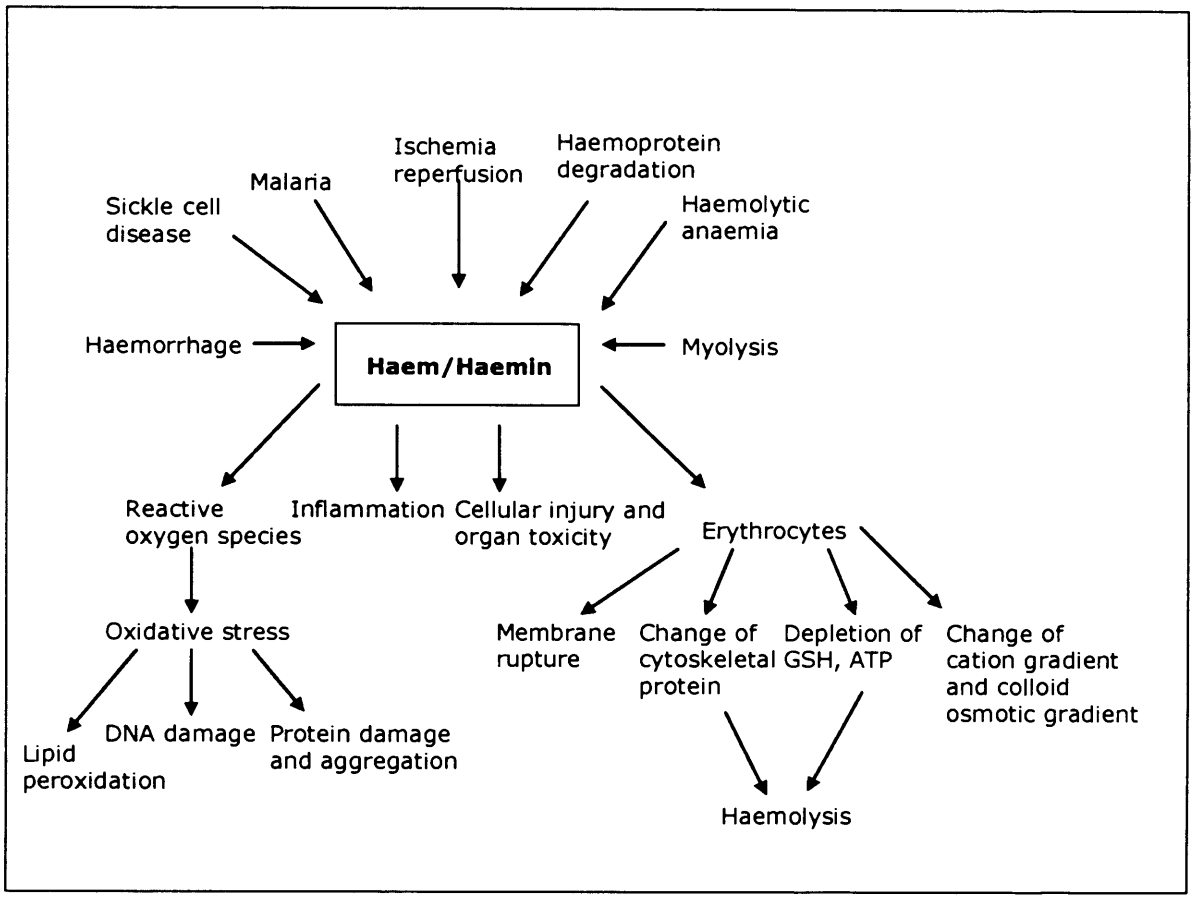

Figure 1-3 Toxic effects of free haem/haemin. Adapted from Kumar & Bandyopadhyay, 2005.

Haem, a ubiquitous iron-containing compound, is quite hydrophobic, readily enters cell membranes, and greatly increases cellular susceptibility to oxidant-mediated killing (Balla *et al.,* 1991). Haem also acts as a catalyst for the oxidation of low-density lipoprotein (LDL), generating products toxic to endothelium (Balla *et al.,* 1991, Miller *et al.,* 1994, Camejo *et al.,* 1998).

The accumulation of haem within the cell can ultimately lead to the accumulation of iron and the production of cell-damaging reactive oxygen species by the Fenton reaction. This is the reaction between ferrous iron and hydrogen peroxide to produce powerful oxidising intermediates, with •OH being the most powerful oxidising species.

$Fe^{2+} + H_2O_2 \rightarrow Fe^{3+} + {\bullet}OH + OH^-$

(Wink *et al.,* 1994)

Haem/porphyrin accumulation also leads to the collapse of mitochondrial function. The regulation of intracellular porphyrin levels is therefore fundamental to cell

survival. In erythroid cells, this regulation is especially important under conditions of low oxygen, when the cellular concentration of haem may increase. This is due to the increased ALAS2 transcription in a hypoxia-inducible factor–1 (HIF-1) independent manner, even though a single putative HIF-1 DNA binding site (HBS) has been identified within the promoter region of murine ALAS2 (Hofer *et al.,* 2003; Kramer *et al.,* 2000). Hypoxia has not been shown to in induce ALAS1 expression.

Once within the cell, haem can promote oxidative damage either directly or, perhaps more importantly, directly via the release of iron. This can occur through either non-enzymatic oxidative degradation of haem, or enzymatic, HO-catalysed haem cleavage. In either case the iron may initially lodge within the hydrophobic interstices of the phospholipid bilayer; within this highly oxidizable matrix, iron acts as an especially active catalyst of oxidation of cell membrane constituents (Balla *et al.,* 2005).

Severe haemolysis occurring during pathological states, such as sickle cell disease, ischemia reperfusion, and malaria results in high levels of free haem (up to 20μM). Under these conditions the physiological mechanisms of removing free haem from the circulation collapse, allowing non-specific haem uptake and haem catalysed oxidation reactions. When large amounts of free haem proteins or haem accumulate, e.g. in a blood clot, the haem detoxification systems get overwhelmed, or are unable to reach them. This enables haem to exert its damaging effects (Kumar & Bandyopadhyay, 2005). These large amounts of exogenous haem, produced in a haemorrhage for example, may be toxic to neurons (Goldstein et al., 2003).

Cellular free haem may increase by pharmacological stimulation with porphyrinogenic agents, by accelerated degradation of intracellular haemoproteins, by impaired incorporation into apo-haemoproteins, or as a result of inhibition of cellular HO activity (Scriver *et al.,* 1995). Cellular stress may also alter haemoprotein turnover. For example, oxidative stress may modify protein structure, causing fragmentation, crosslinking, and changes in charge, hydrophobicity, electrophoretic mobility, and solubility. Such modification, occurring in a haemoprotein, may either trigger the release of the haem, or alter the reactivity of hypervalent states of the protein towards organic molecules in the surrounding cellular context. Oxidative stress generated by UVA (Ultraviolet A) radiation increases degradation of cytochrome p-450 and causes accumulation

of free haem in fibroblasts. This free haem is a potentially dangerous molecule, and therefore, in order to preserve cellular haemostasis, its cellular concentration must be tightly regulated (Ryter & Tyrrell, 2000).

1.5.2 Haem Deficiency

Decreased haem biosynthesis in erythroid cells causes symptoms such as anaemia. The known consequences of decreased levels in non-erythroid cells are loss of mitochondrial complex IV, oxidative stress, accumulation of iron, and cell death whenever stimulation by growth factors occurs. The affects of changes of haem *in vivo* on the brain have not been fully elucidated (Atamna, 2004).

Haem deficiency prevents the assembly of complex IV, the terminal complex of the electron transport chain, by more than 95% and mildly affects complex II and cytochrome c (by 30%) in human fibroblasts (Atamna *et al.,* 2001). The complex IV is tightly coupled to neuronal metabolic activity; therefore brain may be the most susceptible organ for a decrease in complex IV and for oxidative stress, which occur in ageing and Alzheimer's disease (Maurer *et al.,* 2000). Levels of haem *a* in Alzheimer patients decrease by 22%, while haem *b* and *c* remain relatively unchanged, when compared to healthy controls (Atamna *et al.,* 2002).

Haem deficiency obliterates the activation of the Ras-MAPK signalling pathway and its downstream transcription factor, which suggests that haem deficiency should ultimately cause changes in neuronal gene expression. In addition to the genes affected by the Ras-MAPK signalling pathway and CREB, haem deficiency may affect the expression of numerous other neuron-specific genes (Zhu *et al.,* 2002). Research by Zhu *et al* (2002) on haem-depleted PC12 cells, using succinyl acetone in the growth medium, greatly reduces NGF (nerve growth factor)-induced neurite outgrowth. The addition of exogenous haem to the succinyl acetone-treated cells largely restored neurite outgrowth, supporting the idea that the arrest of neurite outgrowth is caused by a lack of haem synthesis and suggesting that haem is critical for NGF signalling (Zhu *et al.,* 2002). NGF is a neurotrophic factor important for both the peripheral nervous system and the CNS (Gage *et al.,* 1990).

As described in section 1.2, haem is the prosthetic group in the P450 cytochromes (CYPs) (Rangarajan & Padmanaban, 1989). CYPs perform their manifold functions as functional holoenzymes saturated with haem (Correia &

Meyer, 1975; Jover *et al.,* 1996). Thus, the regulation of haem availability is of major importance for CYP function. However, regulation of haem availability for CYPs is tissue-dependent. CYP1A1 is involved in the metabolic activation of polyaromatic hydrocarbons (Hankinson *et al.,* 1991), and is expressed in most tissues. However, its function is unclear in the kidney and brain due to a much lower enzymatic activity. In the liver, partial haem deficiency leads to a less potent induction of CYP1A1 mRNA after β-NF treatment. In the brain, CYP1A1 protein is detected not only at the endoplasmic reticulum (ER), but also in the cytosol of transgenic mice with chronic impairment of haem biosynthesis – porphobilinogen deaminase-deficient (PBGD-/-) mice. Therefore, haem deficiency in the brain leads to incomplete haem saturation of CYP1A1, which causes its improper incorporation into the ER membrane and persistence in the cytosol (Meyer *et al.,* 2005).

In the liver, many drugs and chemicals affect haem synthesis, and this may also occur in the brain (De Matteis & Ray, 1982). As in the liver, ALAS1 activity in the brain declines with age, reducing the amount of haem available (Paterniti *et al.*, 1978). Furthermore, the binding of haem to amyloid-β in Alzheimer's disease may also limit its availability to cells (Atamna & Frey, 2004). Chernova *et al* (2006) have shown that inhibition of haem synthesis in neurons results in the earlier lowered expression of the neuron-specific genes *N*-methyl-D-aspartate (NMDA) receptor subunits and neurofilament light peptide (NF-L). Increased expression was then observed when haemin was exogenously added to the cells. In addition, lowered haem concentration caused by an increase in expression of ALAS1 and HO-1 is associated with the senscense of neurons. This may give an indication into how neurons functionality declines with age due to the reduction in haem (Chernova *et al.,* 2006).

1.6 Homeostasis of Haem

Ultimately, the cellular concentration of haem in non-erythroid cells is controlled by its degradation and synthesis, controlled by the haem oxygenases (HOs) and ALAS1, respectively. Therefore, HO will be briefly discussed before moving on to both ALAS1 and ALAS2.

1.6.1 Haem Oxygenase

HO plays a critical role in physiological iron homeostasis, antioxidant defence, and, as previously mentioned, in signalling pathways that employ CO as a messenger (Gilles-Gonzalez *et al.,* 2005). The HO system, oxidatively cleaves haem to produce CO, biliverdin, and free iron (figure 1-4). Three mammalian isoforms of HO have been identified: HO-1, an inducible enzyme that is most highly concentrated in tissues that are heavily involved in the catabolism of haem proteins (reviewed in Maines & Gibbs, 2005); HO-2, a non-inducible isoform that is present in highest concentrations in the brain and testes and is thought to be particularly involved in signalling pathways (Maines *et al.,* 1986); and HO-3, a homologue of HO-2 with low catalytic activity and uncertain physiological role. HO-3 has been described in the rat brain (McCoubrey *et al.,* 1997), however no homologue of this gene is found in either humans or mice and it is best characterized as a processed pseudogene (Hayashi *et al.,* 2004; Maines *et al.,* 2004).

HO-1 and HO-2 both have haem-binding pockets, a stretch of 23 amino acids, a basic sequence mostly made up of hydrophobic residues with a conserved histidine residue (McCoubrey *et al.,* 1993). Outside the haem-binding pocket, the extent of sequence identity between HO-1 and HO-2 is limited to less than 50% (Maines & Gibbs, 2005).

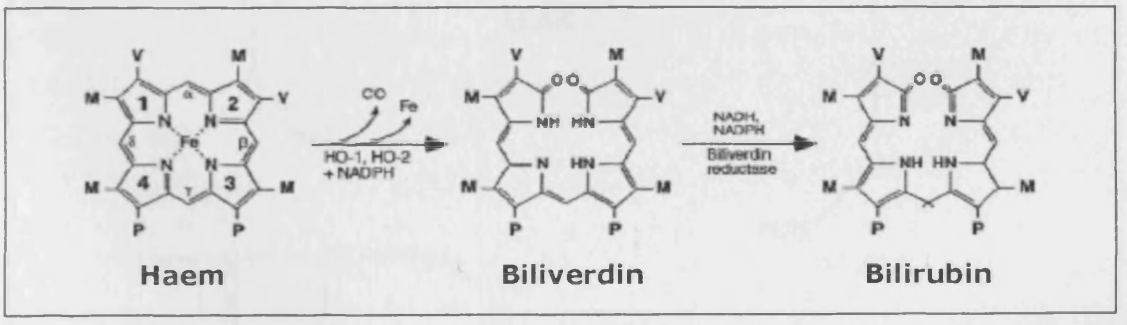

Figure 1-4 The pathway of haem degradation in mammals (reviewed in Maines & Gibbs, 2005).

M=methyl, V=vinyl, P=propionic acid.

Oxidation of haem by the HO proteins requires concerted activity of NADPH-cytP450 reductase (figure 1-4) for providing reducing equivalents for supporting

the reduced state of iron (Fe^{2+}) and activation of molecular oxygen. The specific orientation of bound haem is crucial to specificity of cleavage of the porphyrin ring at the α-meso carbon bridge. The reaction requires 3 molecules of oxygen and 7 electrons. The rate-limiting step in oxidation of haem is the release of the product, biliverdin (Maines & Gibbs, 2005).

1.6.2 Aminolaevulinate Synthase (ALAS)

The reaction catalysed by ALAS involves the condensation of glycine and succinyl-CoA to produce ALA, CoA, and carbon dioxide. This occurs in a wide variety of species including animals, fungi, some protozoa and α-purple bacteria. In contrast, ALA in plants and most other bacteria is made from glutamate by an entirely different biosynthetic pathway involving three enzymatic steps and a glutamyl-tRNA intermediate (Avissar *et al.*, 1989).

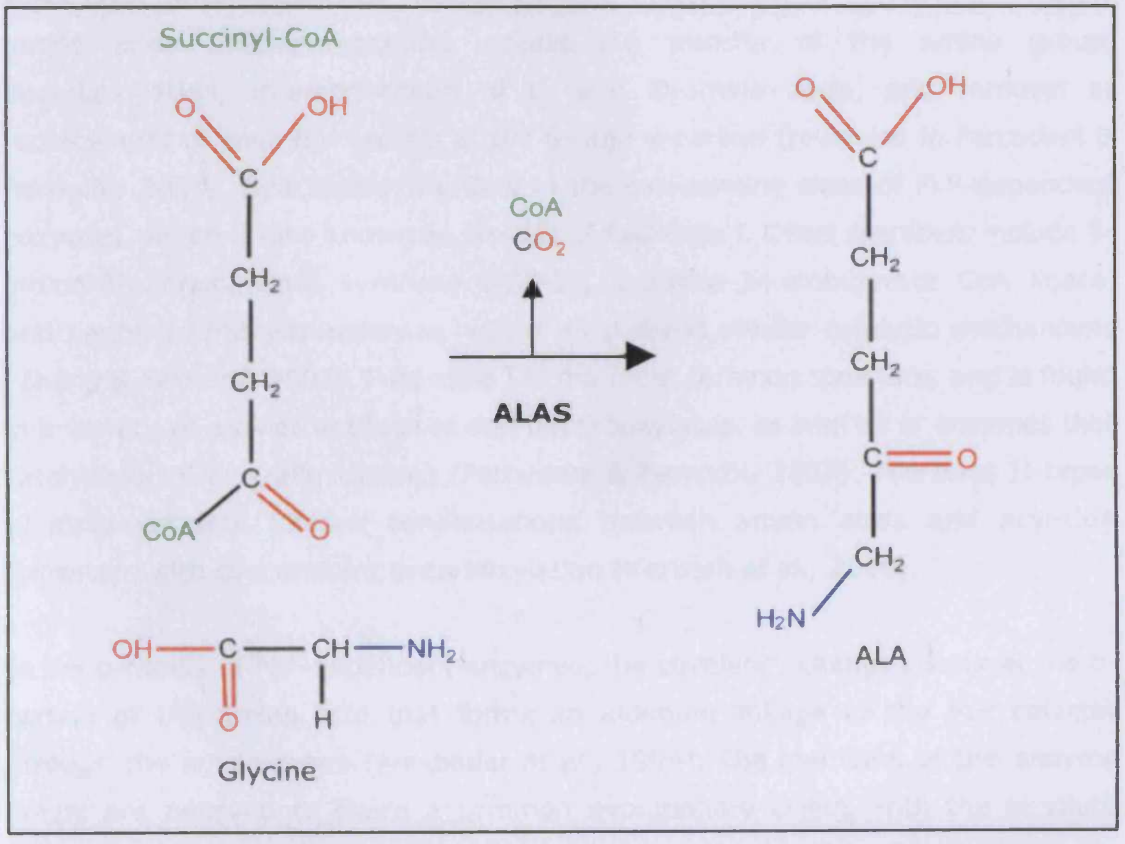

Figure 1-5 Synthesis of ALA by ALAS, adapted from Ajioka *et al.*, 2006.
Decarboxylation of glycine followed by condensation with Succinyl-CoA is catalyzed by ALAS. Pyridoxal Phosphate is required as a co-factor. The products are ALA, CO_2 and CoA.

The crystal structure of the full-length ALAS has only been described in *R. capsulatus,* and so due to the homology between ALASRC and human ALAS2, a model has been derived for the core of human ALAS2 (Astner *et al.,* 2005).

1.6.2.1 ALAS as a PLP-dependent enzyme

ALAS requires pyridoxal 5'-phosphate (PLP, a vitamin B6 derivative) as an essential cofactor, and belongs to the α-oxoamine synthase subfamily of PLP-dependent enzymes (Zhang & Ferreira, 2002). Both forms of ALAS require PLP as a cofactor and both are expressed as homodimers. PLP binds to a specific lysine of ALAS. A PLP-glycine Schiff base complex is then formed which reacts with succinyl Co-A. ALAS catalyses the decarboxylation of glycine followed by condensation of Succinyl-CoA, producing CO_2, CoA and ALA (Ponka, 1999).

Almost all PLP-dependent enzymes, except glycogen phosphorylases are associated with biochemical pathways that involve amino compounds, mainly amino acids. These reactions include the transfer of the amino group, decarboxylation, interconversion of L- and D-amino acids, and removal or replacement of chemical groups at the β- and γ-carbon (reviewed in Percudani & Peracchi, 2003). Specifically, ALAS is in the α-oxoamine class of PLP-dependent enzymes, which is also known as class II of fold-type I. Other members include 8-amino-7-oxononanoate synthase (AONS), 2-amino-3-ketobutyrate CoA ligase, and serine palmitoyltransferase, which all possess similar catalytic mechanisms (Zhang & Ferreira, 2002). Fold-type I is the most common structure, and is found in a variety of aminotransferases and decarboxylases, as well as in enzymes that catalyse α-, β-or γ-eliminations (Percudani & Peracchi, 2003). The class II types typically catalyse Claisen condensations between amino acids and acyl-CoA thioesters with concomitant decarboxylation (Kerbarh *et al.,* 2006).

In the α-family of PLP-dependent enzymes, the covalency changes occur at the α-carbon of the amino acid that forms an aldimine linkage to the PLP cofactor through the amino group (Alexander *et al.,* 1994). The members of this enzyme family are believed to share a common evolutionary origin, with the absolute conservation of an aspartate residue approximately 30-40 residues to the N-terminus of the conserved lysine that forms the Schiff base linkage with the cofactor (Gong *et al.,* 1998).

1.6.2.2 The ALAS catalytic mechanism

To distinguish between the two possibilities for the active site arrangement of ALAS dimer (inter- and intrasubunit), Tan & Ferreira (1996) developed *in vivo* complementation stages in which two inactive mouse mutants were co-expressed in *Escherichia coli* (*E.coli*). Their results support the proposal that the active site of ALAS is shared by the two subunits and that therefore it resides at the subunit interface and dimerization is necessary for the functional ALAS enzyme (Tan & Ferreira, 1996).

ALAS exists in two conformational states, an open conformation in which the substrates bind and a closed conformation induced by the binding of the second substrate, succinyl-CoA. The reaction of glycine with ALAS involves a three-kinetic step (i.*e.* formation of the Michaelis complex and external aldimine and removal of the glycine C-α proton from the external aldimine). The presence of succinyl-CoA accelerates this third step and thus the intermediate formation of two quinonoid species. ALA release is the rate-limiting step in the ALAS catalytic pathway (Zhang & Ferreira, 2002).

Firstly, a transaldimination reaction occurs between the substrate glycine and the internal aldimine, formed between the aldehyde group of PLP and an active site lysine residue. Following the transaldimination reaction and formation of the external aldimine, the *pro*-R proton of glycine is removed, yielding a transient quinonoid species in the presence of succinyl-CoA. This quinonoid intermediate reacts with succinyl-CoA to form, upon removal of the CoA group, an aldimine to α-amino-β-ketoadipate. Subsequently, cleavage of the C-α-carboxylate bond leads to a stabilized quinonoid intermediate. A proton is then returned to the C-5 position of the aldimine between PLP and ALA. Finally, the aldimine dissociates to yield ALA and the holoenzyme (Zhang & Ferreira, 2002).

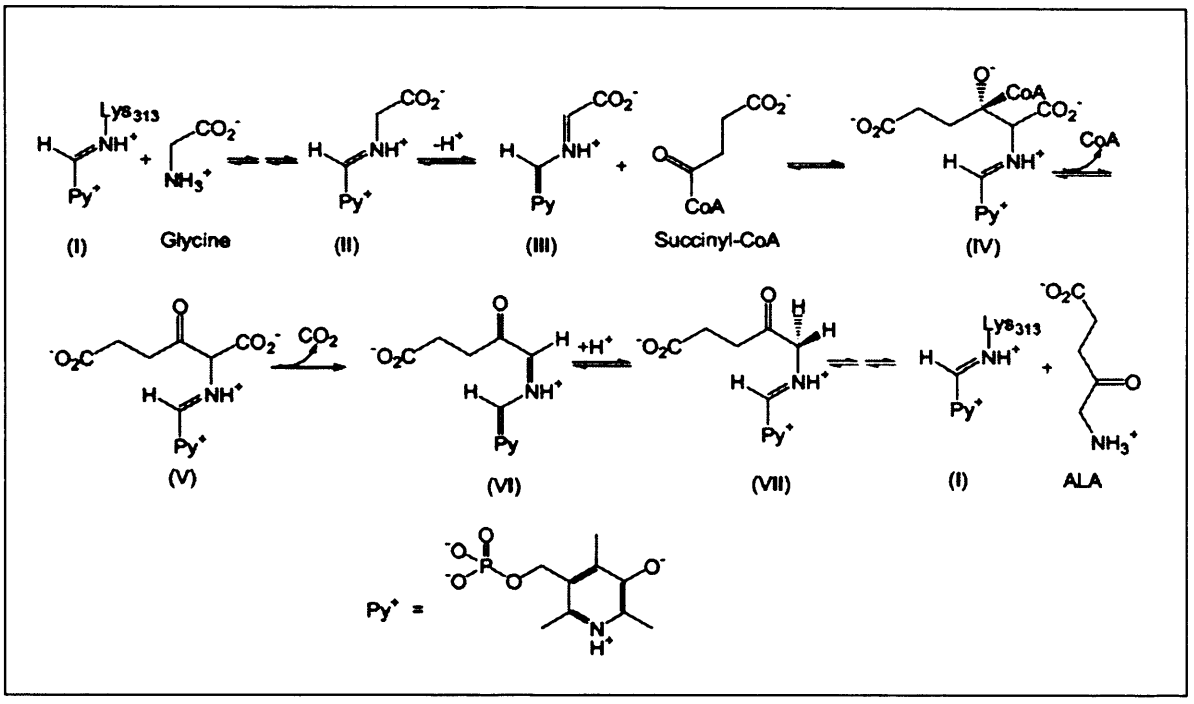

Figure 1-6 Scheme of the ALAS catalytic mechanism, taken from Zhang & Ferreira, 2002.

Radiolabeling studies using *Rhodobacter spheroides* ALAS provided information to develop a model of the ALAS catalytic reaction mechanism (Laghai & Jordan, 1977; Zhang & Ferreira, 2002).

The presence of a lysine residue in the ALAS2 active site, at position 313 appears to be essential to form the quinonoid intermediate in this reaction (Zhang & Ferreira, 2002). K313 of the murine mature ALAS2 acts as a general base to labilize both the pro-R proton of glycine and the pro-R position at C-5 of ALA. The lysine also acts as a general acid to donate a proton to the quinonoid intermediate formed from decarboxylation of the α-amino-β -ketoadipate intermediate (Hunter & Ferreira, 1999).

Also, K313 in mouse ALAS2 appears to be the residue involved in the binding of PLP cofactor, as mutagenesis of this residue to alanine and histidine abolishes the enzyme activity (Ferreira *et al.,* 1995). The arginine 149 (R149) in mouse ALAS2 had also been shown to be catalytically essential, which is highly conserved in all known ALAS enzymes (Gong & Ferreira, 1995).

The mechanism of the human ALAS enzymes have not been elucidated as yet. However, due to the high homology between species of the PLP-binding peptide, it is believed to be similar to the mechanism for murine ALAS2, as described

above. This PLP-binding peptide, consisting of the sequence surrounding the lysine involved in forming the Schiff base linkage with PLP, is present in all known ALAS sequences ranging from human to bacteria, and is present in the conserved catalytic domain (Ferreira *et al.,* 1993). The human ALAS1 lysine residue that corresponds to the essential K313 of murine ALAS2 is K393 (Bawden *et al.,* 1987). The essential lysine in human ALAS2 is K344 (Cox *et al.,* 1991; Borthwick *et al.*, 1985).

1.6.2.3 ALAS Regions

ALAS1 and ALAS2 are composed of three regions: region I is the mitochondrial targeting sequence, region II is the amino-terminal portion of the mature, proteolytically processed protein, and region III is the highly conserved catalytic region of the enzyme (Dailey *et al.,* 2005). The bacterial ALAS enzymes characterised only consist of region III, confirming the catalytically-active domain in this region (Duncan *et al.,* 1999). ALAS is a homodimer, and is translocated into the mitochondrion in a step that proteolytically removes the leader sequence (Region I), and subsequently the cofactor, PLP, is added. Region II, the N-terminal end of the mature protein, of ALAS1 is encoded by exons 2 and 3, and is not required for protein activity; therefore its function is unknown. The ALAS2 region II is encoded by exons 3 and 4 (Dailey *et al.,* 2005).

ALAS is synthesised on cytoribosomes as a precursor form and is translocated to the mitochondria, where it accumulates in the extramitochondrial space. ALAS is then processed to give the mature enzyme (Yamauchi *et al.,* 1980; Urban-Grimal *et al.,* 1986). The capacity of the mitochondria to accommodate ALAS appears to be limited to a certain level, and this also favours the accumulation of ALAS in the extra-mitochondrial fraction in later stages of induction. It accumulates in large amounts in the liver cytosol fraction in chemically-induced porphyria animals, before it is translocated (Kikuchi & Hayashi, 1981).

1.7 Comparison of the ALAS1 and ALAS2 Genes

There are two genes for ALA synthase (ALAS), one of which is expressed ubiquitously with the other specific to erythroid cells. Consequently, there are two corresponding isoforms of the enzyme, named ALAS1 and ALAS2 respectively (Ponka, 1999). In humans, ALAS1 gene is on chromosome band 3p21.1, whilst the ALAS2 gene is in a distal subregion of Xp11.21 (Bishop, 1990; Cotter *et al.,*

1992) (table 1-2). The housekeeping enzyme, ALAS1, is expressed in all tissues to provide haem for respiratory cytochromes and other haemoproteins (May *et al.,* 1995). The ALAS1 gene is expressed in both erythroid and non-erythroid cells, although its expression varies between tissues. Highest levels are found in the liver where ALAS1 transcription can be induced directly by compounds such as phenobarbital to co-ordinate an increased demand for haem with increased apo-cytochrome synthesis (Srivastava *et al.,* 1988).

The ALAS2 pre-protein shows >75% homology to the ALAS1 protein, but the extreme 108 N-terminal residues of ALAS1 is missing from ALAS2. ALAS1 gene expression is also extremely low (2% of total enzyme) in erythroid cells. Nucleotide sequences of the ALAS2 and ALAS1 genes are approximately 60% similar, with the longest stretch of identical sequence being 21 nucleotides. There is very little homology, however, in the N-terminal region, while there is a high homology (~73%) after hepatic residue 197 (Scriver *et al.,* 1995). The full sequence alignment of the ALAS1 and ALAS2 proteins is shown in appendix 1.

About two-thirds of the sequence shows 60-80% amino acid conservation in protein alignments (Duncan *et al.,* 1997). ALAS enzymes in unicellular and multicellular eukaryotes are closely related to those in the α-purple bacteria, which have been suggested to be the closest contemporary eubacterial relatives of mitochondria (Duncan *et al.,* 1997; Gray, 1992). Sequence data of the ALAS gene has been obtained for many species, ranging from bacteria to mammals, including both forms of the human ALAS genes, rat, mouse, one protostome, five fungi, a protist, and some α-proteobacteria (table 1-5). These data conclude that the gene is highly conserved. The carboxy terminal two-thirds of the unprocessed ALAS shows 40-90% amino acid conservation in protein alignments across all taxa, with bacterial ALAS being the most highly conserved (Duncan *et al.,* 1999). The two isoforms of the ALAS gene are suggested to have evolved from a common ancestral gene, by Duncan *et al* (1999). This gene duplication event created two genes that evolved to produce enzymes that perform the same function but are under separate regulatory mechanisms. This duplication event is hypothesised to have occurred between the branching of the cephalochordates and the earliest vertebrates (Duncan *et al.,* 1999). Cephalochordates are lancelets, which have been traditionally viewed as the closest living relative of vertebrates (Delsuc *et al.,* 2006).

The ALAS1 gene is highly conserved in species ranging from bacteria to mammals. The sequence encoded by the second to eleventh exons of rat ALAS1 contains essentially common sequence motifs to those of the corresponding exons of the ALAS2 gene (figure 1-7, Yomogida *et al.,* 1993). The only exception to this structural conservation observed, is that the chicken ALAS1 gene lacks a small exon coding for the 5'-UTR, i.e. an exon which would correspond to the first exon of the other ALAS genes (Yomogida *et al.,* 1993). The rat ALAS1 gene consists of 11 exons and spans more than 14kb in the rat genome, where as the chicken ALAS1 gene is 6.9kb and composed of 10 exons. The size of the exons of rat ALAS1 gene is homologous to that of the chicken ALAS1 gene. The second to eleventh exons of the rat ALAS1 gene correspond to the first to tenth exons of the chicken ALAS1 gene. The structure of the rat ALAS1 gene is also similar to that of the mouse ALAS2 gene which consists of 11 exons. In particular, the boundaries of the fifth to eleventh exons are highly conserved between the rat ALAS1 gene and the mouse ALAS2 gene, signifying that ALAS1 and ALAS2 genes evolved from a common ancestral gene (Yomogida *et al.,* 1993).

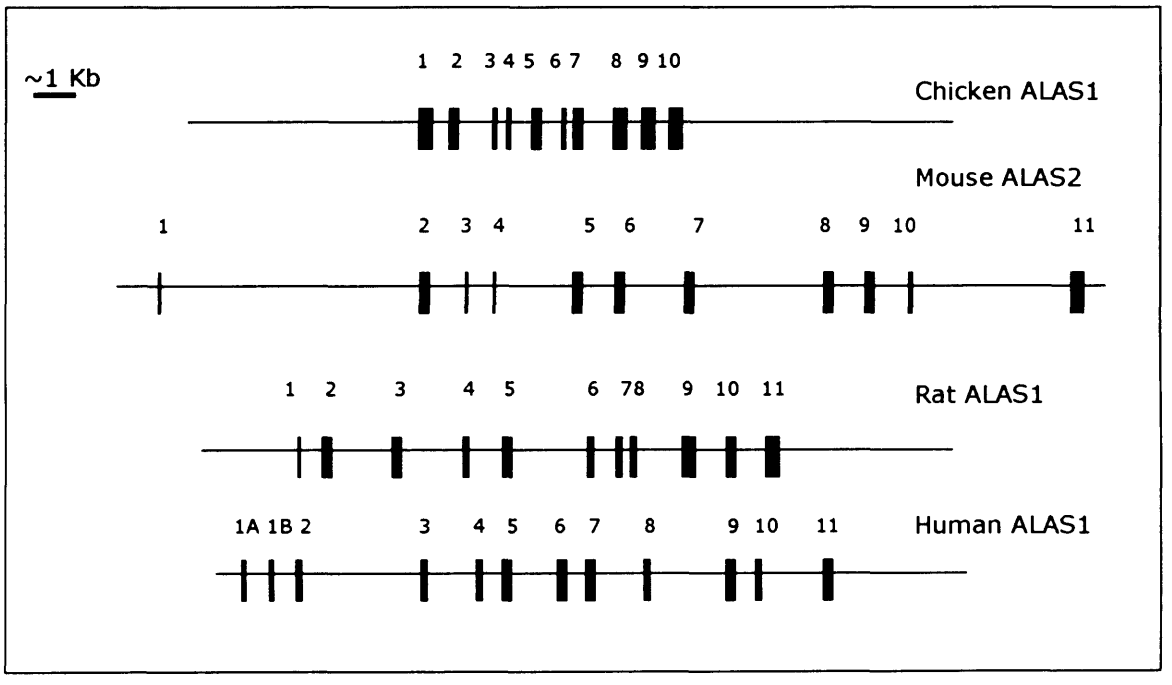

Figure 1-7 Organisation of ALAS1 and ALAS2 genes is highly conserved in animals, figure modified from Yomogida *et al.,* 1993.

The organization of the chicken ALAS1 gene (Maguire *et al.,* 1986), mouse ALAS2 gene (Schoenhaut *et al.,* 1989), and rat and human ALAS1 gene is highly conserved (Yomogida *et al.,* 1993). ALAS1 genes are more compact than the mouse ALAS2 gene. All the genes, except that encoding chicken ALAS1, are composed of 11 exons.

In both chicken and rat, ALAS activity and mRNA is induced in the liver for the synthesis of drug-metabolising CYPs. It can also be induced, to a lesser extent, in the kidney but not in rat heart, brain, skeletal muscle, testis or spleen (May *et al.,* 1995; Maguire *et al.,* 1986; Srivastava *et al.,* 1988). Analysis of the promoter sequences and mRNA transcripts of these genes has identified a single transcription start site about 25 nucleotides (nt) downstream from a TATA box that was used exclusively for basal transcription in all tissues and for induced transcription in the liver (Yomigida *et al.,* 1993, Maguire *et al.,* 1986; Srivastava *et al.,* 1988).

	Species	**Common Name**
Deuterostomes (both ALAS forms)	*Homo sapiens*	Human
	Rattus norvegicus	Rat
	Mus musculus	Mouse
	Gallus gallus	Chicken
	Opsanus tau	Toadfish
	Delphinapterus leucas	Beluga whale
Deuterostomes (single form)	*Myxine glutinosa*	Hagfish
	Strongylocentrotus	Sea urchin
Protostomes	*Drosophila melanogaster*	Fruit fly
	Glycera dibranchiata	Blood worm
	Limulus polyphemus	Horseshoe crab
	Sepia officinalis	Cuttlefish
Fungi	*Agaricus bisporus*	Mushroom
	Schizosaccaromyces pombe	
	Emericells nidulans	
	Saccharomyces cerevisiae	Yeast
	Kluyveromyces lactis	
Protists	*Plasmodium falciparum*	
α-protobacteria	*Rhodobacter sphaeroides* (2 forms, named A and T)	
	Bradyrhizobium japonicum	
	Agrobacterium radiobacter	
	Rhodobacter capsulatus	
	Paracoccus denitrificans	

Table 1-5 ALAS sequences currently available, adapted from Duncan *et al.,* 1999.

1.7.1 The Human ALAS1 Gene

The organisation of the human ALAS1 gene is similar to the orthologous rat, mouse and chicken genes, except that it contains two non-coding regions (1A and

1B) in its 5'-UTR, whereas the rat gene only has one, and the chicken has none (Yomogida *et al.*, 1993; Maguire *et al.*, 1986). The full sequence alignment between species of the ALAS1 gene is shown in appendix 2. All mammalian ALAS1 genes are composed of 11 exons and are homologous to each other.

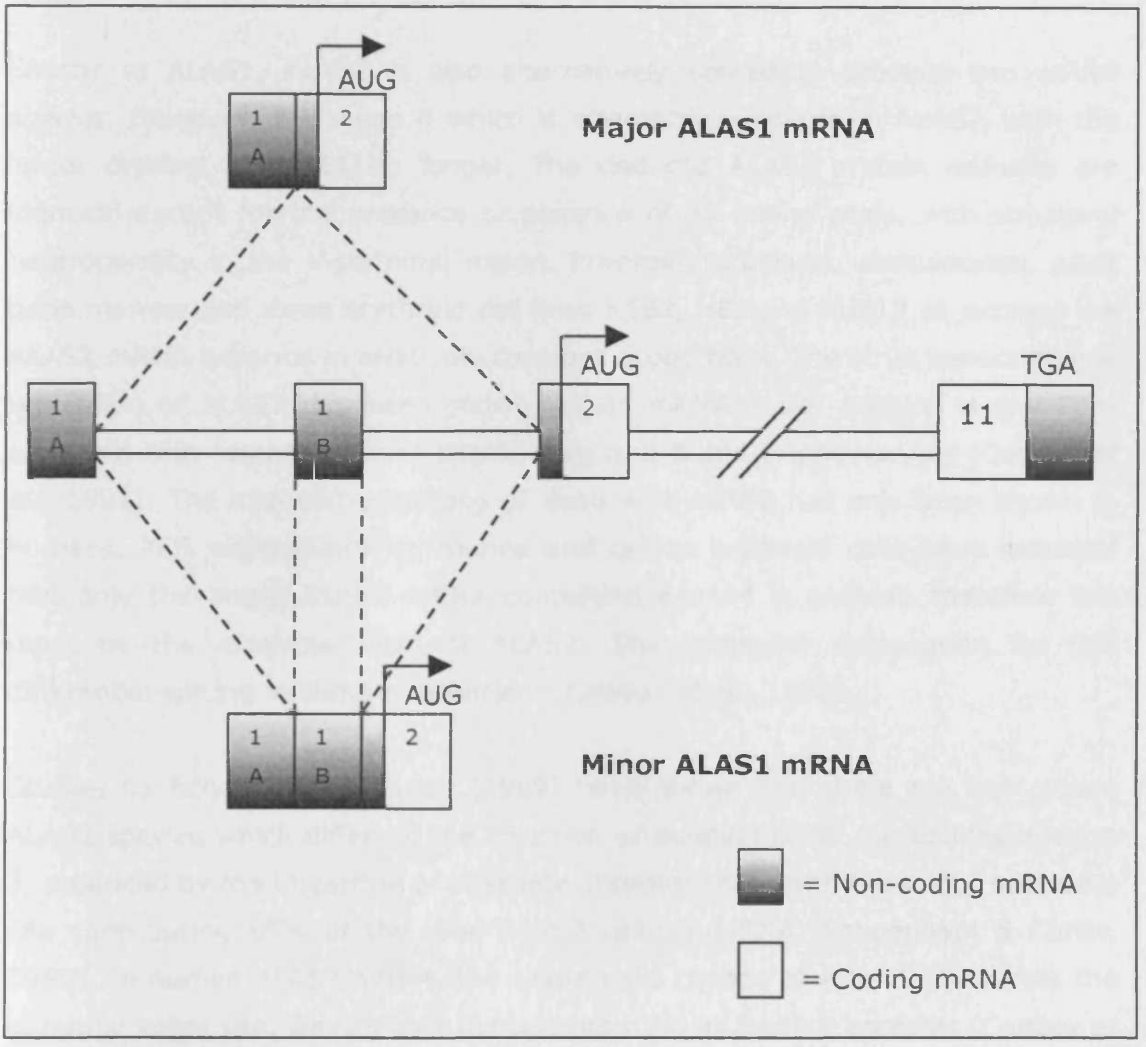

Figure 1.8 Alternative splicing of the human ALAS1 mRNA.
Alternative splicing of human ALAS1 exon 1B produces two isoforms, a major transcript comprising 90% total cellular ALAS1 mRNA and a minor transcript comprising of only 10% total cellular ALAS1 mRNA (Roberts & Elder, 2001).

Exon 1B of the human gene is alternatively spliced resulting in two mRNA species: a major one in which it is omitted and a minor one containing both exons 1A and 1B. This longer transcript is present in all human tissues and cell lines examined and therefore this alternative splicing does not appear to be specific to

particular cell types. Both ALAS1 transcripts have been detected in mRNA from human brain and liver and from K562, HeLa, HepG2 and B-lymphoblastoid cell lines with the percentage of minor transcript ranging from 7-15% of the total steady state concentration of ALAS1 mRNA (Roberts & Elder, 2001).

1.7.2 The Human ALAS2 Gene

Similar to ALAS1, ALAS2 is also alternatively spliced to produce two mRNA species. However, it is exon 4 which is alternatively spliced in ALAS2, with the larger product being 111bp longer. The deduced ALAS2 protein isoforms are identical except for the presence or absence of 37 amino acids, with structural heterogeneity in the N-terminal region. Preproerythroblasts, reticulocytes, adult bone marrow and three erythroid cell lines K562, HEL and KU812 all express the ALAS2 mRNA isoforms in relatively constant proportions. The strict transcriptional regulation of ALAS2 has been shown, as its mRNA is not present in any non-erythroid cells tested, such as HepG2 cells and B and T lymphocytes (Conboy *et al.,* 1992). The alternative splicing of exon 4 in ALAS2 has only been shown in humans. PCR experiments on murine and canine erythroid cells have indicated that only the larger ALAS2 mRNA containing exon 4 is present, therefore this must be the essential form of ALAS2. The molecular explanation for this differential spicing in humans is unclear (Conboy *et al.,* 1992).

Studies by Schoenhaut & Curtis (1989) have shown that there are two mouse ALAS2 species which differ by the insertion or deletion of 45 nucleotides in exon 3, produced by the utilization of alternate acceptor sites, with the major upstream site contributing 85% of the total ALAS2 cellular mRNA (Schoenhaut & Curtis, 1989). In human ALAS2 mRNA, the single base change of A to G inactivates the potential splice site, leaving only the upstream AG as a splice acceptor (Conboy *et al.,* 1992). Both exons 3 and 4 are in region II of the ALAS2 enzyme. As these show species-specific splicing, there must be a specific role for these exons in the regulation, rather than enzymatic activity, of ALAS2.

In 2004, it was demonstrated that another three additional splice isoforms of ALAS2 exist in human erythroid cells. The principal alternatively spliced mRNA is that which lacks exon 4 encoded sequence, constituting around 35-45% of total ALAS2 mRNA in erythroid cells. However, the additional three human mRNA splice forms reported together account for approximately 15% of the total human ALAS2 mRNA in reticulocytes. One of these is characterized by the addition of

exon 1b. The other two mRNAs do not contain exon 2, which contains the normal translation initiation codon. However, it seems unlikely that these two ALAS2 mRNAs which lack exon 2 play a major role in ALAS2 activity in erythroid cells, as they do not contain the sequence necessary for direct translocation to the mitochondria (Cox *et al.,* 2004).

1.8 Transcriptional Control of ALAS

1.8.1 Regulation of ALAS2

The activity of ALAS2 in erythroid cells is controlled mostly be the availability of iron in the cell, which regulates the interaction between iron-binding proteins and an iron responsive element in the 5'-UTR of ALAS2 mRNA to control its translation (Ponka, 1997; Hentze & Kuhn, 1996). Iron-responsive elements (IREs) are identified by the presence of a stem-loop structure in which the loop contains the sequence CAGUGH (H=A/C/U not G) in the 5-untranslated region of an ALAS nucleotide sequence. They are present only in the ALAS2 gene forms and not the ALAS1 gene (Dandekar *et al.,* 1991; Thiel, 1994; Melefors et al., 1993).

Iron regulatory proteins (IRPs) are the regulators of iron metabolism, as this essential element used as a redox centre for proteins has to be tightly regulated in cells due to its toxicity to cells when it reacts with molecular oxygen. These IRPs regulate iron by controlling protein expression of those involved in iron metabolism by binding to the IREs of the mRNA under iron-depleted conditions. To date, two IRPs have been identified, IRP1 and IRP2, which differ in their regulatory mechanism (Ishikawa *et al.,* 2005; Hentze *et al.,* 2004).

1.8.2 Regulation of ALAS1

The liver ALAS1 gene is under multi-component control at the transcriptional level. Its transcription is stimulated by cAMP and respiratory uncoupling, and repressed by phorbal esters and insulin. This pattern of regulation is accomplished by CREB, nuclear respiratory factor-1, and AP-1 transactivation through the *cis*-acting elements CRE, nuclear respiratory factor-1 binding site, and 12-*O*-tetradecanoylphorbol-13-acetate-responsive element, respectively, found in the 5'—regulatory region of ALAS gene (Scassa *et al.,* 2004).

The promoter of the ALAS1 gene contains a TATA box and 2 control elements located immediately upstream of the TATA box that are homologous to the binding site for the transcription factor nuclear respiratory factor–1 (NRF-1), which seems to be involved in the expression of some proteins involved in oxidative phosphorylation (Ponka, 1999).

1.8.2.1 Insulin

Insulin regulates many metabolic responses in a variety of mammalian tissues, principally liver, muscles, and adipose (Scassa *et al.,* 1998). No unique consensus insulin-responsive sequence or element (Ins RE) has been reported. However, an Ins RE with a T(G/A)TTT(T/G)(G/T) core sequence has been associated with insulin-induced transcriptional repression of a number of metabolic genes, including those that encode phosphoenolpyruvate carboxykinase (PEPCK), insulin-like growth factor-binding protein 1, tyrosine aminotransferase (Scassa *et al.,* 2004). Insulin has been reported to inhibit the activity of ALAS1 in rat and chicken hepatocytes cultures. It has been demonstrated that ALAS1 gene expression is stimulated by cAMP and inhibited by phorbal esters. The inhibitory effect of phorbal esters and diacylglycerol is mediated by the activation of protein kinase C (PKC). Scassa *et al* (1998) have provided evidence that insulin negatively regulates transcription of ALAS gene. The 870bp promoter region of ALAS1 sustains the inhibitory effect of insulin in HepG2 cells, and the signal transduction pathway involved is mediated by PKC activation. Treatment of rat hepatic cells with 5nM insulin decreases the amount of ALAS mRNA by five-fold in basal hepatocytes, and by nine-fold in cells exposed to phenobarbital, a known inducer of ALAS1 gene expression. However, it was found that the alterations in the ALAS1 mRNA levels following insulin and/or phenobarbital treatments were not due to changes in its stability and this insulin effect does not require protein synthesis (Scassa *et al.,* 1998).

1.8.2.2 Proliferator-activated receptor γ coativator 1α

Proliferator-activated receptor γ co-activator 1α (PGC-1α) is a co-activator of nuclear receptors and other transcription factors. PGC-1α controls mitochondrial biogenesis and oxidative metabolism in many tissues, including brown adipose tissue, skeletal muscle, heart, and liver. In the liver PGC-1α is induced during fasting, when the liver ceases using glucose as an energy supply and changes to the β-oxidation of fatty acids. This increase in fatty acid β-oxidation and elevation

of hepatic gluconeogenesis are both under control of PGC-1α. Therefore PGC-1α has a key role in liver energy homeostasis and many PGC-1α targets are haem proteins. PGC-1α is an important factor controlling the expression of ALAS1 in the fasted and fed liver. Hepatic PGC-1α is a major determinant of the severity of acute porphyric attacks in mouse models of chemical porphyria (Handschin *et al.*, 2005).

Fasting can be a powerful stimulus to induce an acute porphyric attack and the liver is central to the fasting response in mammals. Experiments where Fao rat hepatoma cells, mouse primary hepatocytes, and rat liver cells were infected with adenovirus expressing PGC-1α, ectopic expression of PGC-1α increased ALAS1 transcript levels in a manner similar to that of glucose-6-phosphatase (Glc6P), a PGC-1α target gene involved in gluconeogenesis. In contrast to ALAS1, none of the other seven genes of the haem biosynthetic pathway were induced by PGC-1α in the liver (Handschin *et al.*, 2005).

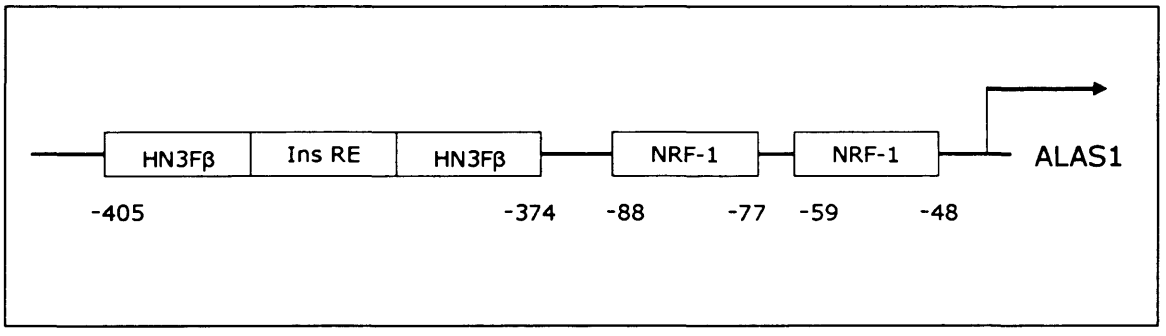

Figure 1-9 Structure of the ALAS1 promoter, adapted from Handschin *et al.*, 2005.

PGC-1α activates the ALAS1 promoter by coactivating NRF-1 and FOXO1, both of which directly bind to the ALAS1 promoter. Insulin has been shown to activate the protein kinase Akt in the liver, and Akt in turn phosphorylates FOXO1 (Brunet *et al.*, 1999; Nakae *et al.*, 2001). Phosphorylation of FOXO1 results in disruption of its binding to PGC-1α and its export from the nucleus (Puigserver *et al.*, 2003), thus inhibiting PGC-1α action.
HN3Fβ = hepatocyte nuclear factor 3β; Ins RE = Insulin responsive element; NRF-1 = nuclear respiratory factor 1.

Regulation of ALAS1 by fasting and feeding is mediated by the counter-regulatory hormones insulin and glucagons, which involves PGC-1α. The induction of PGC-1α has been shown to be a consequence of glucagons action and the transcription factor cAMP element binding protein (CREB), which binds directly to the PGC-1α

promoter (Herzig *et al.,* 2001). In addition, CREB can also directly activate the ALAS1 promoter (Varone *et al.,* 1999).

PGC-1α activates the ALAS1 promoter by coactivating NRF-1 and FOXO1, both of which directly bind to the ALAS1 promoter. It has been established that ALAS1 transcription is inhibited by the insulin pathway, involving Akt. Insulin activates the protein kinase Akt in the liver, and Akt in turn phosphorylates FOXO1. This results in disruption of its binding to PGC-1α and its export from the nucleus (Puigserver *et al.,* 2003), thus inhibiting PGC-1α action (Handschin *et al.,* 2005).

The ability of PGC-1α to positively regulate the ALAS1 gene and the requirement for PGC-1α in the fasting induction of ALAS-1 together provide a direct explanation for how fasting provokes an acute attack in an individual with hepatic porphyria (Handschin *et al.,* 2005).

1.8.2.3 Nuclear respiratory factor-1

There are two binding sites for the nuclear respiratory factor-1 (NRF-1) in the ALAS1 promoter (Braidotti *et al.,* 1993). NRF-1 is a transcription factor that increases expression of nuclear-encoded mitochondrial genes and is known to be activated by PGC-1 (Scassa *et al.,* 2001). NRF-1 appears to have a coordinating role during mitochondrial biogenesis, and functional binding sites for this factor have been identified in the rat and *D. melanogaster* genes (Li *et al.,* 1999; Braidotti *et al.,* 1993; Ruiz de Mena *et al.,* 1999) Braidotti *et al* (1993) established that the NRF- 1 motifs in the rat ALAS1 promoter are critical for promoter activity. They used site-directed mutagenesis of the NRF-1 sites, and fused the 5′ region of the ALAS1 gene to the chloramphenicol acetyltransferase (CAT) gene and measured relative expression levels. Mutagenesis of each NRF-1 motif gave substantially lowered levels of CAT expression, and mutagenesis of both NRF-1 motifs resulted in an almost complete loss of expression. Gene activation of the exon 1 in the rat ALAS1 is dependent on the presence of at least one functional NRF-1 binding site. It has been suggested that NRF-1 may co-ordinate the supply of mitochondrial haem with the synthesis of respiratory cytochromes by regulating ALAS1 expression. Further evidence to support this hypothesis is that ALAS2 lacks any NRF-1 binding sites in its promoter (Braidotti *et al.,* 1993). Increased energy consumption increases expression of the NRF-1 gene, which therefore increases ALAS1 expression by interacting with the NRF-1 binding site (Li *et al.,* 1999).

1.8.2.4 Xenobiotic-sensing Nuclear Receptor

The rate of haem biosynthesis responds to increased demands. For example, for the synthesis of drug-metabolising CYPs, the level of ALAS1 mRNA is quickly up-regulated to provide sufficient haem to the nascent apocytochromes. This increase is not a consequence of haem feedback regulation, but a direct activation of ALAS1 transcription by the drug (Jover *et al.,* 1996; Srivastava *et al.*, 1989). The induction of CYPs by drugs involves parallel increases in the transcription of *ALAS1* and *CYP* genes, with subsequent de-repression of haem-mediated inhibition of synthesis of ALAS1 (Jover *et al.,* 1996; Louis *et al.,* 1998).

Fraser *et al* (2002) have characterised two drug-responsive elements isolated from the 5'-flanking region of the chicken ALAS1 gene in the hepatoma cell line LMH, of 176 and 167 base pairs in length. These regions respond to a wide range of drugs and are referred to as ALAS drug-responsive enhancer sequence (ADRES) elements (Fraser *et al.,* 2002). These enhancer sequences respond to a wide variety of inducer compounds, and closely reflect the induction of ALAS1 mRNA.

Two distal 5' regulatory elements in the human ALAS1 gene that mediate the drug response were identified by Podvinec *et al* (2004). The nuclear receptors (NR): human CAR (constitutive androstane receptor) and PXR (pregnane X receptor) can bind to DR4-type hexamer repeats found in both the ALAS1 regulatory elements and mediate direct transcriptional activation of ALAS1 mRNA in response to drugs. The two elements exhibit a high similarity in their responses to drugs even though there is not extensive similarity at the sequence level (Podvinec *et al.,* 2004).

1.8.4 Circadian Rhythms

Circadian rhythms are an evolutionary conserved property of many biological processes in diverse life forms (Dunlap *et al.*, 1999). In mammals, a master circadian clock resides in the suprachiasmatic nuclei (SCN) of the hypothalamus. In the absence of environmental clues such as light, this clock continues to operate with remarkable precision, stability and persistence with a cycle time that is approximately 24 hours. This internal clock can also be reset to external time cues (Zheng *et al.*, 2001). The first clock mutants were identified in *Drosophilia*, and orthologs of most of these circadian clock genes have been found in

mammals, highlighting a general conservation in the clock mechanism between insects and mammals. In particular, three mammalian *Period* genes (*mPer1*, *mPer2* and *mPer3*), two *Crytochrome* genes (*mCry*1 and *mCry*2), and the genes *Clock*, *Bmal1* and *CK1ε* have been identified (Zheng *et al.*, 2001).

The mRNA transcripts and protein products for the mPer genes are expressed in a circadian manner in the SCN and in peripheral tissues. *In vitro* studies have shown that expression of *mPer*s is driven by the CLOCK/BMAL1 transcription complex, and it was hypothesised that *mPer*s, together with *mCry*s, serve to regulate the CLOCK/BMAL1 transcription complex negatively (Dunlap *et al.*, 1999).

One of the numerous physiological processes that the circadian clock controls in mammals is haem biosynthesis, through the regulation of ALAS1. Several members of the core clock mechanisms are PAS domain proteins, one of which, neuronal PAS2 (NPAS2) has a haem-binding motif (Koudo *et al.*, 2005). Also, haem controls activity of the BMAL1-NPAS2 transcription complex *in vitro* by inhibiting DNA binding in response to CO (Gilles-Gonzalez *et al.*, 2004 & 2005).

To investigate the role of haem in the circadian clock mechanism, Kaasik & Lee (2004) injected mice intraperitoneally (i.p.) with haem or solvent during subjective day and night to determine the effect of haem on clock gene expression *in vivo*. They found that haem but not solvent reduced the expression of mPer2, but enhanced that of mPer1. These effects were most prominent during subjective night. Haem differentially modulates expression of the mammalian genes mPer1 and mPer2 in vivo by a mechanism involving NPAS2 and mPer2 (Kaasik & Lee, 2004).

Loss of both mPER1 and mPER2 function leads to deregulated Alas1 expression1. The BMAL1-NPAS2 transcription complex is a direct and the principal transcriptional regulator of the ALAS1 promoter *in vivo*. Kaasik & Lee (2004) used the ALAS1 gene cloned into a luciferase reporter vector and compared expression levels after incubation with BMAL1-NPAS2, with and without mPer2 and these proteins individually. A 3.5-fold stimulation of promoter activity was observed when NPAS2, BMAL1 and mPER2 were added together. Conversely, mPER2, BMAL1 or NPAS2 added individually did not stimulate Alas1-Luciferase activity (Kaasik & Lee, 2004).

These findings demonstrate a reciprocal regulation between circadian clock regulation of haem biosynthesis and the haem control of circadian clock-complex-regulated transcription. The expression of ALAS1 is dependent on BMAL1-NPAS2 transcription activity under positive control by mPer2. Furthermore, this demonstrates the only way in which haem *indirectly* controls transcription of the ALAS1 gene, and thereby controlling its own synthesis.

1.9 Post-transcriptional Regulation of ALAS1 Expression by Haem

The molecular mechanism by which haem regulates ALAS1 mRNA levels remains poorly characterized and, in particular, the down-regulation of ALAS1 transcription by haem has remained controversial (Srivastava *et al.*, 1988 & 1990; Hamilton *et al.*, 1991). It was thought that in mammals, but not in birds (Hamilton *et al.*, 1991), haem may decrease transcription (May *et al.*, 1995; Srivastava *et al.*, 1998) although the mechanism of this effect is unknown. However, in 2005, Kolluri *et al* showed that haem actually represses transcription of the ALAS1 gene in the chicken hepatoma cell line LMH (leghorn male hepatoma). Furthermore, they identified separate haem and drug-responsive regions in the chicken ALAS1 promoter (Kolluri et al., 2005). Direct interaction of haem with an ALAS1 promoter has only been demonstrated in *D. melanogaster* (Ruiz de Mena *et al.*, 2004).

In the liver, haem represses the expression of ALAS1 through multiple feedback mechanisms at the post-transcriptional levels. In contrast, the level of ALAS2 activity in erythroid cells is not directly related to the intracellular haem concentration. Two mechanisms have been proposed by which haem may regulate the expression of ALAS1:

1. Prevention of the transfer of the newly synthesised enzyme from cytosol to mitochondria
2. End product inhibition of newly synthesised ALAS activity.

Ryan & Ades (1991) have shown that an increase in ALAS1 mRNA due to the addition of translational inhibitors, cycloheximide or ricin, is attributed to the inhibition of protein synthesis. The cycloheximide significantly decreases the rate of degradation of the ALAS1 mRNA. Therefore it has been suggested that a labile protein is involved in the haem-stimulated degradation of ALAS1 mRNA (Hamilton *et al.*, 1991).

1.9.1 Regulatory Haem Pool

Work on adult rat hepatocytes in primary culture provided direct evidence that a free pool of newly synthesised cytosolic haem appears to be central to formation of haem proteins in the liver and is the source of early labelled pigment (figure 1-10). Newly synthesised haem exists transiently in a cytosolic compartment before its transfer to membrane-bound or cytosolic acceptors or its degradation to bilirubin (Grandchamp *et al.*, 1981). Under normal conditions, this regulatory intracellular free haem pool has been estimated to be at concentration of 10-100nM, by examining indirect evidence (Badawy, 1978).

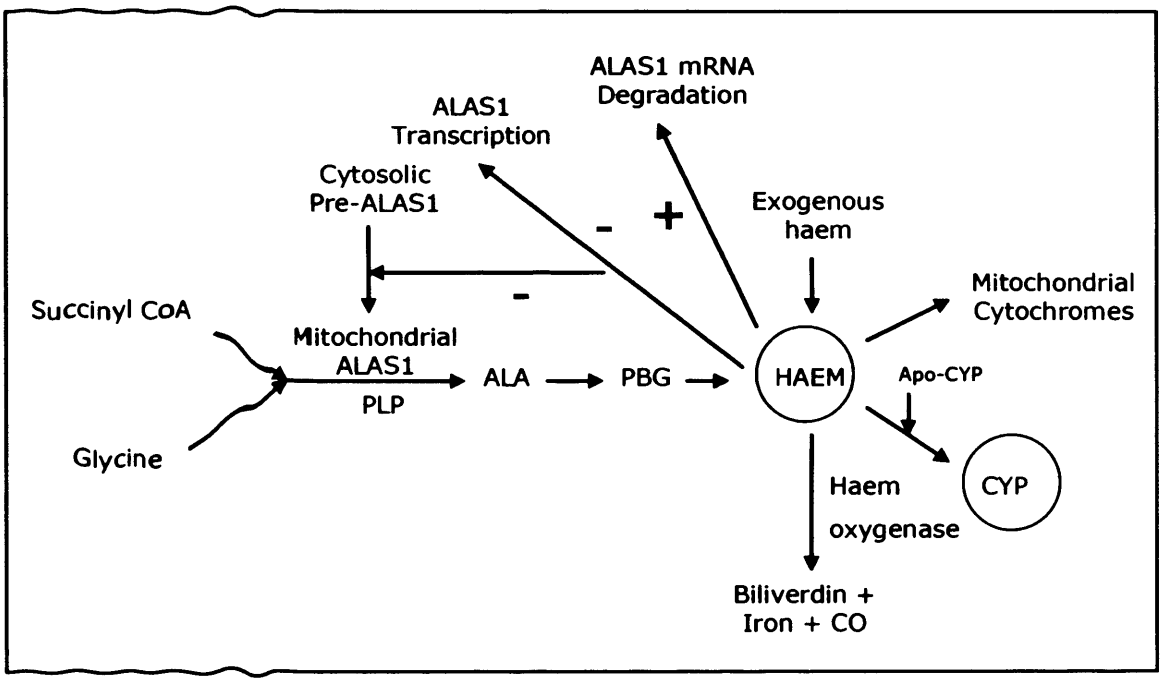

Figure 1-10 Effects of the regulatory haem pool on hepatic haem metabolism, adapted from Kolluri *et al.*, 2005.

Haem exerts regulatory effects on both ALAS1 and HO1 to control both its synthesis and degradation. ALAS1 catalyses the formation of ALA, from glycine and succinyl CoA. Haem is synthesized from ALA through a series of intermediary steps catalysed by the enzymes of the haem biosynthetic pathway. Several steps in the production of functional mature ALAS1 protein are down-regulated by exogenous or endogenous haem, as indicated by the minus signs, or by the plus sign indicating increased degradation of ALAS1 mRNA (Kolluri *et al.*, 2005).

This level of haem is maintained by regulating the amount of haem synthesised within the cell thereby balancing the synthesis and degradation of haem within the cell. Cable *et al* (2000) found that when haem levels within the cell increase; the regulatory haem pool maintains cellular haem levels by first repressing ALAS1, in CWSV17 cells. When the haem levels in this regulatory haem pool are dramatically increased, HO is induced. Therefore there are two mechanisms of reducing the haem concentration, where the more sensitive of the two regulates ALAS1 levels (Cable *et al.,* 2000).

1.9.2 Haem Response Motifs

Haem regulates ALAS1 post-transcriptionally by inhibiting the translocation of newly synthesised ALAS1 enzyme from the cytosol to the mitochondrion, with the use of haem response motifs (HRM)s (Srivastava *et al.*, 1983). Murine ALAS is synthesised as an approximately 70kD cytosolic precursor (Pre-ALAS) that is post-translationally transported into the mitochondrial matrix, where it is proteolytically processed to form a 65kD mature enzyme. High haemin concentrations can inhibit the transport of pre-ALAS1 into mitochondria both *in vitro* and *in vivo* (Lathrop & Timko, 1995).

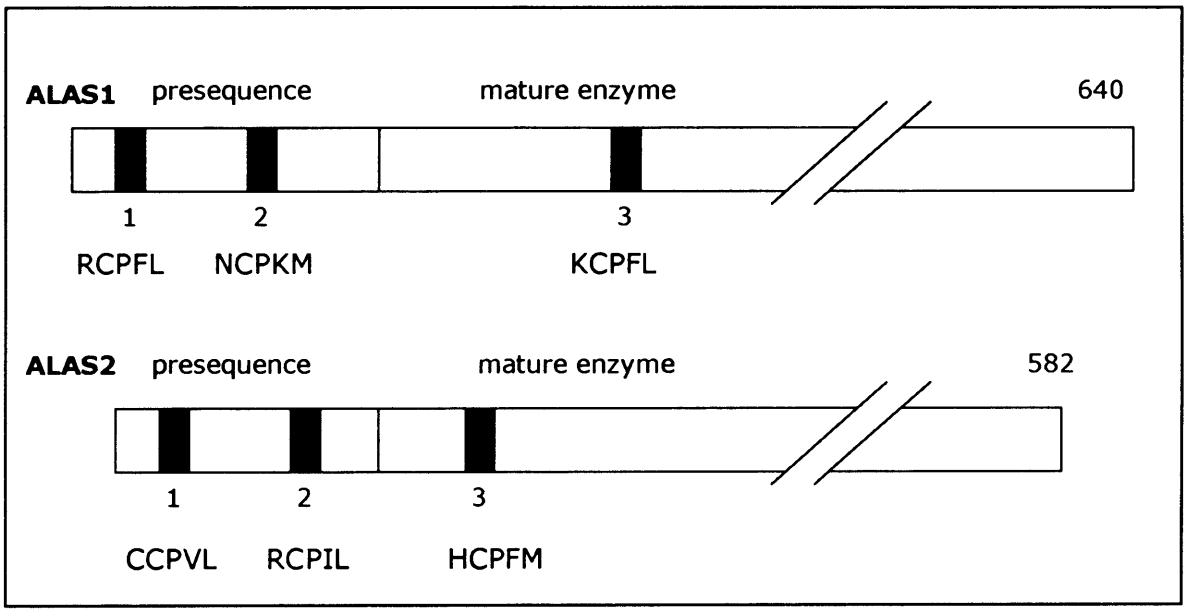

Figure 1-11 – HRM's in human ALAS1 and ALAS2, with the amino acid sequence of each. Diagram adapted from Munakata *et al.,* 2004 and Duncan *et al.,* 1999. Numbers indicate the number of amino acids in each full protein (presequence + mature enzyme).

Both ALAS1 and ALAS2 contain three HRMs, which all contain invariant cysteine and proline residues. Other proteins that contain HRM sequences include haem lyase (which attaches haem to cytochromes), HO-2 and catalase (which degrades hydrogen peroxide). The first two enzymes bind haem as a substrate, and the third uses haem as a cofactor (Zhang & Guarente, 1995).

Generally, the HRM's have been identified in the ALAS sequences in all the species listed in table 1-5, by the amino acid motif R/K/N-C-P-K/hydrophobic residue-L/M, although some minor alterations can be made to this motif (Lathrop & Timko, 1993; Duncan *et al.,* 1999). As HRMs are present in almost all eukaryotic ALAS species, a functional role in the regulation of ALAS has been suggested. The motif is normally present three times near the N-terminus of the ALAS coding sequence, although the known fungal ALAS sequences and the ones for fruit fly and *P.falciparium* appear to be different from this pattern (Duncan *et al.,* 1999).

The HRM motif consists of five amino acids, among which the second cysteine and third proline are completely conserved. Therefore HRM2 differs from the others by its first, fourth and fifth amino acids. The first is neutral in HRM2, but basic in the HRMs 1 and 3. The fourth and fifth amino acids are phenylalanine and leucine in HRM1 and 3, but lysine and methionine in HRM2 (Munakata *et al.,* 2004). Further experiments are required to assess whether this sequence difference in amino acids reflects the HRM activity. Spectral and chromatographic studies by Zhang & Guarente (1995) have shown that peptides containing a HRM bind to haem and change its physical and chemical properties. The cysteine of the HRM serves the critical function of donating electrons to the haem iron. The basic residues which are usually found at the first position and the hydrophobic residues found in the fourth position may enhance binding by interacting with the carboxyl and vinyl side chains of haem, respectively. The proline in the HRM may serve a structural role by exposing the cysteine residue for bonding to the haem iron (Zhang & Guarente, 1995).

Two of these HRM's are in region I and one is in region III. All three of these HRM's in ALAS1 can function *in situ* as haem-responsive regulators of intracellular localisation. In the case of the mammalian ALAS1, haem probably binds to the HRMs in the leader when the protein is still in the cytoplasm, thus preventing unfolding and translocation across the mitochondrial membrane (Lathrop & Timko, 1993; Zhang & Guarente, 1995).

To study the ALAS2 HRM's *in vitro*, Lathrop & Timko (1993) used chimeric proteins transfected into mouse erythroid cells. These proteins consisted of the presequence and a portion of the mature peptide (encompassing the region containing the 15 amino acid deletion in the pre-ALAS2 minor form) linked to the mature ornithine transcarbamoylase precursor (OTC), a normally upregulated mitochondrial protein. Transport of preALAS2 major-OTC (which contains three copies of the HRM) and preALAS2 minor-OTC (which contains two HRMs) was inhibited 89% and 87%, respectively, by 25 μM haemin, an inhibition similar to that observed for the native preALAS2 proteins. The conserved cysteine within the HRM was shown by site-directed mutagenesis to be required for haemin inhibition (Lathrop & Timko, 1993).

Cysteines in the HRM's are essential for their activity, as haem has been shown to bind in a stoichiometric manner to cysteines in synthetic peptides containing an HRM sequence (Zhang & Guarente, 1995). More recently, Munakata *et al* (2004) have found that HRM1 is involved in the haem-mediated inhibition of the mitochondrial import of rat ALAS1, whereas HRM2 is not. Also, HRM3 contributes to the haem-mediated inhibition of ALAS1 transport, ands seems to function together with HRM1. *In vivo* haem does not affect the mitochondrial import of ALAS2 (which is not affected by a wide range of haem concentrations). However, the import of ALAS2 is inhibited by haem using *in vitro* systems (Munakata *et al.,* 2004; Lathrop & Timko, 1993). This suggests that ALAS2 and ALAS1 are controlled by different haem regulation mechanisms *in vivo*, and that the HRMs in the two isoforms of ALAS do not perform the same function (Munakata *et al.,* 2004).

There have been controversial results of the affect of haem on the mitochondrial import of rat ALAS2. Munakata *et al* (2004) found that a wide range of haem concentrations do not affect the import of ALAS2 *in vivo*. In contrast, Lathrop & Timko (1993) showed that the mitochondrial import of mouse ALAS2 was inhibited by haemin *in vitro*. Furthermore, this was mediated by the HRM within the pre-sequence, and only one HRM was required to cause the inhibition. However, it is difficult to compare these two contradictory results as they were performed in different species and Lathrop & Timko used *in vitro* systems (Lathrop & Timko, 1993; Munakata *et al.,* 2004).

1.9.3 Haem-mediated destabilisation of ALAS1 mRNA

Haem has been shown to destabilise ALAS1 mRNA, experimentally, in a wide variety of cells types. For example, in the human hepatoma cell line, HepG2, the addition of haem decreases the ALAS1 mRNA half-life from 8.8 hours to 3.5 hours (Cable *et al.,* 2001; Sassa *et al.*, 1990). In the rat immortalised cell line, CWSV17, the addition of haem decreases the half-life from 2.5 hours to 1.3 hours, while conversely the addition of succinyl acetone (4,6-dioxoheptanoic acid), an inhibitor of haem biosynthesis, increases the ALAS1 half-life to 5.2 hours. In primary chick hepatocytes, haem decreases the mRNA half-life from 3.5 hours to 1.2 hours (Cable *et al.,* 2000; Hamilton *et al.,* 1991).

Haem-dependent decreases of ALAS1 mRNA levels occur more quickly and at lower concentrations than haem-dependent increases of HO. The ALAS1 mRNA remains at reduced levels for extended periods of time, whilst the increases in HO mRNA are much more transient (Cable *et al.,* 2000).

Hamilton *et al* (1991) confirmed that haem acts on ALAS1 post-transcriptionally by decreasing its mRNA stability, by using 2-propyl-2-isopropylacetamide (PIA), which increases the rate of transcription of the ALAS1 gene. The half-life of ALAS1 mRNA is approximately 3.5 hours in both control and PIA-induced primary cultures of chick embryo hepatocytes. Subsequent treatment of PIA-treated cells with either 1 or 10μM haem decreases the half-life of ALAS mRNA to approximately 1.2 hours. Cycloheximide completely blocks the haem-mediated decrease in ALAS1 mRNA half-life. In contrast, cycloheximide alone or in combination with PIA has no effect on the half-life of ALAS1 mRNA. These findings by Hamilton *et al* have therefore suggested that there is labile protein that mediates the effect of haem on ALAS1 mRNA stability. Such a labile protein may function as a haem-binding protein to mediate the effect of haem at specific sites of the ALAS1 mRNA, a haem-induced or activated nuclease for ALAS1 mRNA, or a haem carrier within the cells (Hamilton *et al.,* 1991).

1.9.4 Control of Haem Synthesis in Other Cell Types

Control of haem synthesis in cell types other than hepatic and erythroid cells has not been studied in such depth. A regulatory haem pool tightly regulates haem synthesis in the liver, but apparently less so in extra-hepatic tissue (Bissell and Hammaker, 1976; Giger & Meyer, 1983). ALA formation in these tissues is

presumed to be carried out by ALAS1, but regulation of haem biosynthesis in non-hepatic tissues seems different from that in the liver. For example, potent inducers of hepatic ALAS1 do not increase ALAS1 activity in the Harderian gland of mice, in the heart, adrenal gland, testes, brain and spleen in rats; or in cultured human amniotic cells. The effect of haemin on ALAS1 activity in non-hepatic tissues is also quite different from that in the liver. Haemin does not suppress ALAS1 in the Harderian gland, heart, or adrenal gland of mice, or in the testes of rats. ALAS1 in the foetal liver, which is largely erythroid during the foetal period, is also refractory to inhibition by haemin. Changes in ALAS activity in foetal guinea pig liver are correlated with the change in erythropoietic activity in this organ. Thus, regulation of the enzymatic activity of foetal liver reflects, by and large, that of erythroid cells (Scriver *et al.,* 1995).

1.10 Post-transcriptional Regulation of Gene Expression

In many cases of controlling the flow of genetic information from DNA to protein, the regulation of protein production is principally achieved by controlling mRNA levels (Guhaniyogi & Brewer, 2001). In mammalian cells, physiological signals modulate the rate of mRNA turnover (Bevilacqua *et al.,* 2003). Cytoplasmic mRNA levels represent a balance between the rates of nuclear RNA synthesis, processing, and export, and the rates of cytoplasmic mRNA degradation. The process of mRNA degradation is a major control point in gene expression, and this tightly regulated process dependent on specific *cis*-acting sequences and *trans*-acting factors (Guhaniyogi & Brewer, 2001).

Two major mechanisms of mRNA degradation are active in eukaryotic cells. In the first pathway, deadenylated transcripts are degraded by a complex of 3′-5′ exonucleases known as the exosome. Some mRNAs bearing AREs in their 3′-UTR are degraded by this pathway. The second pathway entails the removal of the seven-methyl guanosine cap from the 5′ end of the transcript by the DCP1-DCP2 complex, allowing 5′-3′ exonucleolytic degradation by XRN1 (reviewed in Meyer *et al.,* 2004; Parker & Song, 2004). In yeast, components of this 5′-3′ decay pathway are concentrated at discrete cytoplasmic foci known as processing bodies (p bodies). Studies of mammalian cells have revealed similar structures that contain DCP1/2, XRN1, GW182, and LSM1-7 heptamer. Little is known about the signaling pathways and specific molecular events that govern p body assembly, although their size and number increase when 5′-3′ mRNA decay is blocked and vary throughout the cell cycle. Stress granules are thought to be

sites of mRNA sorting rather than decay, as p bodies are putative sites of 5'-3' mRNA degradation (reviewed in Parker & Sheth, 2007).

1.10.1 Regulated mRNA Stability

The regulation of both mRNA stability and translation are essential in the control of gene expression and regulation of these two processes allows a cell to rapidly respond to changes in intracellular and extracellular stimuli (Barreau *et al.,* 2005). The regulation of eukaryotic genes by the stability of mRNA was first suggested in 1976. Ouellette & Malt (1976) discovered that the half-life of some murine mRNAs were prolonged, when compared to the majority of murine mRNAs. Since then a large number of genes have found to be regulated by the stability of the mRNA. The mRNA level is controlled post-transcriptionally mainly by specific proteins binding to a specific *cis*-acting element. The majority of these mechanisms, especially in the 5'-UTR affect translation rather than stability of the mRNA. The regulation of mRNA stability constitutes a critical control step in cellular mRNA level. Often, regulatory *cis*-acting elements are found with the coding region of the mRNA, but the mechanism is unknown, for example the regulation of rat CYP2E1 by insulin (Moncion *et al.,* 2002), described in section 1.10.4.

The degradation of mRNA is a highly controlled process in eukaryotic cells and provides a powerful means for controlling gene expression (Chen & Shyu, 1995). The rate of mRNA turnover not only determines the rate of disappearance of mRNA but also its induction. mRNAs with short half-lives respond to changes in transcription more rapidly than those that are relatively stable (Guhaniyogi & Brewer, 2001). Many clinically relevant mRNAs are regulated by differential RNA stability, and the aberrant control of mRNA stability has been implicated in disease states, including cancer, chronic inflammatory responses and coronary disease. The rates at which degradation processes can occur are dictated by both *cis*-acting elements within an mRNA and *trans*-acting factors that bind them. *Cis*-acting elements can regulate the rate of turnover of a transcript, either by promoting (destabiliser elements) or by inhibiting (stabiliser elements) decay (reviewed in Wilusz *et al.,* 2001). The regulated decay of mRNA is achieved by the orchestrated interactions between an mRNA's structural components and specific *trans*-acting factors. These components include the 7-methyl-guanylate (m^7G) 5' cap structure, the 5'-untranslated region (5'-UTR), the protein coding region, the 3'-UTR and the 3' polyadenylate [Poly(A)] tail (Guhaniyogi & Brewer,

2001). Figure 1-12 is a representation of the structure of a typical eukaryotic gene mRNA illustrating the possible types of *cis*-acting regulatory elements that exist. mRNA degradation can be preceded by shortening or removal of the poly(A) tail at the 3′ end and/or by removal of the m^7G cap at the 5′ end. Degradation can also take place following endonuclease activity, independent of both deadenylation and decapping, e.g. the degradation of transferrin receptor (TfR) mRNA in response to iron involves an endonucleolytic rupture in the 3′-UTR (Pesole *et al.*, 2000).

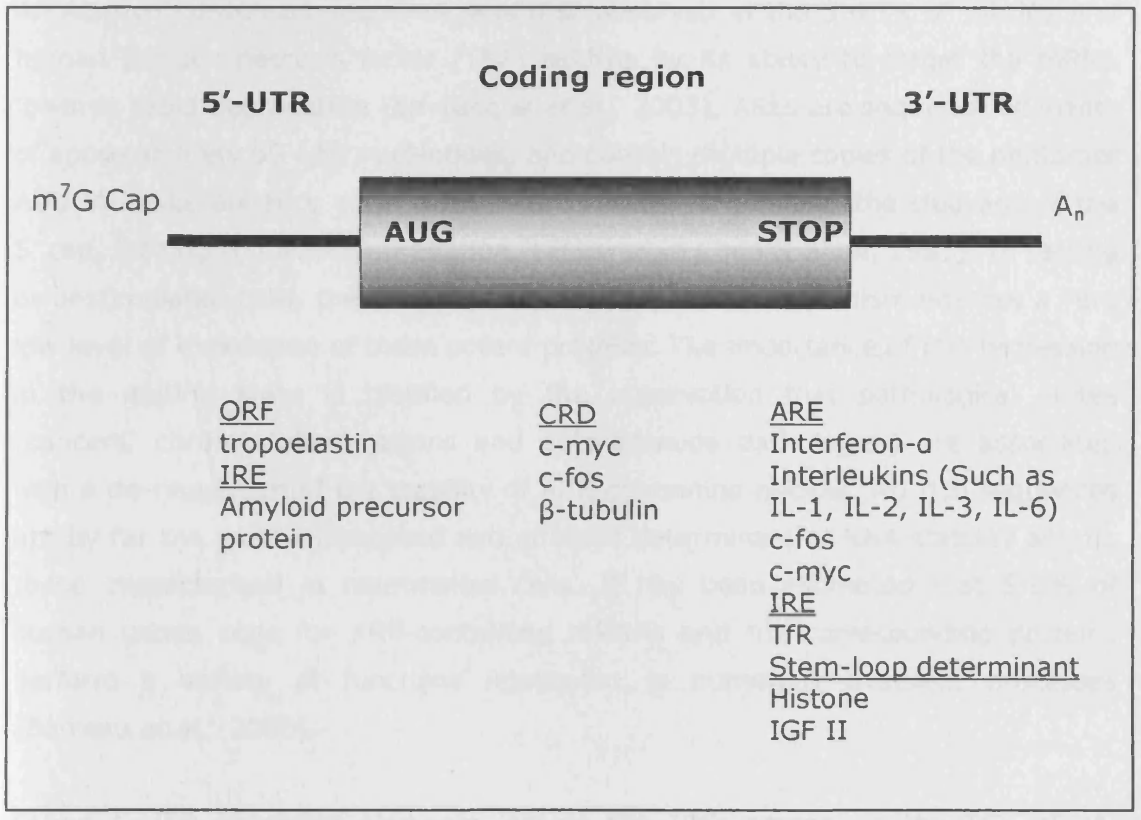

Figure 1-12 The general structure of a eukaryotic mRNA, illustrating examples of *cis*-acting elements involved in mRNA stability mechanisms.
The vast majority of pre-mRNA molecules undergo several steps of processing before they become functional mRNAs. The introns are removed, a m^7G cap structure is added at the 5′ end of the first exon, and a stretch of 100-250 adenine residues is added at the 3′ end of the last exon. The resultant mature mRNA has a tripartite structure consisting of a 5′-UTR, a coding region made up of triplet codons, and a 3′-UTR (Mignone *et al.*, 2002). The 5′ cap structure and 3′ poly(A) tail protect the message from exonucleolytic decay and can also act to regulate translation (Wilusz *et al.*, 2001).

1.10.2 The 3' Untranslated Region

The 3'-UTR has emerged as having a major role in harbouring determinants that control mRNA decay. One of the most prevalent mRNA sequence elements involved in regulating mRNA stability is the adenylate and uridylate (AU)-rich element (ARE), found in the 3'-UTR of numerous mRNAs encoding cytokines, proto-oncogenes and growth factors such as c-fos, c-myc and interferon-α (Wilusz *et al.,* 2001), which consequently have very short half-lives (Mitchell & Tollervey, 2000).

An AU-rich consensus sequence was first observed in the 3'-UTR of murine and human tumour necrosis factor (TNF) mRNAs by its ability to target the mRNA towards rapid degradation (Bevilacqua *et al.,* 2003). AREs are sequence elements of approximately 50-150 nucleotides, and contain multiple copies of the pentamer AUUUA. AREs enhance rapid deadenylation rates and trigger the cleavage of the 5' cap, leading to mRNA degradation (reviewed in Chen & Shen, 1995). In resting or unstimulated cells, the ARE-dependent degradation mechanism ensures a very low level of expression of these potent proteins. The importance of this repression in the resting state is testified by the observation that pathological states (cancers, chronic inflammations and auto-immune pathologies) are associated with a de-regulation of the stability of ARE-containing mRNAs. AU rich sequences are by far the most widespread and efficient determinant of RNA stability among those characterised in mammalian cells. It has been estimated that 5-8% of human genes code for ARE-containing mRNAs and the corresponding proteins perform a variety of functions implicated in numerous transient processes (Barreau *et al.,* 2006).

Other 3'-UTR instability elements include the IREs present in the TfR mRNA. When intracellular levels of iron are low, the IRE binds iron regulatory proteins (IRPs), which prevent endonucleolytic rupture and trigger mRNA degradation (Pesole *et al.,* 2000). Histone mRNAs lack poly(A) tails but their cell-cycle-dependent decay is mediated by a 3' terminal stem-loop motif (6bp stem and a 4 base loop) (Guhaniyogi & Brewer, 2001).

1.10.3 The 5' Untranslated Region

The 5'-UTR can play significant roles in altering stability either in a translation-dependent manner, by containing translation-inhibiting stem-loops, or in a

manner independent of translation. An example of the latter is the stabilisation of the otherwise unstable c-myc mRNA by reciprocal translocations of immunoglobin introns in the 5'-UTR of c-myc mRNA (Guhaniyogi & Brewer, 2001). Upstream initiation codons and open reading frames (ORFs) can cause mRNA decay through the nonsense-mediated mRNA decay (NMD) pathway. Upstream ORFs can also regulate mRNA stability through an NMD-independent mechanism by inhibiting ribosomal scanning, thereby promoting mRNA decay (Mignone *et al.,* 2002). An example of a regulatory ORF occurs in tropoelastin mRNA that encodes the connective tissue protein, elastin, where a specific element within the ORF regulates elastin production in response to transforming growth factor β1 (TGF-β1) (Zhang *et al.,* 1999).

IRE's can also be found in the 5'-UTR of mRNA molecules such as the Alzheimer's Amyloid precursor protein (APP) transcript, ferritin heavy (H) and light (L) chain, ALAS2, mammalian mitochondrial aconitase (mt-acon) and *D.melanogaster* succinate dehydrogenase subunit b, which mediate the mRNA translational efficiency (Thomson *et al.,* 1999; Rogers *et al.,* 2002).

1.10.4 The Coding Region

Instability determinants have also been found within the coding regions of mRNA species, although these are less common than those in the UTR's. The c-myc proto-oncogene contains two instability determinants, an ARE in its 3'-UTR and a 249-nucleotide coding region determinant (CRD) (Bernstein *et al.*, 1992; Doyle *et al.,* 1998). The CRD functions independently of the ARE to make the mRNA unstable (Herrick & Ross, 1994). Other mRNA species with CRDs include the plasminogen activator inhibitor type 2 (PAI-2) and c-fos (Tierney *et al.,* 2001; Chen *et al.,* 1992). The c-fos proto-oncogene mRNA is one of the least stable mammalian messages and is targeted for rapid degradation by at least two distinct mRNA degradation pathways, one involving an ARE, and the other a CRD. Two cellular proteins have been identified that interact with the c-fos CRD to form specific RNA-protein complexes that participate in the CRD-directed mRNA decay (Chen *et al.,* 1992).

Recent experiments using the c-fos mRNA as a model system have demonstrated a clear role for translation in mammalian RNA turnover. Two destabilising regions within the c-fos protein-coding region, termed CRD-1 and CRD-2, have been identified, and CRD-1 is the major determinant (mCRD). Grosset *et al* (2000)

have found that a minimal distance of ~450bp spacer between the mCRD and the poly(A) tail is required for mRNA degradation. They revealed a novel role for the 3' poly(A) tail, a dynamic interaction between the transcribed portion of the message and its poly(A) tail exists to influence the rate of deadenylation, therefore the poly(A) tail plays an active role. They have also provided evidence that the bridging complex contains RNA binding proteins can or have the potential to shuttle between the nucleus and cytoplasm, therefore shuttling RNA binding proteins have nuclear and cytoplasmic functions (Grosset *et al.,* 2000).

Davis *et al* (2001) have identified a ~280 base element residing within the coding region of the MnSOD mRNA that confers cis-mediated destabilisation in the absence of ribosome transit. This element functions during basal and stimulus-dependent MnSOD gene expression (Davis *et al.,* 2001).

Insulin controls the expression of rat CYP2E1 by altering its mRNA stability (De Waziers *et al.,* 1995). However, the mechanism by which insulin achieves this has not been elucidated. A 16bp protein-binding site in the 5'-proximal region of CYP2E1 coding region has been identified as being involved. Although insulin does not modify the binding of proteins to this region, it has been shown to be involved in the mechanism by insertion of the sequence into a luciferase gene. This was sufficient to render the chimeric mRNA sensitive to insulin. There is indirect evidence that the human CYP2E1 mRNA is regulated by insulin similarly to the rat CYP2E1 mRNA. A hairpin loop is present in both the proposed regulatory regions with 88% sequence identity (Moncion *et al.,* 2002). In addition, CYP2E1 is elevated in lymphocytes from patients with insulin-dependent diabetes mellitus (Hannon-Fletcher *et al.,* 2001). As the binding of the regulatory binding protein to its target RNA in CYP2E1 is not regulated by insulin, it is possible that it instead regulates protein-protein interactions mediating the destabilisation of the mRNA (Moncion *et al.,* 2002).

1.11 Aims of the Thesis

Haem regulates its own synthesis in non-erythroid cells through a regulatory haem pool, which is maintained by distinct haem-dependent control of ALAS1 and HO-1. However, the mechanism by which the expression of ALAS1 is post-transcriptionally regulated by haem has not yet been defined.

The overall objective of this thesis was to investigate the mechanism by which haem destabilises the ALAS1 mRNA in human non-erythroid cells. To elucidate this mechanism there were three main aims of the project:

1. To investigate the response of the alternative ALAS1 transcripts to haem.

2. To determine where the ALAS1 *cis*-acting element resides in the mRNA sequence.

3. To investigate protein binding to the ALAS1 mRNA, as this may be involved in its destabilisation in response to haem.

CHAPTER 2

Materials and Methods

2.1 Chemicals

All general laboratory chemicals were of at least AnalaR grade and purchased from Sigma-Aldrich unless otherwise stated.

The full addresses of all suppliers are listed in Appendix 3.

2.2 Cell culture

2.2.1 Mammalian Cell Culture

2.2.1.1 Cell Lines

The human Caucasian hepatoma cell line, HepG2 (ECACC No. 85011430), the human Caucasian neuroblastoma cell line, IMR32 (ECACC No. 86041809), and the human Caucasian chronic myelogenous leukaemia cell line K562 (ECACC No. 89121407) were obtained from the European Collection of Cell Cultures (ECACC).

2.2.1.2 Media and Growth Conditions

HepG2 cells were grown and maintained in Dulbecco's modified Eagle 1x medium (DMEM) supplemented with 10% (v/v) foetal calf serum (FCS) and 2mM L-glutamine. K562 and IMR32 cells were both grown in Roswell park memorial institute 1640 1x medium (RPMI 1640), supplemented with 10% and 5% FCS respectively and 2mM L-glutamine. All cells were grown at 37°C with 5% CO_2 in a humidified incubator.

2.2.1.3 Seeding Cells

Exponentially growing cells were split by washing with saline, followed by treatment with trypsin-EDTA (Sigma) for 5 minutes at 37°C. Cells were reseeded at the appropriate density in complete medium. For RNA extraction, cells were split into 6-well plates at a confluency of approximately 60%. For luciferase assays, cells were split into 12-well plates at a confluency of 60%.

2.2.1.3.1 Determining cell number

Mammalian cells in suspension were counted using a Z2 Coulter Particle Counter and Size Analyser (Beckman Coulter). Briefly, 0.5ml of cell suspension was added to 9.5ml of Isoton II diluent (Beckman Coulter) and analysed for particles in the range of 10 to 30μM. Cell counting was performed three times and the average output given as a number of cells per ml of the original cell suspension.

2.2.1.4 Transfection

Transfections of HepG2, K562 and IMR32 cells for RNA analysis were carried out using Lipofectamine 2000 (Invitrogen) in 6 well plates. One day prior to transfection, cells were seeded into 6-well plates in 2000μl of growth media so that they would be 90% confluent at the time of transfection. For each well, 3μg of DNA was mixed with 250μl of serum-free media (DMEM with 2mM L-glutamine). In a separate tube, 10μl of Lipofectamine 2000 was added to 250μl of serum-free media, and incubated for 5 minutes at room temperature. After the incubation, the DNA solution was combined with the Lipofectamine 2000 solution, mixed gently and incubated for 20 minutes at room temperature. The 500μl transfection mix was added drop-wise to the well and mixed gently. The cells were ready to be used in experiments, 24 hours post transfection.

When transfections were used for reporter assays, 12-well plates were used and the above method was scaled down.

2.2.1.5 Freezing Mammalian Cells

For long-term storage, cells were grown to approximately 2-4 x 10^6 cells/ml in a 75cm^2 flask, washed with saline, trypsinised and resuspended in 10ml of freezing medium (90% FCS, 10% DMSO). 1ml aliquots of the cells were pipetted into cryotubes, and placed in an isopropanol container at –70°C, so that they were frozen at a cooling rate of between 1-3°C/minute. After 24 hours, the cells were transferred to liquid nitrogen for long-term storage.

2.2.1.6 Haem-Depleted Media

For haem-depletion experiments, haem was removed from the FCS, prior to its addition to DMEM. L-ascorbic acid was added to FCS at a final concentration of

10mM, and incubated at 37°C for approximately 12 hours, until the absorbance at 405nm decreased from 2.0 to 0.8. The medium was dialysed in phosphate-buffered saline (PBS) at 4°C overnight in dialysis tubing (Spectra/Por MWCO=2000). The medium was dialysed for a further 8 hours, changing the PBS every 4 hours. The haem-depleted serum was sterilised by filtration through a 0.2µM filter, and stored at −20°C until further use. FCS was added to the cell growth media, at concentrations as described.

2.2.1.7 Preparation of Cytosolic Protein Extracts

Ice-cold PBS (1.5mls) was added to each T75 flask and the cells removed from the surface using a cell scraper. The cell suspensions were transferred to 1.5ml eppendorf tubes and centrifuged at 13000 rpm for 2 minutes. The cell pellet was resuspended in 200µl of ice-cold cytoplasmic extraction buffer (CEB; 10mM Hepes, pH 7.5, 3mM $MgCl_2$, 14mM KCl, 5% glycerol, 0.8% Nonidet P-40, 1mM dithiothreitol [DTT]) with 10µl freshly added protease inhibitor cocktail (104mM AEBSF [4-(2-Aminoethyl)benzenesulfonyl fluoride hydrochloride], 80µM aprotinin, 4mM bestatin, 1.4mM E-64 [N-(trans-Epoxysuccinyl)-L-leucine 4-guanidinobutylamide], 2mM leupeptin, 1.5mM pepstatin A in DMSO [dimethyl sulfoxide] [Sigma]). The tubes were vortexed for 10 seconds and incubated on ice for 20 min, with occasional vortexing. The cell membranes were pelleted by centrifugation for 5 minutes at 8500g. The resultant protein supernatant was removed and stored at −70°C after snap-freezing on dry ice.

2.2.1.8 Dual Luciferase Reporter Assay (DLRA)

To measure the luciferase activity of the transfected HepG2 and IMR32 cells, the cells were washed in saline and lysed in 250µl of 1X Passive Lysis Buffer (PLB) (Promega) with shaking for 15 minutes at room temperature. The assays for firefly luciferase and *Renilla* luciferase activity were performed sequentially from each well of lysed cells. 50µl of LAR II (Promega) and 50µl of the sample were mixed by vortexing in a small glass vial, and assayed in the Luminometer (Lumat LB9507 Luminometer, EG&G Berthold) to measure the firefly luciferase activity. 50µl of Stop & Glo Reagent (Promega) was then added, vortexed briefly and placed in the Luminometer to measure the *Renilla* luciferase activity. Each sample was assayed in duplicate, and the mean *Renilla* luciferase activity was normalised to the mean firefly luciferase activity, to compare the relative expression.

2.2.2 Bacterial Cell Culture

2.2.2.1 Media and Growth Conditions

Bacterial cell culture reagents were purchased from Oxoid and antibiotics from Sigma. All glassware was autoclaved at 126°C for 35 minutes prior to use.

Media	Composition
Luria-Bertani (LB)	1% w/v tryptone 0.5% w/v yeast extract 0.5% w/v NaCl
LB agar	1% w/v tryptone 0.5% w/v yeast extract 0.5% w/v NaCl 1.45% w/v agar
SOC	2% w/v tryptone 0.5% w/v yeast extract 10mM NaCl 2.5mM KCl 20mM $MgCl_2$ 20mM glucose
AX	LB agar plus: 100µg/ml ampicillin 40µg/ml X-Gal

Table 2-1 Compositions of bacterial growth media

Antibiotic	Stock Solution	Working Concentration
Ampicillin	50mg/ml	100µg/ml
Kanamycin	50mg/ml	50µg/ml

Table 2-2 Concentrations of antibiotics used during bacterial cell growth

2.2.2.2 Transformation

For routine subcloning, Library Efficiency™ Chemically Competent DH5α™ *E. coli* cells (Invitrogen) were used (expected tranformation efficiency: >1 x 10^8 cfu/µg supercoiled plasmid), of genotype:
F-Φ80*lac*ZΔM15(*lac*ZYA-*arg*F)U169*rec*A1 *end*AI *hsd*R17(r_k^-,m_k^+)*pho*A *sup*E44 *thi*-1 *gyr*A96 *rel*A1 λ^-.

The DH5α competent cells were thawed on ice before being gently mixed. An aliquot of 50µl was pipetted into a chilled 100mm polypropylene tube on ice. 1-5µl of the ligation reaction (approximately 1-10ng DNA) was added to the cells, and gently tapped to mix. The cells were incubated on ice for 30 minutes, heat-shocked at 42°C for 45 seconds and placed on ice for 2 minutes. 900µl of pre-warmed SOC medium was added to the transformation reaction and incubated at 37°C for 1 hour with shaking at 225rpm. The cells were pelleted by spinning at 6500rpm for 10 seconds, before being resuspended in 100µl of SOC media and spread onto a LB agar plate containing the appropriate concentration of antibiotic, and incubated overnight at 37°C.

2.2.2.3 Small Scale Plasmid Purification

For purification of up to 20µg of high-copy plasmid DNA from *E. coli*, a QIAprep Spin Miniprep Kit (Qiagen) was used. A single bacterial colony was picked from a LB agar plate, freshly streaked with DH5a cells transformed with plasmid DNA, and used to inoculate 5ml of LB with the appropriate antibiotic, and grown overnight at 37°C with shaking at 240rpm. The overnight culture (1.4ml) was transferred to a 1.5ml microcentrifuge tube and the bacteria pelleted by centrifugation at 13,000 rpm in a MSE Micro Centaur for 5 minutes.

The DNA was extracted from the bacterial cells using the alkaline lysis method, whereby SDS in the lysis buffer breaks down the cell membrane, and the NaOH loosens the cell wall and denatures DNA, releasing the plasmid. The bacterial DNA becomes linearised and the strands are separated, whereby the plasmid DNA is circular and remains topologically constrained. Adding potassium acetate to the DNA then renatures the plasmid DNA, whereas the sheared cellular DNA remains denatured as single stranded DNA (ssDNA) and is precipitated since it is insoluble in high salt.

The bacterial pellet was resuspended in 250µl of buffer P1 before 250µl of buffer P2 was added and the sample mixed thoroughly by inverting the tube 4-6 times. Buffer N3 (350µl) was added to the sample and mixed immediately by inversion, before being centrifuged for 10 minutes at 13,000rpm in a MSE Micro Centaur. The supernatant was transferred to a QIAprep spin column, centrifuged at 13,000rpm for 1 minute and the column washed with 0.5ml buffer PB to remove any trace nuclease activity. The spin column was washed with 0.75ml buffer PE and centrifuged twice at 13,000rpm for 1 minute, to remove residual wash buffer. The QIAprep column was placed in a clean nuclease-free microcentrifuge tube

and 50µl of sterile H_2O was added to the centre of the column. The column was left to stand for 1 minute at room temperature, and the DNA was eluted into a clean 1.5ml microcentrifuge tube by centrifugation at 13,000rpm for 1 minute.

2.2.2.4 Large Scale Plasmid Purification

For purification of up to 750µg of high-copy plasmid DNA from *E. coli*, a HiSpeed Plasmid Maxi Kit (Qiagen) was used. A single bacterial colony was picked from a freshly streaked selective LB agar plate and used to inoculate 5ml of LB with the appropriate antibiotic, and grown overnight at 37°C with shaking at 240rpm. 500µl of the starter culture was transferred into 250ml LB media plus any required antibiotics, and grown overnight at 37°C with shaking at 240rpm. The bacterial cells were harvested by centrifugation at 6,000g for 15 minutes at 4°C, and the supernatant was discarded.

The bacterial pellet was resuspended in 10ml buffer P1 by vortexing. Buffer P2 (10ml) was added to the bacteria, and mixed thoroughly by vigorously inverting the tube 4-6 times. The mix was then incubated for 5 minutes at room temperature to lyse the cells. Buffer P3 (10ml) was added to the lysate, and mixed immediately and thoroughly by vigorously inverting the tube. The lysate was poured into a QIAfilter Cartridge, and incubated at room temperature for 10 minutes. The cell lysate was filtered into the previously equilibrated HiSpeed Tip (10ml of buffer QT), and allowed to enter the resin by gravity flow. The HiSpeed Maxi Tip was washed with 60ml of buffer QC, and the plasmid DNA was eluted by the addition of 15ml of buffer QF. The DNA was then precipitated by the adding 10.5ml (0.7 volumes) of room temperature isopropanol, and incubated at room temperature for 5 minutes. The eluate/isopropanol mixture was filtered through a QIAprecipitator Maxi Module, and 2ml of 70% ethanol was passed through to wash the bound DNA. The filter was dried by passing air through the QIAprecipitator and the plasmid DNA was finally eluted into a 1.5ml microcentrifuge tube by passing 1ml of buffer TE through.

2.3 Protein Methodology

2.3.1 Estimation of Protein Concentration

Protein concentrations of samples were measured using the BCA™ Protein Assay Kit (Pierce). This is a detergent-compatible formulation based on bicinchoninic

acid (BCA) for the colorimetric detection and quantification of total protein. The method combines the reduction of Cu^{+2} to Cu^{+1} by protein in an alkaline medium (the biuret reaction) with the highly sensitive colorimetric detection of the cuprous cation (Cu^{+1}) using a reagent containing BCA. The purple-coloured reaction product of this assay is formed by two molecules of BCA chelating with one cuprous ion. This water-soluble complex exhibits a strong absorbance at 562nm that is nearly linear with increasing protein concentrations over a broad range (20-2,000 µg/ml). This method is not a true-end point method as the final colour continues to develop. However, following incubation the rate of continued colour development is sufficiently slow to allow large numbers of samples to be assayed together. Studies have shown that the macromolecular structure of protein, the number of peptide bonds and the presence of four particular amino acids (cysteine, cystine, tryptophan and tyrosine) are responsible for colour formation with BCA by the reduction of Cu^{+2} (Wiechelman *et al*, 1988).

The sample protein and the bovine serum albumin (BSA) standards (diluted with the sample buffer) were incubated at 37°C with the BCA working reagent (BCA™ Reagent A mixed with BCA™ Reagent B, 50:1) for 30 minutes. The tubes were then cooled to room temperature and the absorbencies measured at 562nm. The concentration of the protein was found with reference to a standard curve of the absorbance of the BSA standards, where a series of dilutions of known concentrations of BSA were prepared. These and the samples of unknown concentration were assayed alongside each other.

2.3.2 SDS-Polyacrylamide Gel Electrophoresis (SDS-PAGE)

A resolving gel of 0.8mm thickness was used below a stacking gel to separate proteins according to their size. The stacking gel is only slightly acidic (pH 6.8), with a low acrylamide concentration thereby making it a porous gel. Under these conditions the proteins are poorly separated but form thin, sharply defined bands before entering the resolving gel, where the higher pH and acrylamide concentration causes the proteins to be resolved according to size. Samples were mixed with 4x loading buffer (125mM Tris, 20% (v/v) glycerol, 4% (w/v) 2-mercaptoethanol, 0.04% (w/v) bromo-phenol blue) and heated at 95°C for 2 minutes before loading into the gel. Samples were electrophoresed at a constant current in 1x SDS running buffer (250mM glycine pH8.3, 25mM Tris base, 0.1% SDS) alongside 5µl of kaleidoscope prestained protein standards (Bio-Rad), with a molecular weight range of 6.5–200 kdaltons.

Reagent	Final % Polyacrylamide					
	3.5%	4%	4.5%	7%	10%	12%
Stacking buffer (0.5M Tris-Hcl pH 6.8, 0.4% SDS)	0.625	0.625	0.625	-	-	-
Separating buffer (1.5M Tris-Hcl pH 8.8, 0.4% SDS)	-	-	-	2.50	2.50	2.50
40% Acrylamide:Bisacrylamide	0.220	0.250	0.312	1.75	2.50	3.00
dH2O	1.627	1.597	1.535	5.64	4.89	4.39
10% Ammonium persulphate	0.025	0.025	0.025	0.10	0.10	0.10
100% TEMED	0.0025	0.0025	0.0025	0.01	0.01	0.01

Table 2-3 Compositions of stacking and separating gels used in SDS-PAGE

2.3.3 Coomassie Blue Staining

SDS-polyacrylamide gels were stained in Coomassie blue staining solution (20% methanol, 5% glycerol, 0.25% Coomassie brilliant blue R-250) for 10 minutes and destained in destaining solution (20% methanol, 10% acetic acid) for at least 30 minutes until the desired degree of background was achieved.

2.4 DNA Methodology

2.4.1 Restriction Enzymes and Buffers

Restriction enzymes were purchases from either Promega or New England Biolabs (NEB).

Enzyme	Restriction Site	Supplied NEB Buffer	Percentage Activity in NEB Buffers				Enzyme Assay Temp (°C)
			1	2	3	4	
Kas I	G↓GCGCC	2	75	100	75	75	37

Table 2-4 Enzymes from NEB

NEB Buffer	Composition at 1x
2	10mM Tris-HCl, 10mM $MgCl_2$, 50mM NaCl, 1mM DTT, pH 7.9

Table 2-5 Composition of NEB restriction enzyme buffers

Enzyme	Restriction Site	Supplied Buffer	Percentage Activity in Promega Buffers					Enzyme Assay Temp (°C)
			A	B	C	D	Multi-Core™	
Apa I	GGGCC↓C	A	100	50-75	50-75	<10	75-100	37
*Eco*R I	G↓AATTC	H	25-50	50-75	50-75	50-75	100	37
Hind III	A↓AGCT	E	25-50	100	75-100	10-25	50-75	37
Kpn I	GGTAC↓C	J	100	25-50	25-50	<10	75-100	37
Nco I	C↓CATGG	D	50-75	75-100	75-100	100	75-100	37
Not I	GC↓GGCCGC	D	<10	10-25	25-50	100	25-50	37
Pst I	CTGCA↓G	H	10-25	50-75	50-75	50-75	25-50	37
Sac I	GAGCT↓C	J	75-100	25-50	25-50	<10	100	37
Spe I	A↓CTAGT	B	75-100	100	75-100	75-100	100	37
Xba I	T↓CTAGA	D	50-75	75-100	75-100	100	100	37

Table 2-6 Enzymes from Promega

Promega Buffer	Composition at 1x
A	6mM Tris-HCl, 6mM $MgCl_2$, 6mM NaCl, 1mM DTT, pH 7.5
B	6mM Tris-HCl, 6mM $MgCl_2$, 50mM NaCl, 1mM DTT, pH 7.5
D	6mM Tris-HCl, 6mM $MgCl_2$, 150mM NaCl, 1mM DTT, pH 7.9
E	6mM Tris-HCl, 6mM $MgCl_2$, 100mM NaCl, 1mM DTT, pH 7.5
H	90mM Tris-HCl, 10mM $MgCl_2$, 50mM NaCl, pH 7.5
J	10mM Tris-HCl, 7mM $MgCl_2$, 50mM KCl, 1mM DTT, pH 7.9
Multi-Core™	25mM Tris-Acetate, 100mM K-Acetate, 10mM Mg-Acetate, 1mM DTT, pH 7.5

Table 2-7 Composition of Promega restriction enzyme buffers

2.4.2 Restriction Digests

2.4.2.1 Single Digests

One unit of restriction enzyme activity is defined as the amount of enzyme required to produce complete digestion of 1µg of substrate DNA in 1 hour, at the appropriate assay temperature.

Generally, restriction digestions using a single restriction enzyme were set up as shown in table 2-8.

Reagent	Volume
Substrate DNA	1µg
Restriction Enzyme (10U/µl)	1µl
Restriction buffer 10x	1µl
H_2O	to 10µl final volume

Table 2-8 Single restriction digest reaction

The reactions were incubated at the appropriate temperature (table 2.4 & 2.5) for at least 3 hours.

2.4.2.2 Double Digests

When DNA needed to be digested by two restriction enzymes, the buffer that allows the highest percentage of activity for both enzymes was used (table 2-4 & 2.5)

Generally, restriction digestions using two restriction enzymes were set up as follows:

Reagent	Volume
Substrate DNA	1µg
Restriction Enzyme 1 (10U/µl)	1µl
Restriction Enzyme 2 (10U/µl)	1µl
Restriction buffer 10x	1µl
H_2O	to 20µl final volume

Table 2-9 Double restriction enzyme digest

The reactions were incubated at the appropriate temperature (tables 2-4 & 2-5) for at least 3 hours.

2.4.3 DNA Quantification

DNA was quantified using the GeneQuant DNA/RNA Calculator (Amersham Pharmacia Biotech), which measures absorbance at 260nm and 280nm. 3µl of the DNA sample to be quantified was added to 147µl of water in a quartz cuvette with a path length of 10mm. The GeneQuant was set to interpret either dsDNA or ssDNA as appropriate. The cuvette was placed in the spectrophotometer, and the

concentration of the sample recorded. The purity of the DNA was confirmed by checking the ratio of the absorbance at 260nm and 280nm. DNA with no impurities has a reading of 1.8.

2.4.4 Polymerase Chain Reaction (PCR)

2.4.4.1 Primers

For optimal PCR reactions, the primers were designed with several parameters in mind, such as length, %GC content, internal loop structures or the possibility of primer-dimer formation.

Primers were synthesised and purified by desalting, by Invitrogen's custom primer service. For details of all primers, see appendix 4.

2.4.4.2 Standard PCR Conditions

For routine non-quantitative PCR to confirm ligations were successful during cloning, Taq Polymerase (Promega) was used, with its supplied buffers (table 2-8). Reactions were performed in a PCR Sprint machine (ThermoElectron) as described in table 2.10.

Reagent	Volume (µl)
10x PCR Buffer	5
25mM $MgCl_2$	3
2mM dNTP mix	5
Sense Primer (10pmol/µl)	5
Antisense Primer (10pmol/µl)	5
DNA template	2
Taq Polymerase (4U/µl)	0.5
H_2O	24.5

Table 2-10 Composition of a standard 50µl PCR

Temperature	Time	Number of Cycles
93°C	40 seconds	10
Annealing	1 minute	
73°C	1 minute 40 seconds	
93°C	40 seconds	10
Annealing	1 minutes	
73°C	1 minute 50 seconds	
93°C	40 seconds	10
93°C	1 minute	
Annealing	2 minutes	
73°C	10 minutes	1

Table 2-11 Cycling protocol for standard PCR

Annealing temperatures depended on the length of the primers and the %GC content, and usually ranged from 55°C-65°C.

2.4.4.3 High Fidelity PCR Conditions

For qualitative RT-PCR, or cloning, the polymerases Bio-X-Act and HotStarTaq were used respectively.

2.4.4.3.1 HotStarTaq Polymerase

HotStarTaq DNA polymerase (Qiagen) has a high PCR specificity with reduced non-specific amplification, and leaves an 'A' overhang. Reactions were set up and cycled as described in tables 2.12 and 2.13 respectively.

Reagent	Volume (µl)
10x PCR buffer	5
2mM dNTP mix	5
Sense primer (5pmol/µl)	5
Antisense primer (5pmol/µl)	5
DNA template	2
HotStarTaq Polymerase (5U/µl)	0.5
H_2O	27.5

Table 2-12 Composition of a standard 50µl PCR, using HotStarTaq polymerase

Temperature	Time	Number of Cycles
95°C	15 minutes	1
94°C	1 minute	35
Annealing	1 minute	
72°C	1 minute 40 seconds	
72°C	10 minutes	1

Table 2-13 Cycling protocol for PCR with Taq polymerase

For PCR products longer than 1kb, an extension time of approximately 1 min per kb DNA was used.

2.4.4.3.2 Bio-X-Act Polymerase

Bio-X-Act DNA Polymerases (Bioline) are a high-performance proprietary complex of enzymes and additives specifically designed for difficult or problematic applications requiring high processivity with high-fidelity. The unique composition of different enzymatic activities delivers a 17-fold increase in fidelity in comparison with regular Taq polymerase and is therefore suitable for reactions where accuracy is important. Bio-X-Act also leaves an 'A' overhang which can be utilised in TA cloning.

Bio-X-Act was used with its supplied buffers, as described in table 2.14 and cycled as described in table 2-11.

Reagent	Volume (µl)
10x Optibuffer	5
50mM $MgCl_2$	1.5
2mM dNTP mix	5
Sense primer (10pmol/µl)	5
Antisense primer (10pmol/µl)	5
DNA template	2
Bio-X-Act (4U/µl)	0.5
H_2O	26

Table 2-14 Composition of a high fidelity PCR using Bio-X-Act polymerase

2.4.5 Agarose-TAE Gel Electrophoresis

DNA samples were prepared by the addition of an appropriate volume of 6x loading buffer (Promega) and loaded onto a 0.7-2% electrophoresis grade agarose gel containing ethidium bromide at a final concentration of 0.5µg/ml. The gel was electrophoresed at a constant voltage of 100V in 1x TAE running buffer (pH 8.0; 40mM tris, 40mM acetic acid, 2mM EDTA) for 45-60 minutes. Sizes of DNA fragments were estimated by running alongside a standard DNA marker. The Promega 100bp and 1kb DNA ladders were used for DNA of sizes 100bp – 1kb and 1kb – 10kb respectively (see section 2.4.5.1).

2.4.5.1 DNA Molecular Weight Markers

2.4.5.1.1 100bp Ladder

The Promega 100bp ladder consists of DNA fragments that range in size from 100-1,000bp in 100bp increments, plus a fragment at 1,500bp. To allow easy identification the 500bp fragment is present at increased intensity (figure 2-1)

2.4.5.1.2 1Kb ladder

The Promega 1Kb ladder consists of 13 fragments ranging in size from 250-10,000bp. The 1,000 and 3000bp fragments are of increased intensity relative to the other bands to serve as reference indicators (figure 2-1).

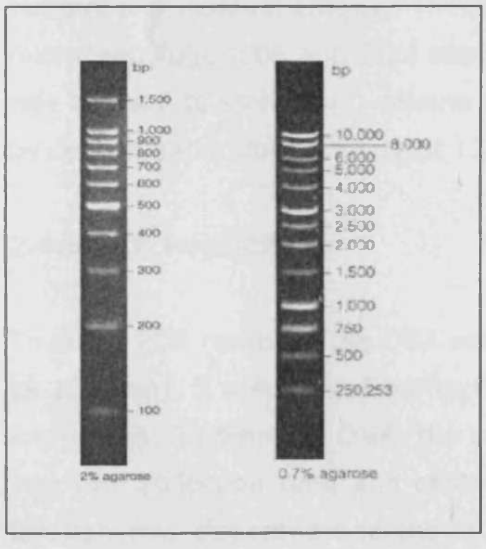

Figure 2-1 100bp and 1kb DNA ladders, adapted from www.promega.com

2.4.6 Gel Visualisation and Documentation

DNA was visualised on a UV transilluminator and photographed using a Syngene gel documentation darkroom system and analysed by GeneSnap Version 2.60.0.14 and GeneTools Version 2.10.03 (Synoptics).

2.4.7 Gel Extraction

To extract and purify DNA from an agarose gel, a QIAquick Gel Extraction Kit (Qiagen) was used, where buffer QG is used to solubilise the agarose and provide appropriate conditions for the DNA to bind to the silica membrane of the column. The DNA is then washed with ethanol and eluted from the column.

The DNA fragment to be extracted was excised from the agarose gel with a clean scalpel. The gel slice was weighed; and three times gel volume of buffer QG was added to the sample and incubated at 50°C for 10 minutes until the gel slice was completely dissolved. One gel volume of isopropanol was added to the sample and mixed. To bind the DNA, the sample was applied to a QIAquick column in a 2ml collection tube and centrifuged for 1 minute at 13,000rpm. The flow-through was discarded and the QIAquick column was placed back in the same collection tube. 0.5ml of buffer QG was added to the column and centrifuged for 1 minute at 13,000rpm. To wash the DNA, 0.75ml of buffer PE was added to the QIAquick column and allowed to stand for 5 minutes at room temperature before centrifuging for 1 minute at 13,000rpm. The flow-through was discarded and the QIAquick column was centrifuged for an additional 1 minute at 13,000rpm to remove any residual ethanol. The QIAquick column was placed into a clean 1.5ml microcentrifuge tube and 30µl sterile H_2O was added to the column. The column was allowed to stand for 1 minute at room temperature and the DNA was eluted by centrifugation for 1 minute at 13,000rpm.

2.4.8 PCR Purification

To purify PCR reactions the DNA was desalted using the QIAquick PCR purification kit (Qiagen). 5 volumes of buffer PB was added to 1 volume of the PCR sample and mixed. To bind the DNA, the sample was applied to a QIAquick spin column in a 2ml collection tube and centrifuged for 1 minute at 13,000rpm. The flow-through was discarded and the QIAquick column was placed back in the same tube. To wash the DNA, 0.75ml of buffer PE was added to the QIAquick column

and centrifuged for 1 minute at 13,000rpm. The flow-through was discarded and the QIA-quick column was placed back into the same tube and centrifuged for an additional 1 minute at 13,000rpm to remove any residual ethanol. The QIAquick column was placed into a clean 1.5ml microcentrifuge tube and 30µl sterile H_2O was added to the centre of the QIAquick membrane and allowed to stand for 1 minute at room temperature. The DNA was eluted by centrifugation for 1 minute at 13,000rpm.

2.4.9 Automated DNA Sequencing

The sequences of all constructs were verified by DNA sequencing, using BigDye v3.1 in the Ready Reaction Premix with the supplied 5x buffer (Applied Biosystems). The reactions were set up as shown in table 2-15, using linearised DNA, and cycled as shown in table 2-16. The sequencing reactions were then cleaned by ethanol/sodium acetate precipitation and analysed on an ABI 377 sequencer (Applied Biosystems) by Central Biotechnology Services, Cardiff University.

Reagent	Volume
Ready Reaction Premix (2.5x)	4µl
BigDye Sequencing Buffer (5x)	2µl
DNA linear template	Single-stranded: 25-50ng Double-stranded: 150-300ng PCR template: 10-50ng
Primer	3.2pmols
H_2O	To 20µl

Table 2-15 DNA sequencing reaction composition

Temperature	Time	Number of Cycles
96°C	1 minute	1
96°C	10 seconds	25
50°C	5 seconds	
60°C	4 minutes	

Table 2-16 Cycling protocol for Big-Dye v3.1 sequencing

2.4.10 Sequencing Clean-Up

To purify the extension product from any unincorporated dye-labelled terminators, ethanol/sodium acetate precipitation was used. The sequencing reaction was briefly microfuged to remove any condensation, followed by the addition of 2µl of 3M sodium acetate (pH5.5) and 50µl of 100% ethanol. The reactions were mixed followed by incubation at room temperature for 15 minutes, and centrifugation at 13,000rpm for 30 minutes in a MSE Micro Centaur. The supernatant was removed and the DNA was washed twice, by the addition of 200µl of 70% ethanol and centrifugation at 13,000rpm for 5 minutes. After the final wash, the supernatant was removed and the DNA was sequenced.

2.4.11 *In Vitro* Transcription

To make labelled RNA probes for use in the RPA, the sequence of the DNA of interest is firstly cloned into the pGEM-T vector, as previously described. The plasmid was linearised by digestion with a restriction enzyme that leaves a blunt or 5' overhang downstream of the DNA of interest. The products of the digestion were visualised using agarose-TAE electrophoresis (section 2.4.5) and fully cut plasmids were extracted using the Qiagen gel extraction kit (section 2.4.7).

To produce the antisense single stranded RNA transcript from the linearised DNA template, T7 phage RNA polymerase was used. The following transcription reaction was assembled at room temperature.

Reagent	Volume
Nuclease-free H_2O	to 20µl
Linear DNA template	1µg
10x Transcription Buffer	2µl
10mM ATP	1µl
10mM CTP	1µl
10mM GTP	1µl
10mM UTP	0.6µl
Biotin-16-UTP	0.4µl
T7 enzyme mix	2µl

Table 2-17 *In Vitro* transcription of biotin-labelled RNA

The reaction was mixed by gently pipetting up and down. The reaction was then microfuged briefly and incubated at 37°C for 2 hr. After which the DNA template was removed by the addition of 1µl DNase I (1U/µl), mixed and incubated at 37°C for 15 min. To stop the reaction, 1µl of 0.5M EDTA was added which chelates metal ions and thereby inhibits DNase I from functioning.

2.4.12 Gel Purification

As the probe was to be used for a ribonuclease protection assay (RPA) it was necessary to primarily have full-length probe by gel purification. After transcription, 20µl of gel loading buffer was added to the probe and incubated at 95°C for 4 minutes to denature any secondary structure, and placed on ice to prevent renaturation. The probe was loaded onto a 5% acrylamide/8M urea denaturing polyacrylamide gel, and run at 200V in 1x TBE buffer for approximately 1 hour until the blue dye front of the bromophenol blue reached the bottom of the gel.

The gel was stained with ethidium bromide in 1x TBE buffer for 5 min and visualised under UV light. The full length RNA probe was excised from the gel, cut into small pieces to increase the surface area and transferred into a nuclease-free microfuge tube. To elute the transcript, the gel fragment was incubated overnight in 350µl elution buffer (0.5M NH_4Oac/1mM EDTA/0.2% SDS). The probe was precipitated by the addition of 3x volume 100% ethanol and centrifugation at 13000rpm for 20 min at 4°C. The supernatant was removed, and the cell pellet consisting of the RNA transcript was resuspended in MMLV Reverse Transcriptase 1x buffer (Promega; 50mM Tris-HCl pH 8.3, 75mM KCl, 3mM $MgCl_2$, 10mM DTT) with 40U of RNasin ribonuclease inhibitor and stored at −70°C prior to its use in the RPA.

2.5 RNA Methodology

2.5.1 RNA Isolation

The RNA working area and pipettes were decontaminated using RNase Away (Merck) prior to handling RNA.

2.5.1.1 Total RNA Isolation

Total RNA was extracted from mammalian cell cultures using Ultraspec™ RNA isolation system (Biotecx USA, purchased from AMS Biotechnology). A monolayer of HepG2/IMR32 cells were scraped from a plate or flask into 1ml Ultraspec and transferred to an RNase/DNase free 1.5ml microcentrifuge tube. For non-adherent K562 cells, the cells were pelleted at 1500rpm for 3 minutes, before being lysed in 1ml Ultraspec. Cell lysates were homogenised by passing them through a pipette several times and incubated at 4°C for 5 minutes.

To extract the RNA, 200µl of chloroform were added per 1ml of Ultraspec and samples shaken for 15 seconds and incubated on ice for 15 minutes. The homogenate was centrifuged for 15 minutes at 13,000rpm in a MSE Micro Centaur at 4°C to separate the lower, organic phase containing the DNA from the upper, aqueous phase containing the RNA. The aqueous phase was transferred to a fresh RNase/DNase free 1.ml microcentrifuge tube and an equal volume of isopropanol added. Samples were incubated on ice for 10 minutes and centrifuged for 10 minutes at 13,000 rpm in a MSE Micro Centaur at 4°C to precipitate the RNA. The supernatant was carefully removed and the RNA pellet washed twice with 75% ethanol by vortexing and centrifugation for 5 minutes at 6,000rpm in a MSE Micro Centaur at 4°C. The RNA was air-dried and resuspended in 30µl nuclease-free water (Sigma) and stored at –70°C until use.

2.5.1.2 mRNA Isolation

To directly extract mRNA from HepG2 cells, the Dynabeads mRNA Direct Kit (Dynal) was used and the manufacturer's instructions were followed.

A monolayer of HepG2/IMR32 cells were scraped from a plate or flask into 1ml ice-cold PBS, transferred to an RNase/DNase free 1.5ml microcentrifuge tube, and centrifuged at 1,500rpm for 3 minutes. The PBS was removed and the cell pellet was stored at -70°C until the mRNA was extracted.

The Dynabeads were prepared by transferring 250µl of beads into an RNase-free 1.5ml microcentrifuge tube placed on a magnet (Dynal MPC-S). After 30 seconds the supernatant was removed, and the beads were resuspended in 250µl of fresh lysis/binding buffer (100mM Tris-HCl pH 7.5, 500mM LiCl, 10mM EDTA pH 8, 1%

LiDS, 5mM DTT). The beads remained in this buffer until the sample lysate was ready for combination with the beads.

The cell pellet was lysed by the addition of 1250µl of lysis/binding buffer. To obtain complete lysis a repeated passage of the solution through a pipette tip was performed. The lysate was then forced through a 21-gauge needle 5 times using a 2ml syringe to shear the DNA. The lysate was transferred to the prepared Dynabeads Oligo $(dT)_{25}$. The beads were mixed with the sample lysate and incubated for 5 minutes at room temperature with continuous mixing to allow the polyA-tail of the mRNA to anneal to the oligo-dT on the beads. The vial was placed on the magnet for 2 minutes, and the supernatant was removed. The beads/mRNA complex was washed twice with 1ml of washing buffer A (10mM Tris-HCl pH 7.5, 150mM LiCl, 1mM EDTA, 0.1% LiDS) at room temperature, and then washed once in 1ml of washing buffer B (10mM Tris-HCl pH 7.5, 150mM LiCl, 1mM EDTA) at room temperature, using the magnet to separate the beads from the solution between each step.

To elute the mRNA from the beads, 25µl of 10mM Tris-HCl was added to the beads/mRNA complex and incubated for 2 minutes at 80°C. The tube was placed immediately on the magnet and the supernatant containing the mRNA was transferred to a new RNase-free microcentrifuge tube and stored at –70°C.

2.5.2 RNA Quantification

Total RNA was quantified using the GeneQuant DNA/RNA Calculator set to interpret RNA, as described in 2.3.3. The purity of the RNA was confirmed by checking the ratio of the absorbance at 260nm and 280nm. RNA with no impurities has a reading of 2.0.

2.5.3 Removal of DNA Contamination

Prior to first strand synthesis, RNA samples were treated with DNase I [Amplification Grade] (Invitrogen) to ensure that any remaining DNA was eliminated from the RNA preparation. Two units of DNase I was added to 1µg of RNA in DNase 10x reaction buffer (20mM Tris-HCl pH 8.4, 2mM $MgCl_2$, 50mM KCl) and incubated for 15 minutes at room temperature. The enzyme was inactivated by the addition of 1µl 25mM EDTA and heating to 65°C for 10 minutes.

2.5.4 First Strand Synthesis

For first strand synthesis of cDNA from RNA, MMLV Reverse Transcriptase was used with its supplied buffer, along with RNasin Ribonucleotide Inhibitor to prevent RNA degradation and Oligo dT primer and dNTP mix, as described in table 2-18. The reaction was incubated for 5 minutes at 25°C, followed by incubation at 42°C for 1 hour and 70°C for 10 minutes to inactivate the reaction. The cDNA was stored at -20°C until further use.

Reagent	Volume (µl)
5x M-MLV-RT Buffer	4
10mM dNTP mix	2
Oligo dT primer (50ng/µl)	1
RNasin Ribonucleotide Inhibitor (40U/µl)	0.25
DNase I-treated RNA	2µg
M-MLV RT (200U/µl)	1
H_2O	To 20µl

Table 2-18 First strand synthesis of RNA

2.5.5 RNase Protection Assay (RPA)

For each experimental tube, labelled probe was mixed with mRNA extracted from the HepG2 cells, in a 1.5ml microcentrifuge tube. For each different probe used, two control tubes were included containing the same amount of labelled probe used for the experimental tubes plus yeast RNA equivalent to the highest amount of sample RNA. 5M NH_4OAc was added to a final concentration of 0.5M, followed by the addition of 2.5 volumes 100% ethanol, and mixed thoroughly. Samples were incubated at -20°C for 15 minutes. The RNA was pelleted by centrifugation at 13,000 RPM in a microcentrifuge for 15 minutes at 4°C. The supernatant was removed and the tubes were spun a second time for 5 seconds to collect any supernatant left on the sides of the tubes, and the remaining supernatant was removed. Pellets were air dried for 5 minutes and resuspended in 20µl of Hybridisation buffer. To denature the RNA and aid its solubilisation, samples were incubated for 4 minutes at 95°C. Samples were incubated overnight at 42°C to hybridise the probe to its complement in the sample RNA.

After hybridisation, the tubes were centrifuged briefly, and 200µl of the diluted RNase mixture was added to each tube, and to one of the two yeast RNA control

tubes that have been prepared for each probe in the experiment. To the remaining yeast RNA control tube, 200µl RNase digestion buffer without RNase was added. Samples were incubated for 30 minutes at 37°C, during which time unprotected single-stranded RNA will be digested. 300µl of RNase inactivation/precipitation solution was then added to the samples, with 2µl Yeast RNA to increase the size and visibility of the final pellets, and incubated at -20°C for 15 minutes. The precipitated products were pelleted by centrifugation at 13,000 RPM at 4°C, and the supernatant was removed. Pellets were resuspended in 6µl Gel Loading Buffer II and incubated for 3 minutes at 95°C to completely solubilise and denature the RNA. RNA samples were loaded onto a 5% polyacrylamide gel and electrophoresed at 25mAmps constant current, until the leading dye band was near the bottom of the gel.

2.5.6 Detection of Non-Isotopic probes

To detect the biotinylated RNA probes used in the RPA, the BrightStar BioDetect kit (Ambion) with its supplied buffers was used, and the manufacturer's instructions were followed. This is a nonisotopic chemiluminescent detection system that does not suffer from the high backgrounds and low sensitivity typical of these systems, and is used to detect the biotinylated RNA on positively charged nylon membrane. All incubations/wash steps were done with gentle agitation at room temperature. The 100cm^2 membrane was washed twice in 100ml 1x Wash buffer for 5 minutes. The membrane was then incubated twice in 50ml Blocking Buffer for 5 minutes each, before a final incubation in 100ml Blocking Buffer for 30 minutes. The membrane was then incubated in 10ml Blocking Buffer, containing 1µl Streptavidin-Alkaline Phosphatase (Strep-AP), for 30 minutes. The membrane was incubated for 10 minutes in 50ml Blocking Buffer, and washed three times in 1x Wash Buffer for 15 minutes each to decrease non-specific background. The membrane was then incubated twice in 50ml 1x Assay Buffer for 2 minutes each, and then in 5ml of CDP-Star. After 5 minutes, the membrane was blotted on filter paper to remove any excess CDP-Star, wrapped in a single layer of plastic wrap, and exposed to film at room temperature. The CDP-Star reaches peak light emission in 2-4 hours, and then emission falls to a plateau which persists for several days.

2.6 Cloning

2.6.1 TA Cloning

DNA fragments to be cloned were amplified using high fidelity PCR as described in 2.3.4. The PCR product was separated on TAE/agarose gel and the specific product band purified by gel extraction. The DNA insert was then ligated into pGEM®-T and the ligation mix used to transform DH5α cells which were plated onto LB-AIX plates for blue/white colour selection.

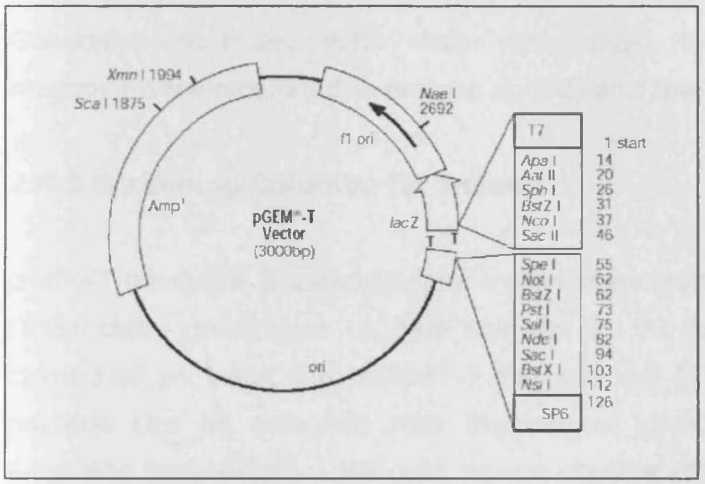

Figure 2-2 Vector map of pGEM®-T from www.promega.com

2.6.2 Ligation

To calculate the appropriate amount of insert DNA to be used in the ligation reaction containing 50ng of vector, the following equation was used:

$$\frac{\text{ng of vector} \times \text{kb size of insert}}{\text{kb size of vector}} \times \text{insert:vector molar ratio} = \text{ng of insert}$$

Reagent	Standard Reaction	Positive Control	Background control
2x Rapid Ligation Buffer	5µl	5µl	5µl
pGEM®-T vector (50ng)	1µl	1µl	1µl
Insert DNA	As calculated by equation	0µl	0µl
Control insert DNA	0µl	2µl	0µl
T4 DNA Ligase (3U/µl)	1µl	1µl	1µl
H_2O	To 10µl	1µl	3µl

Table 2-19 Ligation of insert DNA into the pGEM-T vector

Generally, the insert:vector molar ratios used were 3:1 and 1:1. The ligation reactions were incubated overnight at 4°C, and then transformed into DH5α cells.

2.6.3 Screening Colonies for Inserts

pGEM-T produces β-galactosidase by α-complementation when transformed into DH5a cells, giving rise to blue colonies in the presence of X-gal. Successful cloning of an insert into pGEM®-T disrupts the β-galactosidase gene; therefore bacteria can be screened with the use of LB-AX plates (LB-agar containing ampicillin and X-Gal). DH5 cells do not require IPTG to induce expression from the lac promoter even though the strain expresses the lac repressor, as the copy number of most plasmids exceeds the repressor number in the cells. The insertion of DNA into the cloning site disrupts the *lacZ* gene, therefore preventing α-complementation and producing white colonies.

2.6.4 Colony screening by PCR

To verify if the bacterial colonies contain the correctly ligated construct in the correct orientation they were screened by PCR, using primers that would produce a PCR product that overlaps the plasmid and insert. Each colony was picked and placed into 30µl LB with the appropriate antibiotic and incubated for 1 hour at 37°C with shaking. PCR was then performed on the bacteria, as described in section 2.4.4.2, using Taq polymerase.

2.7 RNA-Protein Interaction Assays

2.7.1 *In Vitro* Transcription

The plasmid was linearised by digestion with a restriction enzyme that leaves a blunt or 5' overhang downstream of the DNA of interest. The products of the digestion were visualised using agarose-TAE electrophoresis (section 2.4.5) and fully cut plasmids were extracted using the Qiagen gel extraction kit (section 2.4.7). For the EMSA's and UV-crosslinking, radiolabelled RNA was made with α32-CTP. The method for *in vitro* transcription in section 2.4.11 was used, but with CTP as the limiting nucleotide. The method for radiolabelled RNA is slightly different to non-radiolabelled RNA, and is therefore described here.

Transcription reactions were performed using the Ambion T7 MAXIscript (similar to section 2.4.11). To 500ng of the linearised DNA template the reagents were added in following order: 1µl 10X transcription buffer, 0.5µl 10mM ATP, 0.5µl 10mM GTP, 0.5µl 10mM UTP, 1µl 0.1mM CTP, 2.5µl ^{32}P CTP, 1µl T7 enzyme mix (15U/µl) and RNase-free H_2O to a final volume of 10µl. The tube was gently flicked to mix and microfuged briefly. The reaction was incubated at 15°C for 1.5 hours and then stopped by the addition of 40µl TE buffer. The RNA was purified from the unincorporated nucleotides by spinning through a Sephadex G-50 column (Amersham-Pharmacia Biotech) at 4,000rpm for 2 minutes in a microfuge. The amount of radioisotope made in each reaction was quantified using a Wallac 1409 DSA liquid scintillation counter (Perkin Elmer Life Sciences) in the Department of Medical Physics, University Hospital of Wales, Cardiff.

To check the integrity and size of the probes, the RNA was electrophoresed on a 1x TBE, 4% polyacrylamide, 8M urea, denaturing gel. 2µl of each probe was incubated with 8µl RNA loading dye and incubated at 95°C for 2 minutes to destabilise any secondary structure, before loading onto the gel and separating at 200V in 1x TBE buffer. The gel was exposed to film for 5-10 minutes to visualise the RNA.

2.7.2 RNA Electrophoretic Mobility Shift Assay (R-EMSA)

The EMSA binding reactions were each carried out in a volume of 10µl using 5x-binding buffer (50mM hepes [4-(2-hydroxyethyl)-1-piperazineethanesulfonic acid] pH7.2, 15mM $MgCl_2$, 25% glycerol, with freshly-added 5mM DTT). The binding

reaction contained 0.1mg/ml bovine liver rRNA, 25µg HepG2 cytosolic protein, 100mM KCl, and 100,000 cpm labelled RNA probe in 1x Binding Buffer and were incubated at room temperature for 15 minutes. Controls of each probe without any protein added were also used. The reactions were incubated for a further 10 minutes with 5µg/µl heparin. After the addition of 2µl of RNA loading buffer (48.5% glycerol, 0.5% bromophenol blue, 0.5% xylene cyanol) the samples were separated on a non-denaturing polyacrylamide gel.

2.7.2.3 Non-Denaturing Gel Electrophoresis

Samples were separated on a 4% non-denaturing polyacrylamide gel (60:1 acrylamide:bis-acrylamide) at 200V, for 5 hours in 0.5x TBE (44.5mM Tris-HCl, 44.5mM boric acid, 1mM EDTA, pH 8). This gel had been pre-run at 200V for 20 minutes to ensure a constant voltage for the EMSA. After electrophoresis, the gel was fixed for 20 minutes with destaining solution (20% methanol, 10% glacial acetic acid), dried for 1 hour at 70°C on 3mm Whatman paper, and exposed to film for up to 3 days at -70°C.

Reagent	**Volume**
40% acrylamide	2.95ml
2% bis-acrylamide	0.98ml
TBE 10x buffer	1.5ml
Ammonium persulphate (25%)	60µl
TEMED	60µl
H_2O	24.45ml

Table 2-20 4% polyacrylamide (60:1 acrylamide:bis-acrylamide) gel

2.7.3 UV-Crosslinking

As for the EMSAs, the UV-crosslinking reactions were carried out in a volume of 10µl, containing 0.1mg/ml bovine liver rRNA, 25µg HepG2 cytosolic protein, 50mM KCl, and 100,000 cpm labelled RNA probe in 1x binding buffer. The reactions were incubated at room temperature for 15 minutes. After which, heparin was added to a final concentration of 5µg/µl, and the reaction was incubated for 15 minutes at room temperature. The microtitre plate was placed on ice and exposed twice to 8600J of Ultraviolet (UV) radiation using a UVC 500 UV Crosslinker (Amersham Lifesciences), which cross-linked any RNA which had bound to the cytosolic proteins. The free RNA and the RNA not protected by cross-linked proteins were digested by incubating the reactions with 4µg of RNase

A and 1U of RNase T1 in RNase dilution buffer (10mM Tris-HCl pH7.5, 1mM $MgCl_2$, 100mM KCl) at 37°C for 30 minutes. Samples were denatured prior to SDS-PAGE analysis by the addition of 5µl of 4x loading buffer (125mM Tris, 20% (v/v) glycerol, 4% (w/v) 2-mercaptoethanol, 0.04% (w/v) bromo-phenol blue) and incubated for 5 minutes at 80°C. The reactions were loaded onto a 10% pre-run SDS-polyacrylamide gel, and electrophoresed at 200V in 1x SDS buffer (25mM Tris, 50mM glycine, 0.1% SDS) until the dye front had reached the bottom of the gel (see section 2.3.2). The gel was fixed by incubating in destaining solution (20% methanol, 10% glacial acetic acid) for 10 minutes and dried for 1 hour at 70°C on 3mm whatman paper. The gel was exposed to X-ray film overnight to up to 3 days at -70°C.

CHAPTER 3

Analysis of the human major and minor ALAS1 5'-UTRs

3.1 Introduction

The organisation of the human ALAS1 gene is similar to the orthologous rat, mouse and chicken genes, except that it contains two non-coding exons (1A and 1B) in its 5'-UTR. This is unlike the rat gene, which contains one (Yomogida *et al.,* 1993), and the chicken, which has no non-coding exons in its 5'-UTR, as explained in the general introduction (Yomogida *et al.,* 1993; Maguire *et al.,* 1986). Roberts *et al* have shown that exon 1B of the human gene is alternatively spliced resulting in two mRNA species: a major one, in which it is omitted, and a minor one containing both exons 1A and 1B (figure 1-8 in the general introduction). This longer minor mRNA is present in all tissues and cell lines that have so far been examined, and represents approximately 10% of the steady state concentration of ALAS1 mRNA (Roberts & Elder, 2001).

Intron 1 of the rat and mouse ALAS1 genes contains sequences that are very similar to the splice donor and acceptor sites of exon 1B in the human gene. However, there is a crucial difference in that the human gene contains an A nucleotide that creates a splice acceptor site in place of the C or T nucleotides in the other species. The inclusion of exon 1B in the minor transcript of the human gene extends its 5'-UTR by 177bp to a minimum of 304bp. Alternative splicing is unlikely to have a significant role in the basal expression of ALAS1, as the percentage of the minor transcript is similar in all tissues (Roberts & Elder, 2001). However, the possibility that it may modulate expression of the downstream mRNA has not yet been explored. Very little is known about the molecular mechanisms that determine either the basal or the drug-induced, tissue-specific regulated transcription of mammalian ALAS1 genes.

It has been reported for various genes, such as pyruvate carboxylase (PC), that increasing the length of the 5'-UTR alters translational efficiency (Jitrapakdee *et al.,* 1998). PC catalyzes the ATP-dependent carboxylation of pyruvate to oxaloacetate, the first regulated step in the gluconeogenic pathway. There is only one copy of the pyruvate carboxylase PC gene (Webb *et al.,* 1997), it generates several forms of PC mRNA, which diverge at their 5'-UTRs but share the same open reading frame encoding a 1178-residue polypeptide (Jitrapakdee *et al.,* 1996). Two tissue-specific promoters are responsible for the production of two primary transcripts, which then are differentially spliced (Jitrapakdee *et al.,* 1998).

Similar to the above example, translational efficiency may be affected by alternative splicing in ALAS1. If this is so, then any change in the proportion of transcripts during induction, or any effect of 5'-UTR lengthening on stability towards haem, provides a potential mechanism for the fine control of its regulated expression. Alternative splicing of exon 1B of ALAS1 does not appear to be specific to a particular tissue or cell line. Both transcripts have been detected by RT-PCR in mRNA from human brain and liver and from K562, HeLa, HepG2 and B-lymphoblastoid cell lines (Roberts & Elder, 2001).

The approach to assessing the differences between the ALAS1 mRNA isoforms involved the analysis of the two different 5'-UTRs in response to haem. Semi-quantitative RT-PCR was used to look at mRNA levels directly, whilst the dual luciferase reporter assay (DLRA) was used to compare ALAS1 expression.

3.1.1 The Dual Luciferase Reporter Assay

Genetic reporter systems are widely used to study eukaryotic gene expression and cellular physiology, and dual reporters are commonly used to improve experimental accuracy. Therefore this assay seemed particularly useful to assess the difference between the expression of the major and minor ALAS1 mRNA isoforms.

Dual luciferase reporter assays involve the simultaneous expression and measurement of two individual reporter enzymes within a single system. The 'experimental' reporter is correlated with the effect of specific experimental conditions, while the activity of the co-transfected 'control' reporter provides an internal control that serves as the baseline response. Normalising the activity of the experimental reporter to the activity of the internal control minimizes experimental variability caused by differences in cell viability or transfection efficiency.

In the Dual Luciferase Reporter Assay system the activities of firefly (*Photinus pyralis*) and *Renilla* (*Renilla reniformis*) luciferases are measured sequentially from a single sample. The firefly luciferase is measured first by adding Luciferase Assay Reagent II (LAR II) to generate a stabilised luminescent signal. After quantifying the firefly luminescence, this reaction is quenched, and the *Renilla* luciferase reaction is initiated by simultaneously adding Stop & Glo Reagent to the same tube. This reagent produces a stabilised signal from the *Renilla* luciferase.

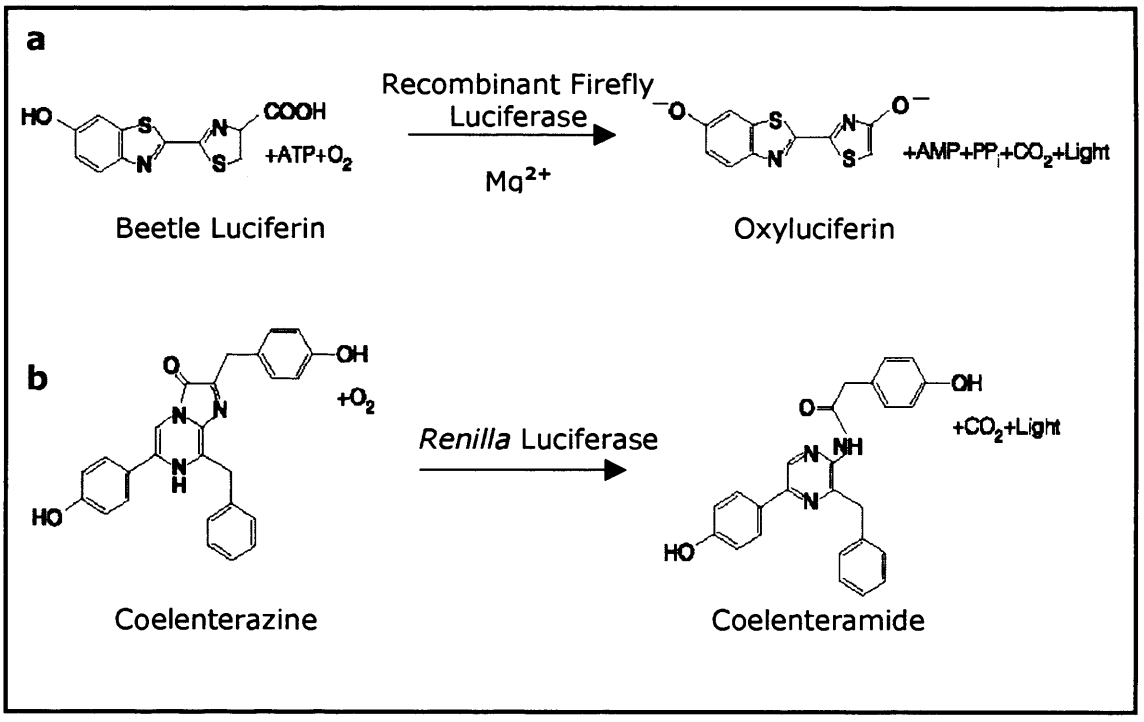

Figure 3-1 Bioluminescent reactions catalysed by firefly and *Renilla* luciferases (adapted from www.promega.com).

a) Photon emission is achieved through oxidation of beetle luciferin in a reaction that requires ATP, Mg^{2+} and O_2. The oxidation occurs through a luciferyl-AMP intermediate that turns over very slowly. As a result, this assay chemistry generates a 'flash' of light that rapidly decays after the substrate and enzyme are mixed.

b) The luminescent reaction of *Renilla* luciferase utilises O_2 and coelenterate-luciferin (coelenterazine). This reaction provides a stabilised luminescent signal that decays slowly over the course of the measurement.

3.1.1.2 Firefly and Renilla luciferases

Firefly and *Renilla* luciferases have distinct evolutionary origins and therefore have dissimilar enzyme structures and substrate requirements, making it possible to selectively discriminate between their respective bioluminescent reactions.

Firefly luciferase is a 61kDa monomeric protein that does not require post-translational processing for enzymatic activity. Therefore, it functions as a genetic reporter immediately upon translation. *Renilla* luciferase is a 36kDa protein, and similar to firefly luciferase, post-translational modification is not required for its activity. The enzyme may function as a genetic reporter immediately following translation.

Firefly and *Renilla* luciferase vectors may be used to co-transfect mammalian cells, and either firefly or *Renilla* luciferase may be used as the control or experimental reporter gene.

3.1.2 Aims and Strategy

It is not known how haem affects the expression of the two different ALAS1 isoforms. Therefore, the major aim of the work in this chapter was to determine whether both ALAS1 mRNA transcripts were destabilised by haem in HepG2 cells and the reasons for this.

This involved:

1. Assessing the stability of the minor and major 5'-UTR mRNA in response to haem.
2. Investigating whether the 5'-UTR affects expression of the downstream heterologous firefly luciferase gene.

In order to achieve these aims, semi-quantitative RT-PCR was used to assess the stability of the major and minor 5'-UTR in response to haem in HepG2 cells. ALAS1-*Renilla* luciferase fusion constructs were also used to determine how the differing 5'-UTRs affects expression of the downstream luciferase gene in response to haem.

3.2 Materials and Methods

This section details the specific materials and methods used in the experimental procedures adopted in the work for this chapter. General materials and methods are detailed in chapter 2.

The core promoter of the human ALAS1 gene contains multiple transcription start sites that are used in a tissue-specific fashion to produce transcripts of different lengths in brain and liver. There are six major transcription initiation start sites in the human and rat ALAS1 gene. However, in the liver, the majority of ALAS1 transcription is initiated from one specific initiation site, approximately 25bp downstream from the TATA element, demonstrated by primer extension analysis and S1 nuclease protection assay. This position is used for greater than 98% of both basal and induced transcription in rat liver. Transcription from upstream sites is less than 2% of the total and not significantly increased during induction. Basal transcription in human liver is also mainly from the same start site (Roberts & Elder, 2001). Therefore, the primers used throughout this chapter were designed to amplify the ALAS1 5'-UTR from the commonly used transcriptional start site in human liver cells.

3.2.1 Semi-Quantitative RT-PCR

To investigate the effect of haem upon the stability of the ALAS1 mRNAs, HepG2 cells were treated with/without haem for up to 8h. HepG2 cells were split into 6-well plates and when approximately 60% confluent, treated with 20μM haem or control medium with actinomycin D (5μg/ml) to inhibit transcription, and harvested at 0h, 1h, 2h, 4h and 8h when total RNA was isolated using Ultraspec, and its concentration and purity determined spectrophotometrically at 260 and 280nm. For RT-PCR, first strand cDNA synthesis was achieved by incubation at 42°C for 1h using 200U MMLV-reverse transcriptase with 2μg total RNA primed by oligo$(dT)_{15}$. Changes in mRNA expression were quantified by PCR with HotStarTaq polymerase (table 3-2).

The two ALAS1 mRNAs was amplified specifically using different sense primers corresponding to the sequences across the exon 1A/1B boundary (primer P1) or the exon 1A/2 boundary (P2), to minimise competition for the two cDNA templates, and an antisense primer (P3) derived from the sequence in exon 3 (figure 3-2). The conditions were optimised for logarithmic amplification using

untreated control cells (section 3.2.1.1). To ensure results were normalised for equivalent concentrations of RNA, a 404bp GAPDH cDNA fragment was also amplified using sense (P4) and antisense (P5) primers (table 3-1). All primer sequences are listed in appendix 4.

Target DNA	Primer Number	Product Size
ALAS1 minor 5'-UTR	Sense - P1, Anti-sense - P3	559bp
ALAS1 major 5'-UTR	Sense - P2, Anti-sense - P3	380bp
GAPDH	Sense - P4, Anti-sense - P5	404bp

Table 3-1 Semi-quantitative RT-PCR

Primer sets used to amplify ALAS1 major, ALAS1 minor and GAPDH cDNA with their respective sizes.

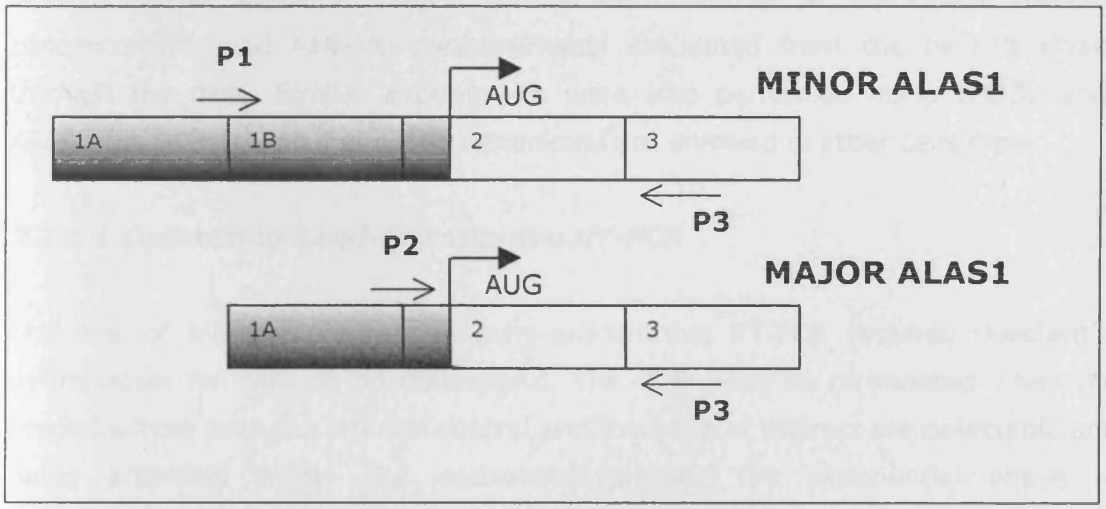

Figure 3-2 Primer Design to Differentiate ALAS1 5'-UTRs

To detect and distinguish between the major and minor ALAS1 5'-UTRs, primers were designed which corresponded to sequences across the exon boundaries of exons 1A and 1B (P1) and exons 1A and 2 (P2). This minimised competition between the two cDNA templates. The same anti-sense primer (P3) in exon 3 was used for both.
Only the 5'-UTR and the beginning of the ALAS1 coding region (exons 2 and 3) are shown.

The PCR of GAPDH was performed in a separate reaction, using primers P4 and P5, with HotstarTaq polymerase, and the conditions described in section 2.4.4.3.1. The cycling protocol for the PCRs was that as described in section 2.4.4.3.1, with 32 cycles, and annealing temperatures of 64°C (table 3-2).

Reagent	Volume (µl)
10x PCR buffer	5
2mM dNTP mix	5
P1 5pmol	5
P2 5pmol	5
P3 5pmol	5
DNA Template (RT product)	5
HotStarTaq Polymerase (5U/µl)	1
H_2O	to 50µl

Table 3-2 Composition of the multiplex RT-PCR

The PCR products were resolved by agarose gel electrophoresis and the band intensities of the products were quantified as raw volume of the peak intensity using Gene Tools software (Syngene), and normalised to GAPDH to calculate the relative mRNA stability. Decay curves were plotted at equivalent GAPDH concentrations and half-life measurements calculated from the best-fit slope through the data. Similar experiments were also performed using IMR32 and K562 cells to establish if similar mechanisms are involved in other cells types.

3.2.1.1 Optimising Semi-Quantitative RT-PCR

The use of internal controls in semi-quantitative RT-PCR requires substantial optimisation for data to be meaningful. The PCR must be terminated when the products from both the internal control and the gene of interest are detectable and being amplified within the exponential phase. The exponential phase of amplification occurs when the reaction components are still in excess and the PCR products are accumulating at a constant rate, so that the quantity of products are proportional to the amount of starting target nucleic acid. To do this, PCRs were set up with a cycle number of 35, with reactions removed from the thermal cycler at cycle numbers ranging from 28 to 35, and resolved by agarose gel electrophoresis. Gene Tools software was used to quantify the intensity of the PCR product, and the PCR cycle number was then plotted against the natural log of the PCR intensity. When a straight line is obtained the samples are in the exponential phase of amplification, and at this cycle number the PCR can be used to quantify the products. This optimisation of PCR cycle number was used for all semi-quantitative PCRs within this thesis (data not shown).

3.2.2 PCR and Plasmid Construction

To investigate the role of the ALAS1 5'-UTRs in haem-mediated stability and to determine their effects upon translation, cDNA fragments for both the major and minor mRNAs were amplified and inserted into the firefly containing vectors, pGL3P and pGL3B (figures 3-3 and 3-4).

Both the major and minor ALAS1 5'-UTR sequences were amplified by PCR from HepG2 cDNA, from the major hepatic transcription start site in exon 1 to the initiating ATG in exon 2, using the sense primer P6 and the antisense primer P7, with 1U of Bio-X-Act Long Polymerase. These primers contained the *Hind* III (A↓AGCT) and *Nco* I (C↓CATGG) restriction sites, respectively (table 3-3). The cDNAs were subsequently purified using a QIAquick PCR Clean-up Kit and cloned into the pGEM-T vector. Recombinant plasmid DNA was purified using a QIAprep spin kit and the identities of the clones for the long and short 5'-UTRs confirmed by automated fluorescent sequencing using Big Dye chemistry and analysis on an ABI Prism 3100 genetic analyser. Inserts from positive clones were removed by digestion with *Hind* III and *Nco* I and subcloned into *Hind* III/*Nco* I digested pGL3-Promoter and Basic vectors (figure 3-3). The *Nco* I site contains the initiating ATG of firefly luciferase thereby excluding any vector-derived 5'-UTR sequence.

Target DNA	Primer Number	Restriction Site	Product Size
ALAS1 mRNA exon 1A - 2	Sense - P6,	*Hind* III	Major ALAS1 = 118bp
	Anti-sense - P7	*Nco* I	Minor ALAS1 = 295bp

Table 3-3 Primers used to amplify the major and minor ALAS1 5'-UTRs, and the restriction enzyme sites within these primers.

To test for intrinsic transcriptional activity, these same ALAS1 fragments were ligated into *Hind* III/*Nco* I digested pGL3-basic vector, which lacks eukaryotic promoter and enhancer sequences (figures 3-3 and 3-4).

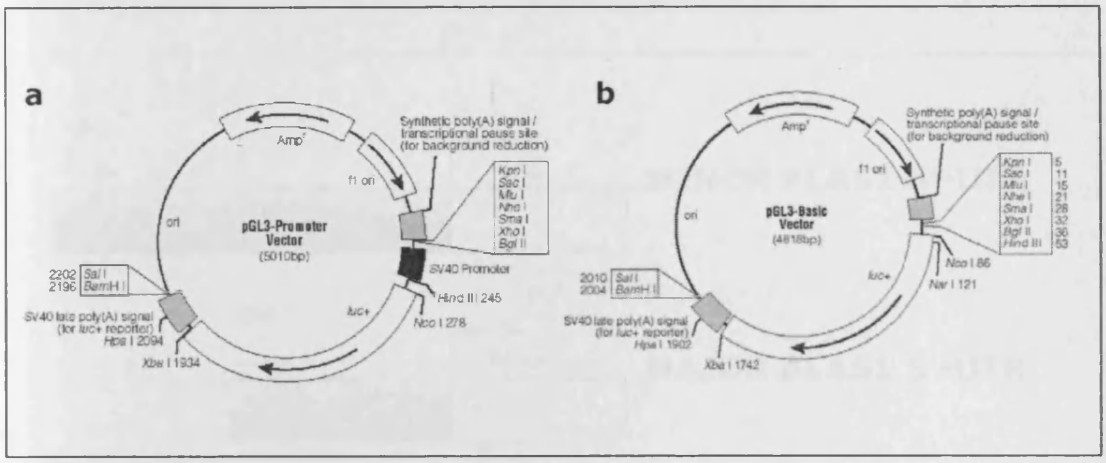

Figure 3-3 Vector maps of pGL3-Promoter and pGL3-Basic.

a) Vector map of the firefly luciferase expression vector pGL3-P from www.promega.co.uk

The pGL3-P vector contains an SV40 promoter upstream of the luciferase gene. DNA fragments containing putative enhancer elements can be inserted either upstream or downstream of the promoter-*luc*+ transcriptional unit.

b) Vector map of the firefly luciferase expression vector pGL3-B from www.promega.co.uk

The pGL3-Basic Vector lacks eukaryotic promoter and enhancer sequences, allowing maximum flexibility in cloning putative regulatory sequences. Expression of luciferase activity in cells transfected with this plasmid depends on insertion and proper orientation of a functional promoter upstream from *luc*+. Potential enhancer elements also can be inserted upstream of the promoter or in the BamHI or SalI sites downstream of the *luc*+ gene.

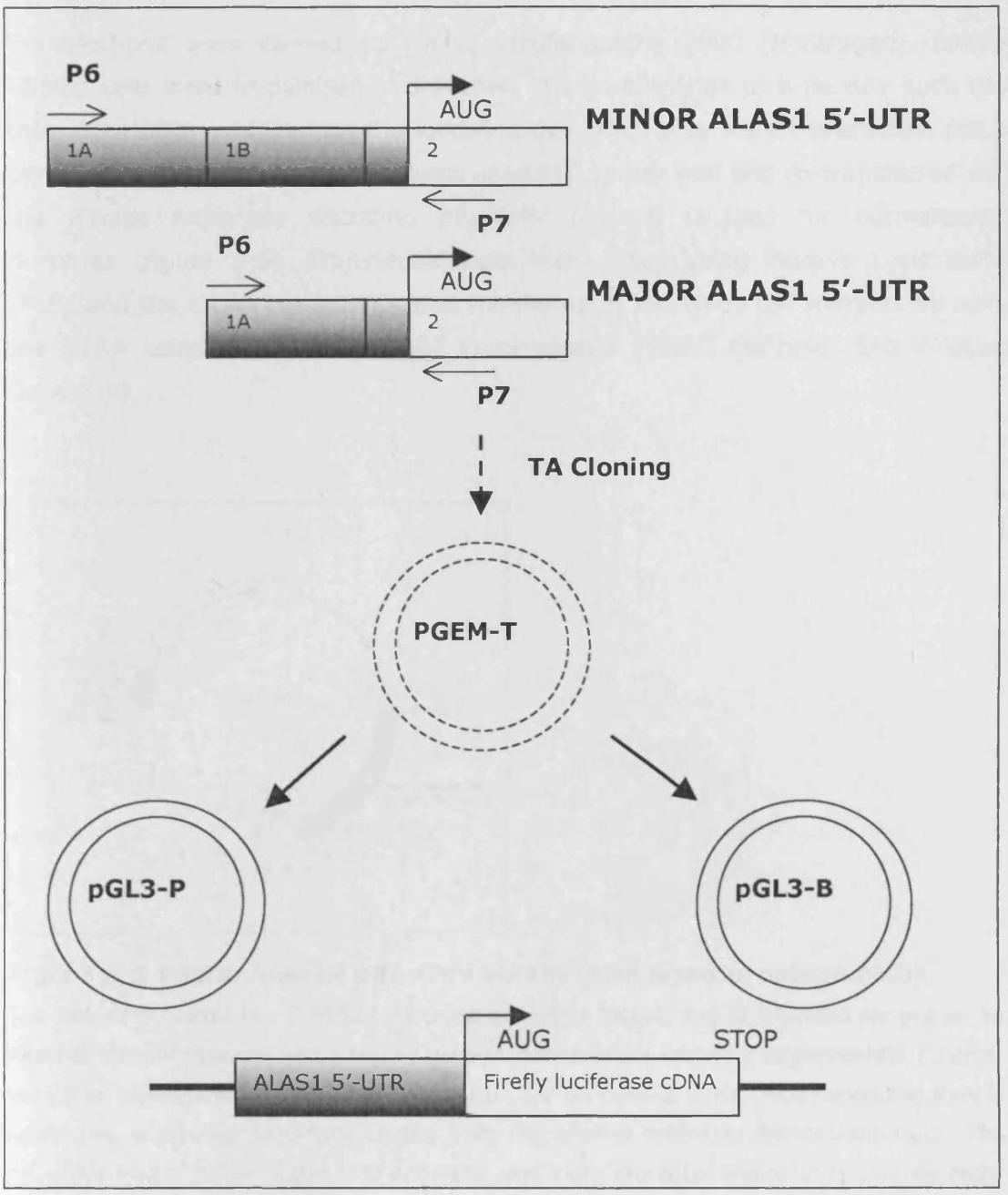

Figure 3-4 Generation of the ALAS1 5'-UTR – Firefly expression vectors.

The major and minor ALAS1 5-UTRs were amplified from HepG2 cDNA from the major hepatic transcription site in exon 1A to the initiating ATG in exon 2. Following TA cloning into pGEM-T, the ALAS1 fragments were excised with appropriate restriction enzymes and cloned into both pGL3-P and pGL3-B at the 5'end of the firefly luciferase gene. The ALAS1 sequences essentially formed the 5'-UTR of the luciferase gene, with the initiating codon derived from the *Nco*I site in the antisense P7 primer.

3.2.3 Transfections and Dual Luciferase Reporter Assay

Transfections were carried out using Lipofectamine 2000 (Invitrogen). Briefly, HepG2 cells were trypsinised and seeded in 12-well plates at a density such that they were 80% confluent on the following day when they were transfected. pGL3-derived experimental constructs were used at 1μg per well and co-transfected with the *Renilla* luciferase encoding pRL-CMV plasmid (0.1μg) for normalisation purposes (figure 3-5). Transfected cells were lysed using Passive Lysis Buffer (PLB) and the luciferase activity was monitored in the lysed cell extracts by using the DLRA using a Lumat LB 9507 Luminometer (EG&G Berthold, Bad Wildbad, Germany).

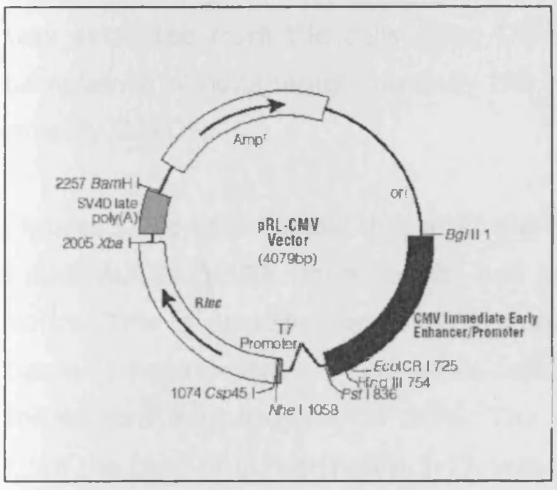

Figure 3-5 Vector map of pRL-CMV vector from www.promega.co.uk.

The pRL-CMV Vector is a *Renilla* Luciferase encoding vector, and is intended for use as an internal control reporter and may be used in combination with any experimental reporter vector to co-transfect mammalian cells. pRL-CMV contains a cDNA (R*luc*) encoding *Renilla* luciferase, which was originally cloned from the marine organism *Renilla reniformis*. The pRL-CMV Vector contains the CMV enhancer and early promoter elements to provide high-level expression of *Renilla* luciferase in co-transfected mammalian cells.

3.3 Results and Discussion

3.3.1 The ALAS1 minor isoform is resistant to haem-mediated decay.

The alternative splicing of the human ALAS1 gene generates two mRNA species: a major one, in which exon 1B is omitted, and a ubiquitously expressed minor one containing both exons 1A and 1B, accounting for only 10% of the steady-state concentration of ALAS1 mRNA (Roberts & Elder, 2001).

To determine whether the major and minor ALAS1 mRNA isoforms were destabilised similarly when exposed to haem, HepG2 cells were subjected to treatment with 5μg/ml actinomycin D to induce transcriptional arrest, and 20μM haemin (or control medium) for up to 8 hours. At specific time points, total RNA was extracted from the cells using Ultraspec. RT-PCR was quantified on all the samples to simultaneously amplify the major and minor ALAS1, and separately amplify GAPDH.

Figures 3-6 and 3-7 show that after the addition of exogenous haem, levels of the major ALAS1 mRNA (lower band) had fallen to 15% of their original levels by 8 hours. This is unsurprising, as it is known that ALAS1 mRNA is destabilised by haem in hepatocytes. In untreated cells, however, the level of the major ALAS1 mRNA had only dropped to 50%. The major ALAS1 mRNA half-life, calculated from the best-fit curve (figure 3-7), was reduced more than two-fold from 6.5h in untreated cells to 2.9h in cells exposed to haem.

In contrast to the major ALAS1 isoform, levels of the minor ALAS1 mRNA (upper band) remained essentially unchanged throughout the duration of the experiment in both the haem-treated and untreated control cells. Therefore, unlike the major ALAS1 form in HepG2 cells, the minor form is resistant to haem-mediated decay, under these experimental conditions. After 8 hours the mRNA of the minor and major ALAS1 isoforms had both decayed, even without haem. This is most probably due to the actinomycin D added to inhibit transcription, and therefore eventually becoming toxic to the cells. Furthermore, a peak in the mRNA concentration is observed in both isoforms at the timepoint t_1. Again, this affect may be attributed to the actinomycin D, rather than a haem effect.

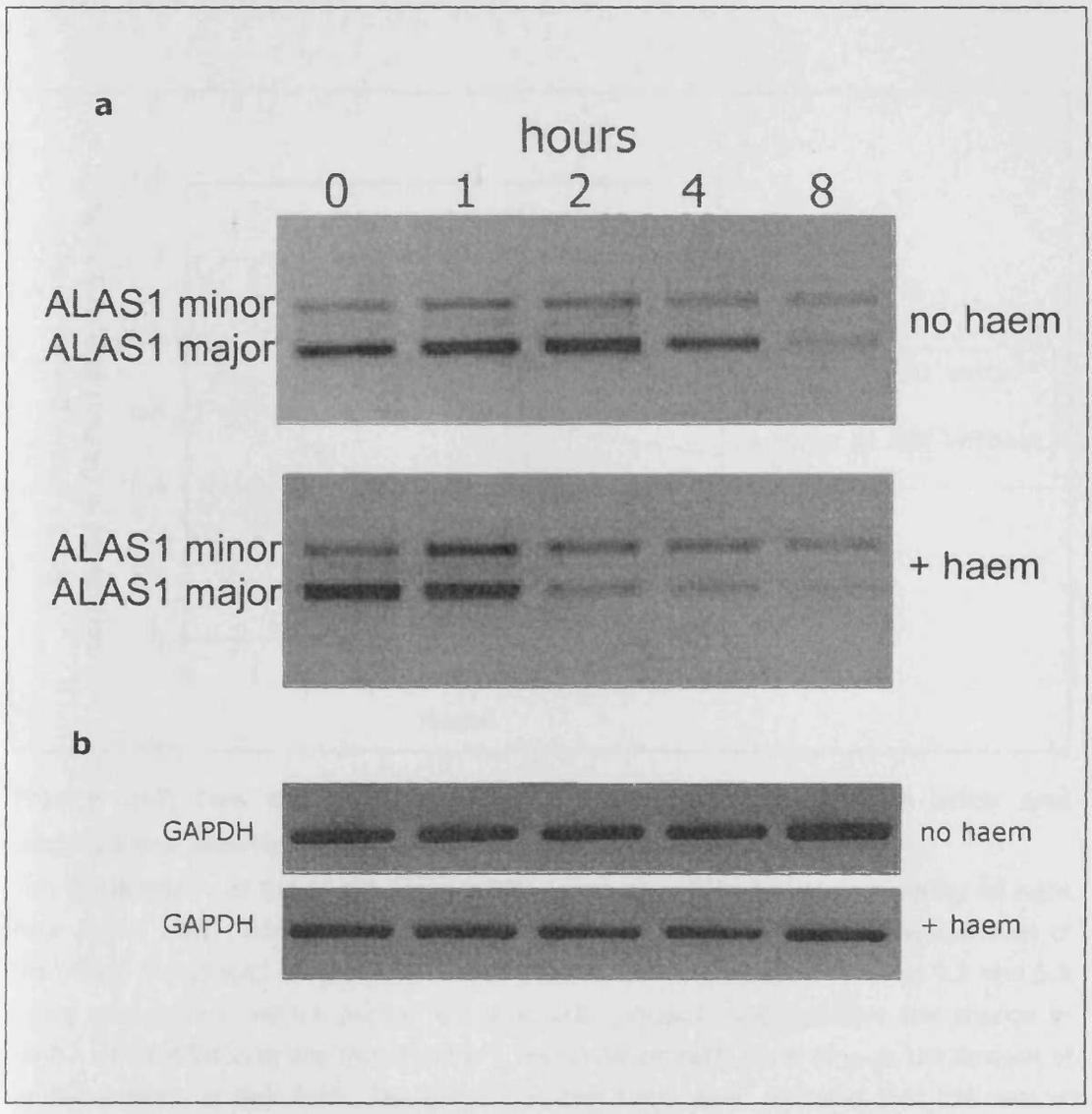

Figure 3-6 ALAS1 Major mRNA is destabilised by haem, whereas the minor ALAS1 mRNA remains relatively stable.

a) Differential detection of endogenous ALAS1 mRNA was achieved by using different primer sets as shown in figure 3-2. HepG2 cells were either treated with 20μM haem or control medium for up to 8 hours, with actinomycin D (5μg/ml). Total RNA was extracted at the indicated time points and RT-PCR was used to assess the relative concentrations of ALAS1 mRNA transcripts. The bottom panel shows the results of cells exposed to haem and the upper panel those without haem.

b) Equivalent total cDNA concentrations between samples were confirmed by amplification of GAPDH cDNA.

Experiments were carried out in triplicate on three separate occasions with similar results achieved each time. The figure is from one representative experiment.

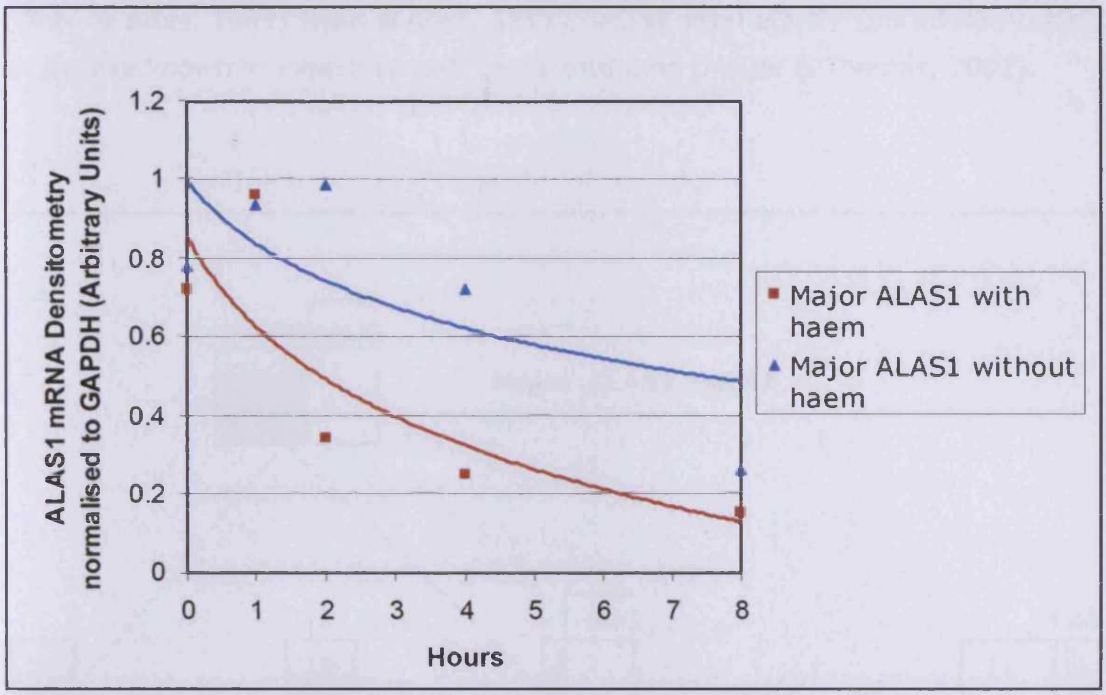

Figure 3-7 The destabilisation of the ALAS1 major mRNA with and without the addition of haem for up to 8 hours.

The densitometry of the ALAS1 major mRNA levels at specific time-points during an eight hour period were normalised to the GAPDH levels, using arbitrary units. The half-lives of the major ALAS1 with and without haem were calculated to be approximately 2.9 and 6.5 hours respectively. mRNA decay, is a stochastic process, and therefore the change in mRNA concentration at any time point is a first-order process, depending on the amount of mRNA present at that time. The graph has two linear axes, showing that the rate of change of mRNA concentration changes over time and is proportional to the amount of mRNA present at that time-point. Data is from one representative experiment.

Decay curves for the major ALAS1 mRNA were plotted at equivalent GAPDH concentrations and $t_{1/2}$ measurements calculated from the best-fit slope through the data. No calculations were made for the minor ALAS1 mRNA since its stability was relatively unaffected by haem.

An explanation for this contrasting stability between the major and minor ALAS1 isoforms is that haem regulation is mediated through a *cis*-acting element located within exons 1A and 2 of the 5'-UTR, which is disrupted in the minor ALAS1 mRNA due to the inclusion of exon 1B. This hypothesis is shown diagrammatically

in figure 3-8. An alternative explanation is that the haem-insensitivity of the minor ALAS1 mRNA might be a result of reduced translation, since inhibition of protein synthesis has been shown to prevent haem-mediated ALAS1 mRNA decay (Drew & Ades, 1989; Ryan & Ades, 1991), whilst alternatively spliced non-coding exons are known to inhibit downstream translation (Meijer & Thomas, 2002).

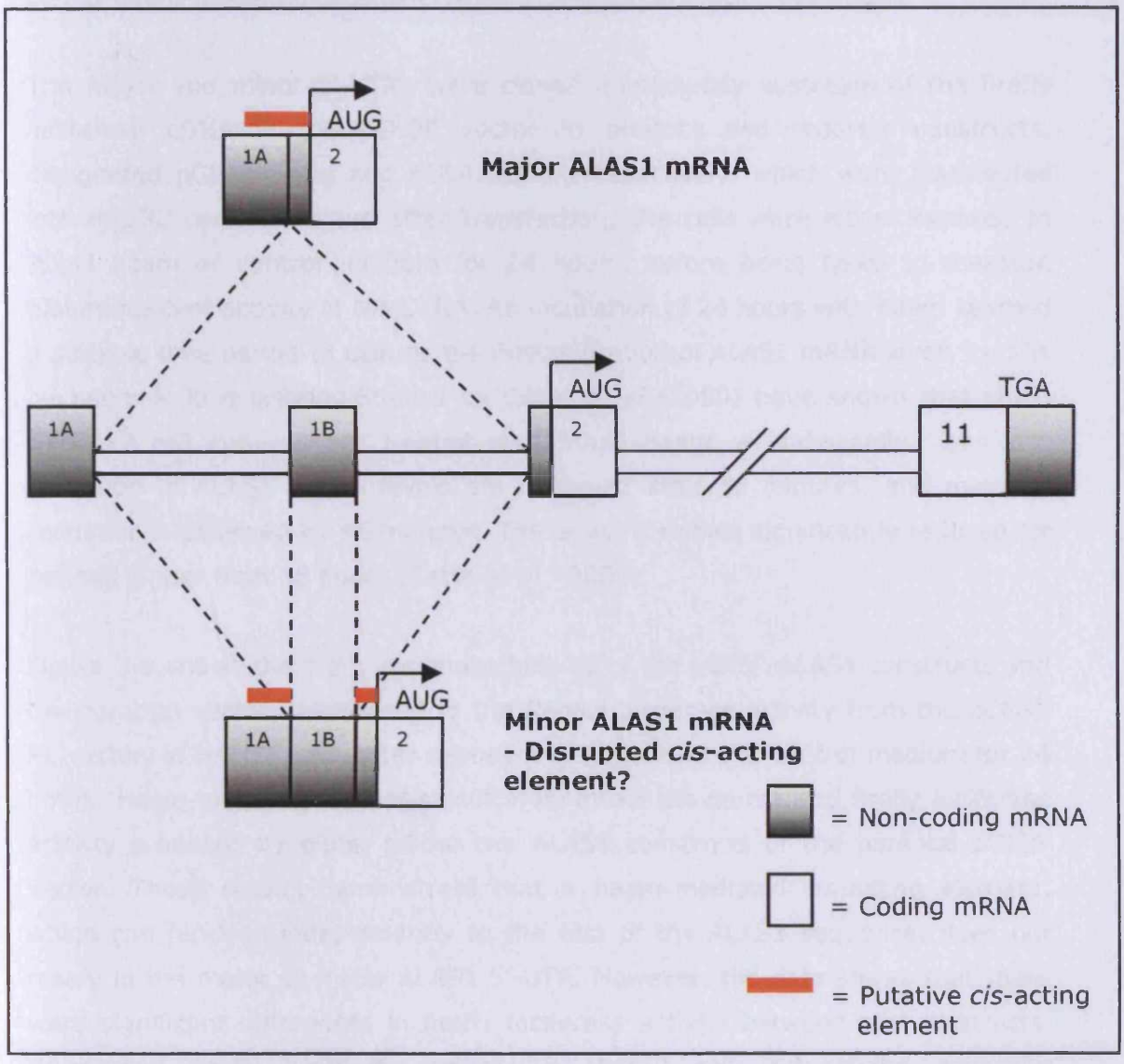

Figure 3-8 Major and Minor ALAS1 5'-UTRs.

Diagram of exons 1A - 2 in the major and minor forms of ALAS1, and a putative haem mediated *cis*-acting element across exons 1A and 2 in the major 5'-UTR. This would be disrupted by the exon 1B in the minor 5'-UTR.

3.3.2 The ALAS1 5'-UTR does not harbour a destabilising element, but the minor isoform inhibits expression of the downstream reporter gene.

It is hypothesised that exon 1B disrupts a *cis*-acting element, and therefore the minor ALAS1 is not destabilised by haem. To test this, heterologous luciferase reporter assays were used to determine if both the ALAS1 5'-UTRs were able to confer haem-mediated sensitivity on the downstream luciferase mRNA.

The major and minor 5'-UTRs were cloned immediately upstream of the firefly luciferase cDNA in the pGL3P vector to produce two reporter constructs, designated pGLALASmaj and pGLALASmin respectively, which were transfected into HepG2 cells. 24 hours after transfection, the cells were either exposed to 20μM haem or control medium for 24 hours, before being lysed to measure bioluminescent activity in the DLRA. An incubation of 24 hours with haem seemed a suitable time period to use, as the destabilisation of ALAS1 mRNA levels in cells by haem is long-lasting. Studies by Cable *et al* (2000) have shown that when CWSV17 cell cultures are treated with 10μM haem, a statistically significant reduction in ALAS1 mRNA levels are observed after 30 minutes, and maximal reduction is achieved by 45 minutes. These levels remain significantly reduced for periods longer than 18 hours (Cable *et al.,* 2000).

Figure 3-9 shows the firefly luciferase activity of the pGL3P-ALAS1 constructs and the parental vector, normalized to the *Renilla* luciferase activity from the pCMV-RL vector, in HepG2 cells, after exposure to 20μM haem or control medium for 24 hours. Haem exposure did not significantly affect the normalised firefly luciferase activity produced by either of the two ALAS1 constructs or the parental pGL3P vector. These results demonstrate that a haem-mediated *cis*-acting element, which can function independently to the rest of the ALAS1 sequence, does not reside in the major or minor ALAS1 5'-UTR. However, the data shows that there were significant differences in firefly luciferase activity between the constructs. Normalised firefly luciferase activity in HepG2 cells transfected with the pGLALASmaj construct was 4.7-fold higher than cells transfected with the parental pGL3P vector. In contrast, normalised firefly luciferase activity in cells transfected with the pGLALASmin construct was nearly 2-fold less than those transfected with pGL3P. Therefore, the minor 5'-UTR reduced the expression of the downstream firefly luciferase approximately 9-fold, compared to the major 5'-UTR.

An explanation for this difference in expression between the major and minor constructs could be that either there was variation in the firefly luciferase expression or that the minor 5'-UTR inhibits translation of the downstream mRNA.

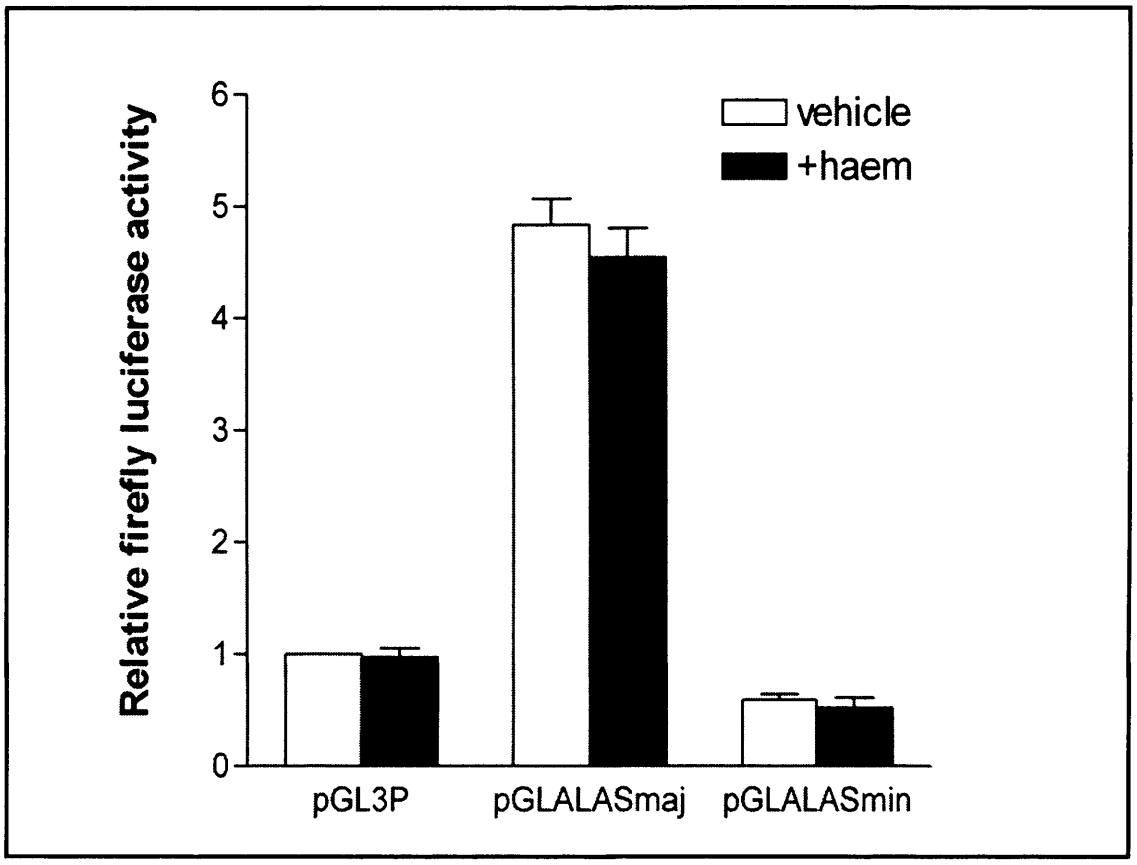

Figure 3-9 Effect of ALAS1 mRNA 5'-UTRs upon firefly luciferase activity and response to haem

The pGL3P, pGLALASmaj and pGLALASmin firefly luciferase constructs were separately co-transfected with the pRL-CMV *Renilla* luciferase vector into HepG2 cells. Luciferase activity was measured using the Dual Luciferase Reporter Assay, 48 hours after transfection. Haem was added for 24 hours before harvesting where indicated. The bars show normalised firefly luciferase activity to *Renilla* activity from pRL-CMV, relative to the pGL3P (minus haem) data, which was arbitrarily considered to be 1. Results represent mean (+ standard deviation) of at least three experiments each performed in triplicate. Statistical analysis was performed using a paired t text, and showed that that the differences plus and minus haem were not statistically significant.

3.3.3 The minor ALAS1 5'-UTR reduces translation of the downstream open reading frame.

RT-PCR was used to ensure that the differences between the firefly luciferase activities of the two ALAS 5'-UTR-firefly constructs were due to mRNA translation efficiency, and not variations in firefly luciferase mRNA expression. Cells were similarly transfected with the pGL3P constructs as in section 3.3.2, and treated with 20μM haem or control medium for 24 hours, after which the total RNA was extracted. Firefly luciferase and GAPDH mRNA were quantified by RT-PCR on cDNA samples derived from the total RNA extracted.

The RT-PCR analysis (figure 3-10) showed that there were no differences in firefly luciferase mRNA levels between cells transfected with the pGLALASmaj or PGLALASmin constructs. In both cases these were approximately 5-fold higher than those from the control pGL3-P-transfected cells. Therefore, insertion of either the major or minor ALAS1 5'-UTR does not affect transcription of the downstream firefly luciferase gene, despite there being a difference in the translation of the luciferase, as shown in the previous figure (figure 3-9).

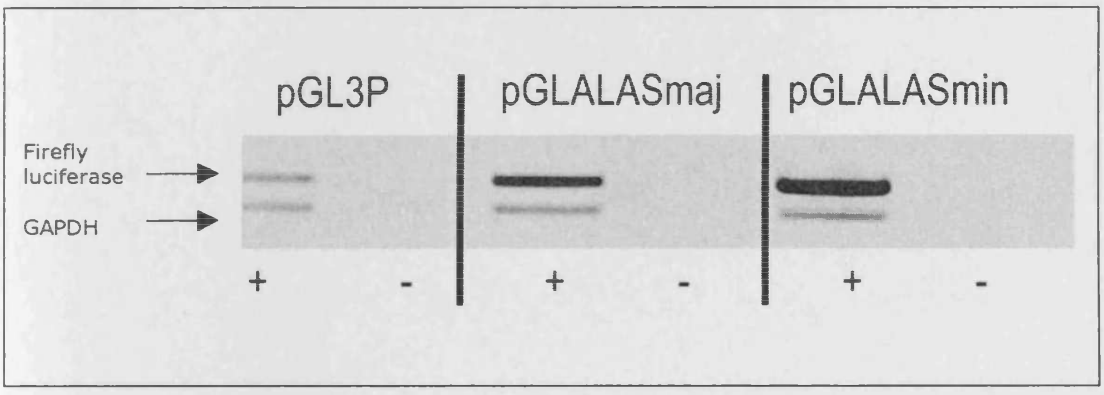

Figure 3-10 Analysis of the firefly luciferase mRNA expression and activity in HepG2 cells transfected with the pGL3-P derived constructs.
cDNA fragments for firefly luciferase (upper band) and GAPDH (lower band) were specifically amplified by RT-PCR using reverse transcribed (+) or control (no reverse transcription step) (-) DNAse I-treated total RNA from transfected HepG2 cells. The image shown is a negative contrast for purposes of clarity. Expression of firefly luciferase mRNA increased from both the pGLALASmaj and pGLALASmin 5'-UTR constructs compared to the parental vector. Experiments were performed on three separate occasions in duplicate with similar results in each case.

Figures 3-9 and 3-10 demonstrate that in pGLALASmaj-transfected cells, the increased firefly luciferase mRNA expression results in a proportionate increase in the firefly luciferase activity. In contrast, however, the increased firefly luciferase mRNA expression in pGLALASmin-transfected cells does not result in an increase in the firefly luciferase activity. The firefly luciferase mRNA expression is similar in both the pGLALASmaj- and pGLALASmin-transfected cells, but the firefly luciferase activity is approximately 90% lower in the pGLALASmin-transfected cells. This data proves that the inclusion of exon 1B in the 5'-UTR of the minor ALAS1 mRNA inhibits the translational mechanism of the downstream firefly luciferase open reading frame. Therefore, in HepG2 cells, the minor ALAS1 mRNA is comparatively poorly translated under normal conditions.

3.3.4 Confirmation of ALAS1 5'-UTR transcriptional activity

Figure 3-10 showed that there is enhanced firefly luciferase mRNA expression observed with both the major and minor ALAS1 5'-UTR constructs, and not the parental pGL3-P vector. It was next examined if this was due to the 5'-UTRs both having intrinsic transcriptional activity, using the promoter-less pGL3-basic vector.

The major and minor 5'-UTRs were cloned into pGL3-basic vector, designated pBALASmaj and pBALASmin respectively. Total RNA was extracted from HepG2 cells transfected with the pGL3B constructs after 24 hours. Firefly luciferase and GAPDH RNA was quantified by RT-PCR of the cDNA samples derived from the RNA extracted. HepG2 cells transfected with these constructs and pRL-CMV for 24 hours were also used for the DLRA, to assess the firefly luciferase activity.

Densitometry derived from RT-PCR (figure 3-11a) showed that there was no substantial firefly luciferase mRNA production and consequently no luciferase activity in cells transfected with the parental pGL3-B vector (data not shown). However, figure 3-11b demonstrates that the ALAS1 5'-UTR constructs both produced firefly activity, but the activity from the pBALASmin construct was approximately 90% lower than that from the pBALASmaj construct.

This data confirms that translation of the minor ALAS1 transcript is inhibited compared to the major ALAS1. Furthermore, this demonstrates that transcription of the ALAS1 5'-UTR constructs in the promoter-less vector pGL3B must originate from sequences upstream of exon 1B, in exon 1A, which is common to both of the ALAS1 isoforms.

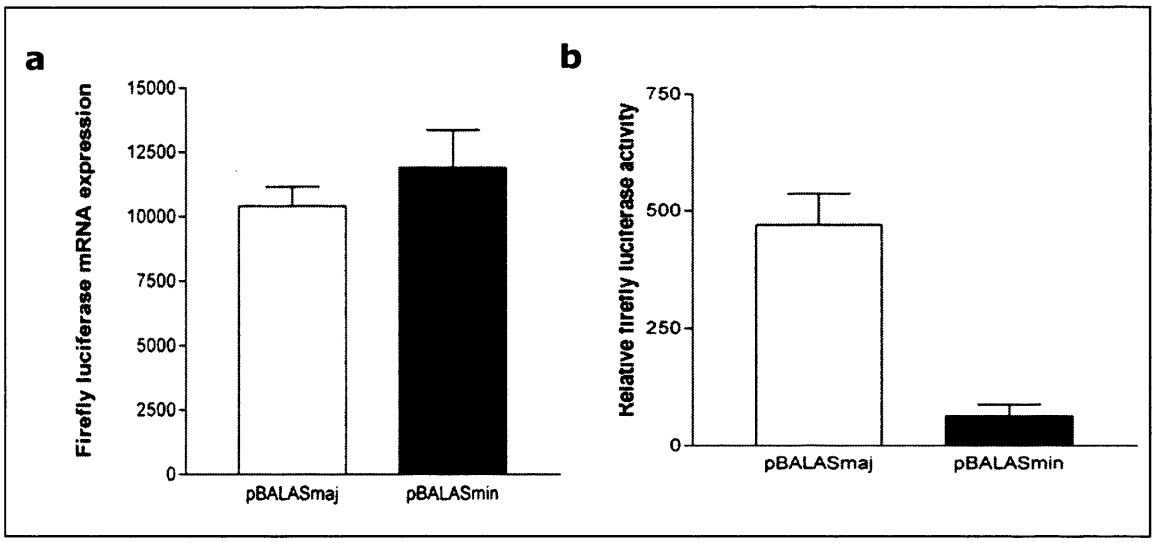

Figure 3-11 Analysis of the firefly luciferase mRNA expression and activity in HepG2 cells transfected with the pGL3-P derived constructs.

a) The cDNA fragments encoding for the major and minor 5'-UTR were ligated into the pGL3-basic vector, to produce the pBALASmaj and pBALASmin constructs. In contrast to the parental pGL3B vector (not shown), both were able to drive transcription producing firefly luciferase mRNA. Values shown on the y axis are arbitrary units from densitometric analysis which are not shown. Results shown represent mean (+ S.D.) of at least three experiments performed in triplicate.

b) The pGL3B, pBALASmaj and pBALASmin firefly luciferase constructs were separately separately co-transfected with the pRL-CMV *Renilla* luciferase vector into HepG2 cells. Luciferase activity was measured using the Dual Luciferase Reporter Assay, 48 hours after transfection. Haem was added for 24 hours before harvesting where indicated. The bars show the relative firefly activity of pBALASmaj (clear bar) and pBALASmin (solid bar), normalised to the activity of the *Renilla* luciferase vector, pRL-CMV. The activity of pBALASmin is reduced by nearly 90% compared to the pBALASmaj construct. Results shown represent mean (+ S.D.) of at least three experiments performed in triplicate.

3.3.5 Reduction in expression of downstream mRNA by the ALAS1 minor 5'-UTR is not restricted to hepatocytes.

To assess if this reduction of expression of the downstream firefly luciferase by the minor ALAS1 5'-UTR was restricted to HepG2 cells, the pGL3P derived constructs were also transfected into IMR32 and K562 cells. The results in figure 3-12 show that similar to the experiments in HepG2 cells, the expression of pGLALASmaj is approximately 4.3- and 6-fold higher than pGALASmin in IMR32 and K562 cells respectively. Therefore it can be assumed that a similar mechanism that controls the ALAS1 expression in HepG2 cells occurs in these cell types. The intrinsic promoter activity in the major ALAS1 5'-UTR, derived from exon 1A, is active in both IMR32 and K562 cells, and not restricted to HepG2 cells.

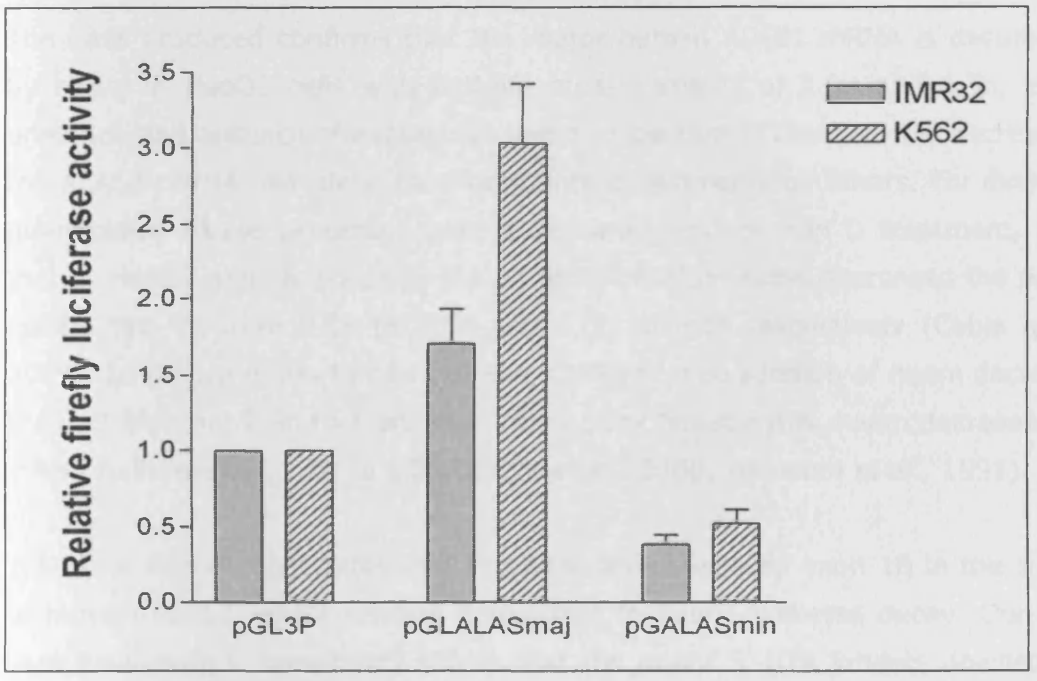

Figure 3-12 A comparison of the firefly luciferase activity of the ALAS1 5'-UTR constructs in the IMR32 and K562 cell lines.

The pGL3P, pGLALASmaj and pGLALASmin firefly luciferase constructs were separately co-transfected with the pRL-CMV *Renilla* luciferase vector into IMR32 and K562 cells. Luciferase activity was measured using the Dual Luciferase Reporter Assay, 48 hours after transfection. In contrast to the HepG2 experiments, no haem was added, as this was to compare the relative expression of the ALAS1 isoforms. The bars show normalised firefly luciferase activity relative to the pGL3P data, which was arbitrarily considered to be 1. Results represent mean (+ standard deviation) of at least three experiments each performed in triplicate. Statistical analysis was performed using a paired t text and shown not to be significantly different between the control and addition of haem.

3.4 Conclusions

In the liver and probably all other non-erythroid cells, haem supply is regulated primarily via feedback regulation of ALAS1 mRNA stability, yet the precise mechanism has not been elucidated.

There are three important observations from the data presented in this chapter:

1. Haem-dependent decay of ALAS1 is not dependent on the 5'-UTR of the mRNA.
2. The minor ALAS1 minor transcript is resistant to haem-mediated decay.
3. The inclusion of exon 1B of the minor 5'-UTR reduces translation of the downstream open reading frame.

The data produced confirms that the major human ALAS1 mRNA is destabilised by haem in HepG2 cells with half-life measurements of 2.9h and 6.5h, in the presence and absence of exogenous haem respectively. This two-fold decrease in the ALAS1 mRNA half-life is consistent with experiments by others. For example, quantitative RNase protection assays, following actinomycin D treatment, show that in HepG2 and Huh-7 cells, the addition of 20μM haem decreases the ALAS1 mRNA half-life from 8.8h to 3.5h and 6.0h to 3.6h respectively (Cable *et al.,* 2001). In the rat immortalised cell line, CWSV17, the addition of haem decreases the half-life from 2.5h to 1.3h. In primary chick hepatocytes, haem decreases the mRNA half-life from 3.5h to 1.2h (Cable *et al.,* 2000; Hamilton *et al.,* 1991).

This data also demonstrates that the alternatively-spliced exon 1B in the 5'-UTR of human ALAS1 mRNA renders it resistant to haem-mediated decay. Our work with RNA assays consistently shows that the minor 5'-UTR inhibits downstream translation. This provides a crucial insight into the underlying mechanism by which haem destabilises ALAS1 mRNA.

Regulation of mRNA stability is an important mechanism in controlling gene expression, involving complex interactions between mRNA binding proteins and *cis*-acting sequence elements, most of which are located in the 3'- or 5'-UTRs (Ross, 1995; Bevilacqua *et al.,* 2003). The resistance of the minor ALAS1 mRNA to haem-mediated decay had suggested that the inclusion of exon 1B might disrupt an important regulatory element within the 5'-UTR. This was investigated and the data showed that the ALAS1 major 5'-UTR was unable to confer haem-

mediated destabilisation on its own. However, these results do not rule out there are elements within the 5'-UTR that interact with others elsewhere in the mRNA to bring about haem-mediated decay. Yet this appears unlikely, since there is poor sequence conservation between the 5'-UTRs of the major human, rat and chicken ALAS1 mRNAs (figure 3-13), and all of which are regulated by haem (Cable *et al.*, 2001; Cable *et al.*, 2000; Hamilton *et al.*, 1991; Drew & Ades, 1989).

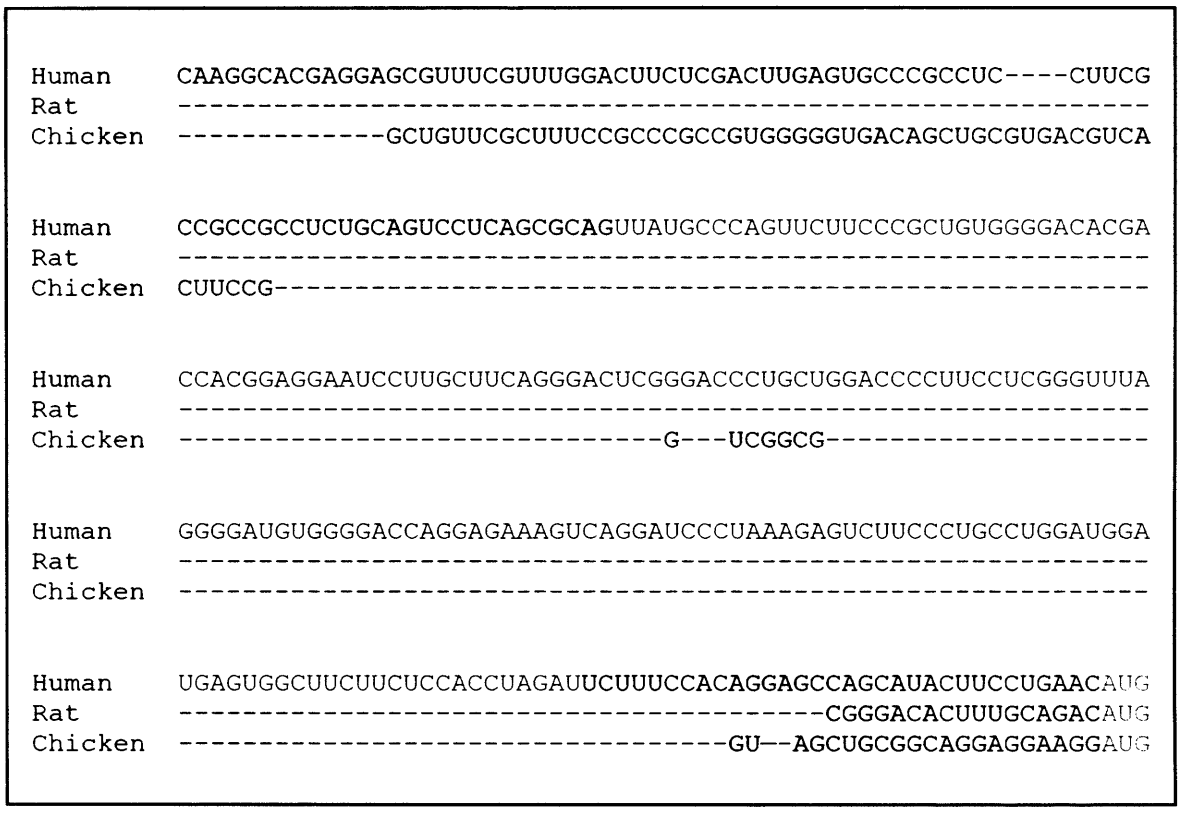

Figure 3-13 Sequences of the human, rat and chicken ALAS1 5'-UTRs.
The sequences of the 5'-UTR of ALAS1 is poorly conserved between species, even though ALAS1 mRNA is always destabilised by haem. This indicates that a haem-mediated *cis*-acting element is not present in the 5'-UTR. Blue text represents exon 1B, which is only present in the minor form of human ALAS1 mRNA. Green text represents the first AUG of the coding region sequence of each species.

The minor 5'-UTR inhibited translation of the downstream heterologous mRNA and so an alternative hypothesis is proposed, where the resistance of the minor ALAS1 mRNA to haem-mediated decay results from its inhibited translation. This alternative theory is consistent with studies where inhibitors of protein synthesis, such as cyclohexamide, have been shown to stabilise ALAS1 mRNA and block

haem-mediated decay, leading to the suggestion that the haem effect requires a labile protein (Drew & Ades, 1989; Ryan & Ades, 1991). Whilst the data does not exclude the involvement of a labile *trans*-acting factor, it suggests strongly that haem-mediated ALAS1 mRNA decay requires translation of ALAS1 mRNA itself. Such regulated co-translational mRNA degradation has been observed for β-tubulin and c-myc (Bachurski *et al.,* 1994; Lemm & Ross, 2002).

Translational control enables a cell to increase the concentration of a protein very rapidly and therefore appears to be especially suited to regulate genes implicated in cell proliferation and damage prevention. The majority of eukaryotic mRNAs are translated according to the scanning model of translation. A pre-initiation complex consisting of the ribosomal 40S subunit and several initiation factors (IFs) is assembled at the 5'-cap structure of mRNA (cap-dependent mechanism of initiation). This initiation complex then migrates along the 5'-UTR in search of an appropriate initiator AUG codon (scanning process). Recognition of an AUG leads to assembly of the 60S ribosomal subunit and initiation of protein synthesis (reviewed in Cazzola & Skoda, 2000).

The process of mRNA turnover is intimately linked to translation and numerous 5'-UTRs have been shown to regulate translation by interfering with efficient translation initiation at the physiological start site. These mRNA-specific characteristics include its size, GC content, secondary and tertiary structure, and the location of potentially active upstream open reading frames (uORFs) (Meijer & Thomas, 2002). For example, the translation of nitric oxide synthase has been shown to be regulated by an alternatively spliced 5'-UTR (Newton *et al.,* 2003). It is thought that multiple UTR's may regulate gene expression through differential expression with respect to cell type or stimulus, or their translational efficiency or stability may differentially modulate the amount of protein synthesised from their mRNAs.

The ALAS1 minor 5'-UTR sequence exhibits a number of features that might be responsible for its role in the reduced translation of the downstream mRNA. In most cases, 5'-UTRs that enable efficient translation are short, have a low GC content, are relatively unstructured and do not contain uAUG codons (Kochetov *et al.,* 1998). The inclusion of exon 1B in the minor isoform creates a much longer 5'-UTR at 303nt than the 125nt major 5'-UTR. Whilst it is not particularly GC rich at 57% compared to exon 1A having a GC content of 64%, RNA folding algorithms predict that exon 1B forms a moderately stable putative stem-loop

structure (ΔG = -38.3 kcal), which might inhibit ribosomal scanning through it (figure 3-14). Secondary structures in the 5'-UTR of several mRNAs have been shown to repress translation of those mRNAs, presumably by stalling the 'scanning' of ribosomal initiation complexes (Kozak, 1989). Studies involving insertion of synthetic oligonucleotides that form stable hairpin structures within the 5'-UTR of pre-pro-insulin (Kozak, 1986) and thymidine kinase (Pelletier & Sonenberg, 1987) mRNAs and subsequent expression in COS cells demonstrated that excessive secondary structure in the 5'-UTR represses translation.

The extent to which scanning is affected is influenced greatly by the size or stability and position of the secondary structure relative to the 5' cap. For example, a hairpin with a free energy of –30 kcal/mol situated close to the cap will impede scanning significantly. This is because secondary structure close to the cap can block access of the 43S pre-initiation complexes to the mRNA. Further from the cap, hairpins with a free energy stronger then –50kcal/mol are required to inhibit the progress of the ribosome. Such stem-loops are stable enough to resist the unwinding activity of eIF4A, the helicase component of the eIF4F complex. Although less stable stem loop can be melted by the helicase, such structures can be further stabilised by the interaction with RNA-binding proteins (Cazzola & Skoda, 2000). Therefore, the inclusion of exon 1B in the minor ALAS1 isoform may inhibit the translation of the ALAS1 protein.

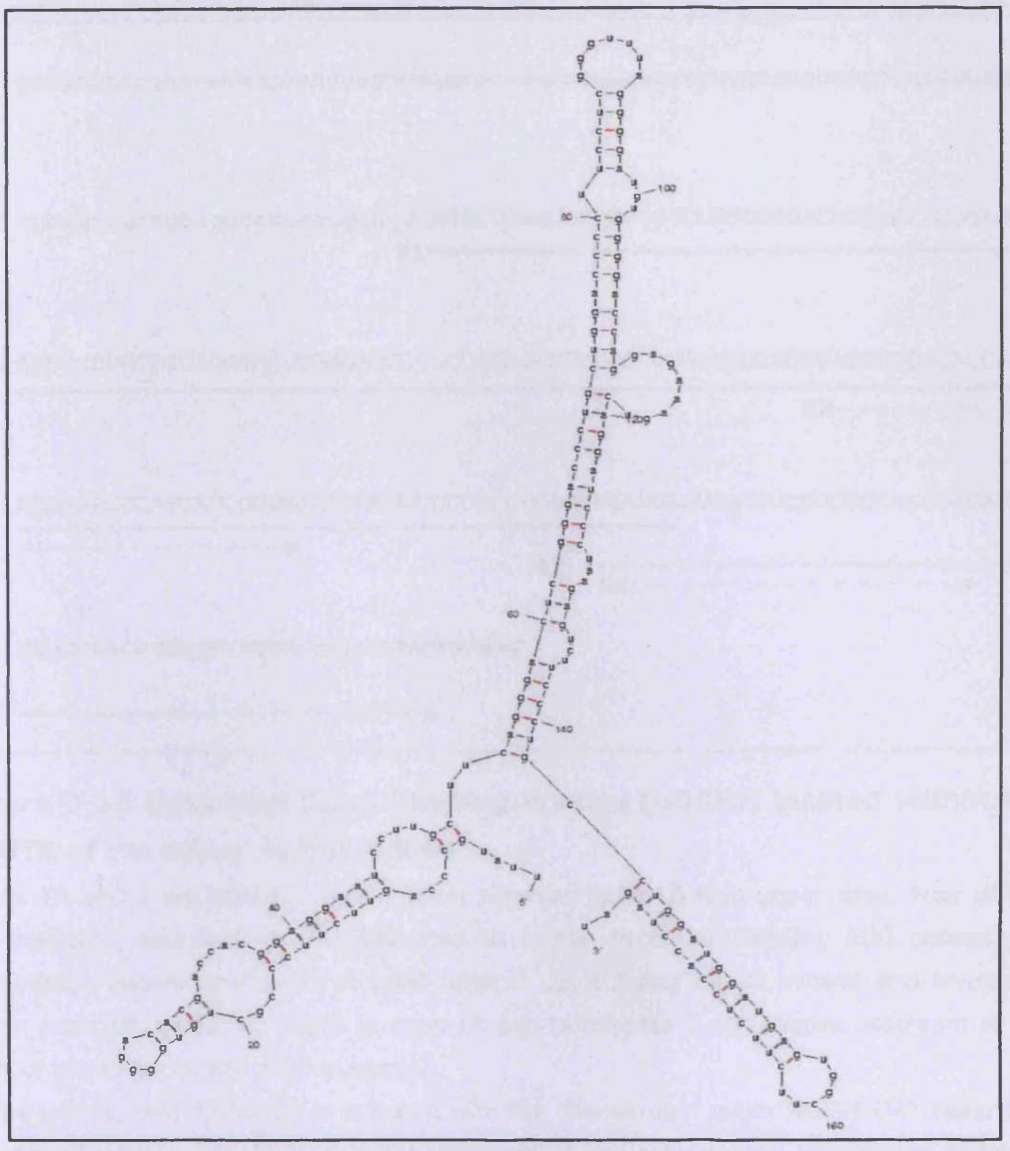

Figure 3-14 The predicted secondary structure of exon 1b in the 5'-UTR

Exon 1B is only present in the minor form of the human ALAS1 gene, in its 5'-UTR. The RNA folding software mfold (http://frontend.bioinfo.rpi.edu/applications/mfold/cgi-bin/rna-form1.cgi) predicts that this exon 1B produces a stem-loop structure with a free energy of -38.3kcal/mol.

In addition to producing a stem-loop structure in the mRNA, exon 1B introduces four potentially active, upstream open reading frames (uORFs): uORFs 1, 2, and 4 are located exclusively within exon 1B whilst uORF3 initiates within exon 1B and terminates 2nt upstream of the ALAS1 initiating codon in exon 2 (figure 3-15).

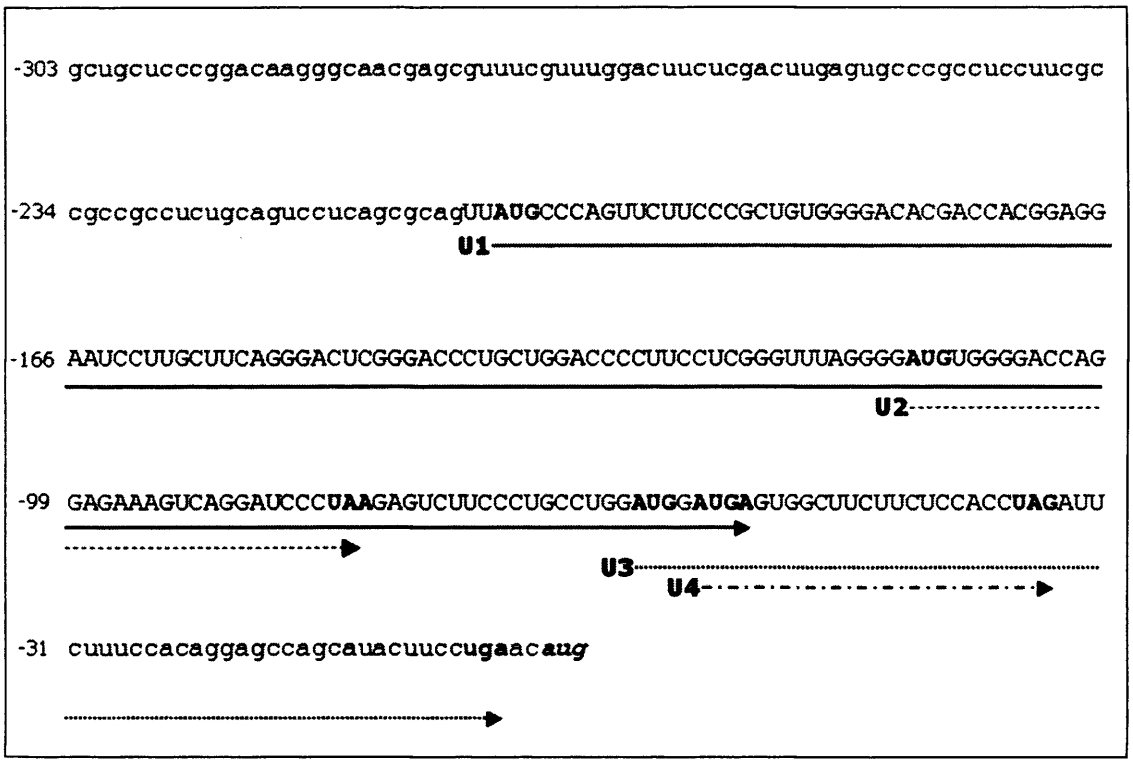

Figure 3-15 Upstream Open Reading Frames (uORFs) located within the 5'-UTR of the minor ALAS1 mRNA

Exons 1A and 2 are shown in lower case, whereas Exon 1B is in upper case. Four uORFs are indicated, and have been designated U1 to U4. Potential initiating AUG codons and termination codons are given in **bold** letters. U1, U2 and U4 all initiate and terminate within exon 1B, whilst U3 starts in exon 1B and terminates 2 nucleotides upstream of the start of the major ALAS1 ORF in exon 2.

Of the uORFs, only 153nt U1 is in frame with the downstream major ALAS1 ORF separated by 54nt of mRNA. The U4 AUG is 1nt upstream of and overlaps the termination codon of U1. The ALAS1 ORF is shown at +1 with all nucleotide positions numbered accordingly.

A typical eukaryotic mRNA contains one major ORF in its 5'-UTR, the sequence between the methyl-guanosine cap and the initiation codon of the ORF, and is typically from 20 to several hundred nucleotides in length. Ribosomes generally begin translation at the first AUG in the mRNA, which encodes the major ORF. The sequence content around an AUG is important in determining whether it is utilised as a translation start site. Upstream open-reading frames are unusual in mammalian mRNAs. Fewer than 10% of the known mammalian genes have upstream open reading frames (uORFs) in their 5'-UTR (Kozak, 1987). Although uncommon, uORFs are found with higher frequency in certain gene families with regulatory importance, including homeobox genes, proto-oncogenes, growth factors, transcription factors, and genes encoding components of signal

transduction pathways. uORFs play important roles in translational regulation of gene expression, either increasing or inhibiting translation of the downstream ORF. The occurrence of uORFs in evolutionary divergent eukaryotes, including yeast, plants, mammals, and animal viruses, suggests that regulation by ORFs is and important mechanism (Morris & Geballe, 2000).

UORFs can have a number of effects on translation. For example, translation of a uORF may affect the translation of the downstream ORF by acting on the translation machinery or the RNA transcript. Both upstream AUGs and secondary structures within the 5'-UTR cause ribosome stalling, the ribosomes spend more time upstream or at the uORF, which may make fewer ribosomes available at the downstream ORF, as in the human ADH5/FDH gene (human x-alcohol dehydrogenase/formaldehyde dehydrogenase) (Meijer & Thomas, 2002; Kwon *et al.*, 2001).

At present, it has not been determined which of these mechanisms might account for the reduced translation. Research in this laboratory (unpublished) has shown that mutagenesis of the uORFs 1, 2 and 4 does not inhibit the repression of translation. Translation of the downstream mRNA is still reduced when these uORFs are mutated. Therefore, it seems likely that it is the secondary structure that retards ribosomal scanning and affects the translation efficiency of the mRNA, rather than the presence of the uORFs.

The functional significance of alternative splicing in the human ALAS1 gene is not known. It is surprising that it has evolved in humans at all as data indicates that the minor mRNA appears to contribute very little of the steady-state concentration of ALAS1 protein, compared to the major mRNA. There is a high sequence homology of the 5'-UTRs of humans and chimpanzees, including the splice donor and acceptor sites, and the four potential uORFs. The presence of putative functional uORFs raises the prospect that regulated translation of the minor mRNA might be involved in developmental or tissue-specific expression of ALAS1.

As a final experiment to this chapter, we also investigated whether the reduction of expression of the downstream luciferase gene by the minor ALAS1 5'-UTR functioned in other cell types, as well as HepG2 cells. Our data indicate that the intrinsic promoter activity in the major ALAS1 5'-UTR, derived from exon 1A, is active in both IMR32 and K562 cells, and not restricted to HepG2 cells.

CHAPTER 4

Delineation of the ALAS1 haem-mediated instability element

4.1 Introduction

Haem primarily controls its own biosynthesis in hepatocytes, and probably all other non-erythroid cells, by post-transcriptional regulation of ALAS1, the first enzyme in its biosynthetic pathway. Haem inhibits the import of the ALAS1 enzyme from entering the mitochondria where it functions (Yamauchi *et al.*, 1980; Hayashi *et al.,* 1983), and also destabilises the ALAS1 mRNA (Drew & Ades, 1989; Cable *et al.,* 2001). However, the mechanism of this destabilisation is unknown. The experiments in chapter 3 demonstrated that the 5'-UTR does not harbour any haem-mediated *cis*-acting elements. Therefore, it is likely that haem destabilises the ALAS1 mRNA by the use of *cis*-acting elements either in its coding region or 3'-UTR. In all cell lines examined so far the addition of haem causes the ALAS1 mRNA half-life ($t_{1/2}$) to reduce by approximately 2-fold. For example, in HepG2 cells, the cell line used throughout this thesis, the addition of 20μM haem causes the $t_{1/2}$ to decrease from 8.8h to 3.5h (Cable *et al.,* 2001). Similarly, RT-PCR experiments in the previous chapter showed that the $t_{1/2}$ of HepG2 ALAS1 mRNA decreased from 6.5h to 2.9h, with the addition of 20μM haem.

The major focus of this chapter was to delineate the exact *cis*-acting element that causes haem-mediated destabilisation of the ALAS1 mRNA, in HepG2 cells. The approach to identify these sequences was to use indirect methods with reporter constructs, to look at the levels of ALAS1-*Renilla* luciferase fusion protein in response to haem. These results were confirmed by direct analysis of the mRNA levels, utilising the techniques RT-PCR and RNase Protection Assay (RPA).

4.1.1 mRNA regulatory elements in the 3'-UTR and coding region

Regulation of mRNA decay rate is an important control point in determining the abundance of cellular transcripts. Decay rates of individual mRNAs differ extensively, whereas some mRNAs decay with half-lives that are 100-fold shorter than cellular generation times, others have half-lives spanning several cell cycles. Moreover, although the decay rates of most transcripts, such as those encoding housekeeping genes, are invariant, the half-lives of numerous mRNAs change markedly in response to environmental cues. These differences in mRNA decay rates have notable effects on the expression of specific genes and upon alterations in the transcription rate; unstable mRNAs will attain steady-state levels in the least amount of time (reviewed in Wilusz *et al.*, 2001).

Localisation of determinant on mRNA	Decay determinant	Functional class/function of mRNA	mRNAs	Reference
3'-UTR	ARE	Immune regulators	Interleukins (e.g. IL-1. IL-2, IL-3)	Stoeklin *et al.*, 2000
			Interferons (e.g. IFN-α)	Ma *et al.*, 1997
			GM-CSF	Carballo *et al.*, 2000
			TNF-α	Lai *et al.*, 1999
		Proto-oncogenes	c-myc	Chen & Shyu, 1995; Wilson & Brewer, 1999; Brewer, 1991; Schiavi *et al.*, 1992
			c-fos	Schiavi *et al.*, 1994
		B-adrenergic receptor	B_1 and B_2 receptors	Pende *et al.*, 1996
		Regulated	VEGF - response to hypoxia	Levy *et al.*, 1998
			PTH in response to calcium	Sela-Brown *et al.*, 2000
	Iron-responsive element	Maintenance of iron homeostasis	TfR	Rouault & Klausner, 1997
	C-rich element	Cell-type specific	α-globin	Kiledjian *et al.*, 1997
	Others	Miscellaneous	Histone stem-loop	Whitfield *et al.*, 2000
			IGF II stem-loop	Scheper *et al.*, 1995
Coding region	CRD	Miscellaneous	c-myc	Yeilding & Lee, 1997; Prokipcak *et al.*, 1994.
			c-fos	Chen *et al.*, 1992
			β-tubulin	Bachurski *et al.*, 1994

Table 4-1 Examples of decay determinants located in the 3'-UTR and coding region, adapted from Guhaniyogi & Brewer, 2001.

One of the most prevalent is the A+U-rich element (ARE), found in the 3'-UTRs of some mRNAs. There are several classes of ARE with slightly different sequence determinants that are characterised by their abilities to promote the rapid deadenylation and subsequent decay of a transcript. A subset of AREs can also mediate mRNA stabilisation in the presence of certain stimuli, illustrating a dual role for these regulatory elements (Wilusz *et al.*, 2001).

The turnover of mRNA is a highly controlled process. Several sequence elements can regulate the rate of turnover of a transcript, either by promoting (destabiliser elements) or by inhibiting (stabiliser elements) decay. These can be located in the 5'- and 3'-UTRs, as well as the coding region of the mRNA. However, those coding region elements are rare and usually specific to the particular mRNA, as opposed to the more common and general elements found in the 3'-UTR (reviewed in Guhaniyogi & Brewer, 2001). Examples of *cis*-acting elements and their mRNA locations are listed in table 4-1. We have looked for these specific elements in the human ALAS1 sequence, and found that none of these are present in the coding region or 3'-UTR.

Group	Motif	Examples
I	WAUUUAW and a U-rich region	c-fos, c-myc
IIA	AUUUAUUUAUUUAUUUAUUUA	GM-CSF, TNF-α
IIB	AUUUAUUUAUUUAUUUA	Interferon-α
IIC	WAUUUAUUUAUUUAW	Cox-2, IL-2, VEGF
IID	WWAUUUAUUUAWW	FGF2
IIE	WWWWAUUUAWWW	u-PA receptor
III	U-rich, non-AUUUA	c-jun

Table 4-2 The classification of AREs and their associated motifs, from Wilusz *et al.*, 2001.

Group II contains reiterations of the AUUUA pentamer. Given the large sequence variation of the ARE, an abundance of ARE-binding factors have been identified.

Cis-acting elements that modulate transcript stability can also be found in the coding region of mRNAs. In some cases these elements act in concert with 3'-UTR elements to regulate mRNA decay, and can only function when both these elements are present. For example, the c-fos mRNA contains both an ARE in the 3'-UTR and two destabilising sequences in its coding region. The most studied is known as the major protein-coding-region determinant (mCRD). This mCRD contains 320 nucleotides, is located near the centre of the mRNA, and encodes the basic and leucine zipper regions critical to c-fos protein function. This *cis*-acting element is position-specific, and needs to be at least 450 nucleotides proximal to the poly(A) tail. Furthermore, it requires continuing translation for its destabilising function (Chen *et al.*, 1992).

As well as in c-fos, functional mRNA stability determinants have been detected within the coding region of a growing list of mammalian mRNAs including the

mRNAs of c-Myc, vascular endothelial growth factor (VEGF), β-tubulin and u-PAR. CRDs are relatively rare in mRNA molecules, in comparison to the number of instability elements found in the 3'- or 5'-UTRs.

4.1.2 Putative ALAS1 *cis*-acting elements

Sequence analysis of the human ALAS1 mRNA shows that it lacks any known regulatory stability motifs. However, this is unsurprising, since the *cis*-acting element may be present in the coding region. These are often specific to the mRNA, and regulation is related to the function of the encoded protein. As ALAS1 mRNA stability is controlled by haem, a specific haem-responsive stability element within the mRNA coding region or 3'-UTR is required.

Cable *et al* (2001) previously identified a specific sequence of the ALAS1 coding region that can bind to cytosolic proteins extracted from Huh-7 cells, a human hepatoma cell line. This 154bp protein-binding region was deleted from the ALAS1 sequence to make a deletion construct, and transfected into Huh-7 cells, along with the full-length ALAS1 as a control. Their results showed that the level of exogenously added deletion construct stayed relatively constant with the addition of haem for 4 hours. Conversely, the level of the full-length construct decreased with the addition of haem (Cable *et al.,* 2001). Therefore, it was concluded that this region is involved in the haem-mediated destabilisation of ALAS1, and may contain a CRD. However, whether this sequence is the sole requirement for haem-mediated destabilisation of the ALAS1 mRNA has not been shown. The experiments in this chapter set out to establish if a haem-responsive element is indeed present in this region, and can function independently of the rest of the ALAS1 sequence.

4.1.3 Aims and Strategy

The major aim of the work in this chapter was to delineate which ALAS1 sequences are responsible for haem-mediated decay in HepG2 cells. We have also assessed the role of haem in the destabilisation mechanism in a non-hepatic cell line.

This involved:

1. Developing reporter assays to indirectly assess the stability of the ALAS1 mRNA in response to haem.
2. Confirming if the 154bp sequence was the only determinant of ALAS1 stability.
3. Identifying other regions within the coding region or 3'-UTR which may be involved in the destabilisation of ALAS1 mRNA by haem.
4. Assessing the role of translation in this mechanism.
5. Confirming the results generated by the DLRA, using RNA-analytical techniques.
6. Investigating the affect of haem on the stability of ALAS1 in neuronal IMR32 cells.

Renilla-ALAS1 Construct	Forward Primer	Reverse Primer	Length of ALAS1 insert (bp)
pR154	P8	P9	153
pRSTOP154	P10	P9	156
pRALAS1	P11	P12	1923
pRSTOPALAS1	P13	P12	1926
pRALAS3UTR	P11	P14	2073
pR3UTR	P15	P14	150
pRA1	P11	P16	480
pRA2	P17	P18	480
pRA3	P19	P20	480
pRA4	P21	P12	483
pRA5	P22	P23	480
pRA6	P24	P25	480
pRA7	P26	P27	480

Table 4-3 Primer combinations used for the cloning of ALAS1 sequences into the *Renilla* luciferase expression vector pRluc-C2.

ALAS1 cDNA comprising the entire coding region of 1923bp, but lacking both 5'- and 3'-UTRs, was amplified using the forward primer P11, containing an *Eco* RI restriction site immediately prior to the initiating ATG codon, and the reverse primer P12, containing a *Kpn* I restriction site immediately after the stop codon utilised in the ALAS1 mRNA. As previously, an additional C nucleotide was added to the sequence in P11, after the *Eco* RI site, so that the ALAS1 coding region remained in frame with the *Renilla* luciferase gene in the pRluc-C2 vector. In order to introduce a stop codon into the *Renilla* luciferase-ALAS1 cDNA fusion immediately prior to the ALAS1 moiety, a modified upstream sense primer, P13, was used with the reverse primer P12. This inserted a stop codon prior to the ATG, ensuring that the ALAS1 sequence is not translated when inserted into the pRluc-C2 vector. The 2073bp DNA fragment, encoding the entire ALAS1 coding region together with the 3'-UTR was amplified using the P11 and P14 primers. To examine the effect of the 3'-UTR alone, a 150bp cDNA fragment corresponding to the ALAS1 mRNA 3'-UTR (positions 1997 – 2146; Genbank sequence, X56351) was amplified using the forward primer P15, and the reverse primer P14.

In order to further delineate the ALAS1 *cis*-acting element, seven smaller overlapping fragments of the ALAS1 coding region were also amplified by PCR, each of approximately 480bp in length, using the primers P11-P12 and P16-P27. Each forward primer contained the restriction site *Eco* RI, and the reverse primer contained the restriction site *Kpn* I, to aid cloning into the pRluc-C2 vector.

All amplified ALAS1 products were purified from agarose gels and ligated into pGEM-T by TA cloning. The ligation mixture was used to transform subcloning efficiency, competent DH5α cells, and the plasmid DNA was isolated and purified. To produce the pRluc-ALAS1 fusion constructs, the pGEM-T-ALAS1 plasmid DNA was digested with the restriction enzymes *Eco* RI and *Kpn* I. The ALAS1 insert was purified using the Qiagen gel extraction kit and subsequently ligated into pRluc-C2 (figure 4-1) that had been previously digested with *Eco* RI and *Kpn* I. Unlike the other constructs, the sequence for the pR154 construct was amplified using the restriction site *Eco* RI in both the forward and reverse primers. Therefore, these were inserted into the pRluc-C2 vector which had been digested with *Eco* RI alone. All cloned sequences were verified by DNA sequencing. The ALAS1 coding region and 3'-UTR constructs are shown diagrammatically in figure 4-2.

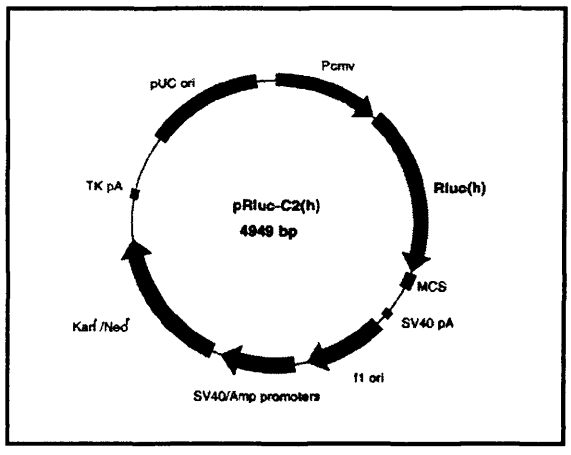

Figure 4-1 Vector Map of pRluc-C2 adapted from www. perkinelmer.com.
The codon humanized pRluc-C vectors contain a multiple cloning site (MCS) located downstream of the codon humanized Renilla Luciferase gene (Rluc(h)), for the subcloning of a gene of interest to create a *Renilla* luciferase fusion protein. The Rluc codons have been humanized to ensure higher expression levels of the fusion protein in mammalian cells. The fusion protein gene is placed under the control of the cytomegalovirus (CMV) promoter, ensuring a very high constitutive expression in a variety of cells.

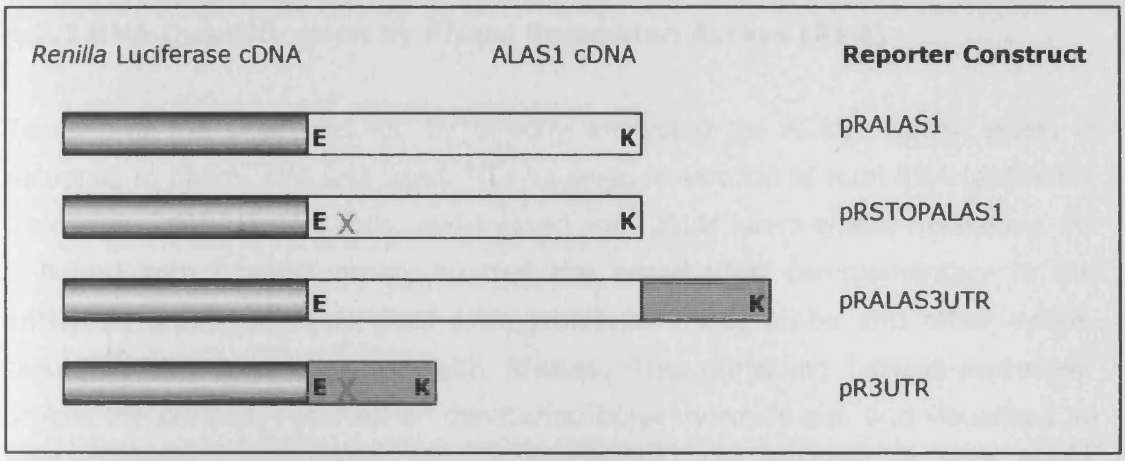

Figure 4-2 Construction of the full-length and 3'-UTR *Renilla*-ALAS1 constructs.

= *Renilla* luciferase cDNA in pRLuc-C2

= ALAS1 coding region cDNA

= ALAS1 3'-UTR cDNA

E= EcoRI site; **K**=KpnI site; **X**=STOP site inserted by modified primer

The ALAS1 sequences were cloned in-frame and downstream of the *Renilla* luciferase gene into the *Eco* RI / *Kpn* I sites within the MCS of pRluc-C2. For the pRSTOPALAS construct, a stop codon was inserted prior to the ALAS1 sequence, with a modified forward primer.

4.2.2 Mammalian Cell Transfection

For the DLRA experiments, confluent HepG2 and IMR32 cells were split into 12-well plates, with 1ml cells/well, in cDMEM 24 hours prior to transfection. The cells were transfected with 1µg/well of each the control vector pRluc-C2 and all other constructs to be tested in triplicate, and co-transfected with 630ng/well of pGL3-P vector. 24 hours after transfection, the cells were treated either with 20µM haem or control medium (vehicle) in triplicate. Luciferase activity was measured 24 hours after incubation with haem/vehicle.

For RNA analysis, confluent HepG2 cells were split into 6-well plates in cDMEM, with 2ml cells/well, so that sufficient RNA was available for cDNA synthesis. Each well of cells were transfected with 2µg of pRALAS1 and 1.26µg of pGL3-P for normalisation purposes, where appropriate.

4.2.3 RNA Quantification by RNase Protection Assays (RPA)

To confirm the DLRA results, by directly analysing the ALAS1 mRNA levels in response to haem, RPA was used. This involved incubation of total RNA (extracted from transfected HepG2 cells, and treated with 20μM haem where necessary, for 6 hours) with labelled probe, so that the sense RNA, complementary to the antisense probe, will hybridise. After which, any free probe and other single-stranded RNA were digested with RNases. The remaining "RNase-protected" probes are purified, resolved on denaturing polyacrylamide gel, and visualised by blotting and UV-crosslinking onto a membrane. The quantity of each mRNA species in the original RNA sample can then be determined based on the intensity of the appropriately sized, protected probe fragment.

4.2.3.1 Biotin-labelled antisense RNA probes

Probe constructs were generated for RPA analysis of *Renilla* luciferase-ALAS1 fusion mRNA and GAPDH mRNA, as a control, by amplification of cDNA fragments from recombinant pRALAS1 plasmid DNA (P28 and P29 primers) and HepG2 RNA (P30 and P31 primers) respectively (figure 4-3). These were ligated into the pGEM-T vector and clones in an orientation to generate antisense RNA using the T7 promoter were selected. The probe for ALAS1 used a sequence that overlapped the *Renilla* luciferase and ALAS1 boundary, to ensure that only the pRALAS1 construct was detected by RPA, and not the endogenous ALAS1. These probes were made as antisense RNA, so that during the RPA they hybridised to the corresponding sense RNA sequence in the HepG2 total RNA extract, thereby protecting this region from degradation by RNase.

The *Renilla* luciferase-ALAS1 and GAPDH probe constructs were linearised by digestion with *Kas* I, which cuts in the *Renilla* luciferase sequence, and *Spe* I which cuts within the SP6 site of the pGEM-T vector, respectively. Antisense biotin-16-UTP probes for *Renilla* luciferase-ALAS1 mRNA (328nt) and GAPDH mRNA (258nt) were generated by *in vitro* transcription using the T7 maxiscript system (Ambion) in accordance with the manufacturer's protocol (section 2.4.11). Labelled RNA probes were gel-purified following electrophoresis through a 5% acrylamide/8M urea denaturing polyacrylamide gel.

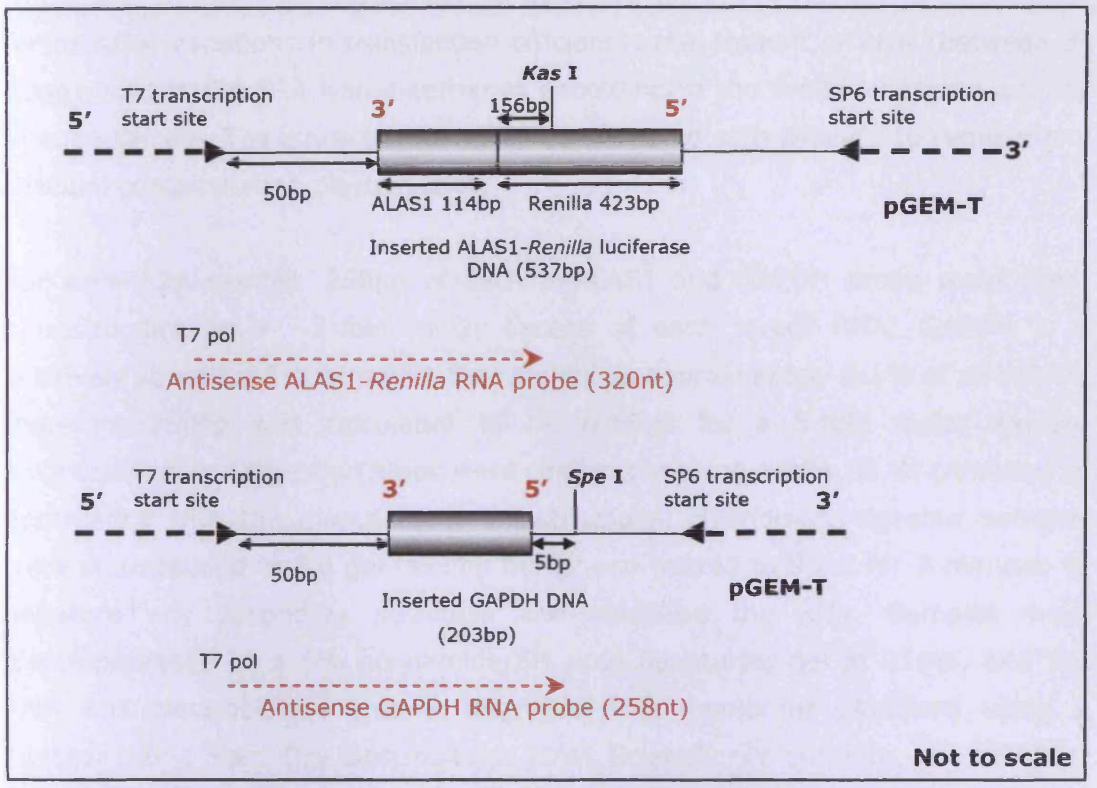

Figure 4-3 Schematic diagram to show the generation of ALAS1 and GAPDH antisense RNA probes for RPA.

Renilla-ALAS1 and GAPDH sequences were amplified by PCR and inserted into the PGEM-T vector by TA cloning, in an antisense (3'-5') direction from the T7 start site. The constructs were excised with *Kas* I and *Spe* I for the ALAS1 and GAPDH probes respectively. The T7 maxiscript kit (Ambion) was used to produce antisense biotin 16-UTP probes by *in vitro* transcription. The labelled RNA probes were gel-purified following electrophoresis through a 5% acrylamide/8M urea denaturing polyacrylamide gel, to ensure that the probes were of the correct size and that any degraded probe or unincorporated dNTPs were removed.

4.2.3.2 RPA

HepG2 cells were co-transfected with pRALAS1 and pGL3P control vector, as in section 4.2.2. After 24h the medium was removed and replaced with DMEM, which contained 20μM haemin, or vehicle medium as appropriate. At t_0, cells in duplicate where trypsinised, harvested and stored at -70°C. Following a further 6h incubation with either haem or control medium, these cells in duplicate were also trypsinised and harvested. A small fraction of the cells were lysed using Passive Lysis Buffer and luciferase activity monitored in lysed cell extracts by a DLRA, whilst the rest were treated with Ultraspec to extract total RNA. To account

for possible variations in transfection efficiency, the amount of RNA (between 3-10μg) used in the RPA was determined according to the firefly luciferase activity in each sample. The extracted RNA was then treated with DNase I to remove any residual contaminating plasmid DNA.

For each RPA sample, 250pg of each pRALAS1 and GAPDH probe were used, corresponding to a ~5-fold molar excess of each target RNA. GAPDH is a relatively abundant target mRNA that makes up approximately 0.1% of all mRNA, therefore 250pg was calculated to be enough for a 5-fold molar excess. Hybridisation and digestion steps were carried out using a RPA III kit (Ambion) in accordance with the manufacturer's instructions. Hybridised, digested samples were resuspended in 6μl gel loading buffer and heated to 95°C for 3 minutes to denature any secondary structure and solubilise the RNA. Samples were electrophoresed on a 5% acrylamide/8M urea denaturing gel at 25mA, and the RNA was electroblotted onto a BrightStar-Plus membrane (Ambion) using a Panther HEP-1 Semi-Dry Electroblotter (OWL Scientific, Portsmouth, NH, USA) for 30 minutes at 400mA, and immobilised by UV crosslinking at 120,000μJ/cm^2 for 30 seconds. Detection was performed following the BrightStar BioDetect protocol (Ambion).

4.2.4 Semi-Quantitative RT-PCR

4.2.4.1 RT-PCR of pRALAS1 and pGL3P

mRNA was isolated from pRALAS1 and pGL3P transfected HepG2 cells (section 4.2.2) using Dynal mRNA Direct Kit. cDNA was synthesised from the mRNA by first strand synthesis, and changes in mRNA expression were assayed by PCR using primer sets specific for cDNA fragments of ALAS1, with pGL3P as a control (tables 4-4 and 4-5). The primers used for ALAS1 amplified a sequence that overlapped the *Renilla* luciferase and ALAS1 boundary, to ensure that only the pRALAS1 construct was detected, and not the endogenous ALAS1. The cycling protocol for the pRALAS1 PCR was that as described in section 2.4.4.3.1, with 34 cycles, and an annealing temperature of 60°C. The pGL3P PCR was similarly of 34 cycles, with an annealing temperature of 65°C. Prior to the quantification by PCR, all the PCR conditions had been optimised for logarithmic amplification using untreated control cells (see section 3.2.1.1).

Target DNA	Primer Number	Product Size	PCR Annealing Temperature
pRALAS1	Sense P28 , Anti-Sense P29	537bp	60°C
pGL3P	Sense P32, Anti-Sense P33	267bp	65°C

Table 4-4 Primers used in semi-quantitative RT-PCR.

Reagent	Volume (µl)
10x PCR buffer	2
2mM dNTP mix	2
Sense Primer 5pmol	5
Antisense Primer 5pmol	5
cDNA Template (RT product)	2
HotStarTaq Polymerase (5U/µl)	0.2
H_2O	to 20µl

Table 4-5 Composition of semi-quantitative RT-PCR.

PCR products were resolved by agarose gel electrophoresis. The band intensities of the products were quantified as raw volume of the peak intensity, using GeneTools software (Syngene), and normalised to GAPDH to calculate the relative induction.

4.2.4.2 RT-PCR of endogenous haem oxygenase-1

Total RNA was isolated from HepG2 cells using Ultraspec, and cDNA was synthesised from the mRNA by first strand synthesis. A change in haem oygenase-1 (HO-1) mRNA expression was assayed by PCR using the forward primer P34, corresponding to a sequence in exon 2, and the reverse primer P35, corresponding to a sequence in exon 3. The PCR product, of 400bp, therefore spanned an exon boundary and ensured that only HO-1 cDNA was amplified, rather than any contaminating genomic DNA. The PCR was quantified as in table 4-5.

4.3 Results and Discussion

4.3.1 The *cis*-acting element in the 154bp region does not confer haem-mediated destabilisation.

Previous work by Cable *et al* has described a 154 nucleotide region that is able to bind cytosolic proteins, and therefore it was suggested that this region contains a haem-responsive *cis*-acting element (Cable *et al.,* 2001). To test this hypothesis we used reporter assays, with a commercially available *Renilla* luciferase expression vector, pRLuc-C2. This vector permitted in-frame cloning of ALAS1 cDNA sequences downstream of the *Renilla* moiety, such that it could be determined whether these conferred haem-mediated destabilisation upon the fusion mRNA, by monitoring effects upon *Renilla* luciferase expression. In these studies, *Renilla* luciferase-ALAS1 fusion constructs were transfected into the human hepatoma cell line, HepG2.

A fusion construct was made with the putative *cis*-acting element of the coding region, to generate a sequence encoding 51 in-frame codons, as described in the materials and methods. Another construct was made with a stop codon (TAA) prior to this sequence to assess whether the sequence needs to be translated to function (pRstop154). The ALAS1 sequences were cloned in-frame to generate a fusion reporter gene construct such that the luminescent signal detected from the *Renilla* luciferase reports on the stability and translation efficiency of the ALAS1 sequence.

These constructs and the control pRluc-C2 vector were transfected separately into HepG2 cells (1µg/well of cells each), together with the firefly luciferase expression plasmid, pGL3-promoter vector (630ng/well of cells) in order to normalise the *Renilla* luciferase data due to any differences in transfection efficiency. Cells were treated with 20µM haem or the vehicle medium, 24h after transfection. The luciferase activities were measured after 24h following exposure to 20µM haem.

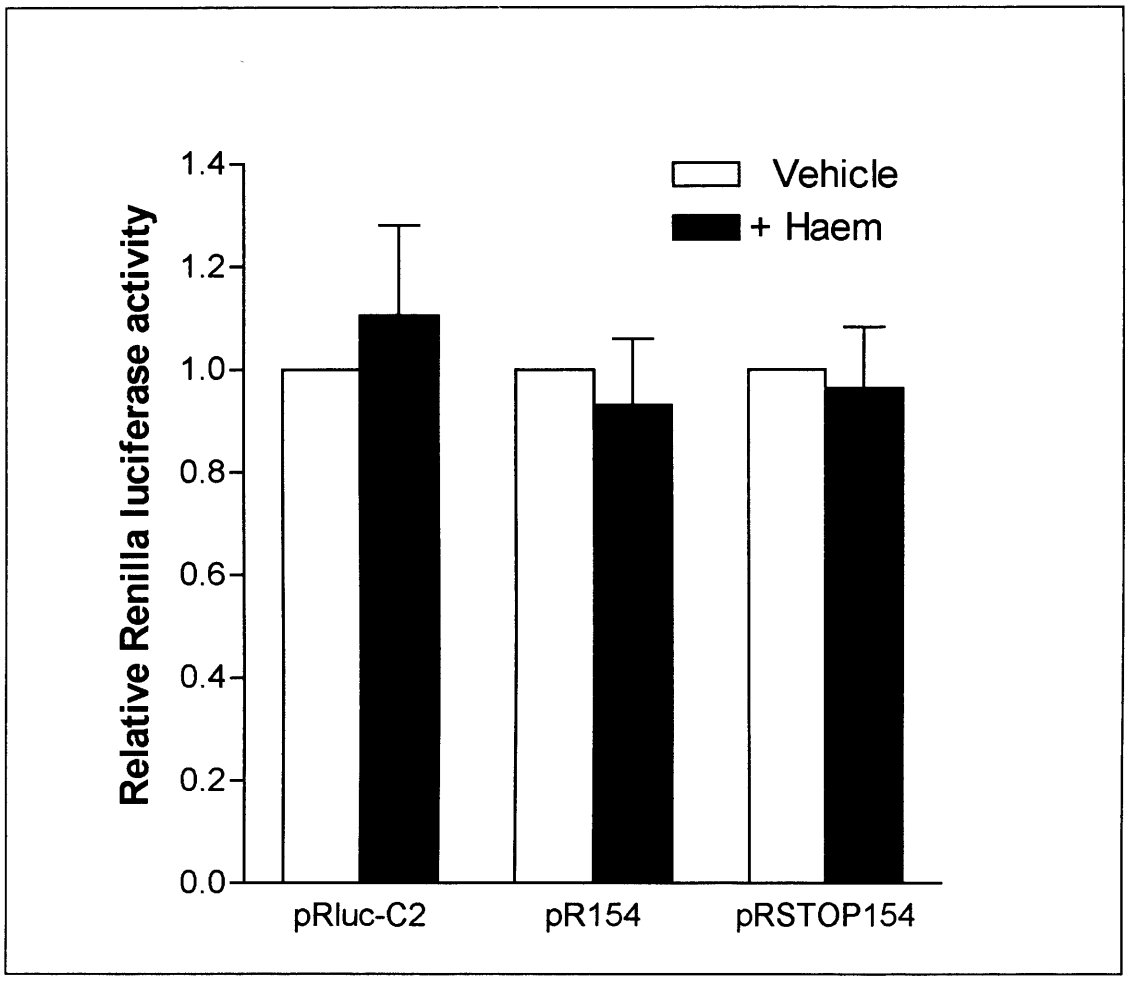

Figure 4-4 The addition of haem does not cause the destabilisation of the ALAS1 153bp – *Renilla* luciferase fusion protein.

The putative cis-acting element of the ALAS1 coding region was cloned in frame to the pRluc-C2 vector at the *Eco* RI site, with and without a stop codon prior to the sequence. Transfection and bioluminescent measurements were performed as previously described. There was no difference between relative Renilla expression of pR154 and pRstop154-transfected cells, treated and untreated with 20μM haem. Bars indicate plus standard deviation. Experiments were on two separate occasions in triplicate.

As expected, *Renilla* luciferase expression from the pRluc-C2 vector alone did not significantly differ between untreated cells and those treated with haem, indicating that neither the activity of *Renilla* luciferase itself nor the CMV promoter driving its expression was affected by increased levels of intracellular haem. Consequently, data from the ALAS1 constructs were normalised to the value of the pRluc-C2 treated cells, which was considered to be 100%. Data from these experiments showed that in both of these constructs the *Renilla* luciferase expression was not reduced with haem treatment (figure 4-4). Although this region has been shown to bind cytosolic proteins in hepatocytes, this data demonstrates that this region alone is not able to confer haem-mediated instability of the mRNA. This suggests that either the 154bp sequence is not significant in the haem destabilisation mechanism, or another sequence elsewhere in the ALAS1 coding region is required for it to function. It is possible that the ALAS1 CRD has a bi-partite structure, which may rely on specific mRNA sequences within the coding region to enable its destabilisation by haem.

4.3.2 The human ALAS1 coding region contains a haem-mediated *cis*-acting element.

The data in chapter 3 eliminated the 5'-UTR as a region harbouring haem-responsive *cis*-acting elements. As section 4.3.1 showed, the haem-response element is not present in the 154bp sequence of the coding region previously identified by Cable *et al* (Cable *et al.,* 2001). Therefore, the next set of experiments set out to establish whether the instability determinant is indeed in the coding region or in the 3'-UTR, and whether it needs sequence elements in both of these regions to function.

Three ALAS1 constructs were generated; one with the coding region added in-frame at the 3' end of the *Renilla* luciferase (pRALAS1), another containing the ALAS1 3'-UTR as well as the coding region (pRALAS3UTR), and a final construct containing just the ALAS1 3'-UTR (pR3UTR) appended to the luciferase gene (figure 4-2).

The ALAS1 sequences were cloned in-frame to generate a fusion reporter gene construct such that the luminescent signal detected from the *Renilla* luciferase reports on the stability and translation efficiency of the ALAS1 sequence. As for the previous section, these constructs and the control pRluc-C2 vector were transfected separately into HepG2 cells (1µg/well of cells each), together with the firefly luciferase expression plasmid, pGL3-promoter vector (630ng/well of cells) for normalisation. Cells were treated with 20µM haem or the vehicle medium, 24h after transfection. The luciferase activities were measured after 24h following exposure to 20µM haem.

Figure 4-5 demonstrates that *Renilla* luciferase expression from the ALAS1-fusion constructs were much lower than that of the pRluc-C2 vector by approximately 15-fold, presumably due to the addition of the long ALAS1 sequence at the C-terminus of *Renilla* luciferase gene. However, *Renilla* expression remained sufficiently high for accurate analysis. Data from each ALAS1 construct was normalised to the value of the untreated cells transfected with the same construct, which was considered to be 100%. *Renilla* luciferase expression from the pRluc-C2 vector alone did not significantly differ between untreated cells and those treated with haem. In contrast, in cells transfected with pRALAS1, exposure to haem decreased *Renilla* luciferase activity consistently and significantly by 40% of that seen in untreated cells. Similarly, haem exposure also resulted in a

significant 33% decrease in *Renilla* luciferase activity in cells transfected with pRALAS3UTR. Paired sample t tests were used to establish that these differences of *Renilla* activity with and without haem were statistically significant.

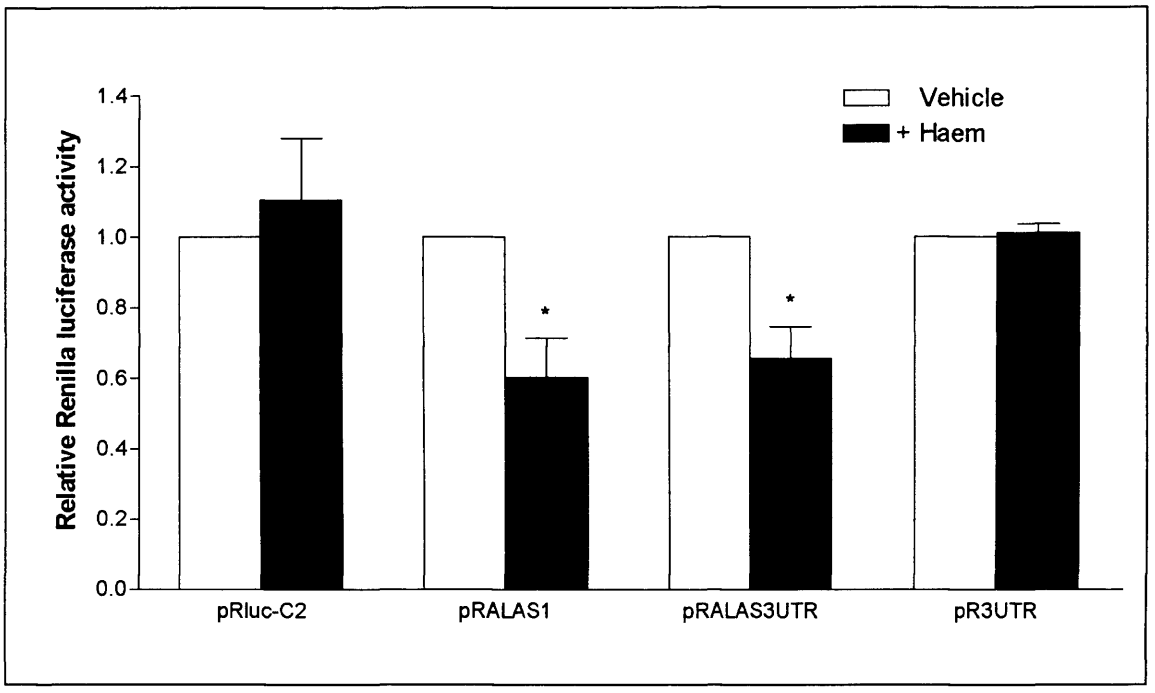

Figure 4-5 ALAS1 mRNA is destabilised by a coding region determinant.
The *Renilla*-ALAS1 fusion constructs and the empty parental vector were co-transfected into HepG2 cells with the pGL3P vector as the internal control. Cells were treated with 20μM haem or the vehicle medium for 24h, and luciferase expression was measured using the DLRA. Data shows the relative *Renilla* expression after the addition of 20μM haem, compared to the expression without haem as 100%. Bars indicate plus standard deviation. Paired sample t tests were performed on the data for pRALAS1 and pRALAS3UTR, and both p values are less than 0.05, indicating a significant difference between *Renilla* expression with and without haem treatment. There was no significant difference between the Renilla expression from pR3UTR with or without the addition of haem. Experiments were on three separate occasions in triplicate. *= statistically significant, p value < 0.05.

There was no significant difference between haem-depressed *Renilla* luciferase activity in pRALAS1 cells and pRALAS3UTR cells indicating that the *cis*-acting haem responsive elements reside within the coding region rather than the 3'-UTR. To confirm this, a fusion construct was generated in which the ALAS1 3'-UTR alone (pR3UTR), with no coding region, was appended to *Renilla* luciferase. Unlike the pRALAS3UTR construct, its *Renilla* luciferase activity was not significantly affected by haem, which substantiated the previous data and conclusions.

4.3.3 The coding region determinant has to be translated to mediate instability of the mRNA in the presence of haem.

The data in chapter 3 demonstrated that the minor ALAS1 mRNA is resistant to haem-dependent degradation compared to the major form. Furthermore, our data suggested that translation of the minor mRNA is reduced approximately eight-fold compared to the major mRNA. This data indicates that ALAS1 mRNA stability is related to its rate of translation. Therefore, having established both that the haem-regulatory element(s) resided within the ALAS1 coding region and that the poorly translated minor ALAS1 mRNA was resistant to haem-mediated degradation, the translational mechanism through the ALAS1 coding region may be required for its haem-mediated destabilisation.

Accordingly, an additional fusion construct was made, designated pRSTOPALAS1, in which a stop codon (TGA) was inserted between the *Renilla* luciferase cDNA and the ALAS1 coding region such that the latter would constitute part of the 3'-UTR and not be translated.

This construct was transfected into HepG2 cells with pGL3P, as in the previous sections. In contrast to the reduced *Renilla* luciferase activity seen in haem-treated cells transfected with either pRALAS1 or pRALAS3UTR constructs, normalised *Renilla* luciferase activity in pRSTOPALAS1-transfected cells was not reduced in response to haem treatment but was in fact slightly elevated, though not significantly so, compared to that in untreated cells (paired samples t test, $p > 0.05$) (figure 4-6). This result indicates that translation through the coding region instability determinant is required for its haem-mediated destabilisation in HepG2 cells.

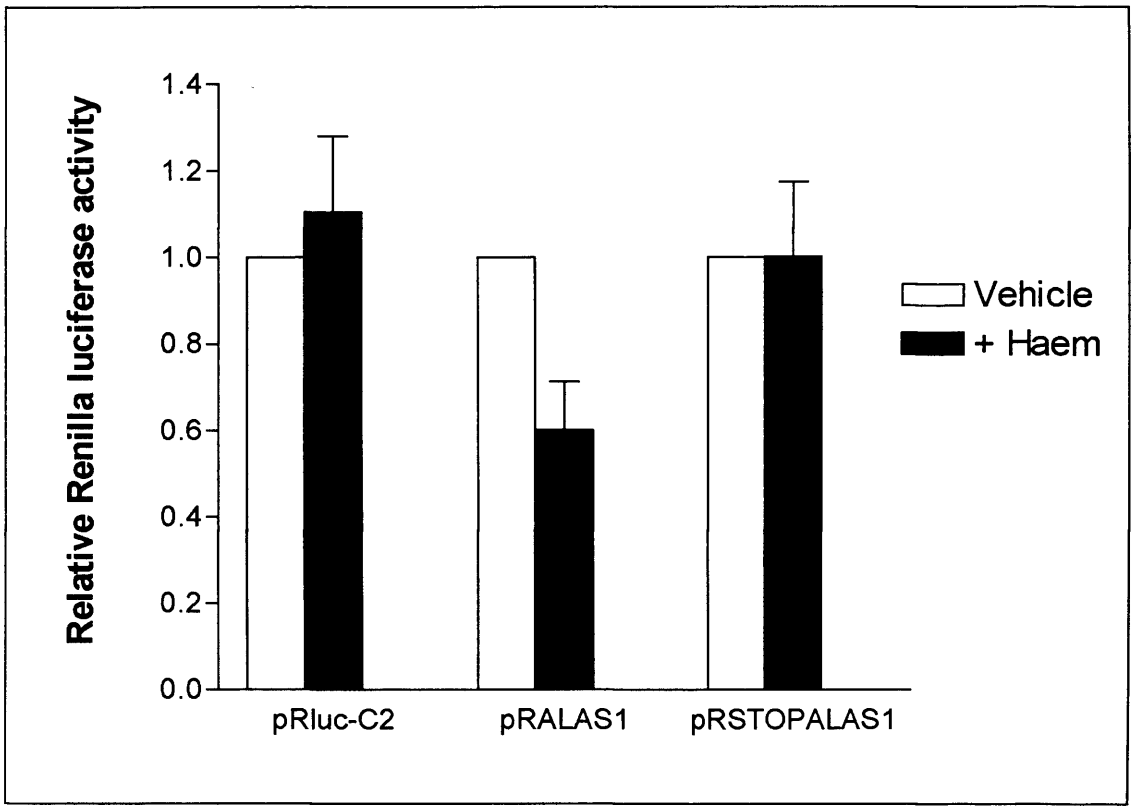

Figure 4-6 The coding region determinant has to be translated to mediate instability of the mRNA in the presence of haem.

The pRstopALAS1 construct was made by introducing a TGA stop codon between the Renilla luciferase gene and the ALAS1 coding region by PCR. Transfection and bioluminescent measurements were as described in figure 4-5. Bars indicate plus standard deviation. There was no significant difference between the relative Renilla luciferase activity of pRSTOPALAS1 with and without haem. Experiments were on three separate occasions in triplicate.

4.3.4 Overlapping deletion experiments to delineate the ALAS1 mRNA coding region determinant(s).

To date, no sequences of ALAS1 mRNA have been shown to bind cytosolic protein, apart from the 154bp sequence at the 3' end of the coding region. Section 4.3.1 demonstrated that this region is not destabilised by haem when used in reporter assays, and therefore this region cannot function alone as a haem-mediated CRD. Additional sequence elements adjacent to the previously identified 154 nucleotide region or other additional elements in the coding region may be needed for haem-mediated instability of the mRNA.

In order to define where other CRDs reside, seven *Renilla* luciferase-ALAS1 fusion constructs consisting of overlapping smaller fragments of the ALAS1 coding region were made (figure 4-7). These all contained ALAS1 sequences of approximately 480bp each, designated pRA1-pRA7. The putative *cis*-acting element, identified by Cable *et al.,* fully resides in the construct pRA4, and partly resides in pRA7 (Cable *et al.,* 2001). The sequences were cloned into the pRluc-C2 vector, co-transfected with pGL3P into HepG2 cells as in the previous sections, and treated with either 20μM haem or the control medium.

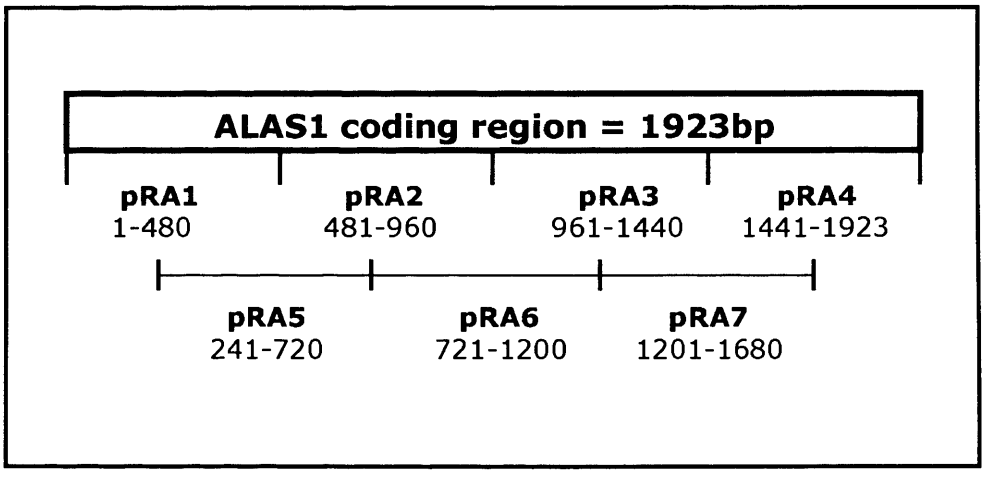

Figure 4-7 The seven overlapping sub-fractions of the ALAS1 coding region that were amplified by PCR, and inserted into the pRluc-C2 vector. Seven regions of the ALAS1 protein-coding region were amplified by PCR, located at the above nucleotides, designated pRA1 - pRA7. The seven overlapping fragments were amplified from HepG2 total RNA, using Bio-X-Act polymerase. These were cloned into the pGEM-T vector, digested with *Eco* RI and *Kpn* I, and cloned into the similarly digested pRluc-C2 vector, to produce the constructs pRA1 – pRA7.

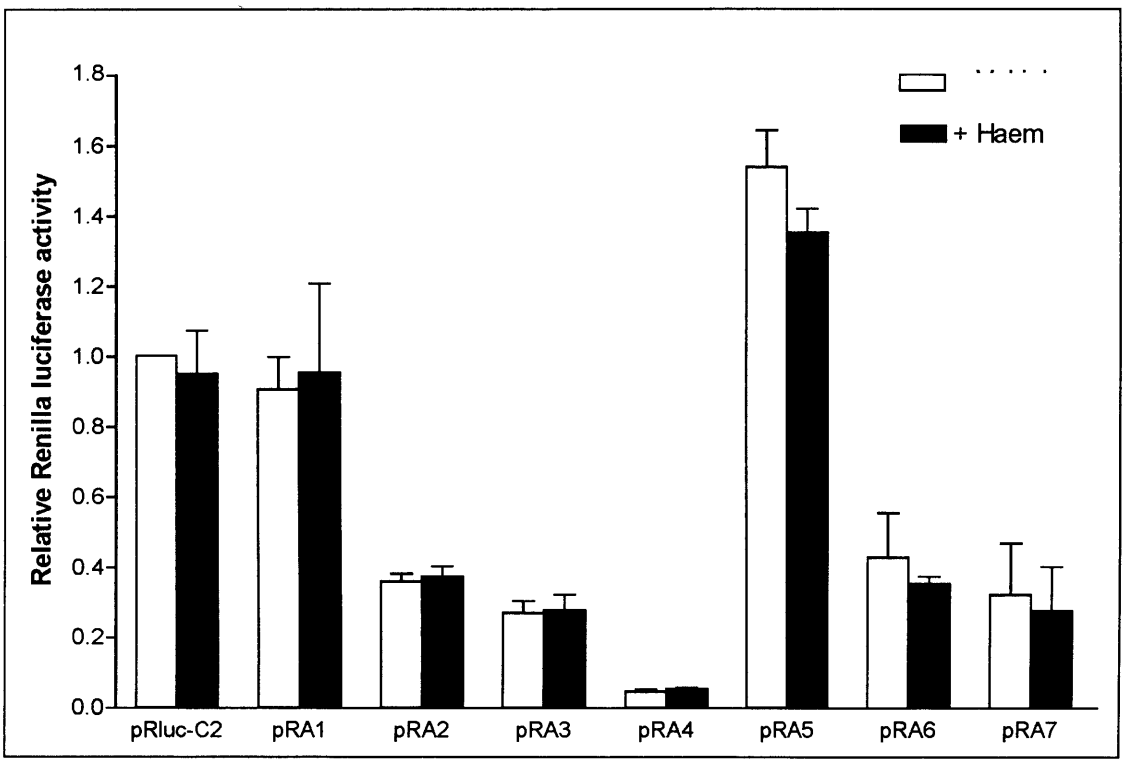

Figure 4-8 The instability element of ALAS1 does not reside in a specific fragment of its coding region mRNA.

Seven fragments of the ALAS1 coding region of approximately 480bp in length were cloned in frame to the pRluc-C2 vector. These were transfected into HepG2 cells, treated with 20μM haem or the vehicle medium for 24 hours, and assayed for bioluminescence as previously described. Unlike the previous graphs, the data was not normalised. Bars indicate plus standard deviation. Experiments were on two separate occasions in triplicate. The pRA4 sequence contains the 154 base pair region, which is able to bind cytosolic proteins.

The relative *Renilla* luciferase expression levels varied greatly between the seven ALAS1 constructs and repeated attempts to demonstrate haem sensitivity on these sequences was unsuccessful. The full-length ALAS1 construct, pRALAS1, was used as a positive control, and on each occasion was shown to be destabilised by haem (data for pRALAS1 not shown here, but demonstrated in figure 4-5). Therefore, these results cannot conclude which fragment the CRD is in.

Due to the unusually high differences between the *Renilla* luciferase expression of each construct, the actual values of relative *Renilla* luciferase expression data to pRluc-C2 was plotted, showing the un-normalised data. Unlike the previous graphs in this study, figure 4-8 shows the *Renilla* expression of the constructs treated with the vehicle medium as its actual value, rather than 100%. This emphasises the variation of *Renilla* luciferase expression between each construct. Interestingly, the expression levels of the ALAS1 fragments closer to the 3′ end of the coding region are much lower that those at the 5′ end, with the *Renilla* expression of pRA4 being only approximately 5% of that of pRA1.

The data in this section confirms the results in section 4.3.1, which showed that the ALAS1 CRD does not fully reside within the 154bp region identified by Cable *et al* (2001). None of the seven ALAS1 deletion constructs were destabilised by haem in this assay, in which the full coding region is always destabilised. To define the specific haem-mediated *cis*-acting element in the coding region by reporter assay methods was not possible. Only the full-length coding region ALAS1 mRNA is unstable in the presence of haem, whereas the short truncated regions are not. The reason for this is unclear, but may be due to the ALAS1 coding region containing multiple sequence elements required for destabilisation by haem. These may require specific spatial and positional separation. Therefore, the methods used in this section are not able to further define the CRD. However, the differences in translational efficiency of these sequences may have a specific role in the haem-destabilisation mechanism.

4.3.5 Confirmation of an ALAS1 CRD by RPA

The previous experiments in this chapter, using reporter assays, have shown that the ALAS1 haem-responsive element is within its coding region. This needed to be confirmed by quantifying the mRNA directly, to establish that the effect of haem upon *Renilla* luciferase activity in the pRALAS1-transfected cells resulted from enhanced instability of the fusion mRNA, rather than an inhibitory effect upon its translation.

The first approach we used was to utilise RNA protection assays (RPA), using RNA extracted from pRALAS1-transfected HepG2 cells at t_0, and those at t_6, which were treated with and without 20μM haem, 24 hours post-transfection. The levels of the fusion mRNA at these time-points were assayed using RPA, with a biotin-UTP labelled 328nt probe that spanned the *Renilla* and ALAS1 mRNA moieties, along with a biotin-UTP labelled 258nt probe for the endogenous GAPDH mRNA as a control.

Figure 4-9 shows a typical result from this RPA experiment. This assay proved to be technically difficult, with the mRNA often being degraded too quickly for it to give reproducible and accurate results. Furthermore, no effect of the addition of haem on the stability of pRALAS1 mRNA was observed. It was thought that the media in which the HepG2 cells grow, already contain haem and haemoproteins in the FCS, which need to be removed so that the affect of haem on the ALAS1 mRNA stability is higher than two-fold, and can therefore be visualised.

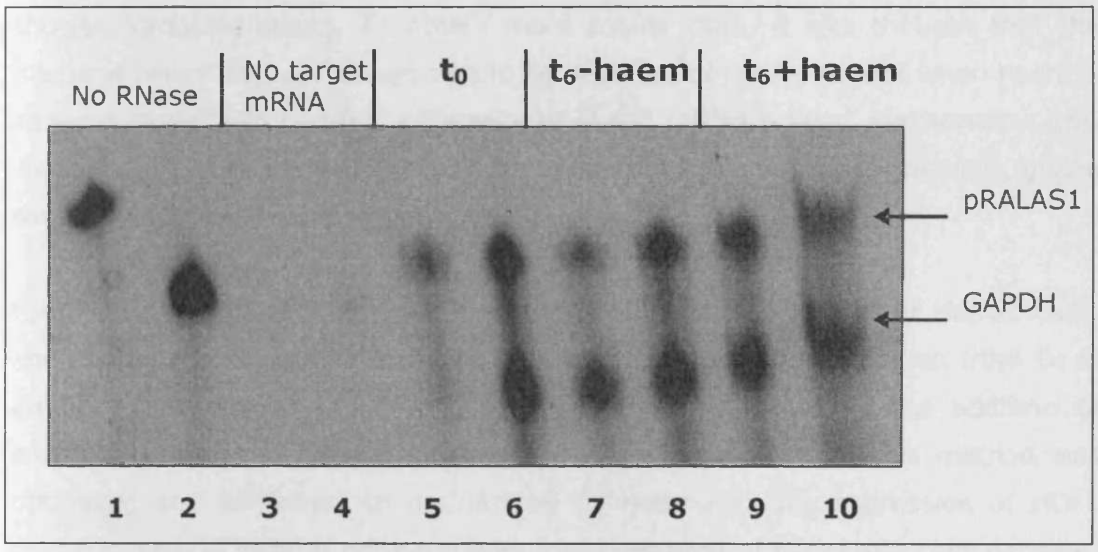

Figure 4-9 RNase protection assay of pRALAS1 and GAPDH mRNA in response to 20μM haem for 6h.

To establish that the effect of haem upon *Renilla* luciferase activity in the pRALAS1 cells resulted from enhanced instability of the fusion mRNA rather than an inhibitory effect upon its translation, levels of the fusion mRNA were analysed using RNase protection analysis. The upper band is the protected fragment of the pRALAS1 *Renilla*-ALAS1 fusion mRNA (328nt) and the lower band that of GAPDH (258nt). The image shown is indicative of a typical experiment.

Lanes 1-2: No RNase control. These serve as a control for probe integrity, showing the gel migration of the full-length probe of pRALAS (1) and GAPDH (2). Any degradation or secondary structure would be seen here. These lanes show a single band for each probe, migrating at the correct size; 3-4: No target RNA control, used 5μg yeast RNA only. These serve as positive controls for the function of the RNases. There is no signal for the pRALAS1 probe (3), and a very faint signal for the GAPDH probe (4) as yeast mRNA also contains this gene; 5-6: RPA of mRNA extracted at t0 in duplicate; 7-8: RPA of mRNA extracted at t6, incubated with control medium only, in duplicate; 9-10: RPA of mRNA extracted at t6, incubated with 20μM haem, in duplicate.

4.3.6 Optimisation of the removal of haem and haemoproteins from FCS

Initial experiments using RPA to assess the stability of ALAS1 mRNA in HepG2 showed variable results. To obtain more robust data, it was thought that the media in which cells are grown should be depleted of haem, so that when haem is added a larger than two-fold difference of ALAS1 mRNA is seen. Furthermore, this would ensure that a controlled amount of haem is being added to the cells, giving consistency between experiments.

Foetal calf serum (FCS) is used to make cDMEM for the growth of HepG2 cells, and contains an unknown quantity of haem. A method was obtained from Dr Li Zhang (University of Columbia), to deplete FCS of haem by the addition of ascorbic acid and dialysis in phosphate-buffered saline (PBS). This method was optimised and confirmed to be working by measuring the expression of HO-1 mRNA in HepG2 cells in normal media, cells depleted of haem and cells depleted of haem for 24h prior to the addition of 20μM haem for a further 4h (the method for haem depletion is in the materials and methods chapter, section 2.2.1.6.).

Since the observed decrease in *Renilla* luciferase activity in the previous DLRA experiments was consistent and reproducible but less than two-fold, we endeavoured to effectively enhance the sensitivity of the experiments. This was by stabilising the fusion mRNA in cells through haem depletion using 100μM 4,6-dioxoheptanoic acid (succinyl acetone), a potent and specific inhibitor of ALA dehydratase, added to the haem-depleted media prior to haem treatment. Structurally, succinylacetone closely resembles ALA and acts as a competitive inhibitor of ALAD. ALAD activity in the liver and erythroid precursors is dramatically reduced and excess ALA is excreted in the urine (De Matteis & Marks, 1983). This ensured that the concentration of haem in the cells is completely reduced, and therefore a high concentration of ALAS1 mRNA is present in the cells.

To confirm that this method of haem-depletion was successful, RT-PCR was used to quantify the HO-1. HO is the rate-limiting enzyme in the degradation of haem, and induction of its isozyme, HO-1, is recognised as a protective response against haem protein-mediated and other insults to diverse tissues (Kanakiriya *et al.*, 2003).

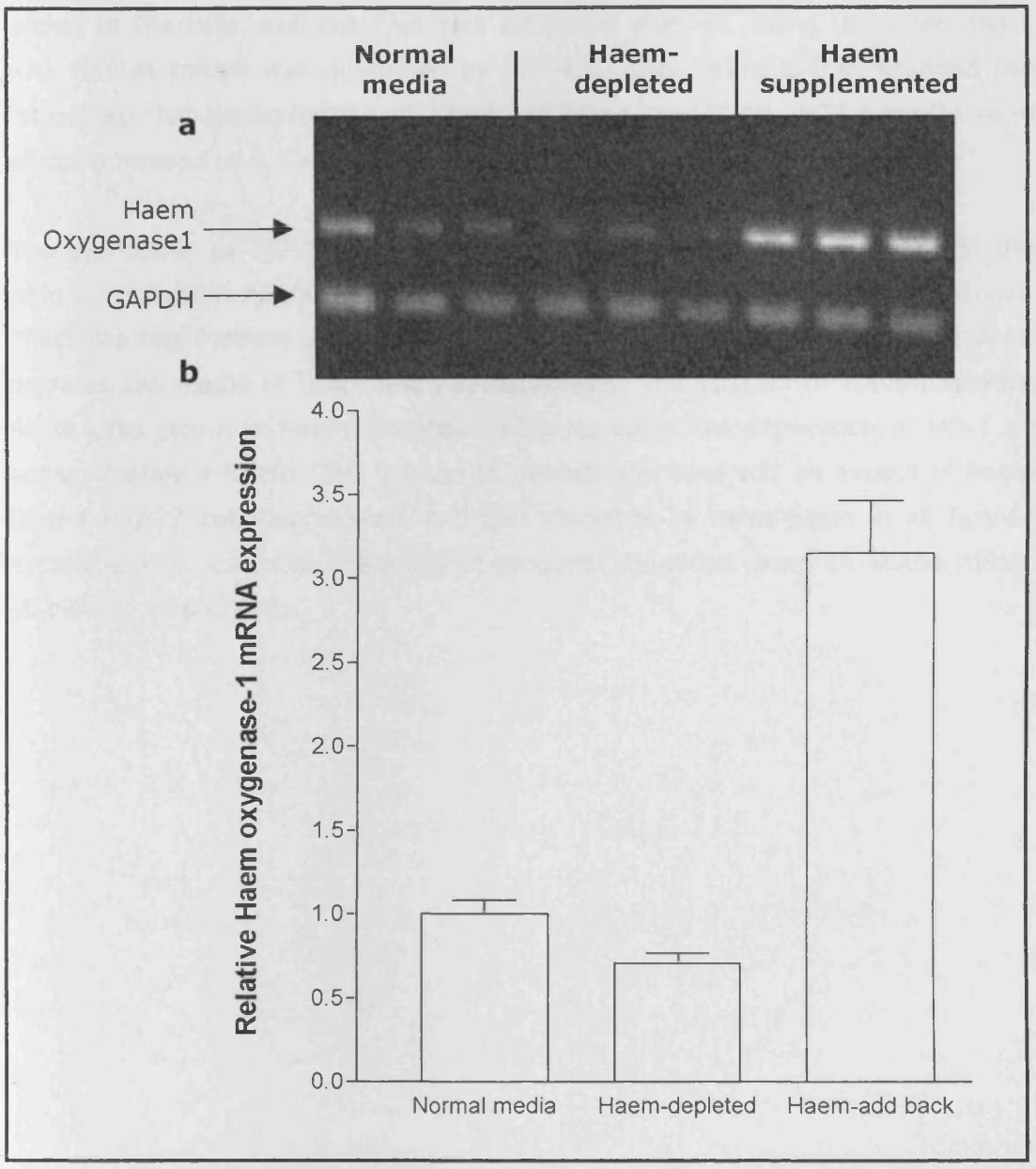

Figure 4-10 HO-1 mRNA expression is reduced in HepG2 cells grown in medium containing haem-depleted FCS.

HepG2 cells, in triplicate, were grown in either normal media or haem-depleted media with/without the addition of 20μM haem for 4 hours prior to the extraction of total RNA.

a) HO-1 and GAPDH mRNA was quantified by RT-PCR, and electrophoresed on a 1.4% agarose gel. Experiments were done on three separate occasions in duplicate. The above gel is an example of a typical experiment.

b) Densitometry of the HO-1 RNA levels normalised to the GAPDH RNA levels from figure 4-10a.

Cells were grown in cDMEM and split into 6-well plates (2ml cells/well). After 24h, the media was replaced with haem-depleted cDMEM, and 500μM succinyl acetone was added to inhibit the synthesis of haem. After a further 24h, 20μM haem was added to the cells, and the RNA was extracted after 4h, using Ultraspec. HO-1 and GAPDH mRNA was quantified by RT-PCR, using primers that spanned the introns so that genomic DNA could be separated from cDNA. PCR samples were electrophoresed on a 1.4% agarose gel.

The expression of HO-1 in HepG2 is reduced by approximately 25% when the cells are grown in haem-depleted media rather than normal media (figure 4-10). Therefore this method of dialysis of the FCS, after the addition of ascorbic acid, depletes the media of haem and haemoproteins. The addition of 20μM haem for 4h to cells grown in haem-depleted media increases the expression of HO-1 by approximately 4.5-fold. The method to deplete and then add an excess of haem to the HepG2 cells works well, and can therefore be relied upon in all further experiments to establish the effect of exogenously added haem on ALAS1 mRNA stability in HepG2 cells.

4.3.7 Confirmation of an ALAS1 CRD by semi-quantitative RT-PCR

Experiments using RPA to confirm the destabilisation of the coding region of ALAS1 by haem proved to be technically difficult and unsuccessful as the addition of haem causes only a two-fold decrease of ALAS1 mRNA levels. Therefore, a method to deplete cell media of haem was used, so that when HepG2 cells where grown in this media, the cellular content of ALAS1 mRNA would be high (and the level of HO-1 mRNA is low, as shown in figure 4-10). Consequently, when haem is added to the cells, the ALAS1 mRNA concentration drops significantly and can be analysed by RNA analysis. To quantify this, RT-PCR was used rather than the previous RPAs, as this is a quicker method, so that the mRNA had less time to degrade as in the RPAs. Furthermore, a two-fold difference is challenging to demonstrate on steady-state levels of mRNA, used in the RPA.

Similar to the DLRA experiments, HepG2 cells in 6-well plates were transfected with pRALAS1 and pGL3P and grown in haem-depleted media and treated with 100μM succinyl acetone. The cells were subjected to treatment with 5μg/ml actinomycin D to induce transcriptional arrest, and 20μM haemin (or control medium) for 6h. After 6h, mRNA was extracted from the cells using the Dynal mRNA direct kit (Ambion). The pRALAS1 and pGL3P cDNA were separately quantified by RT-PCR. As a control, pGL3P was quantified by PCR, so that any differences in transfection efficiency can be visualised.

The results of the RT-PCR in figure 4-11 demonstrate clearly that the addition of 20μM haem to HepG2 cells for 6h causes the destabilisation of the fusion mRNA containing the ALAS1 coding region. Therefore this is likely to be responsible for the decreased *Renilla* luciferase activity seen earlier. This confirms the data from the DLRA's, that ALAS1 mRNA contains a haem-mediated CRD. The reporter assays were done in equilibrium and therefore showed a two-fold change in expression with the addition of haem. However, for the RT-PCR experiments, prior to the addition of haem, the cells were depleted of haem by using specific growth media and succinyl acetone. Furthermore, actinomycin D was used to inhibit transcription. The growth of HepG2 cells in this haem-depleted media, showed a larger than two-fold difference between ALAS1 mRNA with and without haem, visualised by semi-quantitative RT-PCR. We have calculated that the $t_{1/2}$ of ALAS1 mRNA is reduced from 6.5h to 2.9h. Therefore, after incubation with haem for 6h, it is expected that the mRNA will go through at least two half-lives.

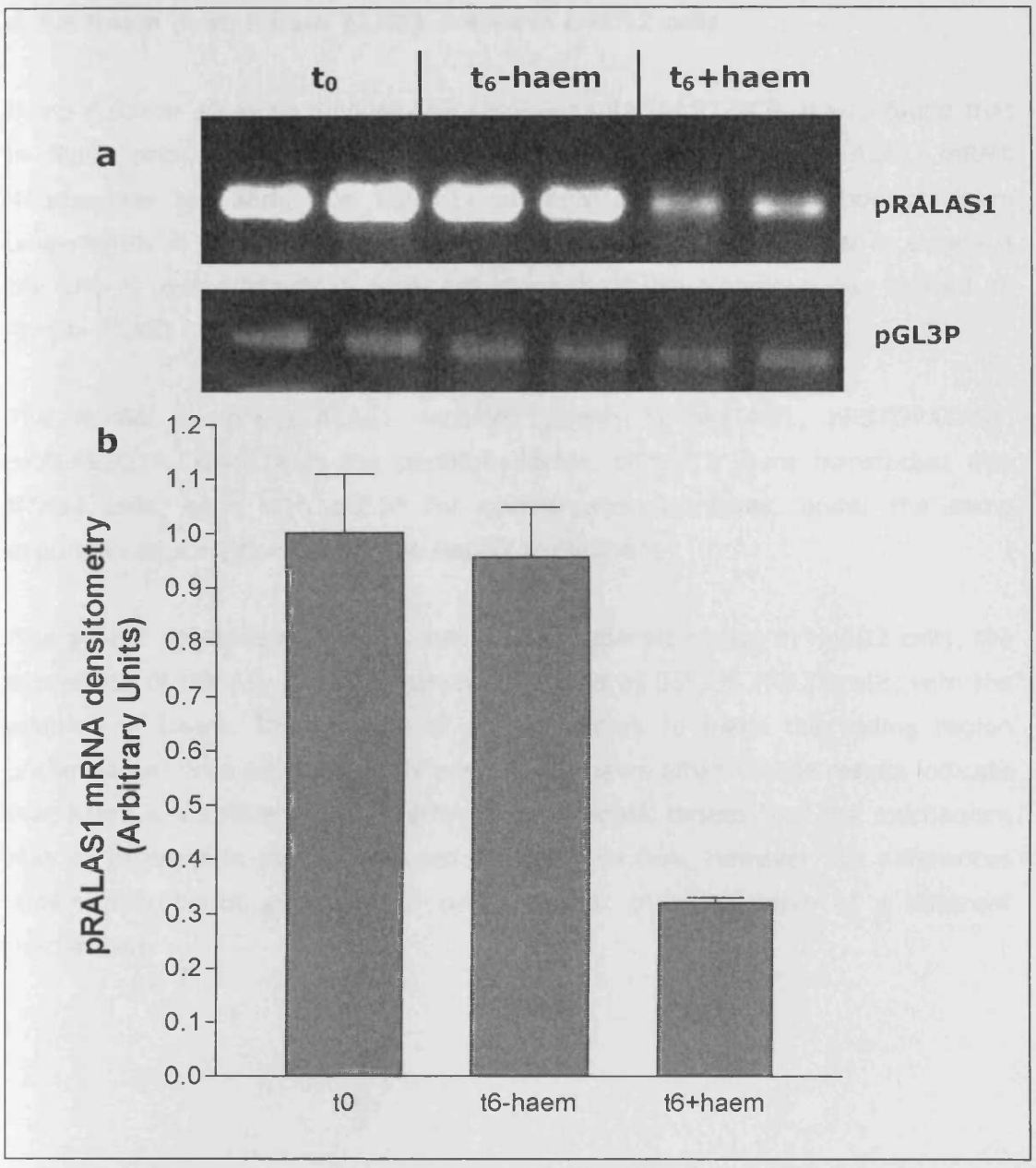

Figure 4-11 The addition of 20μM haem destabilises the fusion *Renilla* - ALAS1 coding region mRNA by more than 2-fold in 6h.

HepG2 cells were grown in haem-depleted media and transfected with pRALAS1 and pGL3P. mRNA was extracted at t_0, t_6 with the addition of control medium (t_6-haem), and t_6 with the addition of 20μM haem (t_6+haem), in duplicate. The addition of haem for 6h caused the ALAS1 mRNA levels to decrease by approximately 70%.

a) cDNA fragments for the pRALAS1 construct and pGL3P were specifically amplified by RT-PCR using reverse transcribed DNAse I-treated mRNA. Experiments were done on three separate occasions in duplicate. The above gel is an example of a typical experiment.

b) Densitometry of the pRALAS1 mRNA levels from figure 4-11a. Values were not normalised to pGL3P, as the densitometry was similar on each occasions, indicating similar transfection efficiency between samples.

4.3.8 Haem destabilises ALAS1 mRNA in IMR32 cells.

Using reporter assay techniques and semi-quantitative RT-PCR, it was found that in HepG2 cells, ALAS1 contains a CRD which functions to destabilise ALAS1 mRNA in response to haem. The majority of research on the regulation of haem biosynthesis in non-erythroid cells has been in hepatocytes. In order to assess if the CRD is used similarly in other cell types the DLRA technique was utilised on *Renilla*-ALAS1 transfected IMR32 cells.

The *Renilla* luciferase ALAS1 reporter constructs pRALAS1, pRSTOPALAS1, pRALAS3UTR, along with the parental vector, pRluc-C2 were transfected into IMR32 cells, each with pGL3P for normalisation purposes, under the same experimental conditions as for the HepG2 experiments.

Figure 4-12 demonstrates that similar to the reporter assays in HepG2 cells, the expression of the full length construct decreased by 35% in IMR32 cells, with the addition of haem. The addition of a stop codon, to make the coding region untranslated, does not completely prevent the haem effect. These results indicate that haem destabilises ALAS1 mRNA in non-hepatic tissues, but the mechanism may be different to the system used in hepatoma cells. However, the differences shown may be of experimental origin, rather than indicative of a different mechanism.

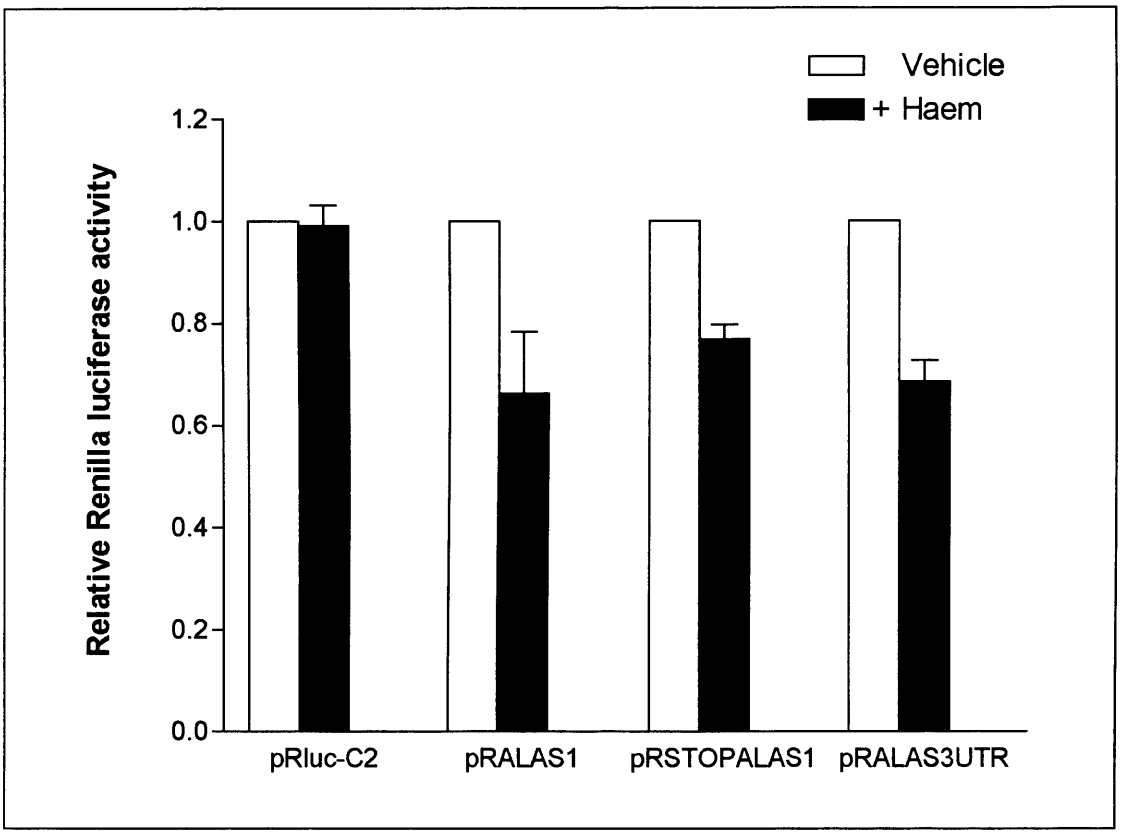

Figure 4-12 Relative *Renilla* luciferase expression of ALAS1 constructs in IMR32 cells in response to the addition of 20μM haem for 24h.

The *Renilla*-ALAS1 fusion constructs and the empty parental vector were co-transfected into IMR32 cells with the pGL3P vector as the internal control. Cells were treated with 20μM haem or the vehicle medium for 24h, and luciferase expression was measured using the DLRA. Data shows the relative *Renilla* expression after the addition of 20μM haem, compared to the expression without haem as 100%. Bars indicate plus standard deviation. Experiments were on two separate occasions in triplicate. Paired sample t tests were performed on the data for pRALAS1, pRSTOPALAS1 and pRALAS3UTR. p values were less than 0.05, indicating a significant difference between *Renilla* expression with and without haem treatment for all constructs.

4.4 Conclusions

The ability of haem to control its own synthesis in all cells is crucial. High intracellular concentrations of haem are cytotoxic, damaging cells through oxidative processes involving Fenton chemistry, whilst haem deficiency may impede the activity of certain haemoproteins with potentially harmful consequences, particularly with regard to neurodegeneration and ageing (Atamna, 2004; Atamna *et al.,* 2002). In liver and probably all other non-erythroid cells, haem supply is regulated primarily via feedback regulation of ALAS1 mRNA stability, yet the precise mechanism has not been elucidated (Ponka, 1999).

There are a number of important observations from the data presented in this chapter:

1. The previously identified putative *cis*-acting element is not sufficient for haem-mediated destabilisation of the mRNA.
2. The haem-mediated element is present in the ALAS1 coding region, and the mechanism of instability does not involve sequence elements in the 5'- or 3'-UTR.
3. Destabilisation of the ALAS1 mRNA could only be demonstrated using the full-length coding region, and not in smaller deletion fragments.
4. In HepG2 cells, the haem-mediated destabilisation of ALAS1 mRNA requires the translation mechanism to occur through a CRD to function.

Neither the 5'- nor 3'-UTR of the major ALAS1 mRNA conferred haem-responsive destabilisation upon a *Renilla* luciferase-ALAS1 fusion mRNA, but instead it was demonstrated by luciferase assays that the *cis*-acting elements responsible for haem-mediated destabilisation reside within the coding region. Methods were optimised to reduce the level of haem in FCS that was used in the medium in which HepG2 cells were grown. This enabled the RNA assays to be optimised, so that the destabilisation of the full-length ALAS1 coding region construct was seen with the addition of haem by using the technique RT-PCR. This confirmed the results from the DLRA's, that ALAS1 contains a haem-mediated CRD.

Cable *et al* (2001) identified a putative haem-mediated CRD due to its ability to bind cytosolic proteins, and that its deletion abolished the haem effect. However, the data in this chapter has shown that this sequence alone is not enough to confer the destabilisation of ALAS1 by exogenously added haem. The ALAS1

instability element resides solely in the coding region, although the 154bp region alone has not been shown to function as a CRD, under these experimental conditions. Thus, it is probable that additional elements surrounding this sequence or elsewhere within the coding region are required for haem-dependent regulation of ALAS1 mRNA. Indirect evidence supporting such a conclusion comes from erythroid cells in which two ALAS isoforms are expressed encoded by ALAS1 and ALAS2 genes (Bishop, 1990). Despite a homology of 61% between them over this 154nt region (figure 4-13), ALAS1 mRNA stability is reportedly regulated by haem in these cells (Fujita *et al.*, 1991; Harigae *et al.*, 2003), but ALAS2 mRNA is not.

```
ALAS1    GCAAUCAAUUACCCUACGGUGCCCCGGGGAGAAGAGCUCCUACGGAUUGCCCCACCCCU
ALAS2    GCCAUCAACUACCCAACUGUCCCCCGGGGUGAAGAGCUCCUGCGCUUGGCACCCUCCCCC

ALAS1    CACCACACACCCCAGAUGAUGAACUACUUCCUUGAGAAUCUGCUAGUCACAUGGAAGCAA
ALAS2    CACCACAGCCCUCAGAUGAUGGAAGAUUUUGUGGAGAAGCUGCUGCUGGCUUGGACUGCG

ALAS1    GUGGGGCUGGAACUGAAGCCUCAUUCCUCAGCUG
ALAS2    GUGGGGCUGCCCCUCCAGGAUGUGUCUGUGGCUG
```

Figure 4-13 Homology between the 154bp sequence of human ALAS1 and ALAS2 mRNA.

There is 61% homology of the putative *cis*-acting element between ALAS1 and ALAS2. Non-homologous nucleotides are indicated in red.

It is hypothesised that a larger region of the mRNA or other sequence elements within the coding region are required for destabilisation to occur, rather than the earlier identified 153bp sequence. *Renilla*-ALAS1 fusion constructs were made using seven overlapping regions of the coding region. Experiments using these constructs in the luciferase assays did not provide evidence to indicate that there is a specific region involved in this instability mechanism. Using reporter assays, we were only able to demonstrate the haem-mediated destabilisation of ALAS1 using the full-length coding region. The approach to define the CRD by using specific sequences on their own is not sufficient for the destabilisation by haem, suggesting that other regions are involved, but cannot function in isolation. Therefore, it is likely that the ALAS1 CRD is a bi- or tri-partite structure, similar to the destabilisation mechanisms of c-myc (Lemm & Ross, 2002), c-fos (Chen *et al.*, 1992) and plasminogen activator type 2 (PAI-2) mRNA (Tierney & Medcalf,

2001). The specific secondary structure of the mRNA may be essential for this mechanism so that these sequence elements are close together in the mRNA molecule.

The data in chapter 3 showed that the minor ALAS1 form is not translated as well as the major form, and is relatively stable in the presence of haem. The data presented in this chapter has demonstrated that by inserting a stop codon prior to the ALAS1 coding region the destabilisation by haem was abolished. This indicates a mechanism in which the haem-mediated decay of ALAS1 mRNA requires translation through its coding region. Like most short-lived mRNAs, ALAS1 mRNA is stabilised in cells exposed to translational inhibitors. Inhibition of translation also prevents its haem-mediated decay (Drew & Ades, 1989; Cable *et al.*, 2001). Although our data does not exclude the possibility that the mechanism involves a labile *trans*-acting factor, we have demonstrated a critical requirement for translation of ALAS1 mRNA itself.

The results showed that 6 of the 7 ALAS1 coding region fragments, when inserted into a *Renilla* luciferase-encoding vector, had high but variable expression. However, the pRA4 construct had much lower expression, which was at an equivalent expression to the full-length construct, pRALAS1, with a much longer ALAS1 insert of 1923bp. This 483bp sequence, at the 3′ end of the coding region, seems to have a lower rate of translation, a factor which may be involved in the destabilisation mechanism. The different rates of translation may, in part, be due to different mRNA 3D structures that impede ribosomal scanning through them. The fact that fragment 4 is so badly translated may indicate a highly structured mRNA. Figure 4-14 indicates that this fragment 4, consisting of the last 483bp of human ALAS1 mRNA, contains multiple stem-loop structures and has a high free energy.

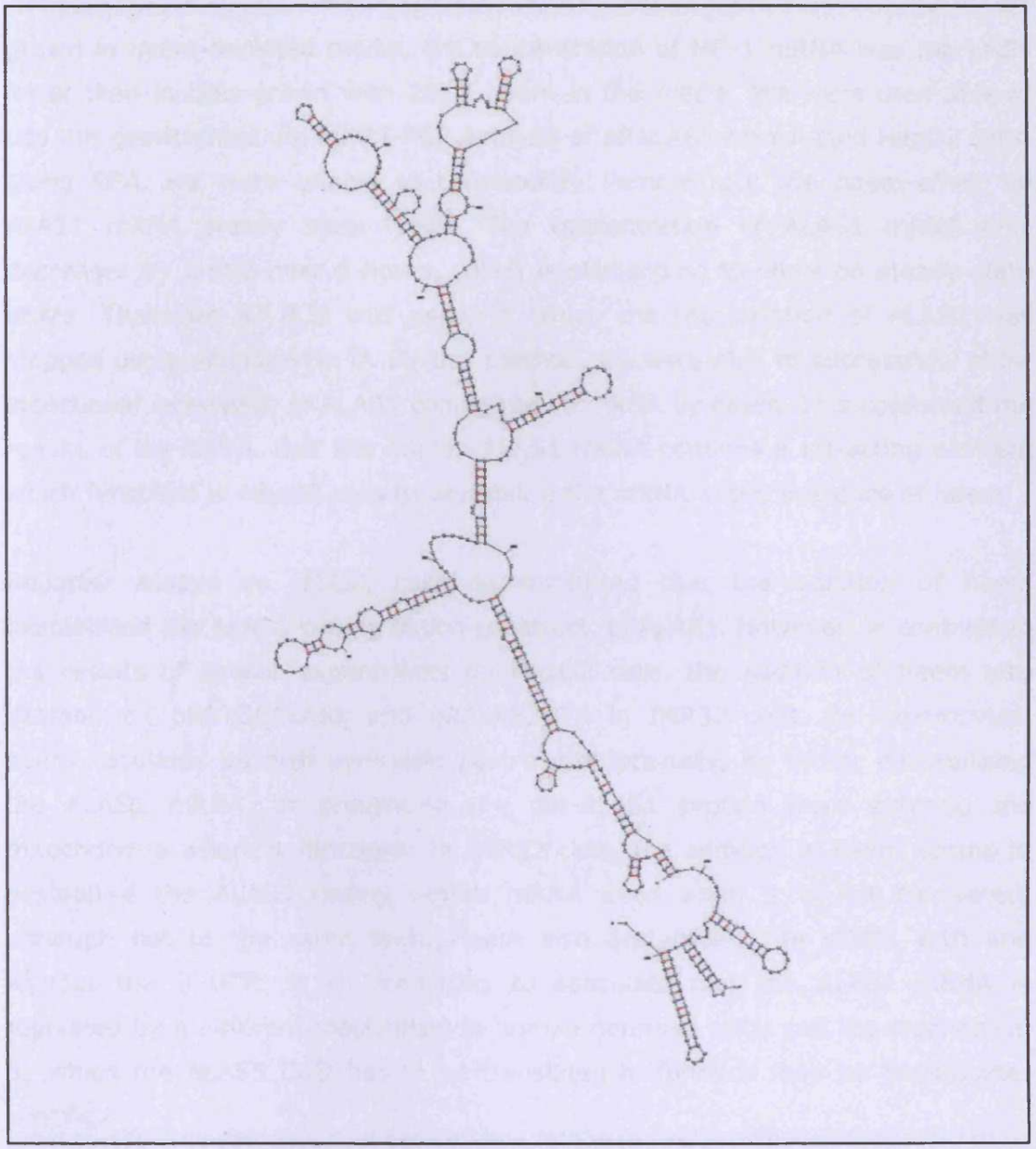

Figure 4-14 The predicted secondary structure of fragment 4 of the ALAS1 coding region

The RNA folding software mfold (http://frontend.bioinfo.rpi.edu/applications/mfold/cgi-bin/rna-form1.cgi) predicts that fragment 4, of 483bp in length, produces a highly structured mRNA with a free energy of -160.7kcal/mol.

FCS used in the growth medium of HepG2 cells contains an unknown concentration of haem and haemoproteins, which may have affected the results of RNA analysis. Therefore, a method to deplete the FCS of haem was optimised and demonstrated to work by RT-PCR of HO-1 in HepG2 cells grown in this media. HO-1 is readily induced by haem proteins and their haem moiety, and in cells

grown in haem-depleted media, the concentration of HO-1 mRNA was markedly lower than in cells grown with 20μM haem in the media. We were then able to use this growth medium for RT-PCR analysis of pRALAS1-transfected HepG2 cells. Using RPA, we were unable to consistently demonstrate the haem-effect on ALAS1 mRNA steady state levels. The concentration of ALAS1 mRNA only decreases by 2-fold over 6 hours, which is challenging to show on steady-state levels. Therefore RT-PCR was used, in which the transcription of ALAS1 was stopped using actinomycin D. By this method, we were able to successfully show inductional repression of ALAS1 coding region mRNA by haem. This confirmed the results of the DLRA, that the human ALAS1 mRNA contains a *cis*-acting element which functions in HepG2 cells to destabilise the mRNA in the presence of haem.

Reporter assays on IMR32 cells demonstrated that the addition of haem destabilised the ALAS1 coding region construct, pRALAS1. However, in contrast to the results of similar experiments on HepG2 cells, the addition of haem also destabilised pRSTOPALAS1 and pRALAS3UTR in IMR32 cells. In hepatocytes, haem regulates its own synthesis post-transcriptionally, by either destabilising the ALAS1 mRNA, or preventing the pre-ALAS1 protein from entering the mitochondria where it functions. In IMR32 cells, the addition of haem seems to destabilise the ALAS1 coding region mRNA even when it is not translated, although not to the same level. Haem also destabilises the mRNA with and without the 3'-UTR. It is interesting to speculate that the ALAS1 mRNA is regulated by a different mechanism in human neuronal cells, and the mechanism by which the ALAS1 CRD has to be translated to function may be hepatocyte-specific.

CHAPTER 5

Identification of ALAS1 mRNA protein-binding regions

5.1 Introduction

The results in the previous chapter demonstrated that ALAS1 contains an element in its coding region that confers haem-mediated destabilisation on the mRNA, and requires translation to function. However, the *cis*-acting element could not be defined further with the use of smaller overlapping sequences of the coding region in reporter assays. An explanation for this is that there may be more than one destabilising element which are required to be spatially distinct to function. An alternative strategy was used to identify protein-binding regions within the human ALAS1 mRNA coding region, to discover whether more than one region binds protein. mRNA stability/instability determinants are also binding sites for proteins; therefore these protein-binding results would give an indication that other sites may be involved in haem-mediated destabilisation of ALAS1 and the coding region determinant could be further delineated. Furthermore, we sought to characterise the size of these ALAS1 binding proteins. In addition to this we also investigated if haem could bind to the ALAS1 mRNA directly.

5.1.1 *Trans*-acting regulatory factors

From the onset of transcription, RNA is associated with RNA-binding proteins. Various RNA-binding proteins are involved in the regulation of splicing and processing, export of mRNA to the cytoplasm, maintenance of mRNA in the cytoplasm for translation, and finally decay of the mRNA. Some RNA-binding proteins shuttle between the nucleus and the cytoplasm (Shyu & Wilkinson, 2000), and a subset of these proteins may stay with an mRNA molecule for its lifespan. Other RNA-binding proteins are transiently associated with the mRNA, and may bind and dissociate in response to different stimuli. Some RNA-binding proteins have been shown to have a role in the regulation of gene expression by stabilizing or destabilizing a particular mRNA. Multiple stimuli can alter the affinity of RNA-binding proteins for their target *cis*-acting elements, including hormones and cytokines, redox changes, UV-light, the cell cycle, and developmental stage (Hollams *et al.,* 2002).

5.1.2 Tetrapyrrole binding to mRNA

In this chapter we examined if haem can bind directly to ALAS1 mRNA to regulate its own synthesis. The binding of haem to mRNA may be likely, as the tetrapyrrole cobalamin (CBL; vitamin B_{12}), synthesised only in prokaryotes, has

been shown to bind to RNA. CBL is an essential cofactor for several important enzymes that catalyze a variety of transmethylation and rearrangement reactions (Martens *et al.,* 2002). Expression of the *Salmonella typhimurium cob* operon, encoding the CBL biosynthetic pathway, and of the *btuB* gene of *Escherichia coli* and *S. typhimurium*, encoding the vitamin B12 transporter, is repressed by addition of vitamin B12 by a post-transciptional regulatory mechanism (Lundrigan *et al.,* 1991; Richter-Dahlfors & Andersson, 1992). The leader mRNAs of the *cob* and *btuB* genes contain an evolutionarily conserved sequence known as the B12-box. Adenosylcobalamin (Ado-CBL) is an effector molecule involved in the regulation of CBL genes (Nou & Kadner, 2000). The B12 RNA element is stabilized by direct binding of adenosylcobalamin. Thus, an adjacent regulatory hairpin terminator folds, which leads to transcriptional or translational repression of the genes. In the absence of the effector, the unstable vitamin-specific RNA element is replaced by an alternative anti-terminator RNA conformation allowing for transcription read-through or translation initiation (Vitreschak *et al.,* 2003).

5.1.3 Aims and Strategy

The major aim of this chapter was to further delineate the ALAS1 CRD by identifying fragments of the mRNA coding region that bind protein. Secondly, it was investigated whether this protein-mRNA interaction is sensitive to haem. It was also examined whether haem is able to bind to the ALAS1 mRNA directly.

In order to achieve these aims, RNA-EMSAs were used to identify fragments of the ALAS1 coding region that bind to HepG2 cytosolic protein extracts. UV-crosslinking was then used to further characterise these proteins. Accordingly, the next part of the introduction details the salient features of the two RNA-binding methods used in this chapter (illustrated in figure 5-1).

To study RNA and haem interactions, haemin-agarose beads were incubated with HepG2 total RNA, and RT-PCR was used to establish if ALAS1 mRNA binds haem directly.

5.1.3.1 RNA-EMSAs

In order to identify if any regions of the ALAS1 mRNA coding region bind HepG2 cytosolic proteins, RNA-EMSAs (Electromobility Shift Assays) were used. EMSA's provide a rapid approach for both qualitative and quantitative analysis of nucleic

acid-protein interactions, and is based on the observation that the electrophoretic mobility of a nucleic acid through a non-denaturing polyacrylamide gel is retarded when a protein(s) is bound to it. This method was originally developed to assay DNA-binding proteins, and was subsequently modified to detect RNA-binding proteins. Whether a band of complexes is seen depends on the strength of the RNA-protein interaction, and for many specific reactions the binding may be quite strong and the complexes long-lived. In addition, the binding is generally enhanced by the relatively low-salt buffer used in the electrophoresis experiment. Any RNA from complexes which dissociate during the run will trail the free RNA band, forming a faint smear between the complex and unbound RNA that is not usually detectable (Walker *et al.,* 1998).

All RNA-EMSA reactions were carried out in the presence of heparin and bovine liver ribosomal RNA (rRNA) at final concentrations of 5µg/µl and 0.1µg/µl respectively, using radiolabelled α^{32}P-CTP RNA. Heparin is a negatively charged anion that mimics the RNA phosphate backbone and is added to reduce non-specific protein binding to mRNA and background binding. Proteins that bind non-specifically to RNA simply because of its negative charge will bind to heparin rather than the RNA of interest. Ribosomal RNA is used as a competitor to bind to general RNA-binding proteins, therefore increasing the specificity of the assay. After incubation with protein, the RNA is electrophoresed on a non-denaturing gel, and exposed to film. Any RNA that has bound to protein will result in a shift on the gel, compared to the same RNA which had not been incubated with protein, run parallel on the gel.

5.1.3.2 UV-Crosslinking

To further characterise any *trans*-acting factors that bind to sequences of the ALAS1 coding region mRNA, UV-crosslinking experiments were carried out. UV-crosslinking of RNP (ribonucleoprotein) complexes takes advantage of the fact that UV light of sufficient intensity generates highly reactive species of RNA that react with molecules, including proteins, with which the RNA is in stable, direct contact. Crosslinking with UV light has several advantages over chemical reagents; it is relatively easy to carry out and the dose level can be accurately controlled. For example, irradiation at 254nm allows the identification of direct RNA-protein interactions since crosslink formation is observed only between molecular entities which are separated by no more than one covalent bond length (Walker *et al.,* 1998). This covalent association of the RNA with proteins makes it

possible to isolate the UV-crosslinked complexes under strongly denaturing and disulphide reducing conditions that ensure that only proteins crosslinked to the RNA are isolated with the RNA. To remove RNA not covalently bound to protein, and to reduce the length of RNA bound to protein for subsequent size estimation, the irradiated reaction is treated with a mix of RNase A and T1. Therefore, the radiolabelled RNA probe is reduced to a stub covalently attached to the protein allowing the visualisation by autoradiography of the RNA-binding protein, and an estimation of its size, by electrophoresis on an SDS-polyacrylamide gel. Similar to the EMSAs, heparin and rRNA is also used in UV-crosslinking to reduce the non-specific binding to the RNA.

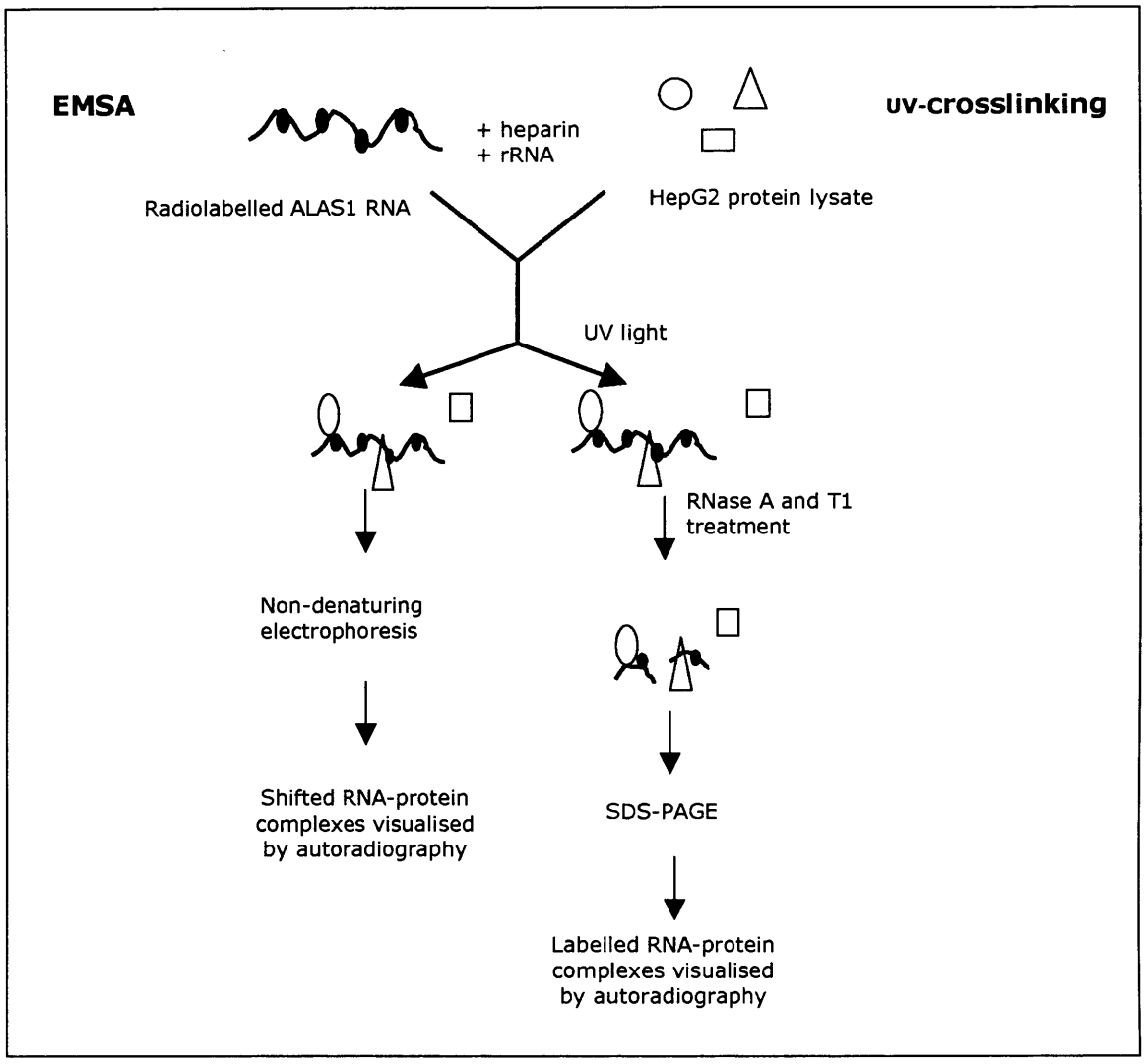

Figure 5-1 Schematic representation of the EMSA and UV-crosslinking reactions.

Cytosolic proteins from HepG2 cells are incubated with a uniformly labelled RNA probe at room temperature for 15 minutes. In the EMSA, the RNA is electrophoresed on a non-denaturing gel, and exposed to X-ray film. RNA-protein complexes are identified by a shift on the gel. In the UV-crosslinking reaction, the exposure to UV light covalently crosslinks closely associated proteins and RNA. The free RNA and the RNA not protected by UV-crosslinked protein are digested by an RNase A and T1 treatment. Finally, UV-crosslinked proteins are separated by SDS-PAGE, and exposed to X-ray film.

5.2 Materials and Methods

For the RNA-binding assays, the overlapping ALAS1 coding region sequences used in chapter 4 were cloned into the pGEM-T vector, in the T7 promoter direction. These were digested with the restriction enzyme, *Not* I to produce a 5' overhang. *In Vitro* transcription, using the Ambion T7 maxiscript kit, was used with 500ng of each linear construct, to produce the radioactive (α^{32}P-CTP) ALAS1 mRNA.

5.2.1 Radiolabelled ALAS1 RNA construction

The seven ALAS1 overlapping coding region sequences were amplified by PCR, using the primers listed in table 4-3 (chapter 4) with Bio-X-Act Long polymerase. These PCR products were gel extracted and inserted into the pGEM-T vector by TA cloning. These were used to transform subcloning efficiency, competent DH5α cells; and the plasmid DNA was isolated and purified. The orientation of each ALAS1 sequence in the pGEM-T vector was verified to be in the T7 sense direction by restriction digest.

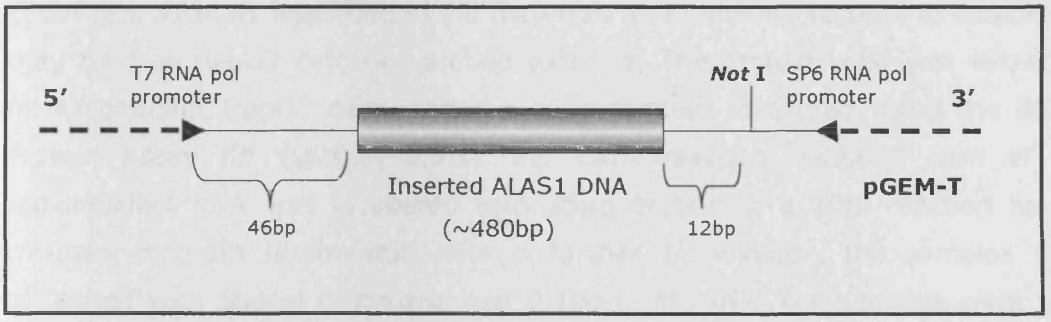

Figure 5-2 Schematic representation of the sub-cloning of ALAS1 DNA into pGEM-T vector.

The ALAS1 inserts, each of approximately 480bp in length, were amplified by PCR with Bio-X-Act Long polymerase and inserted into the pGEM-T vector by TA cloning. The plasmids containing the inserts in the correct orientation were then linearised at the *Not* I site, for *in vitro* transcription from the T7 RNA polymerase start site.

To produce the radiolabelled RNA probes, each pGEM-T-ALAS1 plasmid was digested 5' of the SP6 promoter site with the restriction endonuclease *Not* I, 12bp downstream of the inserted ALAS1 sequence (figure 5-2). *Not* I cuts at the sequence 5'-GC↓GGCCGC-3' to produce a 5' overhang. The digested ALAS1-pGEM-T was then gel purified. T7 RNA Polymerase is an extremely processive

enzyme and will continue to transcribe around a circular template multiple times without disassociating, therefore the construct has to be digested, and specifically with an enzyme that does not produce a 3' overhang. Enzymes which cleave the DNA and leave a 3´ overhang often give rise to aberrant transcripts.

Radiolabelled RNA was transcribed as described in section 2.7.1, using T7 polymerase and α^{32}P CTP as the limiting NTP at a final concentration of 3.125μM, with 10μM of cold CTP. The RNA was purified from the unincorporated nucleotides by spinning through a Sephadex G-50 column, and the amount of radioisotope made was quantified by liquid scintillation counting. Each radiolabelled RNA probe was electrophoresed on a denaturing gel to confirm that it was the correct size, no degradation had occurred, and that any unincorporated nucleotides had been completely removed. The RNA was stored at −70°C until further use, and used within 5 days so that only full-length and intact radiolabelled RNA was used in the experiments.

5.2.2 RNA EMSA

The seven ALAS1 overlapping coding region fragments were used in the RNA-EMSA reactions, as described in the materials and methods section, to establish if they bind to HepG2 cytosolic protein extracts. The protein used was extracted from confluent HepG2 cells, and the concentration measured using the BCA™ Protein Assay Kit (section 2.3.1). For each reaction, 100,000 cpm of the radiolabelled RNA was incubated with 25μg protein in a 10μl reaction for 15 minutes at room temperature. For a further 15 minutes, the samples were incubated with 5μg/μl of heparin and 0.1μg/μl of rRNA. The samples were then subjected to electrophoresis on a non-denaturing 4% polyacrylamide gel. In experiments where the affect of haem on the protein-binding was assayed, 20μM haem or control medium was added to the cells for 24 hours, after the cells had been grown in haem-depleted medium.

5.2.3 UV-Crosslinking of cytosolic proteins to ALAS1

The ALAS1 coding region fragments which were shown to bind to protein by EMSA were also used in cross-linking reactions with HepG2 cytosolic protein extracts. Similar to the EMSAs, 100,000 cpm of the radiolabelled RNA was incubated with 25μg protein in a 10μl reaction for 15 minutes. For a further 15 minutes, the samples were incubated with 5μg/μl of heparin and 0.1μg/μl of rRNA. As

described in the materials and methods section, the reaction was exposed twice to 8600J of UV-light and unbound RNA was degraded by the addition of RNase A and T1. The samples were then subjected to electrophoresis by SDS-PAGE.

5.2.4 Binding of ALAS1 RNA to haemin-agarose

Haemin-agarose has previously been used to identify proteins that bind to haem *in vitro*. Therefore, this part of the chapter endeavoured to modify these protein-binding assays to assess if the ALAS1 mRNA binds to haemin directly, thereby directly inhibiting its transcription. In these experiments, haemin-agarose beads were incubated with total RNA extracted from HepG2 cells, in the presence of 20 µg of glycogen. Glycogen was used as an inert material, allowing the precipitation of pg amounts of RNA. The method used was a modified version of the methods used by Trifillis *et al.,* 1999.

Haemin-agarose beads (60µl) were washed in 1ml of RNA binding buffer (RBB, 10mM Tris-HCl, pH 7.5, 1.5mM $MgCl_2$, 150mM KCl) by resuspending, centrifugation at 6000rpm at 4°C and removal of the supernatant. The beads were resuspended in 350µl of RBB and incubated with 10µg of HepG2 total RNA at 4°C for 1 hour. This incubation was followed by centrifugation at 4000rpm to remove unbound RNA and a wash in 1ml RBB/0.1% TX (Triton X-100), prior to further centrifugation at 4000rpm at 4°C. RNA interacting non-specifically with the haemin-agarose was competed off with 2 washes in RBB containing 1mg/ml heparin for 10 minutes at 4°C and centrifugation. The beads were subsequently rinsed four times in RBB/0.1% TX to remove unbound RNA, and the RNA was isolated from the drained beads by boiling for 5 minutes in 200µl TE/1% sodium dodecyl sulphate (SDS). The RNA was then phenol/chloroform (1:1) extracted, chloroform extracted, ethanol precipitated with 20µg glycogen and washed with 70% ethanol. The dried RNA was resuspended in 10µl sterile H_2O by heating to 65°C for 5 minutes. Washes were collected at varying stages of the procedure for RT-PCR analysis to assess how well specific RNA molecules bound to the haemin-agarose, and at what stage the ALAS1 RNA was eluted.

5.2.4.1 RT-PCR of ALAS1 and GAPDH

RT-PCR was used to amplify ALAS1 (primers P28, P29) and GAPDH (primers P32, P33), and compare elution of these RNA transcripts at varying stages of the assay. Prior to the quantification by PCR, all the PCR conditions had been

optimised for logarithmic amplification using untreated control cells (see section 3.2.1.1).

cDNA was synthesised from the RNA eluted from the haemin-agarose beads by first strand synthesis, and the RNA was quantified by PCR using primer sets specific for cDNA fragments of ALAS1 and GAPDH (table 5-1). The cycling protocol for the ALAS1 PCR was that as described in section 2.4.4.3.1, with 38 cycles, and an annealing temperature of 60°C. The GAPDH PCR used 34 cycles, with an annealing temperature of 65°C. The primers used for ALAS1 and GAPDH spanned exon boundaries, ensuring that only the mRNA was detected, rather than any contaminating genomic DNA in the RNA samples. The PCR products were resolved by agarose gel electrophoresis.

Target DNA	**Primer Number**	**Product Size**	**PCR Annealing Temperature**
ALAS1	Sense P26 , Anti-Sense P27	480bp	62°C
GAPDH	Sense P32, Anti-Sense P33	267bp	65°C

Table 5-1 Primers used in semi-quantitative RT-PCR.

Reagent	**Volume (µl)**
10x PCR buffer	2
2mM dNTP mix	2
Sense Primer 5pmol	2
Antisense Primer 5pmol	2
cDNA Template (RT product)	2
HotStarTaq Polymerase (5U/µl)	0.2
H_2O	to 20µl

Table 5-2 Composition of semi-quantitative RT-PCR.

5. 3 Results and Discussion

5.3.1 HepG2 cytosolic protein binds to two distinct regions of the ALAS1 coding region.

Cable *et al* demonstrated that a specific 154bp sequence of the ALAS1 mRNA coding region binds to Huh-7 cytosolic proteins (Cable et al., 2001). RNA-EMSAs were used in this chapter to confirm that this region binds proteins from hepatocytes using HepG2 cells, and to investigate any other protein-binding regions.

Radiolabelled RNA that corresponded to the seven overlapping ALAS1 fragments of the coding region, designated RNA probes 1-7 (as indicated in figure 5-3b), were incubated with or without protein for 30 minutes, loaded onto a non-denaturing 4% polyacrylamide gel and electrophoresed at 200V for approximately 4 hours. The gel was dried and exposed to radiography film to visualise the RNA.

Figure 5-3a shows the EMSA of the RNA probes corresponding to the specific fragments of the ALAS1 coding region, incubated with and without HepG2 cytosolic protein. The lanes without protein demonstrate that the RNA had not decayed and was of the correct size. When the RNA probes were incubated with the HepG2 cytosolic protein extract, shifts were observed for probes 2, 4, 5 and 6 indicating that these regions of the RNA bind protein. No shifts were seen for probes 1, 3 and 7 of the ALAS1 coding region. These results suggest that no *cis*-acting elements are present in fragments 1, 3 and 7 as they do not bind cytosolic protein.

Interestingly, probe 4, which binds to protein, contains the 154bp sequence element previously identified by cable *et al*. However, our results from probe 2 indicate that an additional sequence towards the N-terminus (corresponding to 481-960bp) also binds protein. It is possible that the *cis*-acting element may still reside in this 154bp region, but it has a bi-partite structure, residing in both fragments 2 and 4. Two shifted bands are observed when probe 2 is incubated with protein. This may be the result of two different proteins binding to the RNA, or that additional secondary structures of the RNA are formed when binding occurs. The binding of protein to probe 2 is confirmed by the EMSAs of probes 5 and 6, which both overlap probe 2 and both bind to protein. This result suggests that there is extensive protein binding over multiple sites within fragment 2.

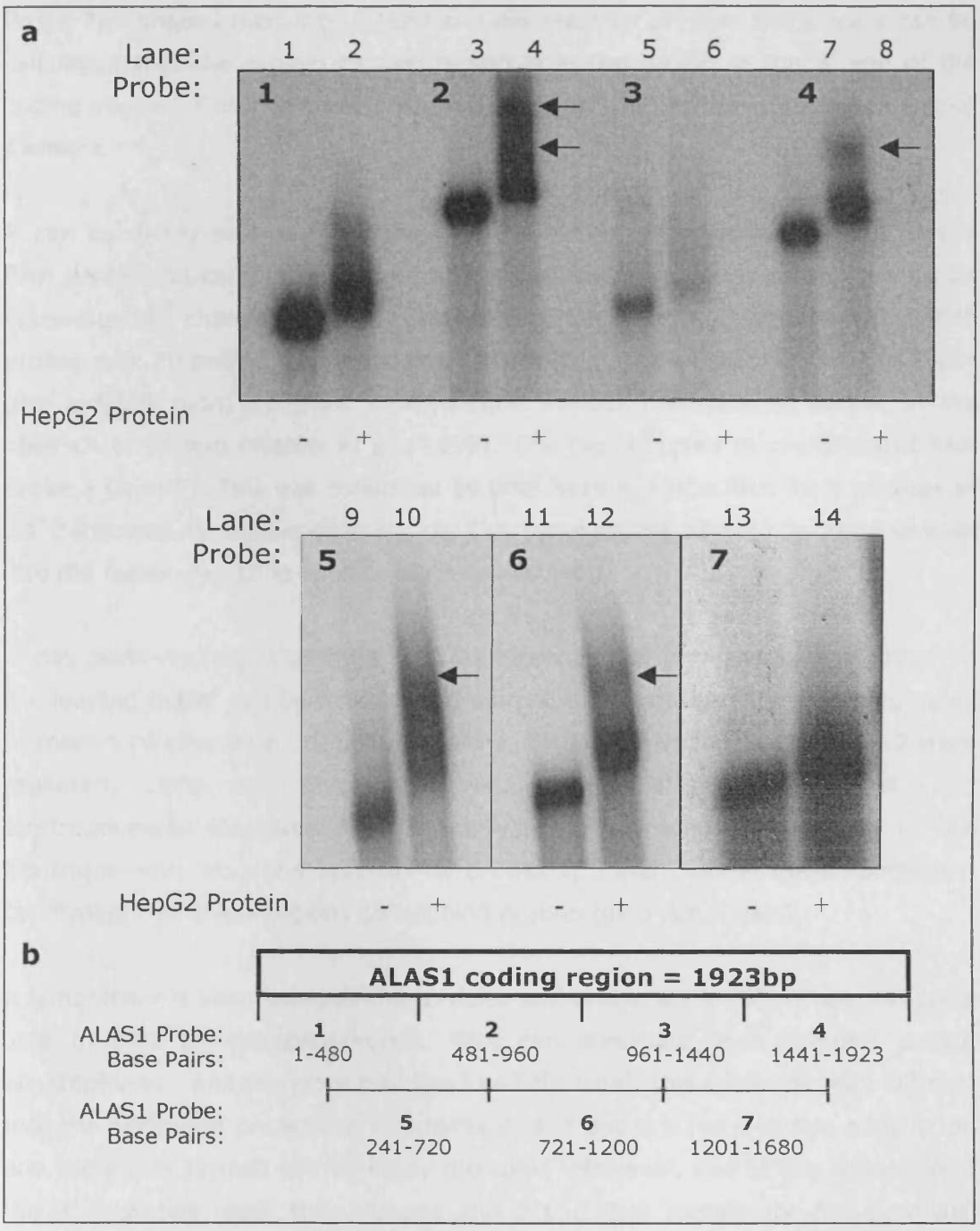

Figure 5-3 RNA-EMSA of overlapping probes of the ALAS1 coding region.

a) Radiolabeled RNA of 7 fragments of the ALAS1 coding region, each of 100,000 cpm, were incubated with 25µg HepG2 cytosolic protein extract or protein-free buffer in an EMSA reaction. The reactions were electrophoresed and visualised by autoradiography. Arrows indicate shifts in the electrophoresis, and indicate that RNA binds to protein. Lanes 1-2: probe 1; 3-4: probe 2; 5-6: probe 3; 7-8: probe 4; 9-10: probe 5; 11-12: probe 6; 13-14: probe 7.

Lanes 1,3,5,7,9,11,13: Protein-free EMSA; 2,4,6,8,10,12,14: Protein in EMSA reaction.

b) A schematic diagram to clarify the sequence of each of the ALAS1 probes. Binding of protein to the mRNA occurred only in fragments 2, 4, 5 and 6; not in 1, 3 and 7.

Probe 7 overlaps probe 4 by 240bp and did not bind protein, therefore it can be calculated that the protein-binding region is in the 243bp at the 3' end of the coding region. This fragment contains 141bp of the 154bp putative *cis*-acting element.

It can be clearly seen in the EMSA that the addition of protein extract to all the RNA probes causes the unbound RNA to shift slightly. This is most likely to be caused by the change in salt concentration of the sample, compared to the RNA probes with no protein extract added. Occasionally, the labelled RNA run in EMSA gels exhibits more than one conformation, resulting in multiple bands, in the absence of protein (Walker *et al.,* 1998). This has occurred in the EMSA of RNA probe 3 (lane 5). This was confirmed by brief heating of the RNA for 3 minutes at 70°C followed by snap cooling on ice. This converts the slower migrating species into the faster migrating species (data not shown).

It has been reported that dyes such as bromophenol blue and xylene cyanol in the loading buffer can be inhibitory to binding and cause problems with complex formation (Walker *et al.,* 1998). Therefore, EMSAs for fragments 1, 3 and 7 were repeated, using only glycerol to load the samples onto the gel, and electrophoresed alongside dye-containing buffer to monitor the extent of the electrophoresis. No shifts occurred for probes 1, 3 and 7 under these conditions, confirming that these regions do not bind protein (data not shown).

A faint smear is seen between the complex and unbound RNA of probes that were able to bind to cytosolic protein. RNA can dissociate from proteins during electrophoresis and therefore trail the free RNA band. This smearing may indicate that the binding of proteins to fragments 2, 4, 5 and 6 is not a strong association and the bonds formed can be easily disrupted. However, due to the large size of the RNA probes used, the unbound and bound RNA probes are not very well resolved which may add to the smearing in lanes 4, 8, 10 and 12.

These EMSA results show that there are two areas in the human ALAS1 coding region mRNA that can bind to Hepg2 cytosolic protein, corresponding to fragment 2 and the last 243bp of fragment 4. Probe 4 corresponds to the region previously identified by Cable *et al* (2001) as able to bind to proteins extracted from Huh-7 cells. This provides independent confirmation that the binding observed in the EMSA for probe 4 is correct.

5.3.2 Binding of HepG2 cytosolic protein to ALAS1 RNA probes with the addition of haemin in the EMSAs

Section 5.3.1 demonstrated that ALAS1 fragments 2 and 4 contain protein-binding sites. Therefore, it was next investigated whether the addition of haemin into the binding reaction of the EMSA affected this binding of cytosolic proteins to the ALAS1 RNA. Fragments 1 and 3 were also used in these EMSAs, to establish if the addition of haemin was able to induce protein binding to these sequences.

During the incubation stage of the EMSA, where the probe is incubated with protein extract for 30 minutes, either 20μM haemin solubilised in DMSO or DMSO alone was also added to the reaction. For each fragment, an EMSA with no DMSO or haemin added to the reaction was also, used as in section 5.3.1, as a further control.

This representative EMSA shown in figure 5-4 of probes 1 and 3 showed no demonstrable difference between samples with or without haemin added in the binding step. This confirms that the sequences corresponding to probes 1 and 3 are not involved in the haem destabilisation mechanism. No consistent effects of haemin could be demonstrated with repeated EMSAs, with haemin sometimes even appearing to increase the protein binding to both probes 2 and 4. However, the results of this EMSA in figure 5-4 show that the addition of haemin to the binding reaction of probe 2 caused a decrease in protein binding, whereas probe 4 decreased its protein binding with the addition of DMSO, and haemin had no effect. However, we were unable to consistently demonstrate effects of haemin on protein binding to probes 2 and 4.

These results confirm that the human ALAS1 mRNA contains two regions, corresponding to fragments 2 and 4 (figure 5-3), which can bind to cytosolic protein. Protein binding to either of these regions is not sensitive to the presence of haemin in the protein-binding step of the EMSA. Therefore, the binding to fragments 2 and 4 does not seem to be haem-sensitive under these experimental conditions.

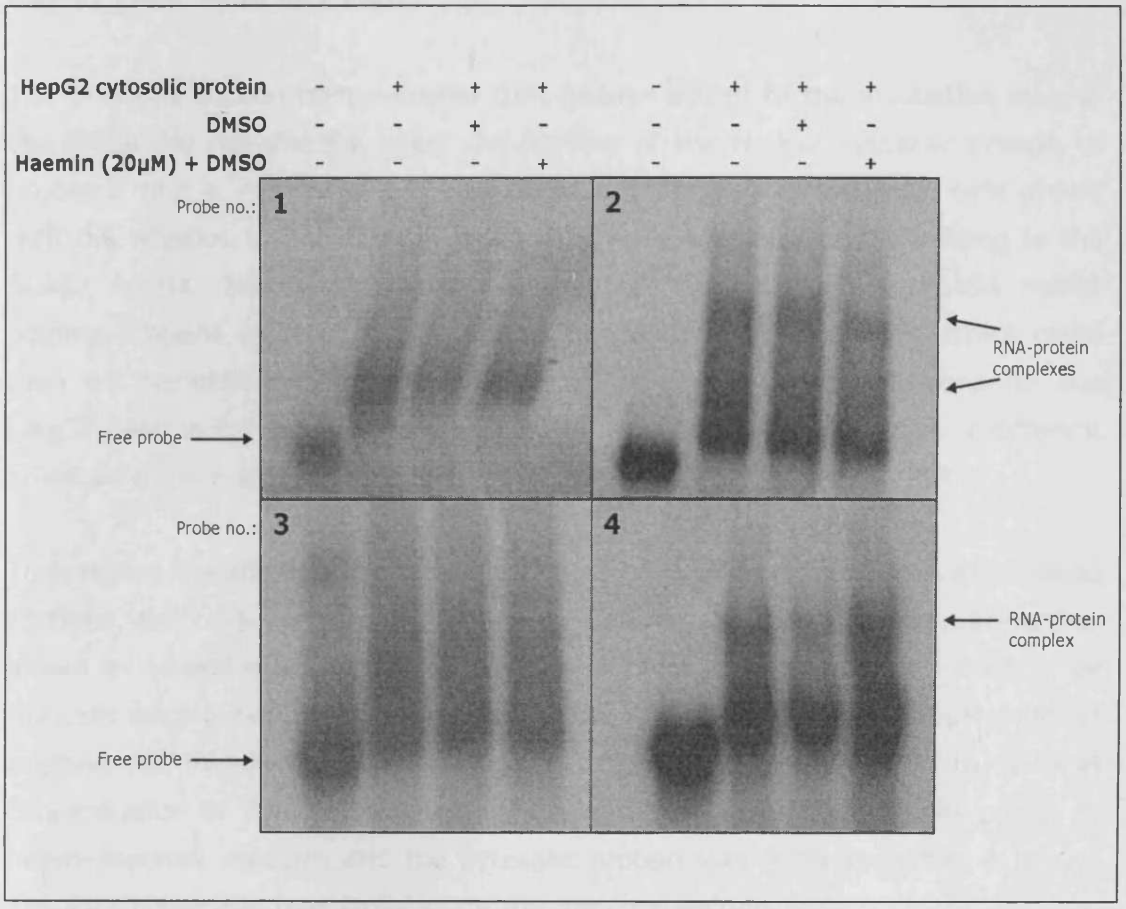

Figure 5-4 RNA EMSA of the 4 ALAS1 coding region fragments incubated with HepG2 cytosolic protein, with haemin or DMSO.

An RNA-EMSA of the ALAS1 coding region fragments was carried out as previously. The radiolabelled RNA was incubated with HepG2 cytosolic protein, with either haemin, solubilised in DMSO, or DMSO alone as a control. For further controls, EMSAs were carried out using radiolabelled probe alone, or incubated with HepG2 cytosolic protein with no DMSO or haemin added. The above EMSA is a representative of the results obtained, when repeated three times.

5.3.3 Binding of cytosolic protein from haem depleted or supplemented HepG2 cells, to ALAS1 RNA

The previous section demonstrated that haemin added to the incubation step of the EMSA did not directly affect the binding of the HepG2 cytosolic protein to probes 2 and 4. However, it is possible that protein extracted from cells grown with the addition or depletion of haem may have an effect on the binding to the ALAS1 mRNA. The haemin added to the cells may cause any ALAS1 mRNA binding-proteins to be either up- or down-regulated within the cell, which could then be demonstrated by the EMSA. The different growth conditions for the HepG2 cells would have more physiological relevance and may have a different affect on protein-binding than the *in vitro* approach used in section 5.3.2.

To compare the affect of haemin added to the cells, prior to extraction of cytosolic proteins, the cells were treated in three different ways. HepG2 cells were either grown in normal media, as for the previous EMSA experiments as a control, or the cells were grown in haem-depleted media with the addition of 500μM succinyl acetone to inhibit haem biosynthesis. After 24 hours, haemin to a final concentration of 20μM or the vehicle medium was added to the cells grown in haem-depleted medium and the cytosolic protein was extracted after 4 hours. The RNA EMSA was performed as for the previous section.

This representative EMSA in figure 5-5 of probes 1 and 3 shows no binding occurred when incubated with the different protein samples. This confirms that the sequences corresponding to probes 1 and 3 are not involved in the haem destabilisation mechanism. The EMSA was repeated in triplicate, and was unable to demonstrate a consistent effect on protein-binding to fragments 2 and 4 by haem depletion/supplementing.

The representative EMSA in figure 5-5 shows that using protein from cells grown in medium *with* haem decreased the binding to probe 4. However, similar to the results seen in the previous section, although binding was decreased by haem the majority of times this EMSA was repeated, it did not occur each time. Haem depletion or add-back to cell medium had no effect on the protein binding to probe 2, compared to proteins from HepG2 cells grown in normal medium, on each occasion the EMSA was repeated. Therefore, this section confirms that fragments 2 and 4 bind to HepG2 cytosolic protein but we cannot conclusively prove that this binding is sensitive to haem.

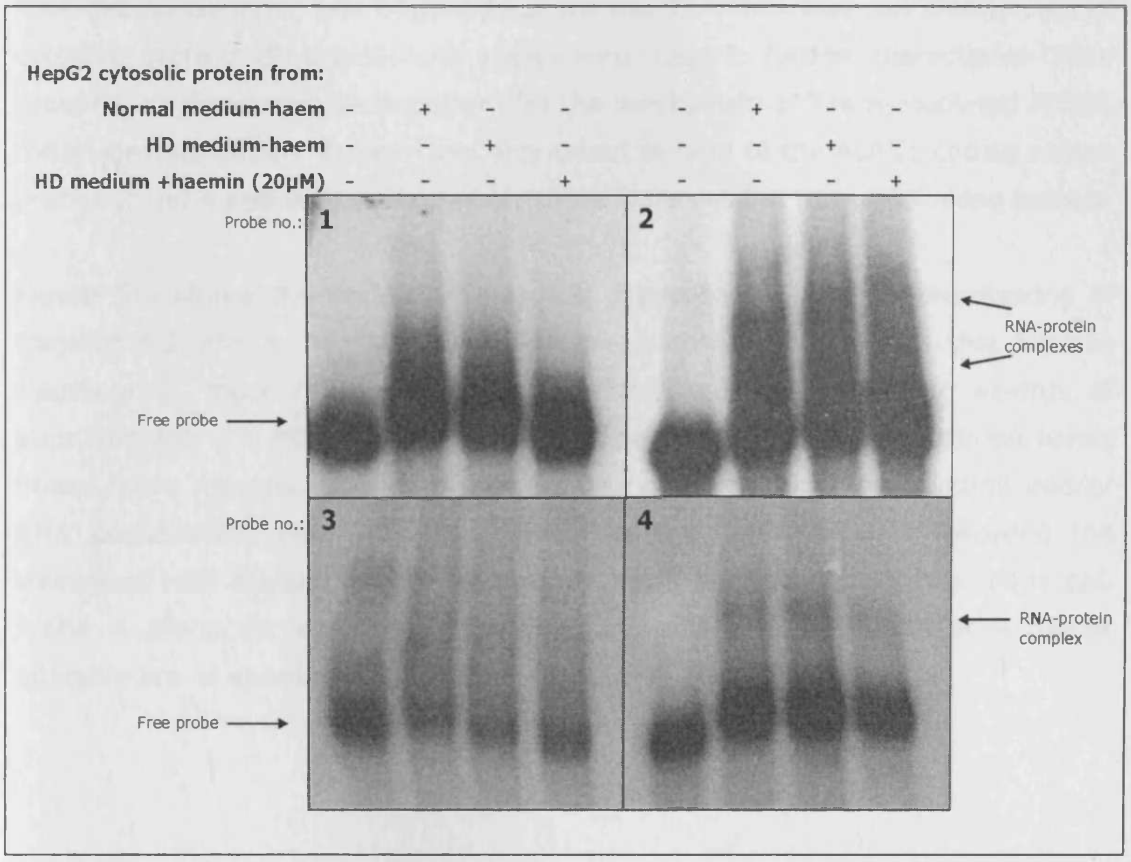

Figure 5-5 RNA EMSA of the 4 ALAS1 coding region fragments incubated with cytosolic protein from cells grown in haem-depleted or supplemented medium.

An RNA-EMSA of the ALAS1 coding region fragments was carried out as previously. The 100,000cpm radiolabelled RNA was incubated with 25μg HepG2 cytosolic protein. As a control, EMSAs were carried out using radiolabelled probe alone. To test the affect of haem in the growth medium of cells on the protein binding, three types of medium were used: normal growth medium, haem-depleted medium, and haem-depleted medium with haem added for 4h before protein extraction. Differences in haem concentration had no effect on probes 1-3, but an excess of haem decreased the binding to probe 4 in the representative EMSA shown. However, this could not be repeated in further replicates of the experiment.

5.3.5 UV-Crosslinking of HepG2 cytosolic proteins bound to ALAS1 RNA

RNA-EMSAs identified two fragments of the ALAS1 mRNA that can bind to HepG2 cytosolic protein. UV-crosslinking assays were used to further characterise these proteins, as these may be important for the mechanism of haem-mediated ALAS1 mRNA destabilisation. Protein was only found to bind to the ALAS1 coding region probes 2 and 4 and consequently only these were used in the crosslinking assays.

Figure 5-6 shows the results of a typical experiment of the UV-crosslinking of fragments 2 and 4, in triplicate. There are a number of proteins that bind to fragment 2; those of the strongest intensity have the molecular weights of approximately 37, 40 and 70kDa (indicated by arrows). The other protein bands below these may be a result of protein degradation during the reaction and/or RNA degradation. However, the majority of the degraded RNA following the treatment with RNases is seen as a strong black band at the bottom of the gel. Probe 4 produced less protein bands than Probe 2. The bands at a higher intensity are of approximately 37 and 48kDa.

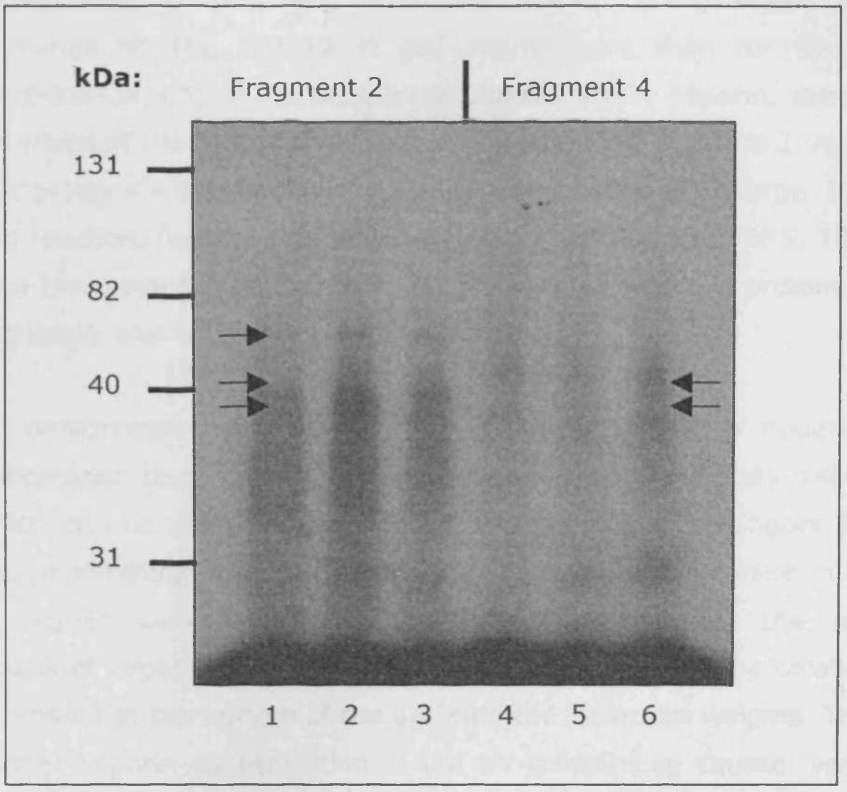

Figure 5-6 UV-crosslinking of ALAS1 radiolabelled RNA fragments 2 and 4 to characterise the binding proteins.

The UV-crosslinking reactions of ALAS1 coding region fragments 2 and 4 were carried out to identify the size of the RNA-binding proteins. For each fragment, the reaction was in triplicate, using 100,000 cpm radiolabelled probe incubated with 25µg HepG2 cytosolic protein, in the presence of 5µg/µl heparin and 0.1µg/µl rRNA to reduce non-specific binding. Samples were analysed by electrophoresis through an SDS-PAGE gel, and the dried gel was exposed to radiography film. The above figure is indicative of a typical gel. The experiment was repeated on three separate occasions.

Lanes 1-3: Radiolabelled ALAS1 coding region fragment 2 in triplicate;

Lanes 4-6: Radiolabelled ALAS1 coding region fragment 4 in triplicate.

5.3.6 Optimisation of UV-crosslinking to fragment 2

The UV-crosslinking of fragment 2 of the ALAS1 coding region produced numerous bands on the SDS-PAGE gel, many more than for fragment 4. Increasing concentrations of the negatively-charged anion, heparin, were used to investigate which of the proteins were specifically binding to probe 2, rather than non-specific proteins which bind to the RNA due to its negative charge. In the UV-crosslinking reaction, heparin was added to a final concentration of 5, 10, 25 and 50µg/µl into the binding reaction, with 25µg of HepG2 cytosolic protein, and the crosslinking assay was carried out as previously.

Figure 5-7 demonstrates that the increasing concentrations of heparin in the reactions increased the intensity of the proteins of approximately 140kDa and 80kDa, which did not seem to be significant on the previous gel (figure 5-6). The bands at approximately 40kDa and 37kDa also seemed to increase in intensity with the higher concentrations of heparin. Furthermore, the increased concentrations of heparin reduced the number and intensity of the smaller bands which are present at the bottom of the gel with low molecular weights. Therefore, using a higher heparin concentration in the UV-crosslinking caused less protein and RNA degradation to occur. It is difficult to analyse further the significance of these proteins which bind to probe 2. Only the molecular weights are known, therefore it cannot be deduced which proteins these actually are and whether the multiple bands are due to multiple proteins binding or numerous subunits of one protein which specifically binds to ALAS1 mRNA.

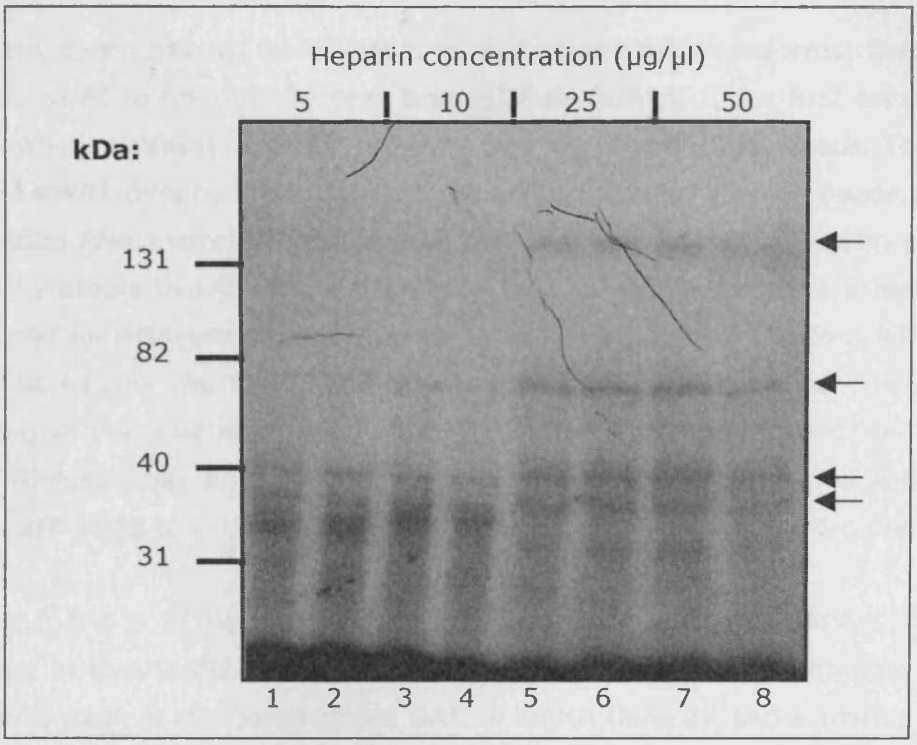

Figure 5-7 UV-crosslinking of RNA fragment 2 with HepG2 cytosolic protein extract and increasing concentrations of heparin.

Heparin at increasing concentrations was added to the binding reaction to compete out any unspecific binding of protein to the ALAS1 mRNA.

Final concentrations of heparin in the binding reaction (in duplicate):

Lanes 1-2: 5µg/µl; 3-4: 10µg/µl; 5-6: 25µg/µl; 7-8: 50µg/µl.

UV-crosslinking was carried out using 100,000cpm radiolabelled RNA probe with 25µg HepG2 cytosolic protein, as described in the methods. The reactions were analysed by SDS-PAGE, and the dried gel was exposed to radiography film.

The above gel is indicative of a typical experiment. The experiment was repeated on two separate occasions, with each heparin concentration in duplicate.

5.3.7 The use of haemin-agarose beads to investigate whether haem binds ALAS1 mRNA directly

To date, haem has not been shown to bind to any mRNA isoforms; therefore we endeavoured to find out if haem directly binds to ALAS1, the first enzyme in its biosynthetic pathway, thereby reducing the rate of its own synthesis. To assess if ALAS1 mRNA directly binds to haem, we utilized haemin-agarose beads incubated with total RNA extracted from HepG2 cells. Haemin-agarose has been previously used by others to investigate if proteins bind to haem; therefore a method was designed for RNA-binding analysis, by a type of affinity purification. RT-PCR was used to amplify the ALAS1 mRNA alongside GAPDH as a control for unspecific binding in the final eluted RNA sample. The RNA was also quantified from the total RNA samples prior to incubation with the haemin-agarose, as well as from two wash steps to establish when each RNA isoform was eluted from the beads.

Lanes 1 and 5 of figure 5-8 confirm that both ALAS1 and GAPDH mRNA are present in the HepG2 total RNA extract, used to incubate with haemin-agarose. The first wash of the beads eluted GAPDH mRNA (lane 2), and a small amount of ALAS1 mRNA (lane 6). In contrast, no GAPDH or ALAS1 mRNA was eluted after the beads were washed in heparin (lanes 3 and 7). The final step to elute the mRNA bound to the haemin demonstrates that both ALAS1 (lane 4) and GAPDH (lane 8) mRNA were able to bind the haemin-agarose, suggesting that the binding to ALAS1 mRNA is non-specific. However, it interesting that only a small quantity of ALAS1 mRNA was eluted from the beads during the first wash step. It may be that both the ALAS1 and GAPDH mRNAs are binding to the agarose rather than the haemin, thereby obscuring any genuine results from the experiment. Despite extensive modification of the wash steps, and even attempting to compete off the ALAS1 mRNA by adding haemin, no specific direct binding of haemin to ALAS1 mRNA was demonstrated in this RNA-binding assay.

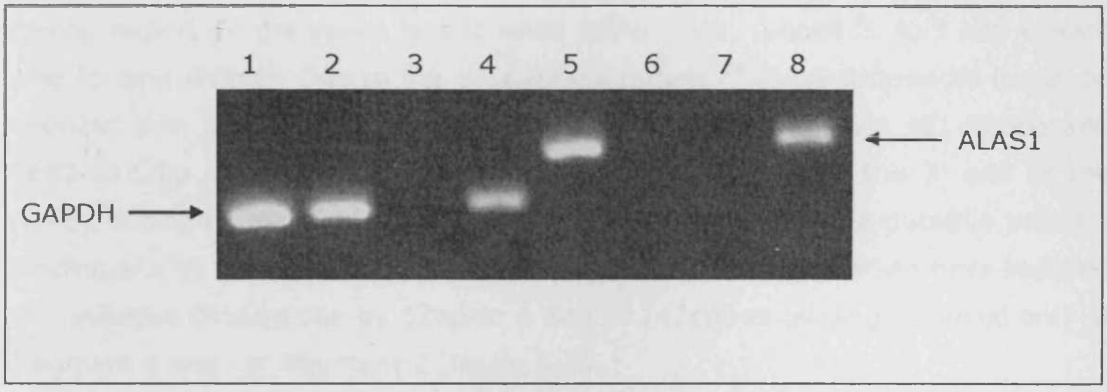

Figure 5-8 RT-PCR analysis of GAPDH and ALAS1 mRNA binding to haemin agarose.

HepG2 total RNA (10µg) was incubated with 60µl haemin-agarose beads for 1h at 4°C. After incubation the sample was washed in RBB, followed by a wash in RBB containing 1mg/ml heparin. The beads were then rinsed four times in RBB and the RNA bound to the haemin-agarose was isolated by boiling for 3min in TE/1% SDS. RNA samples were used at various stages to assess if the ALAS1 and GAPDH mRNA binds to haemin. Each sample was ethanol precipitated and resuspended in 10µl 1x MMLV-RT buffer with 1U of RNasin. Samples were subjected to RT-PCR and the ALAS1 and GAPDH mRNA were separately quantified by PCR.

Lane 1, 5: total RNA; 2, 6: RNA eluted from wash in RBB/0.1%TX; 3, 7: RNA eluted from wash with heparin; 4, 8: Final eluted RNA.

5.4 Conclusions

The data produced in the chapter demonstrates that cytosolic protein extracted from HepG2 cells is able to bind to radiolabelled RNA fragments of the ALAS1 coding region. Of the seven radiolabelled RNAs made, probes 2, 4, 5 and 6 were able to bind protein. Due to the overlapping nature of these sequences it can be deduced that protein binds in two distinct regions ranging from 481-960bp and 1681-1923bp of the coding region. A previous sequence at the 3' end of the ALAS1 coding region of 154bp has previous been identified as a putative protein-binding site by Cable *et al* (2001). The results from the RNA-EMSAs have reduced this putative binding site by 12bp to a size of 142bp, as binding occurred only in fragment 4 and not fragment 7 (figure 5-9).

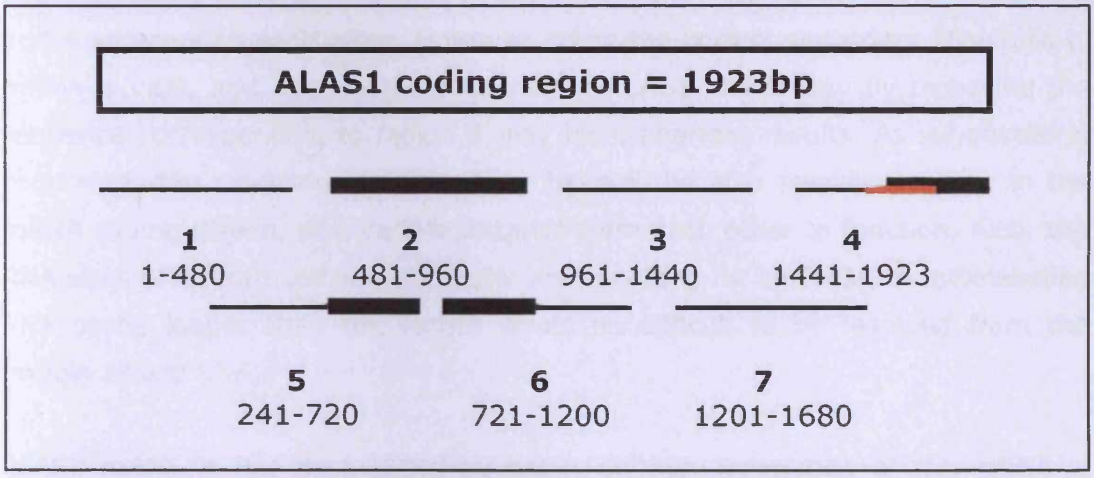

Figure 5-9 Putative cis-acting elements in the ALAS1 mRNA deduced from the protein-binding sites.

RNA-EMSAs were used to establish which of the seven overlapping fragments of the ALAS1 coding region can bind to HepG2 cytosolic protein. Fractions 2, 4, 5 and 6 are able to bind protein, whereas 1, 3 and 7 do not. Therefore, it is concluded that the protein-binding sites are in fragments 2 and at the end of 4. The red line indicates the 154bp *cis*-acting element identified by Cable *et al*. Probe 4 contained the full 154bp sequence and was able to bind protein, whereas probe 7 only contained 12bp of the putative element and did not bind protein. Therefore, this putative *cis*-acting element can be reduced to 142bp.

In these experiments, the addition of haemin in the binding reactions does not affect the binding to probes 2 and 4, and does not induce binding to probes 1 and 3. Furthermore, using protein from HepG2 cells grown in haem-depleted media or

grown in the presence of haem also did not conclusively affect binding to probes 2 and 4, or induce binding to probes 1 and 3. Therefore, fragments 2 and 4 are surmised to contain the haem-mediated *cis*-acting elements from the results of these EMSA experiments, as these bind to proteins, even though a haem-effect was not seen. It is notable that when Cable *et al* carried out EMSAs using Huh-7 protein extracts, they were also unable to show that haem affected the binding of protein to the 154bp sequence of the ALAS1 mRNA, corresponding to our fragment 4 (personal communication).

It has not been established if the putative elements in fragments 2 and 4 are both necessary for the haem-mediated destabilisation of the mRNA. Ways to investigate this may be to use a chimeric protein of fragments 2 and 4 in a DLRA, as used in chapter 4, to assess the stability in response to haem. Secondly, to use a chimeric radiolabelled RNA in the EMSA, with the sequences of regions 2 and 4 adjacent to each other. However, often the correct secondary structure of mRNA is vital, and altering the sequence of ALAS1 in this way by removing the sequence corresponding to region 3 may have aberrant results. As suggested in chapter 4, the *cis*-acing elements may have to be at a specific position in the mRNA coding region, at a certain distance from each other to function. Also, the RNA sizes of 480nt used in this chapter are very long for an EMSA. A radiolabelled RNA probe longer than this length would be difficult to be resolved from the protein bound RNA.

ALAS2 mRNA is not destabilised by haem. Rather, translation of the mRNA is controlled by an iron response element (IRE) in its 5'-UTR, where the higher the iron concentration within the cell, the more ALAS2 and therefore haem is produced. The IRE is bound to an IRP, and at high concentrations of iron this IRP is displaced, allowing translation through it (Dandekar *et al.,* 1991). ALAS2 mRNA is not sensitive to haem concentration and is therefore unlikely to contain a *cis*-acting instability element, as is present in the ALAS1 mRNA. However, ALAS1 gene expression in murine Friend virus-transformed erythroleukemia (MEL) cells appears to be under the haem-mediated feedback control as it is in the liver. Expression of mRNAs encoding the ALAS1 and ALAS2 were examined using *in situ* hybridization. Following DMSO treatment, ALAS2 mRNA increased, whilst ALAS1 mRNA did not increase in wild-type MEL cells (Fujita *et al.,* 1991; Mitani *et al.,* 1992). Furthermore, it has been shown that ALAS1 is up-regulated in ALAS2-knockout erythroblasts, but down-regulated in wild-type erythroblasts (Harigae *et al.,* 2003). Therefore, ALAS1 and ALAS2 mRNAs are under separate controls.

There must be a specific difference between the mRNA sequences of ALAS1 and ALAS2 to enable a haem-mediated destabilising *cis*-acting element to function only in the ALAS1 mRNA.

On comparison of the sequence of fragment 2 in human ALAS1 mRNA and the corresponding fragment of human ALAS2 mRNA, there is 61% homology (figure 5-10). This sequence homology suggests that there may be specific sequences in the fragment that are involved in haem-mediated destabilisation of ALAS1 mRNA.

The fragment 2 of the ALAS1 coding region contains exon 4, and interestingly this exon is often removed in ALAS2 by alternative splicing of the mRNA. There are five alternatively spliced forms of human ALAS2. However, the principal alternatively spliced mRNA is that which lacks exon 4 encoding sequence, constituting around 35-45% of total ALAS2 mRNA in erythroid tissues (Cox *et al.,* 2004; Conboy *et al.,* 1992). Similar proportions of the normal and the spliced exon 4 mRNA isoforms have also been found in foetal liver and normal bone marrow. Exclusion of exon 4-encoded sequence from the ALAS2 protein, which constitutes a major variant *in vivo* does not substantially affect mitochondrial import or its ability to associate with SCSβA (succinyl CoA synthase beta A subunit), but does reduce its catalytic activity *in vitro*. The exclusion of a definitive *in vivo* role for this region between the mitochondrial pre-sequence and the 'catalytic' core remains to be proven. Cox *et al* have postulated that exon 4 may either aid stability of the enzyme, determine whether it is further processed in mitochondria, or may be required for interaction with proteins other than SCSβA (Cox *et al.,* 2004). It is unknown whether the corresponding exon in ALAS1 has a novel function involved in its expression.

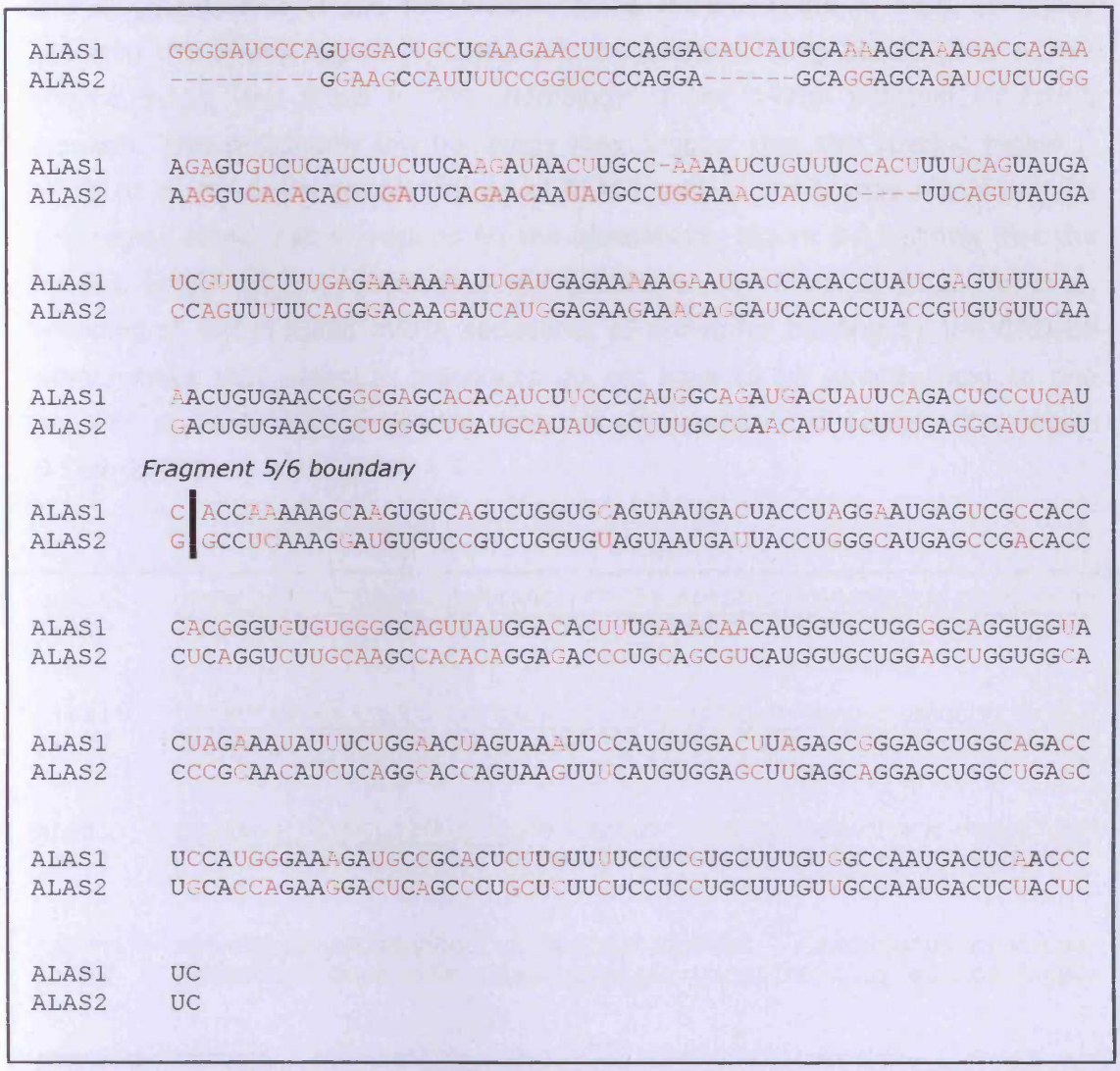

Figure 5-10 mRNA sequence homology of ALAS1 fragment 2, and the corresponding nucleotides of ALAS2.

Using EMSAs of overlapping fragments of the ALAS1 coding region, fragment 2 was shown to bind to HepG2 cytosolic protein. Fragments 5 and 6 which overlap fragment 2 were also shown to bind protein, and their boundary is shown. ALAS1 and ALAS2 have a sequence homology of 61% in this region. The non-homologus nucleotides are in red. The ALAS2 sequence used for this homology analysis contains exon 4 which is often alternatively spliced.

The protein-binding region of fragment 4 has been reduced to the last 243bp of this fragment, and of the full ALAS1 coding region. There is 56% homology between this 243bp region of ALAS1 and the corresponding sequence of ALAS2 (figure 5-11), and there is 59% homology of the 142bp putative *cis*-acting element. This reasonably low homology may suggest that this specific region is involved in the haem-destabilisation of ALAS1 mRNA, but it may not simply be this region alone that is required for the mechanism. Figure 5-11 shows that the longest length of non-homologous nucleotides is only 5 bases long. However, mapping of the required mRNA sequences of c-myc for binding by the CRD-BP demonstrate that essential sequences do not have to be directly next to one another, and only short nucleotide stretches are necessary for binding (Sparanese & Lee, 2007).

```
ALAS1    CCUACGGUGCCCCGGGGAGAAGAGCUCCUACGGAUUGCCCCACCCCUCACCACACACCC
ALAS2    CCAACUGUCCCCCGGGGUGAAGAGCUCCUGCGCUUGGCACCCUCCCCCCACCACAGCCCU

ALAS1    CAGAUGAUGAACUACUUCCUUGAGAAUCUGCUAGUCACAUGGAAGCAAGUGGGGCUGGAA
ALAS2    CAGAUGAUGGAAGAUUUUGUGGAGAAGCUGCUGCUGGCUUGGACUGCGGUGGGGCUGCCC

ALAS1    CUGAAGCCUCAUUCCUCAGCUGAGUGCAACUUCUGCAGGAGGCCACUGCAUUUUGAAGUG
ALAS2    CUCCAGGAUGUGUCUGUGGCUGCCUGCAAUUUCUGUCGCCGUCCUGUACACUUUGAGCUC

ALAS1    AUGAGUGAAAGAGAGAAGUCCUAUUUCUCAGGCUUGAG---CAAGUUGGUAUCUGCUCAG
ALAS2    AUGAGUGAGUGGGAACGUUCCUACUUCGGGAACAUGGGGCCCCAGUAUGUCACCACCUAU

ALAS1    GCCUGA
ALAS2    GCCUGA
```

Figure 5-11 mRNA sequence homology of the protein binding-region of ALAS1 fragment 4 and the corresponding nucleotides of ALAS2.

The use of overlapping RNA sequences in EMSAs enabled a protein-binding region to be defined to a 243nt sequence at the 3′ end of the coding region. ALAS1 and ALAS2 have a sequence homology of 56% in this 243bp region of fragment 4. Underlined is the previous binding site identified by Cable *et al.*, truncated to 142bp as we have ruled out the first 12bp of this sequence. This region has 59% homology between human ALAS1 and ALAS2 mRNA. Non-homologous nucleotides are in red.

In hepatocytes of the rat and chicken, ALAS1 is destabilised by haem, as in human cells (Cable *et al.*, 2000; Hamilton *et al.*, 1991; Drew & Ades, 1989; Cable *et al.*, 2001). Therefore, a similar mechanism of haem-destabilisation of ALAS1 mRNA is surmised to occur amongst these species. The sequence homology of the 142bp putative *cis*-acting element of the rat, chicken and human ALAS1 gene was compared and shown to have 71% homology (figure 5-12). This high homology suggests that this region may contain specific sequences involved in the instability mechanism. The catalytic domain of the enzyme resides in its C-terminus, which may account for the high homology in this region (Dailey *et al.*, 2005; Sadlon *et al.*, 1999). However, the homology of this 142bp sequence between the human, rat and chicken ALAS1 with human ALAS2 is 57%.

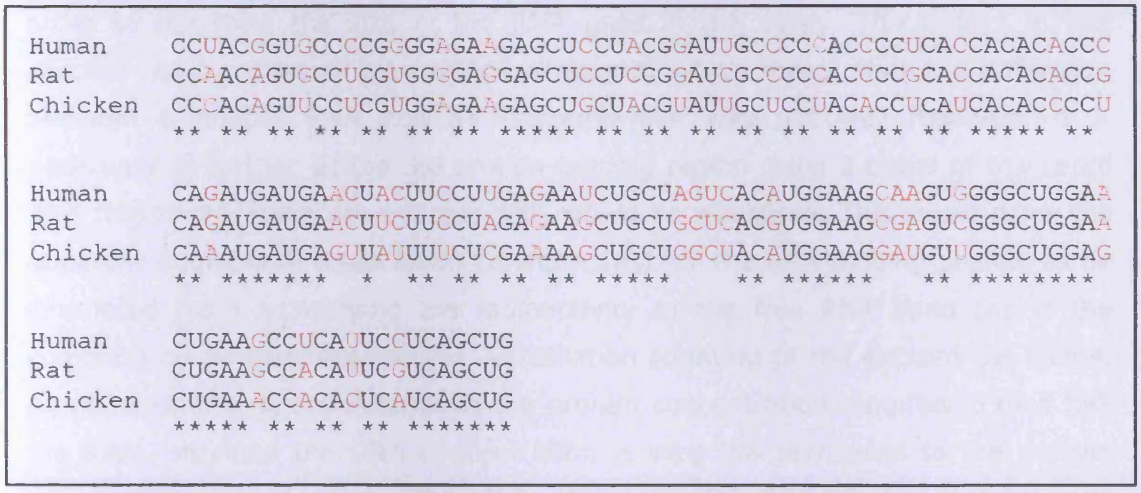

Figure 5-12 Sequence homology of the mRNA 142bp putative protein-binding sequence between species.

Homologies: human and rat – 85%; human and chicken – 77%; rat and chicken – 75%; human, rat and chicken – 71%.

Non-homologous nucleotides of ALAS1 between the three species are shown in red, homologous nucleotides of ALAS1 are indicated by stars.

The EMSAs and UV-crosslinking used in this chapter required extensive optimisation for any protein-binding to the radiolabelled RNA probes to be visualised. In the context of this thesis, it was unfortunate that the crosslinking could be not optimised further to establish the specific proteins that bind and their role in haem-mediated destabilisation of ALAS1 mRNA. The use of increasing concentrations of heparin with rRNA in the UV-crosslinking assays was unable to determine a single band. Instead, it seemed that approximately four proteins bound to probe 2, and two main proteins bound to probe 4. These may be

different proteins or subunits of a single protein binding to each probe. Further analysis of protein-binding to ALAS1 RNA using EMSA and UV-crosslinking would have been useful to analyse the specificity of the binding, define the binding region and characterise the protein.

The majority of EMSAs normally use radiolabelled RNA varying in length from approximately 50 to 350nt. In general, however, short RNAs are easier to analyse since their retarded complexes can be well-resolved from the position of migration of naked RNA. The overall acrylamide content of the bandshift gels as well as their acrylamide:*bis*-acrylamide ratio can be empirically varied to suit the purpose; in practice it becomes very difficult to handle gels of less than 4% polyacrylamide. Therefore, further definition of the binding site is required in order to minimise the size of the RNA used in the assay. The assays in this chapter used probes of over 480nt in length, which meant that the difference between a shifted RNA and an unbound-RNA was not well resolved. It is necessary to further define the protein-binding region using a panel of truncated RNA fragments, therefore a larger shift would be visualised. This would allow the apparent equilibrium dissociation constant (K_d) for the RNA-binding protein to be calculated from quantifying the radioactivity in the free RNA band (or in the complex) by film densitometry or scintillation counting of the excised gel bands. An approximate K_d corresponds to the protein concentration required to bind half the RNA, provided the RNA concentration is very low compared to the protein concentration at midpoint. Therefore, the K_d for the RNA-binding protein could then be accurately compared with protein extracted from HepG2 cells grown in haem-depleted or haem-excess medium, to quantify the haem effect on protein binding (Walker *et al.*, 1998; Ross, 1995).

Using probes of a shorter length than used in the EMSAs in this chapter would allow the specificity of the binding to be analysed, using specific and non-specific competitors. This is a crucial experimental factor, to demonstrate that the interaction is of a specific nature, as proteins can in fact bind to nucleic acids non-specifically. Specific binding can be achieved by carrying out the binding assay in the presence of appropriate competitor molecules, which can be specific or non-specific. Specific competitors would be unlabelled RNAs, identical in sequence to the radiolabelled RNA probes. When added in excess to a binding reaction, a specific competitor should displace the labelled RNA. Non-specific competitors are ideally random portions of RNA, or polyribonucleotides, and should not include the RNA sequence under study. These will not compete with the specific RNA

probe. In the EMSAs and UV-crosslinking experiments in this chapter, rRNA is included in the binding reaction which reduces the number of non-specific complexes formed with the labelled probe. Also, heparin was added to quench the non-specific binding of proteins to RNA. Further experiments using specific competitors with probes 2 and 4 are required. However, our experimental conditions, using heparin and rRNA as non-specific competitors, are highly stringent and provide independent confirmation of protein binding to the 154bp region as published (Cable *et al.,* 2001).

CHAPTER 6

Discussion

The regulation of haem in erythroid cells has been researched extensively. In contrast, however, the mechanism by which haem is regulated in non-erythroid cells, for instance by regulating the ALAS1 mRNA, has been poorly characterised. Therefore, the aim of this thesis was to investigate this post-transcriptional mechanism to examine how haem destabilises ALAS1 mRNA in humans.

In summary, there are a number of important observations made from the data presented in this thesis:

1. The minor ALAS1 isoform is poorly translated and relatively resistant to haem-mediated decay, compared to the major form.
2. The human ALAS1 mRNA contains a CRD that mediates its haem-sensitivity. The 5'- and 3'-UTRs are not involved in this mechanism.
3. The ALAS1 mRNA CRD has to be translated to function.
4. The use of overlapping deletion fragments of the ALAS1 coding region is unable to further delineate the CRD.
5. RNA-EMSAs defined two fragments of the ALAS1 coding region that can bind to HepG2 cytosolic protein.

This thesis has shown that the destabilisation of ALAS1 by haem is not simply a *trans*-acting factor binding to a single *cis*-acting element in the mRNA. The mechanism involved may be more complicated than previously thought. Potential mechanisms of ALAS1 mRNA haem-mediated destabilisation will be discussed in this chapter.

A reason for the previous lack of understanding of the haem-mediated destabilisation of ALAS1 mRNA could be that it has proven difficult to establish continuous cell-culture models that retain high levels of mRNA, protein and activity of ALAS1 as occurs in intact organisms and also retain inductive or repressive responses to chemicals. Virtually all mammalian hepatoma cell lines exhibit very low levels of ALAS1, and these levels are only weakly inducible (1.5 to 2-fold induction), compared to primary cells (Iwasa *et al.,* 1989). Low levels of ALAS1 mRNA in these cell lines have hampered work to understand the mechanism of destabilisation. Indeed, a similar problem was encountered in this project to enable a difference in ALAS1 mRNA levels in response to haem to be visualised in HepG2 cells. Therefore, we successfully used a method to deplete the cells of haem and haemoproteins, with the use of haem-depleted media and

succinyl acetone, to induce the levels of ALAS1 mRNA, prior to the addition of haem to the cells.

A further problem with the experiments throughout this thesis was the dose of haem used to treat the cells. Sassa (2004) identified that free haem within a normal cell is below 1μM. Free haem (0.1-0.3μM) added to the medium of chick embryo liver cell culture specifically inhibited the induction of ALAS1 by one-half. However, free haem concentrations of 1μM caused the induction of HO-1, thereby breaking down the haem. In this thesis a dose of 20μM haem was used to decrease the stability of the ALAS1 mRNA. Therefore, a lower dose may have induced a larger decrease in the mRNA stability with haem. However, the experiments by Sassa (2004) were looking at the endogenous genes rather than reporter assays. Research using reporter assays to monitor ALAS1 mRNA activity, such as that by Kolluri *et al* (2005), used 20μM haem, similar to the concentrations used throughout this thesis. Therefore, ALAS1 within a reporter construct may require a higher concentration of haem to be destabilised. However, in this situation the endogenous HO-1 gene will also be induced, and this may affect the mechanisms involved in ALAS1 mRNA destabilisation within the cell.

6.1 Translationally-dependent haem regulated decay

The major and minor ALAS1 mRNA isoforms were studied to establish if their expression differs in response to haem, and if so, would this offer a clue to the mechanism. The data in this thesis showed that the minor isoform is in fact resistant to haem-mediated decay compared to the major, and its 5'-UTR inhibits translation. We showed that sequence elements that are involved in this haem-stability mechanism are present in the coding region, and not in the 5'- and 3'-UTRs. Furthermore, by using reporter assays and inserting a stop codon prior to the ALAS1 coding region sequence, it was found that haem only destabilises the ALAS1 mRNA when it is translated.

The question arises as to why haem-regulated decay of ALAS1 mRNA should be translationally-dependent. ALAS1 protein is rapidly turned over in the mitochondria with a half-life of approximately 70 minutes in rat liver (Anderson *et al.,* 2000). Cap-mediated translation drops sharply during periods of stress or starvation (Clemens, 2001), whilst translation rates are low during mitosis (Ross, 1997; Pyronnet & Sonenberg, 2001), with general stabilisation of mRNAs, which

may be a survival mechanism that ensures cells are not depleted of labile mRNAs as they enter G1 (Ross, 1997). Transcription and translation are inhibited by approximately 75% between pro-metaphase and telophase. In later telophase or shortly there after, transcription and translation rates return to normal (G1) levels (Prescott *et al.,* 1976). Therefore, the CRD may have to be translated to cause haem-mediated decay to prevent any harmful consequences of ALAS1 depletion during periods when translation rates are low. This preserves the capacity of the cell to synthesise haem immediately upon the end of mitosis, when the cell cycle enters G1 phase again, or the cessation of stress. In addition, it is interesting to speculate that the minor ALAS1 mRNA might be translated under these conditions to ensure that there is sufficient haem for cell viability.

6.2 Delineation of the CRD

This thesis has shown that the destabilisation of ALAS1 by haem is not a simple mechanism of a *trans*-acting factor binding to a single *cis*-acting element in the mRNA. DLRA's showed that a haem-responsive element was present in the ALAS1 mRNA coding region, and was able to function independently of the 5'- and 3'-UTR. However, reporter assays using dissected sequences of the coding region failed to identify a specific region that can confer haem-mediated destabilisation. This demonstrates that a CRD alone is not enough for destabilisation of the ALAS1 mRNA to occur. Furthermore, the ALAS1 mRNA requires active translation through its full-length coding region to be destabilised

6.3 Cytosolic protein binding to ALAS1 mRNA

Cytosolic proteins from HepG2 cells bound to two separate fragments (numbered 2 and 4) of the ALAS1 mRNA coding region, using RNA-EMSAs. Fragment 4 contains the 154bp region previously identified sequence as a putative *cis*-acting element (Cable *et al.,* 2001). By using overlapping ALAS1 coding region sequences we were able to define the putative *cis*-acting element further to a sequence of 142bp. An *in vitro* method of adding haemin to the binding reaction of the EMSA of fragment 4 did not have any affect on protein binding to the ALAS1 coding region. Therefore, HepG2 cells were grown in medium that was either depleted or supplemented with 20μM haem. The representative EMSA in chapter 5 shows that the addition of haem prior to the extraction of protein caused a decrease in protein binding to probe 4. However, this result was not demonstrated each time. Indeed, Cable *et al* were also not able to demonstrate a

reproducible effect of haem on the putative-binding site, even though removal of this site prevented haem-mediated decay (personal communication). A similar observation has been made with the regulation of the CYP2E1 gene by insulin. Insulin controls CYP2E1 expression by destabilising its mRNA. However, Moncion *et al* (2002) were unable to demonstrate that insulin affects protein binding to the CYP2E1 CRD. Therefore, it has been suggested that it may be protein-protein interactions mediating the destabilisation of the mRNA, or alternatively the RNA-binding proteins may constitute a scaffold upon which the actual target of insulin can bind and exert a RNA destabilisation function (Moncion *et al.,* 2002).

Another explanation as to why haem does not seem to affect protein binding to the mRNA of the putative ALAS1 CRD *in vitro* may be that haem directly binds to the ribosomes or regulates endonucleolytic mRNAs. This may be similar to the destabilisation mechanism of c-myc, which will be described in section 6.4.1. Furthermore, haem-regulated binding of protein to ALAS1 mRNA may require active translation of the mRNA. Therefore, this is not observable as a simple RNA/protein interaction, and is not affected by haem in an EMSA.

6.4 Mechanisms of mRNA destabilisation involving CRDs

The emphasis on this thesis was to discover which sequence elements of ALAS1 mRNA are responsible for haem-mediated decay and to study the proteins that interact with them. The actual downstream reactions, including possible poly(A)-shortening, decapping and ribonuclease cleavage that result in its decay are not part of the study. The conclusions from this thesis allow a number of possible mechanisms of the destabilisation of ALAS1 mRNA to be proposed, based on a comparison of mechanisms from known CRDs. These include c-myc, c-fos, β-tubulin and plasminogen activator inhibitor type 2 (PAI-2), which are discussed below.

6.4.1 c-myc

The c-myc mRNA contains an instability sequence within its coding region, located in the last 249 nucleotides. It functions independently of an ARE to make the mRNA unstable (Wisdom & Lee, 1991; Yeilding *et al.*, 1996). When the c-myc CRD is inserted in frame with the coding region of β-globin mRNA, the resulting chimeric mRNA is destabilised (Herrick & Ross, 1994). This CRD must be translated to destabilise the mRNA (Wisdom & Lee, 1991). The CRD interacts with

a 68-kDa CRD-binding protein (CRD-BP), which contains two RNA recognition motifs and four hnRNP K domains (Doyle *et al.*, 1998). When the CRD-BP is bound to the c-myc mRNA, the CRD is shielded from endonucleolytic attack. The mRNA is then only degraded by an ARE-dependent deadenyation pathway. If the CRD-BP dissociates from the mRNA, the CRD becomes exposed to the endonuclease. The mRNA is then rapidly degraded by endonucleolytic cleavage within the CRD (Sparanese & Lee, 2007). Furthermore, ribosomes pause within the 5′ segment of the CRD, at a translation pause site. Pausing generates a ribosome-free downstream region, between the pause site and the translation termination site. Pausing can be induced by several factors, including mRNA structure, the translation product itself, mRNA-binding proteins, signal recognition particle binding and tRNA abundance and rare codons. This unprotected site is attacked by an endonuclease, unless it is protected by CRD-BP during the pause interval. After elongation resumed, the ribosomes would displace the CRD-BP from the mRNA, and translation is completed. The c-myc CRD is a bipartite mRNA instability element, consisting of two juxtaposed sequence elements. The first 72 nucleotides contain the codons that induce pausing. The downstream 177 nucleotides contain sites for CRD-BP binding and endonuclease cleavage (Lemm & Ross, 2002).

6.4.2 c-fos

The c-fos proto-oncogene encodes a transcription factor that appears to play a role in cell growth and differentiation (Sheng & Greenberg, 1990). Transcription of the c-fos gene is transiently induced within minutes after stimulation by growth factors and other agents. Shortly after induction, c-fos transcription shuts-off again, returning to its very low basal level within 30-60 minutes after growth factor addition. The c-fos message persists in the cytoplasm for 30-45 minutes after the period of ongoing c-fos transcription because, upon arriving in the cytoplasm, this labile message is degraded extremely rapidly (Greenberg & Ziff, 1984). The multiple destabilising elements within the c-fos coding region work in concert to achieve the destabilising effect of the intact c-fos coding region. Translation of the c-fos coding region, or at least the assembly of ribosomes at the 5' end of the coding region, is necessary for these determinants to effect swift deadenylation and decay of c-fos mRNA (Schiavi *et al.*, 1994). The requirement for translation could also be explained if there exists a ribosome-associated ribonuclease or degradative factor that is activated when the ribosome interacts with these destabilizing elements.

c-*fos* mRNA contains a 320-nucleotide CRD that functions as an instability element only when the translation mechanism has initiated (Shyu *et al.*, 1991; Schiavi *et al.*, 1994). However, the c-*fos* CRD differs in several ways from the c-*myc* CRD: firstly it is recognized by virtue of its sequence or structure, and secondly it promotes accelerated deadenylation, not endonucleolytic decay. A complex of five proteins (PABP, PABP-interacting protein (PAIP), AUF-1, NS1-associated protein (NSAIP1) and Unr (Upstream of N-ras)) assembles on the mCRD and promotes rapid deadenylation and decay of the mRNA. One model proposes that transit of ribosomes through the mCRD element disrupts the complex and triggers the decay pathway. In this case, the mCRD complex might protect untranslated c-fos mRNA from the rapid deadenylation-dependent decay that is otherwise promoted by the ARE in its 3'-UTR (Grosset *et al.*, 2000).

If the CRD is placed in frame with the globin mRNA coding region, the resulting 5'-globin-fos-globin-3' chimeric transcript is at least four-fold less stable than globin mRNA. If a frameshift mutation is introduced into the globin-*fos*-globin gene, such that the mRNA sequence is changed by only a single nucleotide but the peptide encoded by the c-fos region is entirely different, the frameshifted mRNA is just as unstable as the original globin-*fos*-globin mRNA. Therefore in this case the structure of the c-fos mRNA itself specifies the instability phenotype, independent of the encoded protein (Wellington *et al.*, 1993). In contrast, the destabilisation of β-tubulin mRNA by tubulin monomers depends on the peptides encoded by their CRD's (Yen *et al.*, 1988).

6.4.3 β-tubulin

Microtubules are dynamic filamentous structures that are composed of tubulin monomers. Tubulin is a heterodimer of α- and β-subunits that exist in a dynamic equilibrium with the microtubule polymer (Guhaniyogi & Brewer, 2001). The expression of β-tubulin, one of the two principle constituents of microtubules, is regulated in higher eukaryotes by an autoregulatory mechanism that modulates the stability of the polysome-bound tubulin mRNAs (Cleveland, 1989). The stability of tubulin mRNA is specified by the level of its own translation products, the tubulin subunits themselves (Theodorakis & Cleveland, 1992; Gay *et al.*, 1989). β-tubulin mRNA levels are sensitive to the intracellular concentration of tubulin subunits (Yen *et al.*, 1988). The first 13 translated nucleotides of β-tubulin mRNA are sufficient to confer autoregulated instability onto heterologous RNAs if

present as the first translated nucleotides. Furthermore, for β-tubulin mRNAs to be substrates for autoregulation they must be associated with polysomes and that translation of them must proceed past 41 codons. The binding of cellular cofactors might also be involved (Bachurski et al., 1994). An endonuclease is suspected to be ribosome-associated which is activated to cleave the mRNA by β-tubulin binding to the nascent peptide, although this has not yet been demonstrated (Yen *et al.*, 1988).

6.4.4 Plasminogen activator inhibitor type 2 (PAI-2)

The plasminogen activator system is an important proteolytic cascade that plays a role in the removal of blood clots from the circulation and the turnover of a variety of extracellular matrix proteins. PAI-2 is used in this system as a regulated serine protease inhibitor. Similar to ALAS1 mRNA, the PAI-2 transcript is unstable in the absence of the 3'-UTR (Maurer *et al.*, 1999). Therefore, Tierney & Medcalf (2001) examined the possibility of the PAI-2 mRNA containing CRD's. They demonstrated that individual exons or groups of exons of the PAI-2 gene could confer varying degrees of instability in a reporter assay, suggesting that multiple instability elements reside within the PAI-2 coding region.

To further define one of the protein-binding sites in PAI-2, Tierney & Medcalf (2001) used antisense DNA-masking experiments. In this approach, antisense DNA oligomers that were directed against overlapping sequences within the RNA probe were allowed to anneal. This inhibited binding to a specific *cis*-acting site, allowing this region to be identified. In the ALAS1 RNA-EMSAs in chapter 5, we identified two protein-binding regions of 480bp and 142bp in size. Therefore, it would be useful to use similar DNA masking experiments to further delineate the ALAS1 protein binding regions in human ALAS1 mRNA.

6.5 Potential mechanism of ALAS1 mRNA destabilisation by haem

A proposed mechanism of how haem destabilises the ALAS1 mRNA in hepatocytes needs to involve a number of observations made from this thesis. Firstly, fragment 4 alone is not sufficient to mediate the destabilisation; additional sequence elements in the ALAS1 coding region are required. Secondly, the destabilisation of ALAS1 mRNA is translation-dependent.

Similar to the mechanism used by c-myc, ribosomal pausing may occur in the ALAS1 mRNA. Ribosomal pausing is suggested to account for the following observations:

1. Placing a stop codon prior to the ALAS1 mRNA coding region inhibits its destabilisation in the presence of haem. This demonstrates that translation through the ALAS1 coding region is necessary for its destabilisation.
2. The region of ALAS1 mRNA containing a potential CRD is translated relatively inefficiently. Therefore, this is likely to cause pausing and result in a ribosome-free downstream region.

To establish if there is any ribosome-free regions in the ALAS1 mRNA coding region, ribosome toeprinting assays (translation-couple primer extensions) could be used, similar to those used on c-myc by Lemm & Ross (2002). These would confirm that translational inefficiency of particular fragments of ALAS1, such as fragment 4, is the result of ribosomal pausing.

Similar to the mechanism of c-myc and PAI-2 destabilisation, the ALAS1 CRD may be of a bi-partite structure. Of interest was the observation that fragment 4 dramatically reduced translation of the Renilla luciferase reporter gene. However, this region, by itself, is unable to confer haem-mediated instability on the heterologous protein, suggesting that other important elements in the coding region are also required. These may include another ALAS1 mRNA element that binds to protein, such as fragment 2, identified by the RNA-EMSAs in chapter 5. The downstream site in fragment 4 may be where the CRD-BP binds and cleavage can occur. It could be that an essential ribonuclease or mRNA binding protein is associated with the ribosome, or, that translational elongation is required for the displacement of a stabilising protein bound to a CRD, perhaps through melting of specific mRNA secondary structure.

Interestingly, using a translational-competent cell-free system, Yamamoto *et al* showed that haem rapidly inhibited ALAS1 translation by a mechanism that required translational elongation (Yamamoto *et al.,* 1983). mRNA concentrations were not monitored however and so the contribution of mRNA decay to the reduced rate of ALAS1 production in those experiments cannot be evaluated. However, as suggested earlier, it may be that the initial regulated signal for mRNA decay involves haem-dependent inhibition or pausing of translation within a specific sequence of the ALAS1 coding region. The experiments on ALAS1 used a stop codon prior to the ALAS1 coding region sequence to establish that

translation is essential for the haem-mediated destabilisation of the mRNA. However, we did not investigate whether it is the encoded protein or the structure of the mRNA itself that specifies the haem sensitivity. To test this, as with the c-fos experiments, a frameshift mutation of ALAS1 could be used at the beginning of the coding region. This would establish if the haem-destabilisation mechanism is similar to c-fos or β-tubulin.

A mechanism of ALAS1 destabilisation by haem is proposed in figure 6-1 in which the tertiary structure of the mRNA is involved. This may either involve base pairing between two sequence elements within the coding region, for example between fragments 2 and 4; or involve protein interactions which cause the RNA to fold in a specific way. During translation ribosomes displace the RNA-binding proteins and cause a change in the folding of the mRNA and may expose a site that is degraded by a ribonuclease, or trigger a series of events for the mRNA to be degraded by an unknown mechanism. Furthermore, the ribosomes may have an associated protein such as a haemoprotein or endonuclease (Lee *et al.*, 1998), which is induced by haem. It is not known whether fragment 2 of the coding region is involved in the mechanism. A further part to our proposed mechanism may be that ribosomal pausing occurs over a critical region within the 142bp sequence in the mRNA, allowing a ribosome-free downstream region to be degraded by a ribonuclease, similar to the c-myc mechanism. This would account for the reduced translation of the fragment 4 ALAS1 mRNA used in the reporter assays. Indeed, it is interesting to speculate that haem may regulate this mechanism by binding to the HRMs of the emerging peptide, analogous to the destabilisation mechanism of β-tubulin. As discussed earlier, Yamamoto *et al* (1983) demonstrated that haem inhibits translation of the ALAS1 mRNA, and they also proposed that this might involve a specific interaction of haem with nascent peptide chains of ALAS1 on the polysomes.

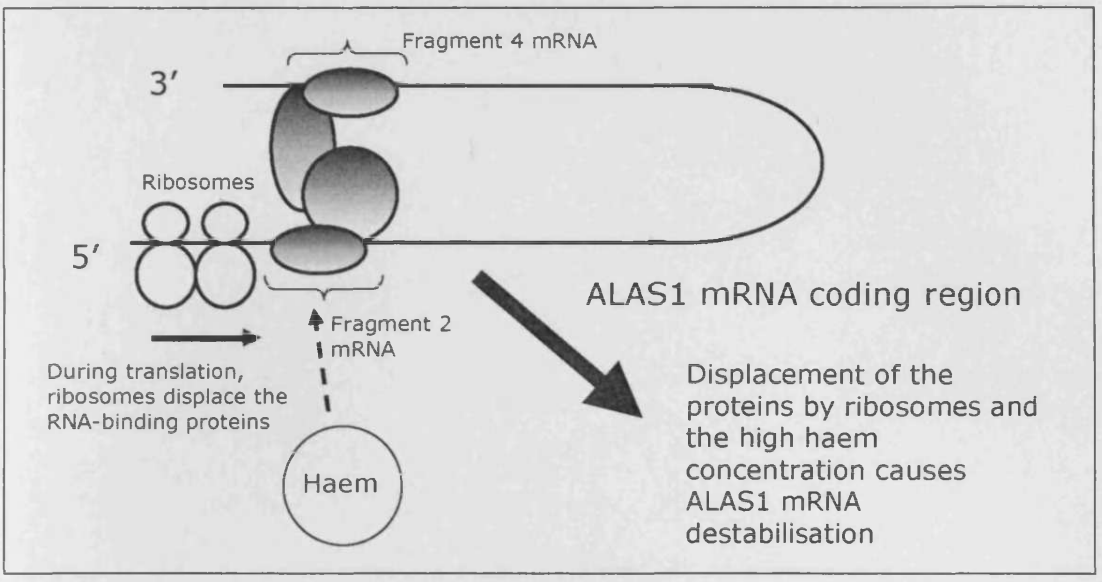

Figure 6-1 A proposed mechanism of human ALAS1 mRNA destabilisation by haem in hepatocytes.

The two fragments (2 and 4) of the ALAS1 coding region are linked by a specific tertiary structure of the mRNA, which binds to a protein-scaffold. During translation, the ribosomes displace the RNA-binding proteins. The high haem concentration within the cell and the displacement of mRNA binding-proteins, trigger a sequence of events to degrade the ALAS1 mRNA by an unknown mechanism.

6.6 Recent literature on the haem control of ALAS1

Specific processes appear to have evolved to rapidly regulate haem concentration within the cell. Recently, Yoshino *et al* (2007) demonstrated that haem regulates its own synthesis by causing the degradation of the ALAS1 enzyme in the mitochondria. The homeostasis of haem is therefore controlled by three post-transcriptional mechanisms: by inhibiting the ALAS1 enzyme from entering the mitochondria; by destabilising the ALAS1 mRNA; and finally by proteolysis of the enzyme within the mitochondria. The homeostatic regulation of haem is likely to be maintained and finely tuned in the mitochondria. The increased instability of ALAS1 mRNA is therefore likely to be more physiologically relevant in reducing the high concentrations following transcriptional induction.

CHAPTER 7

References

Aizencang G, Solis C, Bishop D F, Warner C, and Desnick R J (2000) Human uroporphyrinogen-III synthase: genomic organization, alternative promoters, and erythroid-specific expression. *Genomics* 70: 223-231.

Aizencang G I, Bishop D F, Forrest D, Astrin K H, and Desnick R J (2000) Uroporphyrinogen III synthase. An alternative promoter controls erythroid-specific expression in the murine gene. *J Biol Chem* 275: 2295-2304.

Ajioka R S, Phillips J D, and Kushner J P (2006) Biosynthesis of heme in mammals. *Biochim Biophys Acta* 1763: 723-736.

Alexander F W, Sandmeier E, Mehta P K, and Christen P (1994) Evolutionary relationships among pyridoxal-5'-phosphate-dependent enzymes. Regio-specific alpha, beta and gamma families. *Eur J Biochem* 219: 953-960.

Anderson K, Sassa S, Bishop D F, and Desnick R J (2000) *Disorders of heme biosynthesis: X-linked sideroblastic anemia and the porphyrias.* 8 ed. MacGraw Hill Medical Publishing Division.

Arruda M A, Rossi A G, de Freitas M S, Barja-Fidalgo C, and Graca-Souza A V (2004) Heme inhibits human neutrophil apoptosis: involvement of phosphoinositide 3-kinase, MAPK, and NF-kappaB. *J Immunol* 173: 2023-2030.

Astner I, Schulze J O, van den Heuvel J, Jahn D, Schubert W D, and Heinz D W (2005) Crystal structure of 5-aminolevulinate synthase, the first enzyme of heme biosynthesis, and its link to XLSA in humans. *Embo J* 24: 3166-3177.

Astrin K H, Warner C A, Yoo H W, Goodfellow P J, Tsai S F, and Desnick R J (1991) Regional assignment of the human uroporphyrinogen III synthase (UROS) gene to chromosome 10q25.2----q26.3. *Hum Genet* 87: 18-22.

Atamna H (2004) Heme, iron, and the mitochondrial decay of ageing. *Ageing Res Rev* 3: 303-318.

Atamna H, and Frey W H, 2nd (2004) A role for heme in Alzheimer's disease: heme binds amyloid beta and has altered metabolism. *Proc Natl Acad Sci U S A* 101: 11153-11158.

Atamna H, Killilea D W, and Ames B N (2002) Heme deficiency causes oxidative stress and corrupts mitochondrial integrity, processing of APP, and signal tranduction. *Free Radical Biology and Medicine* 33: 262.

Atamna H, Killilea D W, Killilea A N, and Ames B N (2002) Heme deficiency in brain cells mimics the mitochondrial decay of neurodegeneration and Alzheimer disease. *Free Radical Biology and Medicine* 33: 380.

Atamna H, Killilea D W, Killilea A N, and Ames B N (2002) Heme deficiency may be a factor in the mitochondrial and neuronal decay of aging. *Proceedings of the National Academy of Sciences of the United States of America* 99: 14807-14812.

Atamna H, Liu J K, and Ames B N (2001) Heme deficiency selectively interrupts assembly of mitochondrial complex IV in human fibroblasts - Relevance to aging. *Journal of Biological Chemistry* 276: 48410-48416.

Atamna H, Walter P B, and Ames B N (2002) The role of heme and iron-sulfur clusters in mitochondrial biogenesis, maintenance, and decay with age. *Arch Biochem Biophys* 397: 345-353.

Avissar Y J, Ormerod J G, and Beale S I (1989) Distribution of delta-aminolevulinic acid biosynthetic pathways among phototrophic bacterial groups. *Arch Microbiol* 151: 513-519.

B

Bachurski C J, Theodorakis N G, Coulson R M, and Cleveland D W (1994) An amino-terminal tetrapeptide specifies cotranslational degradation of beta-tubulin but not alpha-tubulin mRNAs. *Mol Cell Biol* 14: 4076-4086.

Badawy A A (1978) Tryptophan pyrrolase, the regulatory free haem and hepatic porphyrias. Early depletion of haem by clinical and experimental exacerbators of porphyria. *Biochem J* 172: 487-494.

Baker H M, Anderson B F, and Baker E N (2003) Dealing with iron: common structural principles in proteins that transport iron and heme. *Proc Natl Acad Sci U S A* 100: 3579-3583.

Balla G, Jacob H S, Eaton J W, Belcher J D, and Vercellotti G M (1991) Hemin: a possible physiological mediator of low density lipoprotein oxidation and endothelial injury. *Arterioscler Thromb* 11: 1700-1711.

Balla G, Vercellotti G M, Muller-Eberhard U, Eaton J, and Jacob H S (1991) Exposure of endothelial cells to free heme potentiates damage mediated by granulocytes and toxic oxygen species. *Lab Invest* 64: 648-655.

Balla J, Vercellotti G M, Jeney V, Yachie A, Varga Z, Eaton J W, and Balla G (2005) Heme, heme oxygenase and ferritin in vascular endothelial cell injury. *Mol Nutr Food Res* 49: 1030-1043.

Barreau C, Paillard L, and Osborne H B (2005) AU-rich elements and associated factors: are there unifying principles? *Nucleic Acids Res* 33: 7138-7150.

Battersby A R, Fookes C J, Matcham G W, and McDonald E (1980) Biosynthesis of the pigments of life: formation of the macrocycle. *Nature* 285: 17-21.

Bawden M J, Borthwick I A, Healy H M, Morris C P, May B K, and Elliott W H (1987) Sequence of human 5-aminolevulinate synthase cDNA. *Nucleic Acids Res* 15: 8563.

Bernstein P L, Herrick D J, Prokipcak R D, and Ross J (1992) Control of c-myc mRNA half-life in vitro by a protein capable of binding to a coding region stability determinant. *Genes Dev* 6: 642-654.

Bevilacqua A, Ceriani M C, Capaccioli S, and Nicolin A (2003) Post-transcriptional regulation of gene expression by degradation of messenger RNAs. *J Cell Physiol* 195: 356-372.

Bishop D F (1990) Two different genes encode delta-aminolevulinate synthase in humans: nucleotide sequences of cDNAs for the housekeeping and erythroid genes. *Nucleic Acids Res* 18: 7187-7188.

Bishop T R, Hodes Z I, Frelin L P, and Boyer S H (1989) Cloning and sequence of mouse erythroid delta-aminolevulinate dehydratase cDNA. *Nucleic Acids Res* 17: 1775.

Bissell D M, and Hammaker L E (1976) Cytochrome p-450 heme and the regulation of delta-aminolevulinic acid synthetase in the liver. *Arch Biochem Biophys* 176: 103-112.

Borthwick I A, Srivastava G, Day A R, Pirola B A, Snoswell M A, May B K, and Elliott W H (1985) Complete nucleotide sequence of hepatic 5-aminolaevulinate synthase precursor. *Eur J Biochem* 150: 481-484.

Bottomley S S, and Muller-Eberhard U (1988) Patho-Physiology of Heme-Synthesis. *Seminars in Hematology* 25: 282-302.

Braidotti G, Borthwick I A, and May B K (1993) Identification of Regulatory Sequences in the Gene for 5- Aminolevulinate Synthase from Rat. *Journal of Biological Chemistry* 268: 1109-1117.

Brewer G (1991) An A + U-rich element RNA-binding factor regulates c-myc mRNA stability in vitro. *Mol Cell Biol* 11: 2460-2466.

Brunet A, Bonni A, Zigmond M J, Lin M Z, Juo P, Hu L S, Anderson M J et al. (1999) Akt promotes cell survival by phosphorylating and inhibiting a Forkhead transcription factor. *Cell* 96: 857-868.

C

Cable E E, Kuhn B R, and Isom H C (2001) Regulation of human hepatic Delta-aminolevulinate synthase and heme oxygenase by heme and non-heme metalloporphyrins. *Hepatology* 34: Abstract 737.

Cable E E, Miller T G, and Isom H C (2000) Regulation of heme metabolism in rat hepatocytes and hepatocyte cell lines: delta-aminolevulinic acid synthase and heme oxygenase are regulated by different heme-dependent mechanisms. *Archives of Biochemistry and Biophysics* 384: 280-295.

Cacheux V, Martasek P, Fougerousse F, Delfau M H, Druart L, Tachdjian G, and Grandchamp B (1994) Localization of the human coproporphyrinogen oxidase gene to chromosome band 3q12. *Hum Genet* 94: 557-559.

Camejo G, Halberg C, Manschik-Lundin A, Hurt-Camejo E, Rosengren B, Olsson H, Hansson G I et al. (1998) Hemin binding and oxidation of lipoproteins in serum: mechanisms and effect on the interaction of LDL with human macrophages. *J Lipid Res* 39: 755-766.

Carballo E, Lai W S, and Blackshear P J (2000) Evidence that tristetraprolin is a physiological regulator of granulocyte-macrophage colony-stimulating factor messenger RNA deadenylation and stability. *Blood* 95: 1891-1899.

Cazzola M, and Skoda R C (2000) Translational pathophysiology: a novel molecular mechanism of human disease. *Blood* 95: 3280-3288.
Chen C Y, and Shyu A B (1995) AU-rich elements: characterization and importance in mRNA degradation. *Trends Biochem Sci* 20: 465-470.

Chen C Y, You Y, and Shyu A B (1992) Two cellular proteins bind specifically to a purine-rich sequence necessary for the destabilization function of a c-fos protein-coding region determinant of mRNA instability. *Mol Cell Biol* 12: 5748-5757.

Chernova T, Nicotera P, and Smith A G (2006) Heme deficiency is associated with senescence and causes suppression of N-methyl-D-aspartate receptor subunits expression in primary cortical neurons. *Mol Pharmacol* 69: 697-705.

Chretien S, Dubart A, Beaupain D, Raich N, Grandchamp B, Rosa J, Goossens M et al. (1988) Alternative transcription and splicing of the human porphobilinogen deaminase gene result either in tissue-specific or in housekeeping expression. *Proc Natl Acad Sci U S A* 85: 6-10.

Clemens M J (2001) Initiation factor eIF2 alpha phosphorylation in stress responses and apoptosis. *Prog Mol Subcell Biol* 27: 57-89.

Cleveland D W (1989) Autoregulated control of tubulin synthesis in animal cells. *Curr Opin Cell Biol* 1: 10-14.

Cleveland D W (1989) Gene regulation through messenger RNA stability. *Curr Opin Cell Biol* 1: 1148-1153.

Conboy J G, Cox T C, Bottomley S S, Bawden M J, and May B K (1992) Human erythroid 5-aminolevulinate synthase. Gene structure and species-specific differences in alternative RNA splicing. *J Biol Chem* 267: 18753-18758.

Correia M A, and Meyer U A (1975) Apocytochrome P-450: reconstitution of functional cytochrome with hemin in vitro. *Proc Natl Acad Sci U S A* 72: 400-404.

Cotter P D, Drabkin H A, Varkony T, Smith D I, and Bishop D F (1995) Assignment of the Human Housekeeping Delta-Aminolevulinate Synthase Gene (Alas1) to Chromosome Band 3p21.1 by Pcr Analysis of Somatic-Cell Hybrids. *Cytogenetics and Cell Genetics* 69: 207-208.

Cotter P D, Willard H F, Gorski J L, and Bishop D F (1992) Assignment of Human Erythroid Delta-Aminolevulinate Synthase (Alas2) to a Distal Subregion of Band Xp11.21 by Pcr Analysis of Somatic-Cell Hybrids Containing X - Autosome Translocations. *Genomics* 13: 211-212.

Cox T C, Bawden M J, Martin A, and May B K (1991) Human Erythroid 5-Aminolevulinate Synthase - Promoter Analysis and Identification of an Iron-Responsive Element in the Messenger-Rna. *Embo Journal* 10: 1891-1902.

Cox T C, Sadlon T J, Schwarz Q P, Matthews C S, Wise P D, Cox L L, Bottomley S S et al. (2004) The major splice variant of human 5-aminolevulinate synthase-2 contributes significantly to erythroid heme biosynthesis. *International Journal of Biochemistry & Cell Biology* 36: 281-295.

D

Dailey H A (1990) *Biosynthesis of Heme and Chlorophylls*. New York: McGraw-Hill Publishing Company.

Dailey H A (2002) Terminal steps of haem biosynthesis. *Biochem Soc Trans* 30: 590-595.

Dailey T A, Woodruff J H, and Dailey H A (2005) Examination of mitochondrial protein targeting of haem synthetic enzymes: in vivo identification of three functional haem-responsive motifs in 5-aminolaevulinate synthase. *Biochem J* 386: 381-386.

Dandekar T, Stripecke R, Gray N K, Goossen B, Constable A, Johansson H E, and Hentze M W (1991) Identification of a novel iron-responsive element in murine and human erythroid delta-aminolevulinic acid synthase mRNA. *Embo J* 10: 1903-1909.

Davis C A, Monnier J M, and Nick H S (2001) A coding region determinant of instability regulates levels of manganese superoxide dismutase mRNA. *J Biol Chem* 276: 37317-37326.

De Matteis F, and Marks G S (1983) The effect of N-methylprotoporphyrin and succinyl-acetone on the regulation of heme biosynthesis in chicken hepatocytes in culture. *FEBS Lett* 159: 127-131.

De Matteis F, and Ray D E (1982) Studied on cerebellar haem metabolism in the rat in vivo. *J Neurochem* 39: 551-556.

De Waziers I, Garlatti M, Bouguet J, Beaune P H, and Barouki R (1995) Insulin down-regulates cytochrome P450 2B and 2E expression at the post-transcriptional level in the rat hepatoma cell line. *Mol Pharmacol* 47: 474-479.

Delfau-Larue M H, Martasek P, and Grandchamp B (1994) Coproporphyrinogen oxidase: gene organization and description of a mutation leading to exon 6 skipping. *Hum Mol Genet* 3: 1325-1330.

Delsuc F, Brinkmann H, Chourrout D, and Philippe H (2006) Tunicates and not cephalochordates are the closest living relatives of vertebrates. *Nature* 439: 965-968.

Deybach J C, da Silva V, Grandchamp B, and Nordmann Y (1985) The mitochondrial location of protoporphyrinogen oxidase. *Eur J Biochem* 149: 431-435.

Doyle G A, Betz N A, Leeds P F, Fleisig A J, Prokipcak R D, and Ross J (1998) The c-myc coding region determinant-binding protein: a member of a family of KH domain RNA-binding proteins. *Nucleic Acids Res* 26: 5036-5044.

Drew P D, and Ades I Z (1989) Regulation of Production of Delta-Aminolevulinate Synthase in Tissues of Chick-Embryos - Effects of Porphyrogenic Agents and of Heme Precursors. *Biochemical Journal* 262: 815-821.

Dubart A, Mattei M G, Raich N, Beaupain D, Romeo P H, Mattei J F, and Goossens M (1986) Assignment of human uroporphyrinogen decarboxylase (URO-D) to the p34 band of chromosome 1. *Hum Genet* 73: 277-279.

Duncan R, Faggart M A, and Cornell N W (1997) Phylogenetic analysis of the 5-aminolevulinate synthase gene. *Biol Bull* 193: 247-248.

Duncan R, Faggart M A, Roger A J, and Cornell N W (1999) Phylogenetic analysis of the 5-aminolevulinate synthase gene. *Mol Biol Evol* 16: 383-396.

Dunlap J C (1999) Molecular bases for circadian clocks. *Cell* 96: 271-290.

E

Elder G H, and Evans J O (1978) Evidence that the coproporphyrinogen oxidase activity of rat liver is situated in the intermembrane space of mitochondria. *Biochem J* 172: 345-347.

F

Ferreira G C, Andrew T L, Karr S W, and Dailey H A (1988) Organization of the terminal two enzymes of the heme biosynthetic pathway. Orientation of protoporphyrinogen oxidase and evidence for a membrane complex. *J Biol Chem* 263: 3835-3839.

Ferreira G C, Franco R, Lloyd S G, Moura I, Moura J J, and Huynh B H (1995) Structure and function of ferrochelatase. *J Bioenerg Biomembr* 27: 221-229.

Ferreira G C, Neame P J, and Dailey H A (1993) Heme biosynthesis in mammalian systems: evidence of a Schiff base linkage between the pyridoxal 5'-phosphate cofactor and a lysine residue in 5-aminolevulinate synthase. *Protein Sci* 2: 1959-1965.

Ferreira G C, Vajapey U, Hafez O, Hunter G A, and Barber M J (1995) Aminolevulinate synthase: lysine 313 is not essential for binding the pyridoxal phosphate cofactor but is essential for catalysis. *Protein Sci* 4: 1001-1006.

Fraser D J, Podvinec M, Kaufmann M R, and Meyer U A (2002) Drugs mediate the transcriptional activation of the 5- aminolevulinic acid synthase (ALAS1) gene via the chicken xenobiotic-sensing nuclear receptor (CXR). *Journal of Biological Chemistry* 277: 34717-34726.

Fujita H, Yamamoto M, Yamagami T, Hayashi N, and Sassa S (1991) Erythroleukemia Differentiation - Distinctive Responses of the Erythroid-Specific and the Nonspecific Delta-Aminolevulinate Synthase Messenger-Rna. *Journal of Biological Chemistry* 266: 17494-17502.

Gage F H, Buzsaki G, and Armstrong D M (1990) NGF-dependent sprouting and regeneration in the hippocampus. *Prog Brain Res* 83: 357-370.

Gay D A, Sisodia S S, and Cleveland D W (1989) Autoregulatory control of beta-tubulin mRNA stability is linked to translation elongation. *Proc Natl Acad Sci U S A* 86: 5763-5767.

Gburek J, Birn H, Verroust P J, Goj B, Jacobsen C, Moestrup S K, Willnow T E et al. (2003) Renal uptake of myoglobin is mediated by the endocytic receptors megalin and cubilin. *Am J Physiol Renal Physiol* 285: F451-458.

Gburek J, Verroust P J, Willnow T E, Fyfe J C, Nowacki W, Jacobsen C, Moestrup S K et al. (2002) Megalin and cubilin are endocytic receptors involved in renal clearance of hemoglobin. *J Am Soc Nephrol* 13: 423-430.

Giger U, and Meyer U A (1983) Effect of succinylacetone on heme and cytochrome P450 synthesis in hepatocyte culture. *FEBS Lett* 153: 335-338.

Gilles-Gonzalez M A, and Gonzalez G (2004) Signal transduction by heme-containing PAS-domain proteins. *J Appl Physiol* 96: 774-783.

Gilles-Gonzalez M A, and Gonzalez G (2005) Heme-based sensors: defining characteristics, recent developments, and regulatory hypotheses. *J Inorg Biochem* 99: 1-22.

Gong J, and Ferreira G C (1995) Aminolevulinate synthase: functionally important residues at a glycine loop, a putative pyridoxal phosphate cofactor-binding site. *Biochemistry* 34: 1678-1685.

Gong J, Hunter G A, and Ferreira G C (1998) Aspartate-279 in aminolevulinate synthase affects enzyme catalysis through enhancing the function of the pyridoxal 5'-phosphate cofactor. *Biochemistry* 37: 3509-3517.

Grandchamp B, Bissell D M, Licko V, and Schmid R (1981) Formation and disposition of newly synthesized heme in adult rat hepatocytes in primary culture. *J Biol Chem* 256: 11677-11683.

Grandchamp B, De Verneuil H, Beaumont C, Chretien S, Walter O, and Nordmann Y (1987) Tissue-specific expression of porphobilinogen deaminase. Two isoenzymes from a single gene. *Eur J Biochem* 162: 105-110.

Gray M W (1992) The endosymbiont hypothesis revisited. *Int Rev Cytol* 141: 233-357.

Greenberg M E, and Ziff E B (1984) Stimulation of 3T3 cells induces transcription of the c-fos proto-oncogene. *Nature* 311: 433-438.

Grosset C, Chen C Y, Xu N, Sonenberg N, Jacquemin-Sablon H, and Shyu A B (2000) A mechanism for translationally coupled mRNA turnover: interaction between the poly(A) tail and a c-fos RNA coding determinant via a protein complex. *Cell* 103: 29-40.

Guhaniyogi J, and Brewer G (2001) Regulation of mRNA stability in mammalian cells. *Gene* 265: 11-23.

Hamilton J W, Bement W J, Sinclair P R, Sinclair J F, Alcedo J A, and Wetterhahn K E (1991) Heme Regulates Hepatic 5-Aminolevulinate Synthase Messenger-Rna Expression by Decreasing Messenger-Rna Half-Life and Not by Altering Its Rate of Transcription. *Archives of Biochemistry and Biophysics* 289: 387-392.

Handschin C, Lin J, Rhee J, Peyer A K, Chin S, Wu P H, Meyer U A et al. (2005) Nutritional regulation of hepatic heme biosynthesis and porphyria through PGC-1alpha. *Cell* 122: 505-515.

Hankinson O, Brooks B A, Weir-Brown K I, Hoffman E C, Johnson B S, Nanthur J, Reyes H et al. (1991) Genetic and molecular analysis of the Ah receptor and of Cyp1a1 gene expression. *Biochimie* 73: 61-66.

Hannon-Fletcher M P, O'Kane M J, Moles K W, Barnett Y A, and Barnett C R (2001) Lymphocyte cytochrome P450-CYP2E1 expression in human IDDM subjects. *Food Chem Toxicol* 39: 125-132.

Harigae H, Nakajima O, Suwabe N, Yokoyama H, Furuyama K, Sasaki T, Kaku M et al. (2003) Aberrant iron accumulation and oxidized status of erythroid- specific delta-aminolevulinate synthase (ALAS2)-deficient definitive erythroblasts. *Blood* 101: 1188-1193.

Hayashi N, Watanabe N, and Kikuchi G (1983) Inhibition by hemin of in vitro translocation of chicken liver delta-aminolevulinate synthase into mitochondria. *Biochem Biophys Res Commun* 115: 700-706.

Hayashi S, Omata Y, Sakamoto H, Higashimoto Y, Hara T, Sagara Y, and Noguchi M (2004) Characterization of rat heme oxygenase-3 gene. Implication of processed pseudogenes derived from heme oxygenase-2 gene. *Gene* 336: 241-250.

Hedlund E, Wyss A, Kainu T, Backlund M, Kohler C, Pelto-Huikko M, Gustafsson J A et al. (1996) Cytochrome P4502D4 in the brain: specific neuronal regulation by clozapine and toluene. *Mol Pharmacol* 50: 342-350.

Hentze M W, and Kuhn L C (1996) Molecular control of vertebrate iron metabolism: mRNA-based regulatory circuits operated by iron, nitric oxide, and oxidative stress. *Proc Natl Acad Sci U S A* 93: 8175-8182.

Hentze M W, Muckenthaler M U, and Andrews N C (2004) Balancing acts: molecular control of mammalian iron metabolism. *Cell* 117: 285-297.

Herrick D J, and Ross J (1994) The half-life of c-myc mRNA in growing and serum-stimulated cells: influence of the coding and 3' untranslated regions and role of ribosome translocation. *Mol Cell Biol* 14: 2119-2128.

Herzig S, Long F, Jhala U S, Hedrick S, Quinn R, Bauer A, Rudolph D et al. (2001) CREB regulates hepatic gluconeogenesis through the coactivator PGC-1. *Nature* 413: 179-183.

Hofer T, Wenger R H, Kramer M F, Ferreira G C, and Gassmann M (2003) Hypoxic up-regulation of erythroid 5-aminolevulinate synthase. *Blood* 101: 348-350.

Hollams E M, Giles K M, Thomson A M, and Leedman P J (2002) MRNA stability and the control of gene expression: implications for human disease. *Neurochem Res* 27: 957-980.

Hunter G A, and Ferreira G C (1999) Lysine-313 of 5-aminolevulinate synthase acts as a general base during formation of the quinonoid reaction intermediates. *Biochemistry* 38: 3711-3718.

Hunter G A, and Ferreira G C (1999) Pre-steady-state reaction of 8-aminolevulinate synthase - Evidence for a rate-determining product release. *Journal of Biological Chemistry* 274: 12222-12228.

Hvidberg V, Maniecki M B, Jacobsen C, Hojrup P, Moller H J, and Moestrup S K (2005) Identification of the receptor scavenging hemopexin-heme complexes. *Blood* 106: 2572-2579.

I

Ishikawa H, Kato M, Hori H, Ishimori K, Kirisako T, Tokunaga F, and Iwai K (2005) Involvement of heme regulatory motif in heme-mediated ubiquitination and degradation of IRP2. *Mol Cell* 19: 171-181.

Iwasa F, Sassa S, and Kappas A (1989) Delta-Aminolevulinate Synthase in Human Hepg2 Hepatoma-Cells - Repression by Hemin and Induction by Chemicals. *Biochemical Journal* 262: 807-813.

J

Jeney V, Balla J, Yachie A, Varga Z, Vercellotti G M, Eaton J W, and Balla G (2002) Pro-oxidant and cytotoxic effects of circulating heme. *Blood* 100: 879-887.

Jitrapakdee S, Booker G W, Cassady A I, and Wallace J C (1996) Cloning, sequencing and expression of rat liver pyruvate carboxylase. *Biochem J* 316 (Pt 2): 631-637.

Jitrapakdee S, Gong Q, MacDonald M J, and Wallace J C (1998) Regulation of rat pyruvate carboxylase gene expression by alternate promoters during development, in genetically obese rats and in insulin-secreting cells. Multiple transcripts with 5'-end heterogeneity modulate translation. *J Biol Chem* 273: 34422-34428.

Jordan P M, and Dailey H A (1990) Biochemistry of Porphyrins. *Molecular Aspects of Medicine* 11: 21-37.

Jover R, Hoffmann K, and Meyer U A (1996) Induction of 5-aminolevulinate synthase by drugs is independent of increased apocytochrome P450 synthesis. *Biochemical and Biophysical Research Communications* 226: 152-157.

Kaasik K, and Lee C C (2004) Reciprocal regulation of haem biosynthesis and the circadian clock in mammals. *Nature* 430: 467-471.

Kanakiriya S K, Croatt A J, Haggard J J, Ingelfinger J R, Tang S S, Alam J, and Nath K A (2003) Heme: a novel inducer of MCP-1 through HO-dependent and HO-independent mechanisms. *Am J Physiol Renal Physiol* 284: F546-554.

Kaplan B H (1977) *Synthesis of Heme*. 2nd ed. New York: McGraw-Hill.

Kauppinen R (2005) Porphyrias. *Lancet* 365: 241-252.

Kaya A H, Plewinska M, Wong D M, Desnick R J, and Wetmur J G (1994) Human delta-aminolevulinate dehydratase (ALAD) gene: structure and alternative splicing of the erythroid and housekeeping mRNAs. *Genomics* 19: 242-248.

Kerbarh O, Campopiano D J, and Baxter R L (2006) Mechanism of alpha-oxoamine synthases: identification of the intermediate Claisen product in the 8-amino-7-oxononanoate synthase reaction. *Chem Commun (Camb)*: 60-62.

Kikuchi G, and Hayashi N (1981) Regulation by heme of synthesis and intracellular translocation of delta-aminolevulinate synthase in the liver. *Mol Cell Biochem* 37: 27-41.

Kiledjian M, DeMaria C T, Brewer G, and Novick K (1997) Identification of AUF1 (heterogeneous nuclear ribonucleoprotein D) as a component of the alpha-globin mRNA stability complex. *Mol Cell Biol* 17: 4870-4876.

Kochetov A V, Ischenko I V, Vorobiev D G, Kel A E, Babenko V N, Kisselev L L, and Kolchanov N A (1998) Eukaryotic mRNAs encoding abundant and scarce proteins are statistically dissimilar in many structural features. *FEBS Lett* 440: 351-355.

Kolluri S, Sadlon T J, May B K, and Bonkovsky H L (2005) Haem repression of the housekeeping 5-aminolaevulinic acid synthase gene in the hepatoma cell line LMH. *Biochem J* 392: 173-180.

Koudo R, Kurokawa H, Sato E, Igarashi J, Uchida T, Sagami I, Kitagawa T et al. (2005) Spectroscopic characterization of the isolated heme-bound PAS-B domain of neuronal PAS domain protein 2 associated with circadian rhythms. *Febs J* 272: 4153-4162.

Kozak M (1986) Influences of mRNA secondary structure on initiation by eukaryotic ribosomes. *Proc Natl Acad Sci U S A* 83: 2850-2854.

Kozak M (1987) An analysis of 5'-noncoding sequences from 699 vertebrate messenger RNAs. *Nucleic Acids Res* 15: 8125-8148.

Kozak M (1989) Circumstances and mechanisms of inhibition of translation by secondary structure in eucaryotic mRNAs. *Mol Cell Biol* 9: 5134-5142.

Kramer M F, Gunaratne P, and Ferreira G C (2000) Transcriptional regulation of the murine erythroid-specific 5-aminolevulinate synthase gene. *Gene* 247: 153-166.

Krishnamurthy P, Ross D D, Nakanishi T, Bailey-Dell K, Zhou S, Mercer K E, Sarkadi B et al. (2004) The stem cell marker Bcrp/ABCG2 enhances hypoxic cell survival through interactions with heme. *J Biol Chem* 279: 24218-24225.

Krishnamurthy P C, Du G, Fukuda Y, Sun D, Sampath J, Mercer K E, Wang J et al. (2006) Identification of a mammalian mitochondrial porphyrin transporter. *Nature* 443: 586-589.

Kristiansen M, Graversen J H, Jacobsen C, Sonne O, Hoffman H J, Law S K, and Moestrup S K (2001) Identification of the haemoglobin scavenger receptor. *Nature* 409: 198-201.

Kumar S, and Bandyopadhyay U (2005) Free heme toxicity and its detoxification systems in human. *Toxicol Lett* 157: 175-188.

Kwon H S, Lee D K, Lee J J, Edenberg H J, Ahn Y H, and Hur M W (2001) Posttranscriptional regulation of human ADH5/FDH and Myf6 gene expression by upstream AUG codons. *Arch Biochem Biophys* 386: 163-171.

L

Laghai A, and Jordan P M (1977) An exchange reaction catalysed by delta-aminolaevulinate synthase from Rhodopseudomonas spheroides. *Biochem Soc Trans* 5: 299-300.

Lai W S, Carballo E, Strum J R, Kennington E A, Phillips R S, and Blackshear P J (1999) Evidence that tristetraprolin binds to AU-rich elements and promotes the deadenylation and destabilization of tumor necrosis factor alpha mRNA. *Mol Cell Biol* 19: 4311-4323.

Lathrop J T, and Timko M P (1993) Regulation by Heme of Mitochondrial Protein-Transport through a Conserved Amino-Acid Motif. *Science* 259: 522-525.

Latunde-Dada G O, Simpson R J, and McKie A T (2006) Recent advances in mammalian haem transport. *Trends Biochem Sci* 31: 182-188.

Latunde-Dada G O, Takeuchi K, Simpson R J, and McKie A T (2006) Haem carrier protein 1 (HCP1): Expression and functional studies in cultured cells. *FEBS Lett* 580: 6865-6870.

Lee C H, Leeds P, and Ross J (1998) Purification and characterization of a polysome-associated endoribonuclease that degrades c-myc mRNA in vitro. *J Biol Chem* 273: 25261-25271.

Lemm I, and Ross J (2002) Regulation of c-myc mRNA decay by translational pausing in a coding region instability determinant. *Mol Cell Biol* 22: 3959-3969.

Levy N S, Chung S, Furneaux H, and Levy A P (1998) Hypoxic stabilization of vascular endothelial growth factor mRNA by the RNA-binding protein HuR. *J Biol Chem* 273: 6417-6423.

Li B, Holloszy J O, and Semenkovich C F (1999) Respiratory uncoupling induces delta-aminolevulinate synthase expression through a nuclear respiratory factor-1-dependent mechanism in HeLa cells. *Journal of Biological Chemistry* 274: 17534-17540.

Lill R, and Kispal G (2001) Mitochondrial ABC transporters. *Res Microbiol* 152: 331-340.

Louis C A, Wood S G, Walton H S, Sinclair P R, and Sinclair J F (1998) Mechanism of the synergistic induction of CYP2H by isopentanol plus ethanol: comparison to glutethimide and relation to induction of 5-aminolevulinate synthase. *Arch Biochem Biophys* 360: 239-247.

Lundrigan M D, Koster W, and Kadner R J (1991) Transcribed sequences of the Escherichia coli btuB gene control its expression and regulation by vitamin B12. *Proc Natl Acad Sci U S A* 88: 1479-1483.

M

Ma W J, Chung S, and Furneaux H (1997) The Elav-like proteins bind to AU-rich elements and to the poly(A) tail of mRNA. *Nucleic Acids Res* 25: 3564-3569.

Maguire D J, Day A R, Borthwick I A, Srivastava G, Wigley P L, May B K, and Elliott W H (1986) Nucleotide sequence of the chicken 5-aminolevulinate synthase gene. *Nucleic Acids Res* 14: 1379-1391.

Maines M D (2004) The heme oxygenase system: past, present, and future. *Antioxid Redox Signal* 6: 797-801.

Maines M D, and Gibbs P E (2005) 30 some years of heme oxygenase: from a "molecular wrecking ball" to a "mesmerizing" trigger of cellular events. *Biochem Biophys Res Commun* 338: 568-577.

Maines M D, Trakshel G M, and Kutty R K (1986) Characterization of two constitutive forms of rat liver microsomal heme oxygenase. Only one molecular species of the enzyme is inducible. *J Biol Chem* 261: 411-419.

Martasek P, Camadro J M, Delfau-Larue M H, Dumas J B, Montagne J J, de Verneuil H, Labbe P et al. (1994) Molecular cloning, sequencing, and functional expression of a cDNA encoding human coproporphyrinogen oxidase. *Proc Natl Acad Sci U S A* 91: 3024-3028.

Martens J H, Barg H, Warren M J, and Jahn D (2002) Microbial production of vitamin B12. *Appl Microbiol Biotechnol* 58: 275-285.

Maurer F, Tierney M, and Medcalf R L (1999) An AU-rich sequence in the 3'-UTR of plasminogen activator inhibitor type 2 (PAI-2) mRNA promotes PAI-2 mRNA decay and provides a binding site for nuclear HuR. *Nucleic Acids Res* 27: 1664-1673.

Maurer I, Zierz S, and Moller H J (2000) A selective defect of cytochrome c oxidase is present in brain of Alzheimer disease patients. *Neurobiol Aging* 21: 455-462.

May B K, Dogra S C, Sadlon T J, Bhasker C R, Cox T C, and Bottomley S S (1995) Molecular Regulation of Heme-Biosynthesis in Higher Vertebrates.*Progress in Nucleic Acid Research and Molecular Biology, Vol 51*. Vol. 51. pp. 1-51.

McCoubrey W K, Jr., Huang T J, and Maines M D (1997) Isolation and characterization of a cDNA from the rat brain that encodes hemoprotein heme oxygenase-3. *Eur J Biochem* 247: 725-732.

McCoubrey W K, Jr., and Maines M D (1993) Domains of rat heme oxygenase-2: the amino terminus and histidine 151 are required for heme oxidation. *Arch Biochem Biophys* 302: 402-408.

Medlock A E, and Dailey H A (1996) Human coproporphyrinogen oxidase is not a metalloprotein. *J Biol Chem* 271: 32507-32510.

Meijer H A, and Thomas A A (2002) Control of eukaryotic protein synthesis by upstream open reading frames in the 5'-untranslated region of an mRNA. *Biochem J* 367: 1-11.

Melefors O, Goossen B, Johansson H E, Stripecke R, Gray N K, and Hentze M W (1993) Translational Control of 5-Aminolevulinate Synthase Messenger- Rna by Iron-Responsive Elements in Erythroid-Cells. *Journal of Biological Chemistry* 268: 5974-5978.

Meyer R P, Lindberg R L, Hoffmann F, and Meyer U A (2005) Cytosolic persistence of mouse brain CYP1A1 in chronic heme deficiency. *Biol Chem* 386: 1157-1164.

Meyer S, Temme C, and Wahle E (2004) Messenger RNA turnover in eukaryotes: pathways and enzymes. *Crit Rev Biochem Mol Biol* 39: 197-216.

Mignone F, Gissi C, Liuni S, and Pesole G (2002) Untranslated regions of mRNAs. *Genome Biol* 3: REVIEWS0004.

Miller Y I, and Shaklai N (1994) Oxidative crosslinking of LDL protein induced by hemin: involvement of tyrosines. *Biochem Mol Biol Int* 34: 1121-1129.

Mitani K, Fujita H, Hayashi N, Yamamoto M, and Sassa S (1992) Differential induction responses of delta-aminolevulinate synthase mRNAs during erythroid differentiation: use of nonradioactive in situ hybridization. *Am J Hematol* 39: 63-64.

Mitchell P, and Tollervey D (2000) mRNA stability in eukaryotes. *Curr Opin Genet Dev* 10: 193-198.

Moncion A, Truong N T, Garrone A, Beaune P, Barouki R, and De Waziers I (2002) Identification of a 16-nucleotide sequence that mediates post-transcriptional regulation of rat CYP2E1 by insulin. *J Biol Chem* 277: 45904-45910.

Moraes C T, Diaz F, and Barrientos A (2004) Defects in the biosynthesis of mitochondrial heme c and heme a in yeast and mammals. *Biochim Biophys Acta* 1659: 153-159.

Morgan R R, Errington R, and Elder G H (2004) Identification of sequences required for the import of human protoporphyrinogen oxidase to mitochondria. *Biochem J* 377: 281-287.

Morgan W T (1976) The binding and transport of heme by hemopexin. *Ann Clin Res* 8 Suppl 17: 223-232.

Morita T, Perrella M A, Lee M E, and Kourembanas S (1995) Smooth muscle cell-derived carbon monoxide is a regulator of vascular cGMP. *Proc Natl Acad Sci U S A* 92: 1475-1479.

Morris D R, and Geballe A P (2000) Upstream open reading frames as regulators of mRNA translation. *Mol Cell Biol* 20: 8635-8642.

Muller-Eberhard U, and Fraig M (1993) Bioactivity of heme and its containment. *Am J Hematol* 42: 59-62.

Munakata H, Sun J Y, Yoshida K, Nakatani T, Honda E, Hayakawa S, Furuyama K et al. (2004) Role of the heme regulatory motif in the heme-mediated inhibition of mitochondrial import of 5-aminolevulinate synthase. *J Biochem (Tokyo)* 136: 233-238.

N

Nakae J, Kitamura T, Silver D L, and Accili D (2001) The forkhead transcription factor Foxo1 (Fkhr) confers insulin sensitivity onto glucose-6-phosphatase expression. *J Clin Invest* 108: 1359-1367.

Namba H, Narahara K, Tsuji K, Yokoyama Y, and Seino Y (1991) Assignment of human porphobilinogen deaminase to 11q24.1----q24.2 by in situ hybridization and gene dosage studies. *Cytogenet Cell Genet* 57: 105-108.

Nelson D R, Koymans L, Kamataki T, Stegeman J J, Feyereisen R, Waxman D J, Waterman M R et al. (1996) P450 superfamily: update on new sequences, gene mapping, accession numbers and nomenclature. *Pharmacogenetics* 6: 1-42.

Newton D C, Bevan S C, Choi S, Robb G B, Millar A, Wang Y, and Marsden P A (2003) Translational regulation of human neuronal nitric-oxide synthase by an alternatively spliced 5'-untranslated region leader exon. *J Biol Chem* 278: 636-644.

Nishimura K, Taketani S, and Inokuchi H (1995) Cloning of a human cDNA for protoporphyrinogen oxidase by complementation in vivo of a hemG mutant of Escherichia coli. *J Biol Chem* 270: 8076-8080.

Nou X, and Kadner R J (2000) Adenosylcobalamin inhibits ribosome binding to btuB RNA. *Proc Natl Acad Sci U S A* 97: 7190-7195.

O

Otterbein L E, Bach F H, Alam J, Soares M, Tao Lu H, Wysk M, Davis R J et al. (2000) Carbon monoxide has anti-inflammatory effects involving the mitogen-activated protein kinase pathway. *Nat Med* 6: 422-428.

Ouellett A J, and Malt R A (1976) Accumulation and decay of messenger ribonucleic acid in mouse kidney. *Biochemistry* 15: 3358-3361.

P

Parker R, and Sheth U (2007) P bodies and the control of mRNA translation and degradation. *Mol Cell* 25: 635-646.

Parker R, and Song H (2004) The enzymes and control of eukaryotic mRNA turnover. *Nat Struct Mol Biol* 11: 121-127.

Paterniti J R, Jr., Simone J J, and Beattie D S (1978) Detection and regulation of delta-aminolevulinic acid synthetase activity in the rat brain. *Arch Biochem Biophys* 189: 86-91.

Pelletier J, and Sonenberg N (1987) The involvement of mRNA secondary structure in protein synthesis. *Biochem Cell Biol* 65: 576-581.

Pende A, Tremmel K D, DeMaria C T, Blaxall B C, Minobe W A, Sherman J A, Bisognano J D et al. (1996) Regulation of the mRNA-binding protein AUF1 by activation of the beta-adrenergic receptor signal transduction pathway. *J Biol Chem* 271: 8493-8501.

Percudani R, and Peracchi A (2003) A genomic overview of pyridoxal-phosphate-dependent enzymes. *EMBO Rep* 4: 850-854.

Pesole G, Grillo G, Larizza A, and Liuni S (2000) The untranslated regions of eukaryotic mRNAs: structure, function, evolution and bioinformatic tools for their analysis. *Brief Bioinform* 1: 236-249.

Podvinec M, Handschin C, Looser R, and Meyer U A (2004) Identification of the xenosensors regulating human 5- aminolevulinate synthase. *Proceedings of the National Academy of Sciences of the United States of America* 101: 9127-9132.

Ponka P (1997) Tissue-specific regulation of iron metabolism and heme synthesis: distinct control mechanisms in erythroid cells. *Blood* 89: 1-25.

Ponka P (1999) Cell biology of heme. *American Journal of the Medical Sciences* 318: 241-256.

Ponka P, Borova J, and Neuwirt J (1973) Accumulation of heme in mitochondria from rabbit reticulocytes with inhibited globin synthesis. *Biochim Biophys Acta* 304: 715-718.

Potluri V R, Astrin K H, Wetmur J G, Bishop D F, and Desnick R J (1987) Human delta-aminolevulinate dehydratase: chromosomal localization to 9q34 by in situ hybridization. *Hum Genet* 76: 236-239.

Prescott D (1976) *Reproduction of eukaryotic cells*. New York: Academic Press.

Prokipcak R D, Herrick D J, and Ross J (1994) Purification and properties of a protein that binds to the C-terminal coding region of human c-myc mRNA. *J Biol Chem* 269: 9261-9269.

Puigserver P, Rhee J, Donovan J, Walkey C J, Yoon J C, Oriente F, Kitamura Y et al. (2003) Insulin-regulated hepatic gluconeogenesis through FOXO1-PGC-1alpha interaction. *Nature* 423: 550-555.

Pyronnet S, and Sonenberg N (2001) Cell-cycle-dependent translational control. *Curr Opin Genet Dev* 11: 13-18.

Q

Quigley J G, Yang Z, Worthington M T, Phillips J D, Sabo K M, Sabath D E, Berg C L et al. (2004) Identification of a human heme exporter that is essential for erythropoiesis. *Cell* 118: 757-766.

R

Rangarajan P N, and Padmanaban G (1989) Regulation of cytochrome P-450b/e gene expression by a heme- and phenobarbitone-modulated transcription factor. *Proc Natl Acad Sci U S A* 86: 3963-3967.

Richter-Dahlfors A A, and Andersson D I (1992) Cobalamin (vitamin B12) repression of the Cob operon in Salmonella typhimurium requires sequences within the leader and the first translated open reading frame. *Mol Microbiol* 6: 743-749.

Roberts A G, and Elder G H (2001) Alternative splicing and tissue-specific transcription of human and rodent ubiquitous 5-aminolevulinate synthase (ALAS1) genes. *Biochimica Et Biophysica Acta-Gene Structure and Expression* 1518: 95-105.

Roberts A G, Redding S J, and Llewellyn D H (2005) An alternatively-spliced exon in the 5'-UTR of human ALAS1 mRNA inhibits translation and renders it resistant to haem-mediated decay. *FEBS Lett* 579: 1061-1066.

Rogers J T, Randall J D, Cahill C M, Eder P S, Huang X, Gunshin H, Leiter L et al. (2002) An iron-responsive element type II in the 5'-untranslated region of the Alzheimer's amyloid precursor protein transcript. *J Biol Chem* 277: 45518-45528.

Romana M, Dubart A, Beaupain D, Chabret C, Goossens M, and Romeo P H (1987) Structure of the gene for human uroporphyrinogen decarboxylase. *Nucleic Acids Res* 15: 7343-7356.

Ross J (1995) mRNA stability in mammalian cells. *Microbiol Rev* 59: 423-450.

Ross J (1997) A hypothesis to explain why translation inhibitors stabilize mRNAs in mammalian cells: mRNA stability and mitosis. *Bioessays* 19: 527-529.

Rouault T, and Klausner R (1997) Regulation of iron metabolism in eukaryotes. *Curr Top Cell Regul* 35: 1-19.

Ruiz de Mena I, Fernandez-Moreno M A, Bornstein B, Kaguni L S, and Garesse R (1999) Structure and regulated expression of the delta-aminolevulinate synthase gene from Drosophila melanogaster. *J Biol Chem* 274: 37321-37328.

Ryan G, and Ades I Z (1991) On the Mechanism of Induction of Chick-Embryo Hepatic Delta- Aminolevulinate Synthase by Translational Blockers. *Biochemical Journal* 274: 619-621.

Ryter S W, and Tyrrell R M (2000) The heme synthesis and degradation pathways: role in oxidant sensitivity. Heme oxygenase has both pro- and antioxidant properties. *Free Radic Biol Med* 28: 289-309.

Sadlon T J, Dell'Oso T, Surinya K H, and May B K (1999) Regulation of erythroid 5-aminolevulinate synthase expression during erythropoiesis. *International Journal of Biochemistry & Cell Biology* 31: 1153-1167.

Sassa S (2000) Hematologic aspects of the porphyrias. *Int J Hematol* 71: 1-17.

Sassa, S (2004) Why heme needs to be degraded to iron, biliverdin IXα, and carbon monoxide? *Antioxid. Redox. Signal* 6 (5): 819-824.

Sassa S (2006) Modern diagnosis and management of the porphyrias. *Br J Haematol* 135: 281-292.

Sassa S, Iwasa F, and Kappas A (1990) 5-Aminolaevulinic Acid Synthase in Human Hep-G2 Hepatoma-Cells - Heme-Mediated Feedback Repression and Induction by Dimethyl-Sulfoxide. *Molecular Aspects of Medicine* 11: 140-140.

Sato E, Sagami I, Uchida T, Sato A, Kitagawa T, Igarashi J, and Shimizu T (2004) SOUL in mouse eyes is a new hexameric heme-binding protein with characteristic optical absorption, resonance Raman spectral, and heme-binding properties. *Biochemistry* 43: 14189-14198.

Scassa M E, Guberman A S, Ceruti J M, and Canepa E T (2004) Hepatic nuclear factor 3 and nuclear factor 1 regulate 5-aminolevulinate synthase gene expression and are involved in insulin repression. *J Biol Chem* 279: 28082-28092.

Scassa M E, Guberman A S, Varone C L, and Canepa E T (2001) Phosphatidylinositol 3-kinase and Ras/mitogen-activated protein kinase signaling pathways are required for the regulation of 5- aminolevulinate synthase gene expression by insulin. *Experimental Cell Research* 271: 201-213.

Scassa M E, Varone C L, Montero L, and Canepa E T (1998) Insulin inhibits delta-aminolevulinate synthase gene expression in rat hepatocytes and human hepatoma cells. *Experimental Cell Research* 244: 460-469.

Scheper W, Meinsma D, Holthuizen P E, and Sussenbach J S (1995) Long-range RNA interaction of two sequence elements required for endonucleolytic cleavage of human insulin-like growth factor II mRNAs. *Mol Cell Biol* 15: 235-245.

Schiavi S C, Belasco J G, and Greenberg M E (1992) Regulation of proto-oncogene mRNA stability. *Biochim Biophys Acta* 1114: 95-106.

Schiavi S C, Wellington C L, Shyu A B, Chen C Y, Greenberg M E, and Belasco J G (1994) Multiple elements in the c-fos protein-coding region facilitate mRNA deadenylation and decay by a mechanism coupled to translation. *J Biol Chem* 269: 3441-3448.

Schoenhaut D S, and Curtis P J (1989) Structure of a mouse erythroid 5-aminolevulinate synthase gene and mapping of erythroid-specific DNAse I hypersensitive sites. *Nucleic Acids Res* 17: 7013-7028.

Scriver C R, Beaudet A L, and Sly W S (1995) *The metabolic and molecular bases of inherited disease. Volume I. Volume II. Volume III.* 7th. ed. New York: McGraw-Hill.

Sela-Brown A, Silver J, Brewer G, and Naveh-Many T (2000) Identification of AUF1 as a parathyroid hormone mRNA 3'-untranslated region-binding protein that determines parathyroid hormone mRNA stability. *J Biol Chem* 275: 7424-7429.
Shayeghi M, Latunde-Dada G O, Oakhill J S, Laftah A H, Takeuchi K, Halliday N, Khan Y et al. (2005) Identification of an intestinal heme transporter. *Cell* 122: 789-801.

Sheng M, and Greenberg M E (1990) The regulation and function of c-fos and other immediate early genes in the nervous system. *Neuron* 4: 477-485.

Shyu A B, Belasco J G, and Greenberg M E (1991) Two distinct destabilizing elements in the c-fos message trigger deadenylation as a first step in rapid mRNA decay. *Genes Dev* 5: 221-231.

Shyu A B, and Wilkinson M F (2000) The double lives of shuttling mRNA binding proteins. *Cell* 102: 135-138.

Smith A, and Morgan W T (1984) Hemopexin-mediated heme uptake by liver. Characterization of the interaction of heme-hemopexin with isolated rabbit liver plasma membranes. *J Biol Chem* 259: 12049-12053.

Sparanese D, and Lee C H (2007) CRD-BP shields c-myc and MDR-1 RNA from endonucleolytic attack by a mammalian endoribonuclease. *Nucleic Acids Res* 35: 1209-1221.

Srivastava G, Bawden M J, Anderson A, and May B K (1989) Drug Induction of P450iib1/Iib2 and 5-Aminolevulinate Synthase Messenger-Rnas in Rat-Tissues. *Biochimica Et Biophysica Acta* 1007: 192-195.

Srivastava G, Borthwick I A, Brooker J D, Wallace J C, May B K, and Elliott W H (1983) Hemin Inhibits Transfer of Pre-Delta-Aminolevulinate Synthase into Chick-Embryo Liver-Mitochondria. *Biochemical and Biophysical Research Communications* 117: 344-349.

Srivastava G, Borthwick I A, Maguire D J, Elferink C J, Bawden M J, Mercer J F B, and May B K (1988) Regulation of 5-Aminolevulinate Synthase Messenger-Rna in Different Rat-Tissues. *Journal of Biological Chemistry* 263: 5202-5209.

Srivastava G, Hansen A J, Bawden M J, and May B K (1990) Hemin Administration to Rats Reduces Levels of Hepatic Messenger-Rnas for Phenobarbitone-Inducible Enzymes. *Molecular Pharmacology* 38: 486-493.

Stoecklin G, Ming X F, Looser R, and Moroni C (2000) Somatic mRNA turnover mutants implicate tristetraprolin in the interleukin-3 mRNA degradation pathway. *Mol Cell Biol* 20: 3753-3763.

Strobel H W, Geng J, Kawashima H, and Wang H (1997) Cytochrome P450-dependent biotransformation of drugs and other xenobiotic substrates in neural tissue. *Drug Metab Rev* 29: 1079-1105.

T

Taketani S, Inazawa J, Abe T, Furukawa T, Kohno H, Tokunaga R, Nishimura K et al. (1995) The human protoporphyrinogen oxidase gene (PPOX): organization and location to chromosome 1. *Genomics* 29: 698-703.

Taketani S, Inazawa J, Nakahashi Y, Abe T, and Tokunaga R (1992) Structure of the human ferrochelatase gene. Exon/intron gene organization and location of the gene to chromosome 18. *Eur J Biochem* 205: 217-222.

Tan D, and Ferreira G C (1996) Active site of 5-aminolevulinate synthase resides at the subunit interface. Evidence from in vivo heterodimer formation. *Biochemistry* 35: 8934-8941.

Theodorakis N G, and Cleveland D W (1992) Physical evidence for cotranslational regulation of beta-tubulin mRNA degradation. *Mol Cell Biol* 12: 791-799.

Thomson A M, Rogers J T, and Leedman P J (1999) Iron-regulatory proteins, iron-responsive elements and ferritin mRNA translation. *Int J Biochem Cell Biol* 31: 1139-1152.

Thomson A M, Rogers J T, Walker C E, Staton J M, and Leedman P J (1999) Optimized RNA gel-shift and UV cross-linking assays for characterization of cytoplasmic RNA-protein interactions. *Biotechniques* 27: 1032-1039, 1042.

Tierney M J, and Medcalf R L (2001) Plasminogen activator inhibitor type 2 contains mRNA instability elements within exon 4 of the coding region. Sequence homology to coding region instability determinants in other mRNAs. *J Biol Chem* 276: 13675-13684.

Tschudy D P, Hess R A, and Frykholm B C (1981) Inhibition of Delta-Aminolevulinic-Acid Dehydrase by 4,6- Dioxoheptanoic Acid. *Journal of Biological Chemistry* 256: 9915-9923.

Tsiftsoglou A S, Tsamadou A I, and Papadopoulou L C (2006) Heme as key regulator of major mammalian cellular functions: molecular, cellular, and pharmacological aspects. *Pharmacol Ther* 111: 327-345.

Tugores A, Magness S T, and Brenner D A (1994) A single promoter directs both housekeeping and erythroid preferential expression of the human ferrochelatase gene. *J Biol Chem* 269: 30789-30797.

U

Urban-Grimal D, Volland C, Garnier T, Dehoux P, and Labbe-Bois R (1986) The nucleotide sequence of the HEM1 gene and evidence for a precursor form of the mitochondrial 5-aminolevulinate synthase in Saccharomyces cerevisiae. *Eur J Biochem* 156: 511-519.

V

Varone C L, Giono L E, Ochoa A, Zakin M M, and Canepa E T (1999) Transcriptional regulation of 5-aminolevulinate synthase by phenobarbital and cAMP-dependent protein kinase. *Archives of Biochemistry and Biophysics* 372: 261-270.

Vitreschak A G, Rodionov D A, Mironov A A, and Gelfand M S (2003) Regulation of the vitamin B12 metabolism and transport in bacteria by a conserved RNA structural element. *Rna* 9: 1084-1097.

Volk B, Meyer R P, von Lintig F, Ibach B, and Knoth R (1995) Localization and characterization of cytochrome P450 in the brain. In vivo and in vitro investigations on phenytoin- and phenobarbital-inducible isoforms. *Toxicol Lett* 82-83: 655-662.

W

Walker J, Neto O, and Standart N (1998) *Protein Synthesis - Methods and Protocols: Section 26*. Totowa: Humana Press Inc.

Webb G C, Jitrapakdee S, Bottema C D, and Wallace J C (1997) Assignment of the pyruvate carboxylase gene to rat chromosome band 1q43 by in situ hybridization. *Cytogenet Cell Genet* 79: 151-152.

Wellington C L, Greenberg M E, and Belasco J G (1993) The destabilizing elements in the coding region of c-fos mRNA are recognized as RNA. *Mol Cell Biol* 13: 5034-5042.

Whitfield M L, Zheng L X, Baldwin A, Ohta T, Hurt M M, and Marzluff W F (2000) Stem-loop binding protein, the protein that binds the 3' end of histone mRNA, is cell cycle regulated by both translational and posttranslational mechanisms. *Mol Cell Biol* 20: 4188-4198.

Wiechelman K J, Braun R D, and Fitzpatrick J D (1988) Investigation of the bicinchoninic acid protein assay: identification of the groups responsible for color formation. *Anal Biochem* 175: 231-237.

Wilson G M, and Brewer G (1999) The search for trans-acting factors controlling messenger RNA decay. *Prog Nucleic Acid Res Mol Biol* 62: 257-291.

Wilusz C J, Wormington M, and Peltz S W (2001) The cap-to-tail guide to mRNA turnover. *Nat Rev Mol Cell Biol* 2: 237-246.

Wink D A, Nims R W, Saavedra J E, Utermahlen W E, Jr., and Ford P C (1994) The Fenton oxidation mechanism: reactivities of biologically relevant substrates with two oxidizing intermediates differ from those predicted for the hydroxyl radical. *Proc Natl Acad Sci U S A* 91: 6604-6608.

Wink D A, Wink C B, Nims R W, and Ford P C (1994) Oxidizing intermediates generated in the Fenton reagent: kinetic arguments against the intermediacy of the hydroxyl radical. *Environ Health Perspect* 102 Suppl 3: 11-15.

Wisdom R, and Lee W (1991) The protein-coding region of c-myc mRNA contains a sequence that specifies rapid mRNA turnover and induction by protein synthesis inhibitors. *Genes Dev* 5: 232-243.

Y

Yamamoto M, Hayashi N, and Kikuchi G (1983) Translational inhibition by heme of the synthesis of hepatic delta-aminolevulinate synthase in a cell-free system. *Biochem Biophys Res Commun* 115: 225-231.

Yamauchi K, Hayashi N, and Kikuchi G (1980) Translocation of delta-aminolevulinate synthase from the cytosol to the mitochondria and its regulation by hemin in the rat liver. *J Biol Chem* 255: 1746-1751.

Ye W Z, and Zhang L (2004) Heme controls the expression of cell cycle regulators and cell growth in HeLa cells. *Biochemical and Biophysical Research Communications* 315: 546-554.

Yeilding N M, and Lee W M (1997) Coding elements in exons 2 and 3 target c-myc mRNA downregulation during myogenic differentiation. *Mol Cell Biol* 17: 2698-2707.

Yeilding N M, Rehman M T, and Lee W M (1996) Identification of sequences in c-myc mRNA that regulate its steady-state levels. *Mol Cell Biol* 16: 3511-3522.

Yen T J, Gay D A, Pachter J S, and Cleveland D W (1988) Autoregulated changes in stability of polyribosome-bound beta-tubulin mRNAs are specified by the first 13 translated nucleotides. *Mol Cell Biol* 8: 1224-1235.

Yen T J, Machlin P S, and Cleveland D W (1988) Autoregulated instability of beta-tubulin mRNAs by recognition of the nascent amino terminus of beta-tubulin. *Nature* 334: 580-585.

Yomogida K, Yamamoto M, Yamagami T, Fujita H, and Hayashi N (1993) Structure and Expression of the Gene Encoding Rat Nonspecific Form Delta-Aminolevulinate Synthase. *Journal of Biochemistry* 113: 364-371.

Yoo H W, Warner C A, Chen C H, and Desnick R J (1993) Hydroxymethylbilane synthase: complete genomic sequence and amplifiable polymorphisms in the human gene. *Genomics* 15: 21-29.

Yoo Y M, Kim K M, Kim S S, Han J A, Lea H Z, and Kim Y M (1999) Hemoglobin toxicity in experimental bacterial peritonitis is due to production of reactive oxygen species. *Clin Diagn Lab Immunol* 6: 938-945.

Yoshino K, Munakata H, Kuge O, Ito A, and Ogishima T (2007) Heme-regulated Degradation of {delta}-Aminolevulinate Synthase 1 in Rat Liver Mitochondria. *J Biochem* 142: 453-458.

Zhang J S, and Ferreira C (2002) Transient state kinetic investigation of 5-aminolevulinate synthase reaction mechanism. *Journal of Biological Chemistry* 277: 44660-44669.

Zhang J S, and Ferreira G C (2002) Transient-state kinetic investigation of the mechanism of 5- aminolevulinate synthase reaction. *Abstracts of Papers of the American Chemical Society* 223: 383-PHYS.

Zhang L, and Guarente L (1995) Heme binds to a short sequence that serves a regulatory function in diverse proteins. *Embo J* 14: 313-320.

Zhang M, Pierce R A, Wachi H, Mecham R P, and Parks W C (1999) An open reading frame element mediates posttranscriptional regulation of tropoelastin and responsiveness to transforming growth factor beta1. *Mol Cell Biol* 19: 7314-7326.

Zheng B, Albrecht U, Kaasik K, Sage M, Lu W, Vaishnav S, Li Q et al. (2001) Nonredundant roles of the mPer1 and mPer2 genes in the mammalian circadian clock. *Cell* 105: 683-694.

Zhu Y, Hon T, Ye W, and Zhang L (2002) Heme deficiency interferes with the Ras-mitogen-activated protein kinase signaling pathway and expression of a subset of neuronal genes. *Cell Growth Differ* 13: 431-439.

Zhu Y H, Lee H C, and Zhang L (2002) An examination of heme action in gene expression: Heme and heme deficiency affect the expression of diverse genes in erythroid K562 and neuronal PC12 cells. *DNA and Cell Biology* 21: 333-346.

APPENDIX

Appendix 1

Amino acid alignment of the human ALAS1 and ALAS2 proteins (using the amino acid letter code)

Homologous amino acids are starred and indicated in blue text. The amino acids are numbered at the end of each line.

```
                  ** * * *   * *  *   *           *  *    * *      *
ALAS1    ---MESVVRRCPFLSRVPQAFLQKAGKSLLFYAQNCPKMMEVGAKPAPRALSTAAVHYQQ
                                                                    57
ALAS2    MVTAAMLLQCCPVLARGPTSLLGKVVKTHQFLFG-------IGRCP---ILATQGPNCSQ
                                                                    50

         *          *                                 *    *    ***
ALAS1    IKETPPASEKDKTAKAKVQQTPDGSQQSPDGTQLPSGHPLPATSQGTASKCPFLAAQMNQ
                                                                   117
ALAS2    IHLKATKAGGDS----------------------------PSWAKG---HCPFMLSELQD
                                                                    79

           *    **  * ****             *    * ***       **         * *
ALAS1    RGSSVFCKASLELQEDVQEMNAVRKEVAETSAGPSVVSVKTDGGDPSGLLKNFQDIMQKQ
                                                                   177
ALAS2    GKSKIVQKAAPEVQEDVKAF--------KTDLPSSLVSVSLR-KPFSGPQE------QEQ
                                                                   124

             * ** * * *     * ** **  ** *** ************ *   * *   *
ALAS1    RPERVSHLLQDNLPKSVSTFQYDRFFEKKIDEKKNDHTYRVFKTVNRRAHIFPMADDYSD
                                                                   237
ALAS2    ISGKVTHLIQNNMPGNY-VFSYDQFFRDKIMEKKQDHTYRVFKTVNRWADAYPFAQHFSE
                                                                   183

              * ***************** *  *   **  ******************* ** **
ALAS1    SLITKKQVSVWCSNDYLGMSRHPRVCGAVMDTLKQHGAGAGGTRNISGTSKFHVDLEREL
                                                                   297
ALAS2    ASVASKDVSVWCSNDYLGMSRHPQVLQATQETLQRHGAGAGGTRNISGTSKFHVELEQEL
                                                                   243


         * ** ** ********************  ******** *************   *  **
ALAS1    ADLHGKDAALLFSSCFVANDSTLFTLAKMMPGCEIYSDSGNHASMIQGIRNSRVPKYIFR
                                                                   357
ALAS2    AELHQKDSALLFSSCFVANDSTLFTLAKILPGCEIYSDAGNHASMIQGIRNSGAAKFVFR
                                                                   303

         ***  **  **  * *  *************** ********* *  ** **********
ALAS1    HNDVSHLRELLQRSDPSVPKIVAFETVHSMDGAVCPLEELCDVAHEFGAITFVDEVHAVG
                                                                   417
ALAS2    HNDPDHLKKLLEKSNPKIPKIVAFETVHSMDGAICPLEELCDVSHQYGALTFVDEVHAVG
                                                                   363

         *** ** *** *** * * *********************  * * **************
ALAS1    LYGARGGGIGDRDGVMPKMDIISGTLGKAFGCVGGYIASTSSLIDTVRSYAAGFIFTTSL
                                                                   477
ALAS2    LYGSRGAGIGERDGIMHKIDIISGTLGKAFGCVGGYIASTRDLVDMVRSYAAGFIFTTSL
                                                                   423
```

```
          *** * ******* **  **  *** ****** *** *** ****  ******* **  *
ALAS1     PPMLLAGALESVRILKSAEGRVLRRQHQRNVKLMRQMLMDAGLPVVHCPSHIIPVRVADA
                                                                    537
ALAS2     PPMVLSGALESVRLLKGEEGQALRRAHQRNVKHMRQLLMDRGLPVIPCPSHIIPIRVGNA
                                                                    483

          * *   ** * * * ******************** ** *** ****  * * **  *  *
ALAS1     AKNTEVCDELMSRHNIYVQAINYPTVPRGEELLRIAPTPHHTPQMMNYFLENLLVTWKQV
                                                                    597
ALAS2     ALNSKLCDLLLSKHGIYVQAINYPTVPRGEELLRLAPSPHHSPQMMEDFVEKLLLAWTAV
                                                                    543

          ** *   * * ******* *** *** * ***       *   *
ALAS1     GLELKPHSSAECNFCRRPLHFEVMSEREKSYFSGLS-KLVSAQA
                                                    640
ALAS2     GLPLQDVSVAACNFCRRPVHFELMSEWERSYFGNMGPQYVTTYA
                                                    587
```

Appendix 2

Alignment of the full ALAS1 genes of the human, rat and chicken.

Homologous nucleotides are indicated by stars.

```
HUMAN     CTGTATATTAAGGCGCCGGCGATCGCGGCCTGAGGCTGCTCCCGGACAAGGGCAACGAGC
RAT       ------------------------------------------------------------
CHICKEN   ------------------------------------------------------------

HUMAN     GTTTCGTTTGGACTTCTCGACTTGAGTGCCCGCCTCCTTCGCCGCCGCCTCTGCAGTCCT
RAT       ------------------------------------------------------------
CHICKEN   ------------------------------------------------------------

HUMAN     CAGCGCAGTTATGCCCAGTTCTTCCCGCTGTGGGGACACGACCACGGAGGAATCCTTGCT
RAT       ------------------------------------------------------------
CHICKEN   ------------------------------------------------------------


HUMAN     TCAGGGACTCGGGACCCTGCTGGACCCCTTCCTCGGGTTTAGGGGATGTGGGGACCAGGA
RAT       ------------------------------------------------------GAA
CHICKEN   ------------------------------------------------------------


HUMAN     GAAAGTCAGGATCCCTAAGAGTCTTCCCTGCCTGGATGGATGAGTGGCTTCTTCTCCACC
RAT       GAAGGGCACTGGTCGGTTTAGCGTCCTCCGCTCGAGTGCCCA-----CCGCCGTCTCGTC
CHICKEN   -------GCTGTTCGCTTTC-CGCCCGCCGTGGGGGTGACAG------CTGCGTGACGTC
                        *           * * *   *  **                  *  *

HUMAN     TAGATTCTTTCCACAGGAGCCAGCATACTTCCTGAACATGGAGAGTGTTGTTCGCCGCTG
RAT       GAGAGCCCG--CGCAGGACCCGGGACACTTTGCAGACATGGAGACTGTCGTTCGCAGATG
CHICKEN   -ACTTCCGGTCGGCGGTAGCTGCGGCAGGAGGAAGG-ATGGAGGCGGTGGTGCGGCGCTG
           *    *      * * * *      *          ******   ** ** **  * **

HUMAN     CCCATTCTTATCCCGAGTCCCCCAGGCCTTTCTGCAGAAAGCAGGCAAATCTCTGTTGTT
RAT       CCCATTCTTATCCCGAGTCCCTCAGGCCTTTCTGCAGAAGGCAGGGAAATCTCTGCTGTT
CHICKEN   CCCGTTCCTGGCCCGCGTCTCGCAGGCCTTCCTGCAGAAGGCCGGGCCTTCCCTGCTCTT
          *** *** *  **** *** * ******** ******** ** **    ** *** * **

HUMAN     CTATGCCCAAAACTGCCCCAAGATGATGGAAGTTGGGGCCAAGCCAGCCCCTCGGGCATT
RAT       CTATGCTCAAAACTGCCCCAAGATGATGGAAGTCGGGGCCAAGCCGGCTCCTCGGACCGT
CHICKEN   TTATGCCCAGCACTGTCCCAAAATGATGGAGGCGGCGCCGCCGGCCGCCGCCCGAGGCCT
           ***** **  **** ***** ******** *  * * *   * * **  * **     *

HUMAN     GTCCACTGCAGCAGTACACTACCAACAGATCAAAGAAACCCCTCCGGCCAGTGAGAAAGA
RAT       GTCCACTTCAGCAGCACAGTGCCAGCAGGTCAAAGAAACCCCTCCAGCCAATGAGAAAGA
CHICKEN   CGCCACATCCGCCGCCCGCGGGCAGCAGGTAGAGGAGACCCCTGCGGCCCAGCCGGAGGC
            ****  * ** *  *     ** *** *  * ** ****** * ***     * * *

HUMAN     CAAAACTGCTAAGGCCAAGGTCCAACAGACTCCTGATGGATCCCAG------CAGAGTCC
RAT       GAAAACTGCCAAAGCCGCAGTCCAGCAGGCTCCTGACGAGTCCCAGATGGCACAGACTCC
CHICKEN   CAAGAAAGCCAAAGAAGTGGCCCAGCAG--------------------------AACAC
           ** *  ** ** *     * *** ***                           *   *

HUMAN     AGATGGCACACAGCTTCCGTCTGGACACCCCTTGCCTGCCACAAGCCAGGGCACTGCAAG
RAT       AGACGGCACACAGCTCCCGCCTGGACACCCGTCACCCTCTACAAGCCAGAGCTCTGGGAG
CHICKEN   AGATGGGTCACAGCCTCCTGCTGGCCACCCACCTGCTGCTGCTGTCCAGAGCTCTGCTAC
          *** **  ******  **  **** *****     *  *  *   **** ** ***  *
```

```
HUMAN     CAAATGCCCTTTCCTGGCAGCACAGATGAATCAGAGAGGCAGCAGTGTCTTCTGCAAAGC
RAT       CAAGTGCCCTTTCCTGGCAGCACAGCTGAGCCAGACGGGCAGCAGCGTCTTCCGCAAGGC
CHICKEN   AAAATGCCCATTCCTGGCAGCTCAGATGAACCACAAGAGCAGCAATGTGTTCTGCAAAGC
           ** ***** ********** *** ***  ** *   ******  ** *** **** **

HUMAN     CAGTCTTGAGCTTCAGGAGGATGTGCAGGAAATGAATGCCGTGAGGAAAG------AGGT
RAT       CAGTCTGGAGCTTCAGGAGGACGTGCAGGAAATGCATGCTGTGAGGAAAG------AGGT
CHICKEN   CAGCTTGGAACTGCAGGAGGATGTGAAGGAAATGCAGGTGGACAGGAAAGGTAAAGAATT
          ***  * ** ** ******** *** ******** * *  *  *******      *  *

HUMAN     TGCTGAAACCTCAGCAGGCCCCAGTGTGGTTAGTGTGAAAACCGATGGAGGGGATCCCAG
RAT       TGCTCAAAGCCCAGTGCTCCCCAGCTTGGTCAATGCAAAAAGGGATGGAGAAGGTCCAAG
CHICKEN   TGCCAAAATACCAACTAATTCCGTGGTGAGGAACACTGAGGCTGAGGGAGAAGAGCAGAG
          ***  ***   **       **    **   *      *    ** ****  *  *  **

HUMAN     TGGACTGCTGAAGAACTTCCAGGACATCATGCAAAAGCAAAGACCAGAAAGAGTGTCTCA
RAT       CCCACTGCTGAAGAACTTCCAGGACATCATGAGAAAGCAAAGGCCAGAAAGAGTGTCTCA
CHICKEN   TGGCTTGCTCAAGAAGTTTAAGGATATTATGCTGAAGCAAAGACCCGAAAGTGTGTCTCA
               **** ***** **  **** ** ***   ******** ** ***** ********

HUMAN     TCTTCTTCAAGATAACTTGCCAAAATCTGTTTCCACTTTTCAGTATGATCGTTTCTTTGA
RAT       TCTTCTTCAGGATAACTTGCCAAAGTCCGTTTCCACTTTTCAATATGATCATTTCTTTGA
CHICKEN   TCTGCTTCAGGATAACTTGCCAAAATCTGTATCCACCTTCCAGTATGACCAGTTCTTTGA
          *** ***** ************** ** ** ***** ** ** ***** *  ********

HUMAN     GAAAAAAATTGATGAGAAAAAGAATGACCACACCTATCGAGTTTTTAAAACTGTGAACCG
RAT       GAAGAAAATTGACGAGAAAAAAAATGACCACACCTACCGAGTTTTTAAAACTGTGAACCG
CHICKEN   GAAAAAGATAGATGAAAAGAAGAAAGATCATACCTACCGAGTGTTCAAAACGGTGAACCG
          *** ** ** ** ** ** ** ** ** ** ** ***** ***** ** ***** ********

HUMAN     GCGAGCACACATCTTCCCCATGGCAGATGACTATTCAGACTCCCTCATCACCAAAAAGCA
RAT       GAGAGCACAGATCTTCCCTATGGCAGATGACTACACGGACTCCCTCATCACCAAAAAGCA
CHICKEN   AAAGGCGCAGATCTTTCCCATGGCAGATGACTACTCTGATTCCCTGATCACCAAGAAAGA
              ** ** ***** ** **************  * ** ***** ******** **  *

HUMAN     AGTGTCAGTCTGGTGCAGTAATGACTACCTAGGAATGAGTCGCCACCCACGGGTGTGTGG
RAT       GGTGTCGGTCTGGTGCAGCAACGACTATCTAGGCATGAGTCGACACCCACGGGTGTGTGG
CHICKEN   GGTGTCTGTGTGGTGCAGCAATGATTACCTGGGCATGAGTCGTCACCCTCGTGTGTGCGG
          ***** ** ******** ** ** ** ** ** ******** ***** ** ***** **

HUMAN     GGCAGTTATGGACACTTTGAAACAACATGGTGCTGGGGCAGGTGGTACTAGAAATATTTC
RAT       GGCCGTCATAGAGACTGTGAAACAGCATGGTGCCGGAGCAGGTGGAACTAGAAATATTTC
CHICKEN   AGCGGTTATGGATACACTGAAACAACATGGTGCTGGAGCAGGAGGCACAAGGAATATCTC
           ** ** ** ** **  ******* ******** ** ***** ** ** ** ***** **

HUMAN     TGGAACTAGTAAATTCCATGTGGACTTAGAGCGGGAGCTGGCAGACCTCCATGGGAAAGA
RAT       TGGAACGAGCAAGTTCCATGTGGAACTGGAGCAGGAGCTGGCTGACCTCCACGGCAAGGA
CHICKEN   AGGAACAAGCAAATTTCATGTCGACTTGGAGAAAGAACTGGCTGATCTTCATGGAAAAGA
          ***** ** ** ** ***** **  * ***   ** ***** ** ** ** ** ** **

HUMAN     TGCCGCACTCTTGTTTTCCTCGTGCTTTGTGGCCAATGACTCAACCCTCTTCACCCTGGC
RAT       CGCGGCGCTCTTGTTCTCTTCCTGCTTCGTGGCCAACGACTCCACTCTCTTCACCCTGGC
CHICKEN   TGCAGCCTTGTTGTTCTCATCTTGCTTTGTAGCCAATGATTCCACCCTCTTCACTCTTGC
          ** **  * ***** ** ** ***** ** ***** ** ** ** ******** ** **

HUMAN     TAAGATGATGCCAGGCTGTGAGATTTACTCTGATTCTGGGAACCATGCCTCCATGATCCA
RAT       TAAGATGATGCCAGGCTGTGAAATTTACTCTGATTCCGGGAACCATGCCTCCATGATCCA
CHICKEN   TAAAATGCTGCCAGGTTGTGAGATCTACTCTGATTCTGGAAACCATGCCTCCATGATCCA
          *** *** ******* ***** ** *********** ** ******************
```

```
HUMAN    AGGGATTCGAAACAGCCGAGTGCCAAAGTACATCTTCCGCCACAATGATGTCAGCCACCT
RAT      AGGGATTCGCAACAGTCGAGTGCCAAAGTATATCTTCCGCCACAATGATGTCAACCATCT
CHICKEN GGGGATTCGAAACAGCAGGGTGCCAAAACACATCTTCCGCCATAACGACGTCAACCATCT
         ******** *****  * ********  * ********** ** ** **** *** **

HUMAN    CAGAGAACTGCTGCAAAGATCTGACCCCTCAGTCCCCAAGATTGTGGCATTTGAAACTGT
RAT      CAGAGAACTGTTGCAGAGATCCGACCCCTCGGTCCCCAAGATCGTAGCATTCGAAACTGT
CHICKEN TCGAGAGCTGTTGAAGAAGTCTGATCCATCGACCCCTAAAATTGTTGCGTTTGAAACTGT
          **** *** ** * *  ** ** ** **   *** ** ** ** ** ** ********

HUMAN    CCATTCAATGGATGGGGCGGTGTGCCCACTGGAAGAGCTGTGTGATGTGGCCCATGAGTT
RAT      CCATTCAATGGATGGAGCAGTGTGCCCCCTGGAAGAGCTGTGTGATGTGGCCCATGAGTT
CHICKEN GCACTCCATGGATGGTGCTGTCTGCCCTCTGGAAGAGCTGTGTGATGTGGCCCACGAGCA
         ** ** ******** ** ** ***** ************************** ***

HUMAN    TGGAGCAATCACCTTCGTGGATGAGGTCCACGCAGTGGGGCTTTATGGGGCTCGAGGCGG
RAT      TGGAGCGATCACGTTTGTGGACGAGGTCCATGCAGTAGGGCTCTATGGGGCTTCAGGTGG
CHICKEN CGGGGCAATCACTTTTGTGGATGAAGTGCATGCTGTGGGGCTGTATGGAGCTCGAGGTGG
         ** ** ***** ** ***** ** ** ** ** ** ***** ***** ***  *** **

HUMAN    AGGGATTGGGGATCGGGATGGAGTCATGCCAAAAATGGACATCATTTCTGGAACACTTGG
RAT      AGGGATCGGTGATCGGGATGGAGTCATGCCAAAAATGGACATCATTTCTGGAACACTCGG
CHICKEN TGGCATAGGGGACCGGGATGGAGTCATGCACAAGATGGACATCATCTCTGGAACGCTCGG
         ** ** ** ** ****************  ** ********** ******** ** **

HUMAN    CAAAGCCTTTGGTTGTGTTGGAGGGTACATCGCCAGCACGAGTTCTCTGATTGACACCGT
RAT      TAAAGCGTTCGGCTGTGTTGGAGGATACATTGCCAGCACGAGTTTGCTGATCGACACCGT
CHICKEN CAAGGCCTTTGCGTGTGTGGGAGGATACATCTCCAGTACAAGTGCCCTGATAGACACTGT
         ** ** ** *  ***** ***** *****  **** ** ***   ***** ***** **

HUMAN    ACGGTCCTATGCTGCTGGCTTCATCTTCACCACCTCTCTGCCACCCATGCTGCTGGCTGG
RAT      CCGGTCCTACGCTGCGGGCTTCATCTTCACCACCTCCCTGCCACCAATGCTGCTGGCTGG
CHICKEN CCGTTCGTATGCTGCTGGCTTTATCTTCACAACATCCCTGCCACCCATGCTCCTGGCTGG
         ** ** ** ***** ***** ******** ** ** ******** ***** ********

HUMAN    AGCCCTGGAGTCTGTGCGGATCCTGAAGAGCGCTGAGGGACGGGTGCTTCGCCGCCAGCA
RAT      AGCCCTGGAGTCTGTGCGGATCCTGAAGAGCAATGAGGGACGTGCCCTTCGCCGCCAGCA
CHICKEN TGCCCTCGAATCTGTCCGAACTCTGAAAAGTGCTGAGGGCCAAGTCTTGAGGCGCCAGCA
         ***** ** ***** ** *  ***** **   ****** *  *   *  * ********

HUMAN    CCAGCGCAACGTCAAACTCATGAGACAGATGCTAATGGATGCCGGCCTCCCTGTTGTCCA
RAT      CCAGCGCAATGTCAAGCTTATGAGGCAGATGCTAATGGACGCTGGCCTCCCAGTCATCCA
CHICKEN CCAACGCAATGTGAAGCTCATGAGACAGATGCTGATGGATGCAGGGCTTCCTGTAGTGCA
         *** ***** ** ** ** ***** ******** ***** ** ** ** ** **  * **

HUMAN    CTGCCCCAGCCACATCATCCCTGTGCGGGTTGCAGATGCTGCTAAAAACACAGAAGTCTG
RAT      CTGCCCCAGCCACATCATCCCTGTGCGGGTTGCCGATGCTGCTAAAAACACAGAAATCTG
CHICKEN TTGCCCGAGTCACATCATTCCAATAAGGGTTGCAGATGCTGCTAAAAATACAGAGATCTG
         ***** ** ******** **  *  ******* ************** *****  ****

HUMAN    TGATGAACTAATGAGCAGACATAACATCTACGTGCAAGCAATCAATTACCCTACGGTGCC
RAT      TGATGAGTTGATGACCAGGCATAATATCTACGTCCAGGCCATTAATTACCCAACAGTGCC
CHICKEN TGACAAGCTGATGAGCCAACACAGCATCTATGTCCAAGCAATCAACTACCCCACAGTTCC
         ***  *  * **** *   ** *  ***** ** ** ** ** ** ***** ** ** **

HUMAN    CCGGGGAGAAGAGCTCCTACGGATTGCCCCCACCCCTCACCACACACCCCAGATGATGAA
RAT      TCGTGGGGAGGAGCTCCTCCGGATCGCCCCCACCCCGCACCACACACCGCAGATGATGAA
CHICKEN TCGTGGAGAAGAGCTGCTACGTATTGCTCCTACACCTCATCACACCCCTCAAATGATGAG
         ** ** ** ***** ** ** ** ** ** ** ** ** ***** ** ** *******
```

```
HUMAN    CTACTTCCTTGAGAATCTGCTAGTCACATGGAAGCAAGTGGGGCTGGAACTGAAGCCTCA
RAT      CTTCTTCCTAGAGAAGCTGCTGCTCACGTGGAAGCGAGTCGGGCTGGAACTGAAGCCACA
CHICKEN TTATTTTCTCGAAAAGCTGCTGGCTACATGGAAGGATGTTGGGCTGGAGCTGAAACCACA
         *  ** ** ** ** *****    ** ******   ** ******** ***** ** **

HUMAN    TTCCTCAGCTGAGTGCAACTTCTGCAGGAGGCCACTGCATTTTGAAGTGATGAGTGAAAG
RAT      TTCGTCAGCTGAATGCAACTTCTGCAGGAGGCCCTTACACTTCGAAGTGATGAGCGAGAG
CHICKEN CTCATCAGCTGAATGCAACTTCTGCAGAAGACCTCTACACTTTGAAGTGATGAGTGAAAG
         ** ******** ************** ** **  * ** ** ********** ** **

HUMAN    AGAGAAGTCCTATTTCTCAGGCTTGAGCAAGTTGGTATCTGCTCAGGCCTGAGCATGACC
RAT      AGAGAAAGCCTATTTCTCAGGCATGAGCAAGATGGTGTCTGCCCAGGCCTGACTGTGAC-
CHICKEN GGAAAGATCCTACTTCAGTGGCATGAGCAAACTATTATCTGTCAGTGCATGAGAGTAAC-
         ** *   **** ***   *** *******  *  * ****     ** ***   * **

HUMAN    TCAATTATTTCACTTAACCCCAGGCCATTATCATATCCAGATGG--TCTTCAGAGTTGTC
RAT      TCAGTTATT-CACA-AACCCCAGACCATTACCATACCCAAATAG--TAGCCAGAATTGTC
CHICKEN AGTGTTAATCCACTCATATCCA-ATCAGTAGCATTTTTAAATTACTTAATAAGCATTTTA
            *** * ***  *   ***   ** ** ***    * **    *    **  ** *

HUMAN    TTTATATGTGAATTAAGTTATAT--TAAATTTTAATCTATAGTAAAAACATAGTCCTGGA
RAT      TTTATATGTGAAGTAAATTATATATTAAATCTTAATCTATAGTAAAAAAAAAAAAAAAAA
CHICKEN ATCATAGTTAAAGCA--CTACGCTCTGAAAATAAATTTCTAGAGCCCCTG----------
         * ***  * **  *   **     * **  * *** * ***

HUMAN    AATAAATTCTTGCTTAAATGGTG----------
RAT      AAAAAAAAAAAAAAAAAAAAAAAAAAAAAAG
CHICKEN ---------------------------------
```

Appendix 3

Suppliers' full addresses

Ambion	Applied Biosystems Lingley House 120 Birchwood Boulevard Warrington WA3 7QH
Amersham Pharmacia Biotech	Amersham Biosciences UK Ltd Amersham Place Little Chalfont Buckinghamshire HP7 9NA
Beckman Coulter	Beckman Coulter (UK) Ltd Oakley Court Kingsmead Business Park London Road High Wycombe Buckinghamshire HP11 1JU
Bioline	Bioline Ltd. 16 The Edge Business Centre Humber Road London NW2 6EW
Biotecx	AMS Biotechnology (Europe) Ltd 63B Milton Park Milton Abingdon Oxon OX4 3LY
ECACC	http://www.ecacc.org.uk/
Fisher Scientific	Fisher Scientific UK Ltd Bishop Meadow Road Loughborough Leicestershire LE11 5RG
Invitrogen	Invitrogen Ltd 3 Fountain Drive Inchinnan Business Park Paisley PA4 9RF

New England Biolabs	New England Biolabs (UK) Ltd. 75/77 Knowl Piece, Wilbury Way Hitchin, Herts. SG4 0TY
Oxoid	Oxoid Ltd Wade Road Basingstoke Hampshire RG24 8PW
Pierce Biotechnology, Inc.	P.O. Box 117 Rockford IL 61105
Promega	Promega UK Ltd Delta House Chilworth Research Centre Southampton SO10 7NS
Qiagen	Qiagen Ltd Boundary Court Gatwick Road Crawley West Sussex RH10 9AX
Sigma-Aldrich	Sigma-Aldrich Company Ltd The Old Brickyard New Road Gillingham Dorset SP8 4XT

Appendix 4 – Primers

Primers used in this thesis

The restriction enzyme sites within a primer sequence are shown in *italics*. Primers are labelled as P1-P35 and used throughout chapters 3-5. The table is continued on the next page.

Primer Name	Target sequence	Restriction Enzyme Site	5'-3' Sequence	Orientation
P1	ALAS1 mRNA minor 5'-UTR exons 1A/B boundary	-	CAGCGCAGTTATGCCCA	sense
P2	ALAS1 mRNA major 5'-UTR exons 1A/2 boundary	-	CAGCGCAGTCTTTCCAC	sense
P3	ALAS1 coding region mRNA exon 3	-	CTGTGCTGCCAGGAAGAAGCA	antisense
P4	GAPDH mRNA	-	CCATCACCATCTTCCAGGAG	sense
P5	GAPDH mRNA	-	GGATGATGTTCTGGAGAGCC	antisense
P6	ALAS1 5'-UTR mRNA exon 1A	*Hind* III	*AAGCTT*CTGCTCCCGGACAAGGGCAAC	sense
P7	ALAS1 5'-UTR mRNA exon 2	*Nco* I	*CCATGG*TCAGGAAGTATGCTGGCTCC	antisense
P8	ALAS1 153bp region	*Eco* RI	GGGA*GAATTC*GCAAGCAATCAATTACCCTACG	sense
P9	ALAS1 153 end	*Eco* RI	GGG*AATTC*GCTGAGGAATGAGGCTTCAGTTC	antisense
P10	ALAS1 153bp region - with STOP codon	*Eco* RI	GGGA*GAATTC*GTAAGCAATCAATTACCCTACGGTG	sense
P11	ALAS1 coding region exon 2 from the ATG start site	*Eco* RI	GGGA*GAATTC*GATGGAGAGTGTTGTTCGC	sense
P12	ALAS1 end of coding region	*Kpn* I	GGG*GTACC*TCAGGCCTGAGCAGATAC	antisense
P13	ALAS1 coding region exon 2 with **STOP** codon	*Eco* RI	C*GAATTC*G**TGA**GGTATGGAGAGTGTTGTTCGC	sense
P14	ALAS1 end of 3'-UTR	*Kpn* I	GGG*GTACC*CACCATTTAAGCAAG	antisense
P15	ALAS1 start of 3'-UTR	*Eco* RI	CC*GAATTC*GTGAGCATGACCTC	sense
P16	ALAS1 fragment 1	*Kpn* I	CGG*GGTAC*CTCCATCGGTTTTCACAC	antisense
P17	ALAS1 fragment 2	*Eco* RI	CA*GAATTC*GGGGGATCCCAGTGGAC	sense

Primer Name	Target sequence	Restriction enzyme site	5'-3' Sequence	Orientation
P18	ALAS1 fragment 2	*Kpn* I	CG*GGTACC*GAGGGTTGAGTCATTGGC	antisense
P19	ALAS1 fragment 3	*Eco* RI	GGG*GAATTC*GTTCACCCTGGCTAAG	sense
P20	ALAS1 fragment 3	*Kpn* I	GA*GGTACC*CATGGGTGGCAGAG	antisense
P21	ALAS1 fragment 4	*Eco* RI	GGGA*GAATTC*GCTGCTGGCTGGAG	sense
P22	ALAS1 fragment 5	*Eco* RI	GGAA*GAATTC*GGGATCCCAGCAGAG	sense
P23	ALAS1 fragment 5	*Kpn* I	GG*GGTACC*GATGAGGGAGTCTGAATAG	antisense
P24	ALAS1 fragment 6	*Eco* RI	GGGGA*GAATTC*GACCAAAAAGCAAGTG	sense
P25	ALAS1 fragment 6	*Kpn* I	CG*GGTACC*CACATCACACAGCTC	antisense
P26	ALAS1 fragment 7	*Eco* RI	GG*GAATTC*GGCCCATGAGTTTGG	sense
P27	ALAS1 fragment 7	*Kpn* I	CG*GGTACC*GTAATTGATTGCTTGCAC	antisense
P28	ALAS1 coding region radiolabelled probe	-	TTCGTGGAGACCATGCTGCCCAG	sense
P29	ALAS1 coding region radiolabelled probe	-	TTCCATCATCTTGGGGCAGTT	antisense
P30	GAPDH coding region radiolabelled probe	-	CAAGAAGGTGGTGAAGCAGC	sense
P31	GAPDH coding region radiolabelled probe	-	CCACCACCCTGTTGCTGTAG	antisense
P32	pGL3P	-	GGGCCTCCCGGTTTTAATGAATACG	sense
P33	pGL3P	-	GGGGCCACATATCAAATATCCGAGTG	antisense
P34	HO-1 coding region exon 2	-	CCCAGGATTTGTCAGAGGCCC	sense
P35	HO-1 coding region exon 3	-	CCAGACAGGTCACCCAGGTAGC	antisense

(Table continued)